

DISS. ETH NO. 28297

**ACUTE BENEFITS OF TRANSCRANIAL RANDOM NOISE STIMULATION  
ON SENSORY AND MOTOR PROCESSING**

A thesis submitted to attain the degree of  
DOCTOR OF SCIENCES of ETH ZURICH

(Dr. sc. ETH Zurich)

presented by

**WERONIKA KINGA POTOK**

Magister in Cognitive Science, Adam Mickiewicz University in Poznań

Magister in Psychology, Adam Mickiewicz University in Poznań

born on 24.07.1992

citizen of Poland

accepted on the recommendation of

*Prof. Dr. Nicole Wenderoth*

*Prof. Dr. Rafael Polania*

*Prof. Dr. Daniel Kiper*

2022



## Acknowledgements

The last four years were an extremely important chapter of my life. My PhD was a remarkably enlightening experience not only on the professional but also on the personal level. This journey would have not been the same or even possible without all the great people involved, to whom I am sincerely grateful.

First, I would like to thank my amazing supervisor Nici Wenderoth for giving me the fantastic opportunity of working in the NCM lab. I could not wish for a better working environment. Your leadership makes it a dream place to run a project with the highest scientific standards and in a wonderful, friendly atmosphere. Thank you for challenging me, your thoughtful guidance, and all the inspiring discussions.

I would like to truly thank my co-supervisors Rafa Polania and Daniel Kiper for the valuable and critical feedback and insightful comments on my project. I am also grateful for your support, and flexibility in arranging our not-so-annual committee meetings.

I wish to thank the collaborators, Dylan Edwards for his valuable contribution in our first ever tRNS review presented in Chapter 2, and Laszlo B. Kish for inspiring us with an exciting research idea, and his contribution to the manuscript presented in Chapter 5.

To my dear friend and mentor Marc Bächinger, thank you for all your help with my project, inestimable mental support, endless discussions, and for your irresistible work on boosting my self-confidence during countless coaching sessions over walks and drinks.

Warmest and full of love gratitude goes to my lovely ladies Andreea Cretu, Sanne Kikkert, and Sarah Meissner! You are my inspiration. Thank you for being my role models, providing me with endless support, sharing all the laughs, and for making my (not only) lab life more vibrant, and without doubts more fun!

Special thanks to Onno van der Groen for starting the electrifying, noisy line of research aiming to create a 'Super Human' that I was lucky to continue. Also, for his valuable advice and feedback on the project and manuscripts.

Huge thanks to all my colleagues from the NCM lab! It was a real honor and pleasure to work with you!

Snow (Xue) Zhang, thank you for sharing your brain stimulation knowledge and experience with me and for giving me constant support and guidance in the lab.

Dan Woolley, thank you for your support in the lab, invaluable feedback on my projects, proofreading, and correcting all my manuscripts.

Miriam Schrafl-Altermatt, thank you for your great help and advice on running brain stimulation experiments.

Maria Willecke and Nicole Hintermeister, thank you for making my life so much easier with all your priceless administrative help.

Presentations Masters, Valerio Zerbi and Caroline Lustenberger, thank you for your valuable feedback and critical comments on all the talks I presented in the lab.

Charlie Lambelet and Jan Stutz, thank you for bringing a huge smile to my face at all times, no matter the circumstances!

Ernest Mihejl, Finn Rabe, Stephi Huwiler, Gabs Zbären, thank you for all the fruitful discussions, constant support, lots of fun, laughs, and drinks that we shared! Special thanks to my writing Buddy Gabs for proofreading my writing and for giving me always helpful feedback.

Felix Thomas and Ingrid Odermatt, thank you for sharing passion and excitement for brain stimulation and for the great pleasure of teaching together!

To all the other NCMers, Marija Markicevic, Rea Lehner, Michel Wälti, Christina Grimm, Iurii Savvateev, Caro Heimhofer, and Manu Carro Dominguez, thank you for the time we shared in the lab, for your support over the years and inspiring working environment.

I would also like to thank all the volunteers that participated in my research and all students who were involved in my project, Sahana Sivachelvam, Stella Oberlin, Marta Stępień, Lena Salzmann, Alexandra Bürgler, Luana Giacone, Lydia Kämpf, and Marcel Fellmann. Special thanks to Alain Post for his invaluable contribution to the study presented in Chapter 4.

To all the amazing people accompanying me in Switzerland, Kasia, Jaan, Kasia 'Czoli', Ambra, Kamil, Aga, Mati, Ewelina, Misiiek, Agatka, Monika, Milena, Adrian, Kasztan, and all the *Feminno* Ladies, thank you for being a substantial part of this adventure.

To all my dear friends in Poland, Jagoda, Gosia, Julia, Zosia, Marta, and Witek, thank you for the special bond between us no matter time and place, all the fun we have together, your support, and for motivating me throughout the years! I miss you all so much and cannot wait to live closer to you. Special thanks to my dearest nomad friend Alik for our never-ending stimulating and insightful discussions, for constantly challenging me and cheering me up at the same time, having you in my life is such a blessing.

I am beyond grateful to my beloved family, Mom, Dad, Grandmas, my Sister and best Friend Madzia and my Brother(-in-law) Miki! Thank you for your unconditional love, constant encouragement and believing in me. Dziękuję, że wspieracie mnie niezmiennie całe moje życie i akceptujecie moje często nieoczywiste wybory. Nie mogłam wymarzyć sobie cudowniejszej rodziny. Bardzo Was Kocham i nie mogę się doczekać aż będziemy dzielić ze sobą więcej czasu w przyszłości.

And foremost, I would like to thank my Kubi, for sharing your life with me, being my love, my joy, my best friend, and my greatest inspiration. You are always on my side, supporting and motivating me - it means the world to me. I am immensely grateful for every moment we spend together. Kocham Cię!

## Abstract

In everyday life countless stimuli are delivered to our central nervous system from the environment. The processing of incoming information is not free of noise. Even though it is counterintuitive at first, some level of background noise can have a positive impact on signal processing in the central nervous system. It has been hypothesized that neural processing can benefit from added noise via a Stochastic Resonance (SR) phenomenon. SR is a general mechanism that enhances the response of nonlinear systems to weak subthreshold signals by adding an optimal level of random noise. Using transcranial random noise stimulation (tRNS), electrical noise can be added centrally to cortical circuits to modulate brain function. In this thesis, we investigated the immediate online effects of noise on the central nervous system. We probed the responsiveness of motor and visual systems in the presence and absence of electrical noise. Additionally, we explored the effects of high-frequency *non*-stochastic electrical stimulation on sensory processing.

We began by reviewing the current literature and delineating the effects of electrical noise at the cellular, systems, and behavioral levels. We discussed the putative mechanism underpinning the effect of electrical noise stimulation on neural processing and how electrical noise might be utilized to augment sensory and motor function.

In the first study, we investigated the acute effects of noise on the neural population level in awake human participants. We showed that the responsiveness of the primary motor cortex (M1) increases immediately when electrical noise is added via tRNS.

In the second study, we explored the acute effects of tRNS delivered to two connected yet anatomically remote neural populations within the visual system, namely the primary visual cortex (V1) and the retina. We observed a significant decrease in the visual contrast detection threshold compared to baseline during tRNS delivery to V1 but not to the retina, suggesting that tRNS affects these neural populations differently.

In the third study, we empirically tested the theoretical prediction that in addition to stochastic signals, *non*-stochastic signals can also cause resonance effects. We found that non-random high-frequency transcranial alternating current stimulation (hf-tACS) applied to V1 lowers the contrast detection threshold, reflecting enhanced visual detection performance.

Altogether our work addresses the potential use of acute electrical noise added to cortical circuits to modulate physiology and enhance brain function. Our findings are consistent with the hypothesis that neural processing can benefit from added noise via a SR phenomenon, but also demonstrate the potential use of alternative waveforms to induce resonance-like effects. More broadly, our work sheds new light on a possible mechanism underpinning the

effect of acute electrical noise stimulation on neural processing and provides a new paradigm for testing SR theory predictions in the human brain. Our results highlight the general importance and relevance of SR-like mechanisms in the human brain and will potentially lead to new developments and applications across various disciplines, including basic neuroscience, neurophysiology, computational biology, and clinical research.

## Zusammenfassung

Im Alltag begegnen wir unzähligen Reizen, die aus der Umgebung in unser Nervensystem gelangen. Die Verarbeitung der eingehenden Informationen ist nicht frei von Rauschen. Auch wenn es zunächst kontraintuitiv erscheint, kann ein gewisses Maß an Hintergrundrauschen einen positiven Einfluss auf die Signalverarbeitung in einem erregbaren Nervensystem mit Schwellenwert haben. Frühere Studien stellten die Hypothese auf, dass die neuronale Verarbeitung durch das Vorhandensein zusätzlichen Rauschens über das Phänomen der Stochastischen Resonanz (SR) verbessert werden kann. SR ist ein allgemeines mechanistisches Phänomen, das beschreibt, wie sich die Reaktion nichtlinearer Systeme auf schwache, unterschwellige Signale durch Hinzufügen eines optimalen zufälligen Rauschpegels verbessert. Im Kontext der Hirnforschung kann mittels transkranieller Rauschstimulation (tRNS) elektrisches Rauschen im zentralen Nervensystem zu kortikalen Schaltkreisen hinzugefügt werden, um die Hirnfunktion zu modulieren. In der vorliegenden Doktorarbeit wurden die unmittelbaren Effekte während der Rauschstimulation auf das Nervensystem untersucht. Wir untersuchten die Erregbarkeit von motorischen und visuellen Systemen in Gegenwart und Abwesenheit elektrischen Rauschens. Darüber hinaus wurden die Effekte hochfrequenter, aber nicht-stochastischer Elektrostimulation auf die sensorische Verarbeitung untersucht.

Diese Arbeit bietet zunächst einen Überblick über die aktuelle Literatur und umreißt die Auswirkungen elektrischen Rauschens auf Zell-, System- und Verhaltensebene. In diesem Überblick diskutierten wir den vermeintlichen Mechanismus, der der Wirkung elektrischer Rauschstimulation auf die neuronale Verarbeitung zugrunde liegt, sowie die Frage, wie elektrisches Rauschen genutzt werden könnte, um sensorische und motorische Funktionen zu verbessern.

In der ersten experimentellen Studie untersuchten wir die akuten Auswirkungen von tRNS auf der Ebene neuronaler Populationen des primären motorischen Kortex (M1) im Menschen. Wir konnten zeigen, dass die Erregbarkeit von M1 unmittelbar steigt, wenn elektrisches Rauschen mittels tRNS hinzugefügt wird.

In der zweiten Studie untersuchten wir die akute Wirkung der tRNS-Stimulation auf zwei miteinander verbundene, aber anatomisch entfernte neuronale Populationen im visuellen System – auf den primären visuellen Kortex (V1) und auf die Netzhaut. Wir konnten eine signifikante Abnahme der visuellen Kontrasterkennungsschwelle im Vergleich zum Ausgangswert beobachten, wenn V1 mittels tRNS stimuliert wurde. Dies war nicht der Fall

während der Stimulation der Netzhaut. Dies deutet darauf hin, dass tRNS diese beiden neuronalen Populationen unterschiedlich beeinflusst.

In der dritten Studie überprüften wir die theoretische Vorhersage, dass auch nicht-stochastische Signale Resonanzeffekte verursachen können, empirisch. Wir konnten zeigen, dass die nicht zufällige, hochfrequente transkranielle Wechselstromstimulation (hf-tACS) von V1 ebenfalls die Kontrasterkennungsschwelle senkt, was eine verbesserte visuelle Erkennungsleistung widerspiegelt.

Insgesamt befasst sich die vorliegende Arbeit mit der möglichen Verwendung von akutem elektrischem Rauschen in kortikalen Schaltkreisen, mit dem Ziel die physiologische Verarbeitung kortikaler Signale zu modulieren und die Gehirnfunktion zu verbessern. Unsere Ergebnisse stimmen mit der postulierten Hypothese überein, dass die neuronale Verarbeitung von zusätzlichem Rauschen durch ein SR-Phänomen profitieren kann. Wir weisen aber auch auf die mögliche Verwendung alternativer Wellenformen zur Induktion resonanzähnlicher Effekte hin. Allgemein werfen die Studien dieser Doktorarbeit ein neues Licht auf einen möglichen Mechanismus, der der Auswirkung akuter elektrischer Rauschstimulation auf die neuronale Verarbeitung zugrunde liegt. Darüberhinaus liefern sie ein neues Paradigma für das Testen von Vorhersagen der SR-Theorie im menschlichen Gehirn. Unsere Ergebnisse unterstreichen die allgemeine Bedeutung und Relevanz von SR-ähnlichen Mechanismen im menschlichen Gehirn und könnten zu neuen Entwicklungen und Anwendungen in unterschiedlichsten Disziplinen wie den Neurowissenschaften, der Neurophysiologie, der computergestützten Biologie sowie der klinische Forschung führen.



# Contents

Acknowledgements.....	i
Abstract.....	iii
Zusammenfassung.....	v
List of Figures.....	xi
List of Boxes.....	xii
List of Tables.....	xii
1 Introduction.....	1
1.1 Motivation.....	1
1.2 Nonlinear systems.....	2
1.3 Stochastic resonance.....	2
1.3.1 Stochastic resonance in the nervous system.....	3
1.4 Threshold tracking methods in sensory and motor systems.....	4
1.4.1 Motor threshold measures.....	4
1.4.2 Sensory threshold measures.....	5
1.5 Aims of this thesis and chapter overview.....	6
1.5.1 Chapter 2.....	6
1.5.2 Chapter 3.....	7
1.5.3 Chapter 4.....	7
1.5.4 Chapter 5.....	7
1.5.5 Chapter 6.....	7
2 Transcranial Random Noise Stimulation modulates neural processing of sensory and motor circuits – from potential cellular mechanisms to behavior: a scoping review.....	9
2.1 Abstract.....	9
2.2 Introduction.....	10
2.3 Methods.....	10
2.4 Results.....	11
2.5 Discussion.....	12
2.5.1 Stimulation properties.....	12
2.5.2 tRNS causes physiological after-effects leading to increased cortical excitability.....	14
2.5.3 tRNS causes acute physiological effects.....	17
2.5.4 tRNS induces behavioral after-effects and modulates perceptual learning and motor function in health and disease.....	20

2.5.5	tRNS acutely affects perceptual and motor performance .....	22
2.6	Conclusions and outlook.....	24
3	Transcranial Random Noise Stimulation acutely lowers the response threshold of human motor circuits.....	26
3.1	Abstract .....	26
3.2	Introduction .....	26
3.3	Materials and Methods .....	28
3.3.1	Participants .....	28
3.3.2	General study design.....	28
3.3.3	Transcranial Random Noise Stimulation .....	30
3.3.4	Transcranial Magnetic Stimulation .....	30
3.3.5	Electromyography.....	31
3.3.6	Data processing and analysis.....	31
3.3.7	Statistical analysis.....	32
3.3.8	Additional information for specific experiments.....	32
3.4	Results .....	38
3.4.1	Exp. 1 – tRNS induced increase in MEP probability for subthreshold TMS .....	38
3.4.2	Exp. 2 - increase in MEP probability for higher tRNS intensity over M1 .....	39
3.4.3	Exp. 3 - tRNS over M1 induced decrease in RMT .....	40
3.4.4	Exp. 4 - decrease in RMT is specific for M1 stimulation .....	41
3.4.5	Additional control analyses .....	41
3.5	Discussion.....	44
3.5.1	Acute tRNS-induced noise benefits are partly consistent with SR theory .....	45
3.5.2	Alternative accounts of the observed acute tRNS-induced noise benefits.....	45
3.5.3	Possible neurophysiological substrate mediating tRNS-induced noise benefits	46
3.5.4	Increased cortical responsiveness via tRNS is unlikely to result from tactile stimulation.....	47
3.6	Conclusions.....	48
4	Transcranial random noise stimulation of the primary visual cortex but not retina modulates visual contrast sensitivity. ....	49
4.1	Abstract.....	49
4.2	Introduction .....	50
4.3	Materials and methods .....	50
4.3.1	Participants .....	51
4.3.2	General Study design .....	52
4.3.3	Visual stimuli .....	53

4.3.4	Four-alternative forced choice visual detection task .....	54
4.3.5	tRNS characteristics .....	55
4.3.6	Statistical Analysis .....	58
4.4	Results .....	59
4.4.1	tRNS over V1 modulates visual contrast threshold.....	60
4.4.2	tRNS over the retina does not modulate visual contrast threshold consistently	61
4.4.3	No effects of simultaneous tRNS of V1 and retina on visual contrast threshold	62
4.5	Discussion.....	63
4.5.1	tRNS improves visual sensitivity in V1 .....	63
4.5.2	Inconsistencies in the effects of noise on retinal processing of contrast.....	64
4.5.3	Intersession variability in the effects of individualized tRNS protocol on contrast sensitivity .....	66
4.6	Conclusions.....	66
5	Contrast detection is enhanced by non-stochastic, high-frequency transcranial alternating current stimulation .....	68
5.1	Abstract.....	68
5.2	Introduction .....	68
5.2.1	On stochastic resonance .....	68
5.2.2	Non-stochastic resonance with triangle (or sawtooth) waves.....	70
5.2.3	Stochastic resonance effects on neural processing.....	73
5.3	Materials and methods .....	74
5.3.1	Participants .....	74
5.3.2	General Study design .....	76
5.3.3	Experimental setup and visual stimuli .....	77
5.3.4	Four-alternative forced choice visual detection task.....	78
5.3.5	Hf-tACS characteristics.....	79
5.3.6	Statistical analysis.....	80
5.4	Results .....	82
5.4.1	Hf-tACS <sub>triangle</sub> over V1 modulates visual contrast threshold .....	83
5.4.2	Hf-tACS <sub>sine</sub> over V1 modulates visual contrast threshold.....	84
5.4.3	Comparison of hf-tACS <sub>triangle</sub> , hf-tACS <sub>sine</sub> , and hf-tRNS-induced modulation.....	85
5.5	Discussion.....	88
5.5.1	Hf-tACS with triangle and sine waveform improve visual sensitivity potentially via a resonance-like signal enhancement mechanism.....	88
5.5.2	Comparison of hf-tACS <sub>triangle</sub> , hf-tACS <sub>sine</sub> , and hf-tRNS.....	91
5.6	Conclusions.....	91

6	General Discussion .....	92
6.1	Significance of the main findings .....	92
6.1.1	tRNS modulates neural processing of sensory and motor systems .....	92
6.1.2	tRNS delivered centrally acutely lowers the responsiveness of neuronal populations in human cortex .....	93
6.1.3	tRNS affects distinct neuronal populations within the visual system differently ..	93
6.1.4	Signal processing in the visual cortex can be enhanced by non-stochastic, high-frequency transcranial alternating current stimulation .....	93
6.2	Neural substrate and computational underpinnings of stochastic and non-stochastic electrical stimulation effects.....	94
6.3	Methodological implications.....	95
6.4	Outstanding questions .....	96
6.5	Potential applications .....	99
6.6	Conclusions.....	100
	References.....	101
	Appendix .....	112
	Supplementary material Chapter 2 .....	112
	Curriculum Vitae .....	128

## List of Figures

Figure 1.1 Stochastic Resonance phenomenon in a threshold system .....	3
Figure 2.1 Data charting process .....	11
Figure 2.2 tRNS characteristics.....	13
Figure 2.3 Conceptual representation of how electrical random noise stimulation (RNS) may enhance the neural signal and influence neural response according to the Stochastic Resonance phenomenon.....	18
Figure 3.1 Conceptual representation of how tRNS may enhance the neural signal and influence RMT .....	28
Figure 3.2 Stimulation protocol, electrode placement (grey rectangles) and electric field modelling for experiments 1-4 .....	29
Figure 3.3. Representative data of an individual participant to exemplify the threshold estimation procedure. ....	36
Figure 3.4 tRNS induced an increase in motor evoked potential (MEP) probability relative to the probability of eliciting MEPs in the no tRNS control condition. ....	39
Figure 3.5 Probability of eliciting MEPs ( $p(\text{MEP}_{0.05\text{mV}})$ ) at different tRNS intensities .....	40
Figure 3.6 Results of experiment 3 .....	40
Figure 3.7 Results of experiment 4 .....	41
Figure 3.8 Average MEP amplitude elicited by single-pulse TMS in the experimental and control conditions .....	42
Figure 3.9 Changes in the adjusted TMS intensity between measurement blocks in experiments 2-4 .....	44
Figure 4.1 Flow diagram of the data collection progress through the phases of the study....	52
Figure 4.2 Stimulation protocol in V1, Retina and V1+Retina sessions .....	53
Figure 4.3 Experimental design.....	55
Figure 4.4 Baseline VCT measured in the no tRNS condition in both blocks in V1, Retina and V1+Retina sessions .....	60
Figure 4.5 Results of V1 and Retina sessions .....	61
Figure 4.6 Results of V1+Retina session .....	63
Figure 5.1 Deterministic transfer of sub-threshold binary signal through simple threshold-based stochastic resonators with a Threshold Element and an additive triangle wave at the input.....	70
Figure 5.2 The triangle wave vs. the threshold. ....	72
Figure 5.3 Experimental design.....	77
Figure 5.4 Average baseline VCT measured in the no hf-tACS conditions in hf-tACS <sub>triangle</sub> and hf-tACS <sub>sine</sub> experiments.....	83
Figure 5.5 Results of experiment 1 .....	84
Figure 5.6 Results of experiment 2 .....	85
Figure 5.7 Average baseline VCT measured in the no tES conditions in hf-tACS <sub>triangle</sub> , hf-tACS <sub>sine</sub> , hf-tRNS experiments .....	86

Figure 5.8 Comparison of effects of hf-tACS<sub>triangle</sub>, hf-tACS<sub>sine</sub>, hf-tRNS.....87

List of Boxes

Box 2.1 Definitions of Stochastic Resonance phenomenon and nonlinear system. .... 19

List of Tables

Table 2.1 Summary of the purpose, stimulation parameters and findings of tRNS and RNS studies..... 112

# 1 Introduction

## 1.1 Motivation

Imagine a walk in the late afternoon on a cloudy day or listening to a low-level background sound. In such situations, the stimuli you are perceiving are weak and you struggle to extract specific features, making it difficult to interpret them. In everyday life, the human brain receives numerous and complex inputs. The way in which stimuli are processed depends on the intrinsic properties of the nervous system, for example its response threshold, and external factors such as stimulus strength or accompanying noise. While the relationship between stimulus strength and the nonlinear response of the system (see *Nonlinear systems* below) is mostly understood, the influence of noise is much less clear. Surprisingly, the response of a nonlinear system can be enhanced by an optimal level of added noise. This phenomenon, which seems counterintuitive at first, is referred to as stochastic resonance (SR, see *Stochastic resonance* below). The SR effect was previously demonstrated for visual processing (Simonotto et al., 1997), where noise added to the *periphery*, by superimposing visual noise on weak visual stimuli, improved signal detection. However, the idea of delivering noise *centrally* to the brain to enhance brain function is relatively new (van der Groen and Wenderoth, 2016). A noninvasive brain stimulation technique called transcranial random noise stimulation (tRNS) provides us with a unique tool to deliver *noise* to the brain in the form of electric current and test its effects on brain function. The acute effects of tRNS on visual processing were tested in the context of SR using a behavioral paradigm where tRNS was delivered to the visual cortex, with the results revealing a beneficial effect of electrical noise on signal detection (van der Groen and Wenderoth, 2016; van der Groen et al., 2018; Pavan et al., 2019).

What remains unclear is (i) what neurophysiological mechanisms underlie these acute effects emerging from tRNS, (ii) what are the effects of tRNS when delivered over divergent neural populations within the nervous system, and (iii) whether beneficial resonance-like effects are bound to a specific type of stimulation waveform (stochastic vs deterministic). The overall aim of this thesis is to answer these questions by probing the thresholds of sensory and motor systems in the presence and absence of electrical stimulation, and to validate the effects of stimulation on input signal processing.

In this chapter, we introduce the general concepts related to the influence of noise on signal processing. First, we present the nervous system as a nonlinear excitable threshold system. We then outline the properties of the stochastic resonance phenomenon, in particular in the

nervous system. We finally describe neuroscientific and psychophysical methods to probe system threshold that can be utilized to assess the influence of noise on system performance. We conclude this chapter by delineating the main goals of the thesis and presenting an overview of the next chapters.

## 1.2 Nonlinear systems

Nonlinearity is a property of systems in which the change in the system *output* is not proportional to the system *input*. Nonlinear systems are described across many disciplines including mathematics, physics, engineering, and in particular biology (Scott, 2007). The response of many biological systems is based on whether the level of a stimulus is above or below a given threshold. This is a characteristic of nerve cells, which are the fundamental units of the brain and nervous system. In neurons, any stimulus or input signal needs to induce depolarization by reaching a certain threshold in order to evoke an action potential (Longstaff, 2000).

## 1.3 Stochastic resonance

Even though it is counterintuitive at first, noise introduced to a nonlinear system can have a positive impact on signal processing. In their influential review, McDonnell and Abbott (2009) proposed a broad definition of stochastic resonance (SR), which describes the phenomenon where the presence of internal noise or external input noise in a nonlinear system provides a better system response to a given input signal than the absence of noise:

$$\textit{performance (noise + nonlinearity)} > \textit{performance (nonlinearity)}$$

In other words, noise can have a beneficial influence on signal processing and the performance of a nonlinear system can be better with added noise compared to without (McDonnell and Abbott, 2009).

Different types of SR have been described in the past (see McDonnell et al., 2008 for a review). The two main subtypes include dynamical SR and non-dynamical SR. For the purpose of this thesis we will focus on the type of SR that can occur in excitable systems with only one stable state, known as non-dynamical or threshold SR (Wiesenfeld et al., 1994). In its simplest manifestation, SR results from the concurrence of a threshold, a subthreshold stimulus, and noise (Gingl et al., 1995). SR occurs if the presence of additive noise allows the input signal to be detected (i.e., to cross the response threshold), which is reflected in a higher output signal-to-noise ratio (SNR; McDonnell and Ward, 2011). As the brain is an example of an excitable threshold system that has to detect and transmit signals in a noisy environment, it is



a good candidate to benefit from SR effects. We discuss examples of SR in neural models below.

### 1.3.1 Stochastic resonance in the nervous system

SR has been demonstrated in a variety of naturally occurring processes including biological systems (Moss et al., 2004; Vázquez-Rodríguez et al., 2017). Demonstrations of SR in the nervous system were carried out on crayfish mechanoreceptors (Douglass et al., 1993), neurons in crickets (Levin and Miller, 1996), mice (Onorato et al., 2016; Huidobro et al., 2017), rats (Collins et al., 1996b; Gluckman et al., 1996; Remedios et al., 2019), and cats (Manjarrez et al., 2002), with studies consistently reporting enhanced system performance. In particular, it has been demonstrated that electrical random noise stimulation increases action potential firing in neurons in response to weak electrical stimuli (see **Figure 1.1**; Onorato et al., 2016; Remedios et al., 2019).

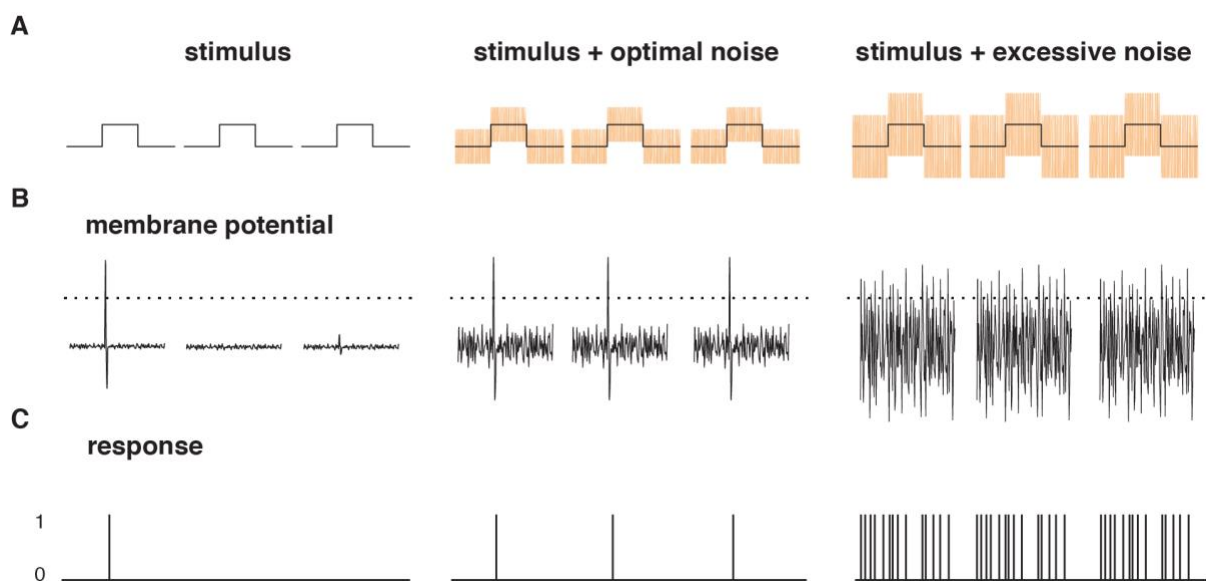


**Figure 1.1** Stochastic Resonance phenomenon in a threshold system. Conceptual representation of how electrical random noise stimulation may enhance the neural signal and influence the neural response. **A.** Weak stimuli of depolarizing steps (left) or steps combined with white electrical noise of various powers (optimal or excessive noise level, middle and right, respectively). **B.** Stimuli evoke passive changes in membrane potentials resulting in occasional action potentials. **C.** Binary output response is observed when membrane potential reaches a response threshold (dotted line in B). Stimulus input alone is too weak to evoke an accurate system response (left). For stimuli accompanied by the optimal noise level, the output response corresponds to the exact timing of input stimuli (middle). Excessive noise added to the stimuli results in false alarms in the output response (right). Adapted from (Onorato et al., 2016).

In humans, SR-related phenomena may arise both in the peripheral and the central nervous system. So far, SR-related research investigated mostly different perception models. It has

been shown that adding an optimal level of random noise to weak visual (Simonotto et al., 1997), tactile (Collins et al., 1996a; Iliopoulos et al., 2013), or auditory (Zeng et al., 2000) stimuli improves detection performance. In this regard, SR effects induced by auditory noise were also observed across different sensory modalities (Lugo et al., 2008).

Interestingly, it has been recently demonstrated that adding electrical transcranial random noise stimulation (tRNS) directly to the cerebral cortex improves sensory detection as well as perceptual decision making in accordance with the SR mechanism (van der Groen and Wenderoth, 2016; van der Groen et al., 2018). There is an increasing interest in utilizing tRNS as a tool to investigate brain function, especially in the context of the influence of noise on signal processing (Battaglini et al., 2020, 2019; Ghin et al., 2018; Pavan et al., 2019; van der Groen et al., 2019, 2018; van der Groen and Wenderoth, 2016; see Potok et al., 2022 for review). A detailed literature review on the effects of tRNS is presented in Chapter 2.

## **1.4 Threshold tracking methods in sensory and motor systems**

System excitability can be described either as the strength of the system response to external input signals (e.g., response amplitude or accuracy) or as system responsiveness characterized by a certain response threshold. The level of neural tissue responsiveness can be determined by assessing how probable it is that a signal within the system reaches the system's threshold and evokes a response (Vázquez-Rodríguez et al., 2017). Probing the threshold of a measured system in the presence and absence of noise can help us understand how noise influences system responsiveness.

### **1.4.1 Motor threshold measures**

In the motor system, neural responsiveness is operationalized via the well-known concept of the resting motor threshold (RMT, Hallett, 2000). The RMT can be probed using single-pulse transcranial magnetic stimulation (TMS). TMS, when applied over the primary motor cortex (M1), elicits motor evoked potentials (MEPs). MEPs can be recorded in the muscle and reflect the summation of multiple cortical components (i.e., the resultant of excitatory and inhibitory interneuron interactions) activating a chain reaction in the corticospinal tract neurons (Di Lazzaro and Rothwell, 2014). The RMT is typically defined as the lowest intensity needed to elicit MEPs with peak-to-peak amplitude  $\geq 0.05$  mV in the relaxed muscle, in 50% of consecutive trials (Rossini et al., 1994). RMT is one of the most robust and stable TMS measures to assess the individual membrane excitability of corticospinal tract neurons (Kobayashi and Pascual-Leone, 2003; Nitsche et al., 2005; Hallett, 2007; Rossi et al., 2009). Threshold tracking techniques provide measures of system excitability and reflect the membrane properties at the site of stimulation (Bostock et al., 1998). Threshold tracking is

often utilized in TMS studies (Fisher et al., 2002; Awiszus, 2003, 2011; Vucic et al., 2006; Menon et al., 2015; Shibuya et al., 2016), whereby the estimated threshold is based on the probability with which a certain stimulus intensity effectively evokes a response. In this approach, shifts in threshold rather than MEP amplitude represent outcome measures (Vucic et al., 2018). Threshold estimation with TMS serves as a good alternative to investigate disturbances in the stability of the nervous system under various conditions without the influence of variable fluctuations in MEP amplitude (Howells et al., 2018; Vucic et al., 2018). We used the estimated motor threshold as our physiological outcome parameter to assess the responsiveness of M1 in the study presented in Chapter 3.

#### **1.4.2 Sensory threshold measures**

In research on sensory and perceptual systems, psychophysical methods are often utilized to quantify the relationship between behavioral performance and the input signal (Grondin, 2016). In a psychophysical task, behavior can be modeled using a parametric function that is characterized by a few parameter values. During task performance, changes in stimulus strength or other characteristics are associated with changes in the ability of the sensory system to detect or discriminate such stimuli (Moss et al., 2004). Resulting measures of performance as a function of the level of input stimulus constitute a psychometric function (i.e., input-output curve). Each psychometric function provides information about two key features describing behavior, i.e., threshold and slope. The threshold is estimated as a level of detection (or discrimination) performance. The performance criterion for the threshold is chosen as a measure of the function from random (i.e., chance level) execution to perfect execution. The second parameter describing behavior is the slope of the psychometric function, which assesses how changes in performance correspond to changes in stimulus values (Leek, 2001; Moss et al., 2004).

The individual psychometric function for a given stimulus is typically assessed by the method of constant stimuli. One drawback of this method is that it requires tedious and multiple sampling over many possible stimulus levels and collecting an observation response after each presentation. The psychometric function is then evaluated based on the percentage of presentations of each member of the stimulus set that is correctly recognized (Leek, 2001). Adaptive procedures have been developed in psychophysical research to overcome the problem of inefficient placement of trials along the stimulus array in order to extract a relevant measure. The main characteristic of all adaptive procedures is that information about the outcome (e.g., a threshold) increases systematically as the procedure progresses (Leek, 2001). In other words, in an adaptive experimental procedure, characteristics of the stimuli on each trial are determined by the input stimuli and respective system responses that occurred

in the previous sequence of trials (Leek, 2001). One commonly used example of an adaptive procedure in psychophysical experiments is a Bayesian adaptive psychometric method called QUEST (Watson and Pelli, 1983). We used this threshold assessment tool to estimate individual visual contrast detection threshold in the studies presented in Chapter 4 and Chapter 5. In this maximum-likelihood adaptive procedure, information from all trials in an experiment are considered in order to determine a threshold (Watson and Pelli, 1983; Leek, 2001).

## **1.5 Aims of this thesis and chapter overview**

The aim of this PhD thesis was to investigate the effects of stochastic noise on the nervous system. We probed thresholds of motor and visual systems to obtain information about their responsiveness in the presence versus absence of noise. Additionally, we tested a high-frequency deterministic equivalent of noise on the nervous system.

The main open questions addressed in this thesis are:

- (i) What are the potential neurophysiological underpinnings of the effects of tRNS?
- (ii) Can SR-like effects of tRNS be shown at the neural population level using neurophysiological readouts of human cortex responsiveness?
- (iii) Does tRNS-induced modulation depend on the neuronal population level of delivery within a certain system?
- (iv) Are the SR-like effects specific to the stochastic noise waveform of transcranial electrical stimulation?

### **1.5.1 Chapter 2**

Chapter 2 entails our recently published scoping review where we collect the existing evidence of neuromodulation induced by tRNS. We discuss findings from behavioral, physiological, and cell studies demonstrating the beneficial influence of electrical random noise stimulation on sensory and motor processing manifested either as after-effects following prolonged stimulation or as acute noise benefits. Additionally, we compiled a table summarizing detailed methodology and conclusions from 70 tRNS publications. This review provides an overview of the current state of knowledge about tRNS and its effects on the brain, to better understand how electrical random noise influences the nervous system from cellular mechanisms to behavior. More broadly, the review sheds new light on a putative mechanism underpinning the effect of electrical noise stimulation on neural processing.

### **1.5.2 Chapter 3**

In the first research chapter, we investigated the physiological effects of online tRNS on neuronal populations in humans. This chapter entails a peer-reviewed paper in which we extended the principle that weak neural signals can be enhanced by adding the appropriate level of electrical noise from single-cell preparations to the neural population level in awake human participants. We showed that the responsiveness of motor cortex increases immediately when electrical noise is added via transcranial stimulation. These electrophysiological findings contribute to our understanding of acute behavioral benefits resulting from the application of tRNS to cortical areas.

### **1.5.3 Chapter 4**

In the second research chapter, we focused on the behavioral effects of online tRNS applied over two connected yet anatomically remote neural populations. We built on our previous findings and tested whether our electrophysiological findings extend to acute behavioral benefits caused by tRNS. We stimulated two independent neuronal populations within the visual system, namely the retina and primary visual cortex (V1) and estimated the visual contrast detection threshold while participants were performing a visual contrast detection task. We found that tRNS significantly decreases the visual contrast detection threshold compared to baseline when delivered to the V1 but not when applied to the retina. Our results indicate that the effect of tRNS depends on the targeted neural population since we did not find equal modulation within two distinct areas of the visual system.

### **1.5.4 Chapter 5**

In the third research chapter, we explored the potential of alternative stimulation protocols to induce benefits for signal processing. Knowing that electrical random noise applied over V1 can improve contrast sensitivity, we tested whether this effect is specific to stochastic signals only and repeated our experimental procedure, this time stimulating V1 with two additional types of non-stochastic high-frequency alternating currents, namely triangle and sine waves. We observed that all three stimulation types resulted in comparable effects in decreasing visual detection thresholds. These findings are the first evidence that a stochastic component is not necessary to induce resonance effects.

### **1.5.5 Chapter 6**

In Chapter 6, the main findings from chapters 3-5 are summarized, followed by a discussion of the potential underlying mechanism of stochastic and non-stochastic electrical stimulation.

We then present the remaining outstanding questions, methodological implications of our results and their potential clinical relevance.

## 2 Transcranial Random Noise Stimulation modulates neural processing of sensory and motor circuits – from potential cellular mechanisms to behavior: a scoping review

**Potok, W.**, van der Groen, O., Bächinger, M., Edwards, D. and Wenderoth, N. (2022). Transcranial Random Noise Stimulation modulates neural processing of sensory and motor circuits—from potential cellular mechanisms to behavior: a scoping review. *eNeuro*.

### **Contributions:**

Experimental Design, Literature Review, Literature Selection and Analysis, and Manuscript Writing.

### **2.1 Abstract**

Noise introduced in the human nervous system from cellular to systems levels can have a major impact on signal processing. Using transcranial stimulation, electrical noise can be added to cortical circuits to modulate neuronal activity and enhance function in the healthy brain and in neurological patients. Transcranial random noise stimulation (tRNS) is a promising technique that is less well understood than other non-invasive neuromodulatory methods. The aim of the present scoping review is to collate published evidence on the effects of electrical noise at the cellular, systems, and behavioral levels, and discuss how this emerging method might be harnessed to augment perceptual and motor functioning of the human nervous system. Online databases were used to identify papers published 2008–2021 using tRNS in humans, from which we identified 70 publications focusing on sensory and motor function. Additionally, we interpret the existing evidence by referring to articles investigating the effects of noise stimulation in animal and sub-cellular models. We review physiological and behavioral findings of tRNS induced offline after-effects and acute online benefits which manifest immediately when tRNS is applied to sensory or motor cortices. We link these results to evidence showing that activity of voltage-gated sodium ion channels might be an important cellular substrate for mediating these tRNS effects. We argue that tRNS might make neural signal transmission and processing within neuronal populations more efficient, which could contribute to both (i) offline after-effects in the form of a prolonged increase in cortical excitability and (ii) acute online noise benefits when computations rely on weak inputs.

## 2.2 Introduction

Transcranial random noise stimulation (tRNS) is a transcranial electrical stimulation (tES) modality which has received increasing scientific attention during the last decade (Paulus, 2011; Miniussi et al., 2013; Antal and Herrmann, 2016; Antal et al., 2016; Fertonani and Miniussi, 2017). Here we review the available evidence on how tRNS might modulate neural processing within cortical sensory or motor systems. The majority of previous studies utilizing tRNS, stimulated the brain continuously for several minutes, investigating both physiological and behavioral after-effects. More recently acute effects of tRNS have also been explored, showing that tRNS can exert immediate neuromodulatory effects. Even though it is not completely clear which biological substrate underpins these effects, experiments using pharmacological interventions or specific preparations in animals have generated testable hypotheses of how tRNS modulates neuronal function.

In this scoping review we focus on the effects of tRNS on sensory and motor functions. We first provide a summary of tRNS properties. We then summarize evidence showing that tRNS modulates physiological and behavioral outcome parameters either in form of offline after-effects, i.e., changes which are measured after prolonged continuous tRNS application, or in the form of acute online effects which are immediately observable when tRNS is applied.

## 2.3 Methods

We followed a reviewing process according to the PRISMA guidelines extension for scoping reviews (Tricco et al., 2018). Our central goal was to synthesize the effects of tRNS on sensory and motor function in humans. To address this, we defined our eligibility criteria as primary studies published after 2008 (the year when tRNS was first introduced), written in English, investigating modulation of sensory or motor function using tRNS in humans. Our search was conducted using the PubMed and BioRxiv databases, with the search phrase “transcranial random noise stimulation”. From this search we only included research articles describing studies using tRNS to modulate sensory and motor functions in humans. We screened the identified articles first based on the titles, then abstracts and finally the full-text. From the initial search pool (163 titles found), we excluded non-research articles (reviews and conference abstracts), studies that did not use tRNS or were not written in English. We then screened the remaining tRNS research articles to exclude all studies that did not concern sensory or motor functions. In the last screening step, we removed case reports. The search process is summarized in **Figure 2.1**.

Screening identified 163 papers of which 70 met the criteria. In order to interpret these studies and integrate the provided insights into the broader concept of non-invasive brain stimulation,



we refer to additional literature that (i) has investigated the effect of electrical noise in animal models or (ii) has used other forms of electrical brain stimulation. This review protocol was not pre-registered.

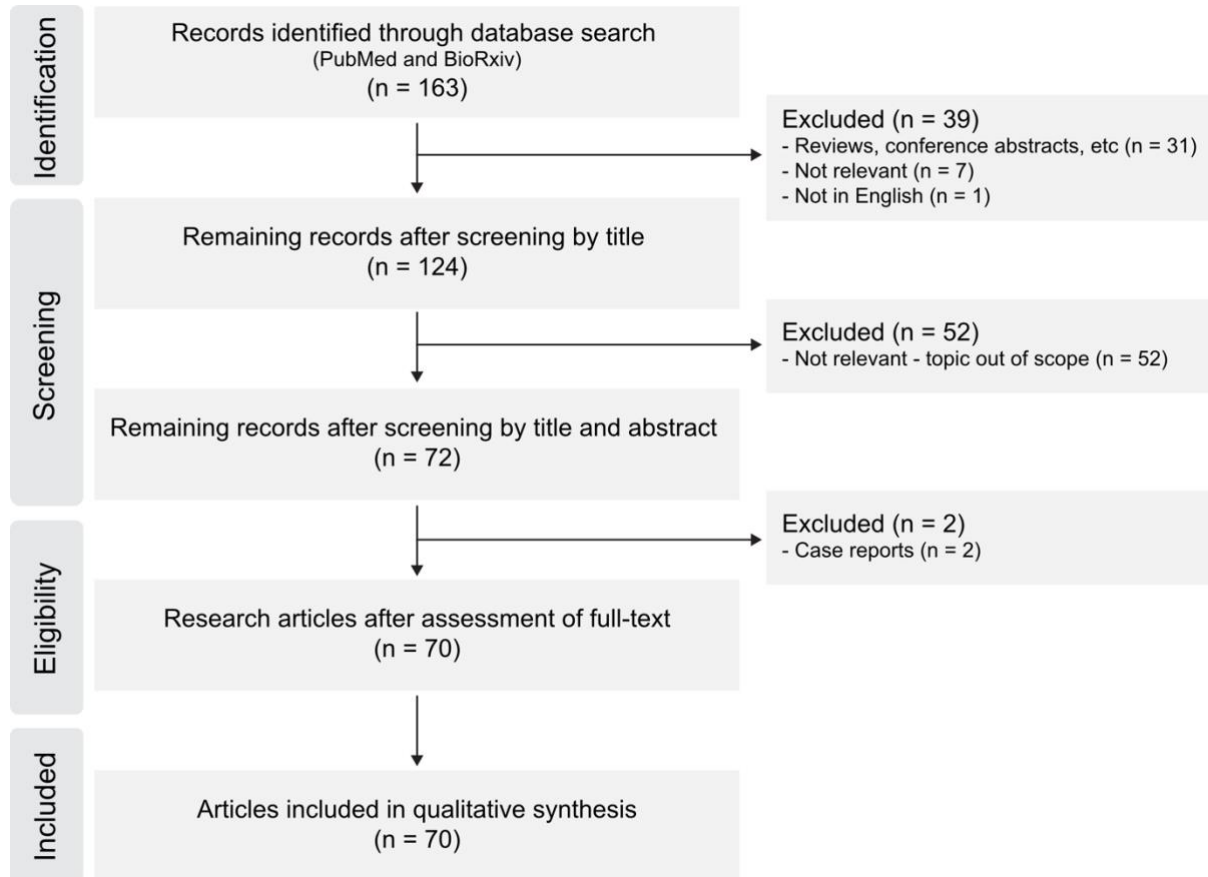


**Figure 2.1** Data charting process.

## 2.4 Results

We reviewed 70 articles investigating tRNS effects on sensory and motor function in human participants. We divide the eligible studies into those measured with physiology or behavior, assessing either offline after-effects and learning or acute online effects.

We found 19 articles focusing on the physiological effects of tRNS in healthy individuals. 18 studies investigated offline after-effects in excitability of the primary motor cortex (M1, N=15), primary visual cortex (V1, N=1), and auditory cortex (AC, N=2). One study tested the acute online effects of tRNS on M1 excitability.

50 reviewed studies investigated whether tRNS modulates behavior. Of these studies, 31 in the visual (N=7), somatosensory (N=1), and motor (N=6) systems examined offline after-

effects or learning following tRNS in healthy volunteers. Moreover, offline after-effects on visual (N=5), auditory (N=7) and, pain and motor function (N=5) were tested in clinical populations. 20 studies focused on the acute online effects of tRNS on visual (N=10) and auditory processing (N=5), somatosensation caused by stimulation (N=2) and motor function (N=1) in healthy volunteers. Again, acute online effects on visual (N=1) and motor function (N=1) were also tested in clinical populations.

The purpose, methodology and main findings of each tRNS study in humans are summarized in the table provided as **Table 2.1** in **Appendix**. We further combine the evidence from the reviewed studies and discuss the findings in the context of potential underlying mechanisms in the *Discussion* section below.

## 2.5 Discussion

This scoping review found 70 primary research studies that investigated the effects of tRNS on sensory and motor function in humans. Here, we first discuss a summary of tRNS properties. We then synthesize the findings from studies examining tRNS modulation of physiological and behavioral outcome parameters measured either as offline after- and learning effects, or acute online effects during tRNS. We interpret this evidence by referring to additional literature on the effect of electrical noise in animal models or other forms of electrical stimulation.

### 2.5.1 Stimulation properties

During tRNS, alternating currents travel between two electrodes with constantly changing polarity (Pirulli et al., 2016) (**Figure 2.2A**). The biphasic sinusoidal current is delivered at random frequencies within a predefined range and can be described as “white noise”, i.e., the induced power spectral density (the squared amplitude for a given frequency band) is constant for all frequencies (**Figure 2.2B**). The maximum frequency range is often determined by the device and typically ranges between 0.1 and 700Hz (Terney et al., 2008; Moret et al., 2019). Two commonly utilized subtypes are high-frequency tRNS (>100 Hz, hf-tRNS) and low-frequency tRNS (<100 Hz, lf-tRNS). The amplitude of tRNS signals is usually drawn from a Gaussian-distribution with a mean current of zero (**Figure 2.2C**). Thus, the net effect of tRNS is 0 mA unless an offset is introduced by adding a direct current component. tRNS intensity has traditionally been reported as “peak-to-baseline” or “peak-to-peak” amplitudes (**Figure 2.2D**). To allow replication and comparison across studies, it is important to explicitly state which convention is used. Additionally, it might be more informative to report the overall power of the current signal (which corresponds to the variance of the intensities distribution) rather

than the maximum amplitude because of the distributed characteristic of the waveform (see **Figure 2.2C**).

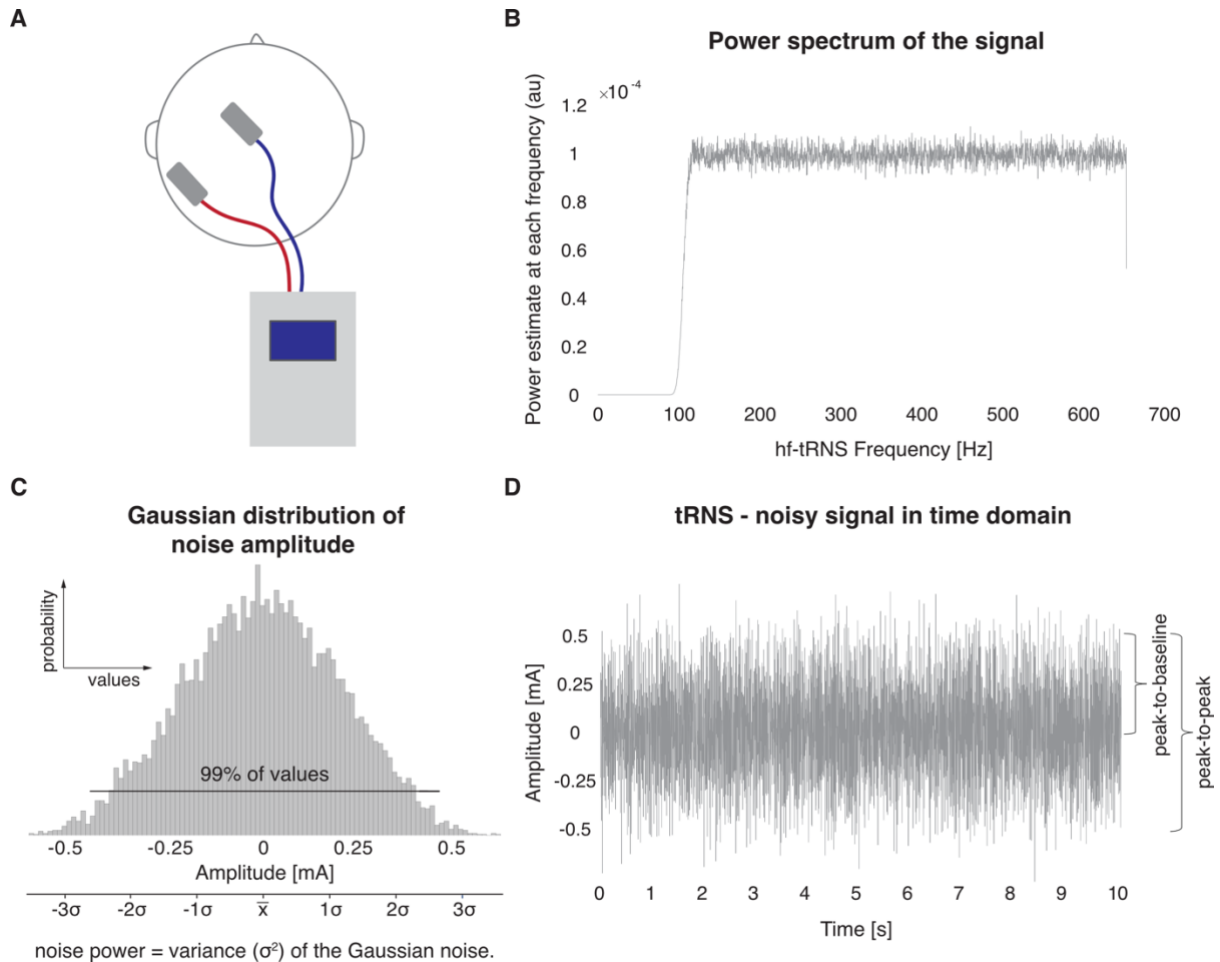


**Figure 2.2** tRNS characteristics. **A**. Example of a tRNS montage. The battery-driven stimulator applies current which travels in a biphasic manner between two stimulation electrodes (positioned anterior and posterior to the M1; Potok et al., 2021; Rawji et al., 2018), resulting in polarity independent stimulation (Pirulli et al., 2016). **B**. Power spectrum of a typical tRNS signal, shown for high frequency tRNS (hf-tRNS, 101-640Hz). The signal can be characterised as “white noise”, i.e., power is approximately constant for all frequencies. **C**. The random current intensities are normally distributed with 99% of the values lying between the peak-to-peak amplitude (see D). The noise power can be expressed as the variance of the signal. **D**. tRNS signal in the time domain. Stimulation intensity is traditionally described as the peak-to-baseline or peak-to-peak amplitude of the current output signal. This example shows a tRNS signal with the frequently used intensity of 1mA peak-to-peak (Terney et al., 2008; Parkin et al., 2019; Qi et al., 2019).

tRNS is a safe method if used according to general safety guidelines for tES (Fertonani et al., 2015; Woods et al., 2015; Bikson et al., 2016, 2018). It has been shown that after delivering tRNS with an intensity of 1mA peak-to-peak amplitude for 10 min, the concentration of serum neuron-specific enolase, a sensitive marker of neuronal damage, remains unchanged (Terney et al., 2008). Also, the induced discomfort due to cutaneous sensation is low in comparison to

transcranial direct current stimulation (tDCS) (Ambrus et al., 2010, 2011), which is advantageous for experimental blinding.

Low-intensity tES as used in human volunteers, including tRNS, is unlikely to directly elicit changes in neural spiking activity (Liu et al., 2018) since invasive recordings and modelling demonstrated that electrical fields induced by common tES protocols do not exceed 1 V/m in the brain (Opitz et al., 2015, 2016; Huang et al., 2017). However, networks of many synaptically connected active neurons reveal higher sensitivity to field modulation than a single-neuron threshold, thus, amplifying the stimulation effect (Fröhlich and McCormick, 2010; Reato et al., 2010). Therefore, even subthreshold stimulation at intensities well below the action potential threshold can substantially modulate neural activity (Gluckman et al., 1996; Francis et al., 2003; Bikson et al., 2006). It is known that the electric field induced in the brain is independent of the stimulation frequency (Vöröslakos et al., 2018). However, high frequencies might be filtered out by the neural structures (Deans et al., 2007; Liu et al., 2018) which gives rise to the concern that hf-tRNS might result in seemingly little modulation of neuronal activity. Despite the evidence showing effective modulation of single cells responses in animal models with electrical random noise (Onorato et al., 2016; Remedios et al., 2019; see *tRNS causes acute physiological effects*), the exact mechanism by which high frequency stimulation affects neural structures is currently unknown. Nevertheless, there is a growing body of evidence in the literature for *invasive* electrical stimulation, that high and ultra-high frequencies ( $> \sim 1$  kHz) can effectively modulate neuronal activity and cause clinically meaningful effects in humans (Kilgore and Bhadra, 2014; Hottinger et al., 2016; Kapural et al., 2016; Harmsen et al., 2019), supporting the merit of transcranial application.

### **2.5.2 tRNS causes physiological after-effects leading to increased cortical excitability**

18 studies investigated the physiological after-effects of tRNS on cortical excitability. A vast majority of studies in humans have investigated whether tRNS modulates cortical excitability, as measured via motor evoked potentials (MEP, N=15) or phosphene thresholds (N=1) which were elicited by single-pulse transcranial magnetic stimulation (TMS) over motor cortex and visual cortex, respectively. Most of these studies have tested tRNS induced after-effects, i.e., excitability was measured at baseline as well as after applying tRNS for a stimulation period of several minutes over M1. Specifically, 10 min of tRNS has been shown to increase corticospinal excitability (CSE) of primary motor cortex for up to 60 min, in both upper (Terney et al., 2008; Moliadze et al., 2012; Abe et al., 2019), lower extremities (Laczó et al., 2014), and pharyngeal muscle (Zhang et al., 2021), with occasional reports suggesting inhibitory effects for low intensities (Moliadze et al., 2012). A similar increase in excitability was observed in visual cortex where hf-tRNS decreased the TMS-evoked phosphene threshold for up to 60

minutes post-stimulation (Herpich et al., 2018). While 5 min of tRNS is most likely the minimum stimulation duration for enhancing CSE of the motor system (Chaieb et al., 2011) it is not clear whether there is also a maximum duration which should not be exceeded. Previous work suggests that hf-tRNS stimulation periods between 10 and 20 min seem to be appropriate to increase cortical excitability (Van Doren et al., 2014; Herpich et al., 2018; Parkin et al., 2019).

After-effects of tRNS have been suggested to depend on the stimulation frequency spectrum, with hf-tRNS inducing stronger after-effects than lf-tRNS (Terney et al., 2008), especially when the full hf-tRNS spectrum (100-700Hz) is delivered (Moret et al., 2019). When directly compared to other brain stimulation methods, tRNS resulted in stronger increase in CSE than anodal tDCS (a-tDCS) (Moliadze et al., 2014; Inukai et al., 2016), intermittent theta-burst stimulation (Moliadze et al., 2014), or 140Hz transcranial alternating current stimulation (tACS) (Inukai et al., 2016). It has been hypothesized that hf-tRNS including a direct current offset results in a stronger increase in CSE than hf-tRNS alone (Ho et al., 2015), however, this was only observed at a trend level and the direct comparison between stimulation conditions did not reveal significant differences.

Previous studies have used different electrode montages. When stimulating motor cortex, most studies placed one electrode over M1 and the other over the contralateral (supra)orbital cortex to modulate CSE (Terney et al., 2008; Moliadze et al., 2012, 2014; Chaieb et al., 2015; Ho et al., 2015; Inukai et al., 2016; Moret et al., 2019). This choice seems to be justified since a recent study found that applying hf-tRNS via the conventional M1/contralateral orbit montage caused larger CSE after-effects than a bilateral M1-M1 montage (i.e., targeting motor cortex of both hemispheres; Parkin et al., 2019). However, a bilateral montage might have its merit, particularly when sensory areas are stimulated. This was demonstrated for the auditory (Van Doren et al., 2014) and visual domain (Herpich et al., 2018) where delivering hf-tRNS bilaterally, i.e., with the electrodes placed on both hemispheres, was shown to enhance cortical excitability. The effectiveness of a bilateral montage was further demonstrated by several studies which tested the effect of tRNS on sensory detection tasks (see below, *tRNS induces behavioral after-effects and modulates perceptual learning and motor function in health and disease* and also see below, *tRNS acutely affects perceptual and motor performance*). A recent study (Potok et al., 2021) utilized an unilateral electrode montage positioned anterior and posterior to the M1 (45° away from the nasion-inion mid-sagittal line; Rawji et al., 2018). In this arrangement current oscillates perpendicular to the central sulcus, which has been hypothesized to be more efficient in modulating cortico-spinal excitability (Rawji et al., 2018). Additionally, this montage enables positioning the TMS coil directly on the scalp and not on top of the electrode. One study showed that the effects of tRNS on the targeted area seem to be dependent on the distance between the electrodes (Moliadze et al.,

2010a). To obtain the optimal electrode placement for targeted brain stimulation, it is highly recommended to use electric field modelling (Bikson et al., 2018; Bergmann and Hartwigsen, 2020). Note, however, that until now there is no software providing a reliable simulation of the electric field induced when current waveform of variable intensities and frequencies are used, as with tRNS.

Physiological after-effects outside of motor or visual cortex are less well understood. Studies investigating cortical excitability within auditory cortex (N = 2) show contradictory evidence regarding tRNS influence on auditory steady state responses measured with EEG (Van Doren et al., 2014; Schoiswohl et al., 2021).

Similar to other tES paradigms, there is a variability in effectiveness across tRNS studies and study populations. It is currently unclear whether these variable result patterns reflect small or inconsistent effects induced by tRNS or depend on participant-specific determinants. For example, the after-effects following tRNS were suggested to vary depending on interindividual differences such as age (Fertonani et al., 2019) or a person's susceptibility to placebo effects (Kortuem et al., 2019), but probably independent of the BDNF gene polymorphism (Antal et al., 2010). Long-term modulation of CSE with tRNS was suggested to be task-dependent and specific to the underlying brain state (Chaieb et al., 2009; Saiote et al., 2013; Jooss et al., 2019; Qi et al., 2019). However, many of these potential participant-specific determinants still await replication.

It is not fully understood which biological mechanism underlies long-lasting physiological effects of tRNS. A first pharmacological pilot study suggests that the facilitatory effects of tRNS are suppressed by a voltage-gated sodium channel blocker, as well as by a  $\gamma$ -Aminobutyric acid type A (GABA<sub>A</sub>) receptor agonist, while they were unaffected by N-methyl-D-aspartate (NMDA) receptor antagonists (Chaieb et al., 2015). In line with the proposal that tRNS modulates excitatory circuits it has been shown that tRNS increases intracortical facilitation in motor cortex (Terney et al., 2008) and evoked responses in somatosensory cortex (Saito et al., 2019). Evidence for the potential involvement of a GABAergic mechanism is, however, much more mixed. A recent animal study investigated histological changes after chronic tRNS in juvenile mice (Sánchez-León et al., 2021). After 9 tRNS sessions, each lasting 20min, GABA levels (quantified via GAD65-67 immunoreactivity markers) were decreased suggesting that cortical disinhibition might contribute to tRNS-induced effects. However, studies investigated the activity of GABAergic inhibitory circuits after a single session of tRNS did not support the hypothesis that a reduction of GABA<sub>A</sub> and GABA<sub>B</sub> mediated inhibition (Terney et al., 2008; Ho et al., 2015; Saito et al., 2019) contributes to after-effects on excitability in primary motor cortex.

Taken together, tRNS-induced after-effects seem to rely on a mechanism which is probably not driven by NMDA-receptor activity. High GABA<sub>A</sub> activity has been shown to prevent tRNS effects to be expressed, however, evidence is mixed as to whether tRNS modulates cortical excitability via a GABAergic disinhibition mechanism. The strongest evidence up-to-date is that tRNS induced after-effects are associated with increased activity within facilitatory cortical circuits which might facilitate neural transmission at the population level, thereby bringing the cortex into a plasticity-supporting state. At the cellular level this might be achieved by modulating the transmission at voltage-gated sodium channels, however, most of the available evidence supporting this mechanism was obtained when random noise stimulation (RNS) was *acutely* applied as discussed next.

### 2.5.3 tRNS causes acute physiological effects

The majority of the available neurophysiological studies in humans investigated tRNS-induced after-effects on cortical excitability, while only one study tested the acute physiological effects of tRNS (see below). By contrast, many in-vitro studies and research in animal models have focused on how neural activity is changed during RNS. For example, it has been demonstrated that electrical RNS increases action potential firing in mouse primary sensory neurons of dorsal root ganglia in response to weak stimuli (Onorato et al., 2016). One likely cellular substrate for mediating this acute RNS effect are voltage-dependent ion channels. Externally applied electrical white noise was shown to increase the signal transduction capacity at a sub-cellular level in artificial lipid bilayers, where it facilitated openings of voltage-dependent alamethicin ion channels (Bezrukov and Vodyanoy, 1995, 1997). Additionally, it has been demonstrated that subthreshold electrical stimulation opens sodium channels, causing a small influx of Na<sup>+</sup> which in turn causes a rapid, local depolarization of the cell membrane. Repolarization, by contrast, is a passive process which occurs over a longer time period. If the electrical stimulation is quickly repeated, as may be the case with tRNS, multiple Na<sup>+</sup> influxes occur in rapid succession and the membrane potential is gradually shifted towards depolarization (Schoen and Fromherz, 2008). An alternative account for how RNS affects sodium channels was provided by a recent study which directly probed whether applying RNS simultaneously with voltage-clamp ramps, affects the kinetics and peak amplitude of Na<sup>+</sup> currents in rat somatosensory and auditory pyramidal neurons in vitro (Remedios et al., 2019). One main finding of this study was that the observed RNS effects can be explained by modulating the kinetics of activation and inactivation of Na<sup>+</sup> channels as demonstrated by a Hodgkin–Huxley neuron model which replicated the experimental data.

Most of the above studies were motivated by the idea that neurons might be sensitive to the Stochastic Resonance (SR) phenomenon (McDonnell and Abbott, 2009) (see **Box 2.1**). SR

describes that the response of nonlinear systems to weak, subthreshold signals can be enhanced by adding an *optimal* level of random noise (McDonnell and Abbott, 2009) (**Figure 2.3**). The SR mechanism has been confirmed for neural systems and has been argued to be beneficial for neural processing by increasing the signal-to-noise ratio. For example, potentials evoked by experimental stimuli were enhanced by the optimal level of optogenetic noise photostimulation (Huidobro et al., 2017), acting on the Na<sup>+</sup> current (Mabil et al., 2020). Furthermore, the electrical RNS delivered to neurons in rat hippocampal slices increased extracellular electrical activity (Gluckman et al., 1996) and enhanced their firing activity for a particular noise level (Stacey and Durand, 2000). Similarly, subthreshold sinusoidal and stochastic noise can modulate the sensitivity of individual neurons in the medial vestibular nucleus without affecting basal firing rates (Stefani et al., 2019). Finally the two studies cited above (Onorato et al., 2016; Remedios et al., 2019) further demonstrated that neural responses to externally applied stimuli were maximally enhanced when an optimal level of electrical RNS was applied and linked this effect specifically to the induced Na<sup>+</sup> current.

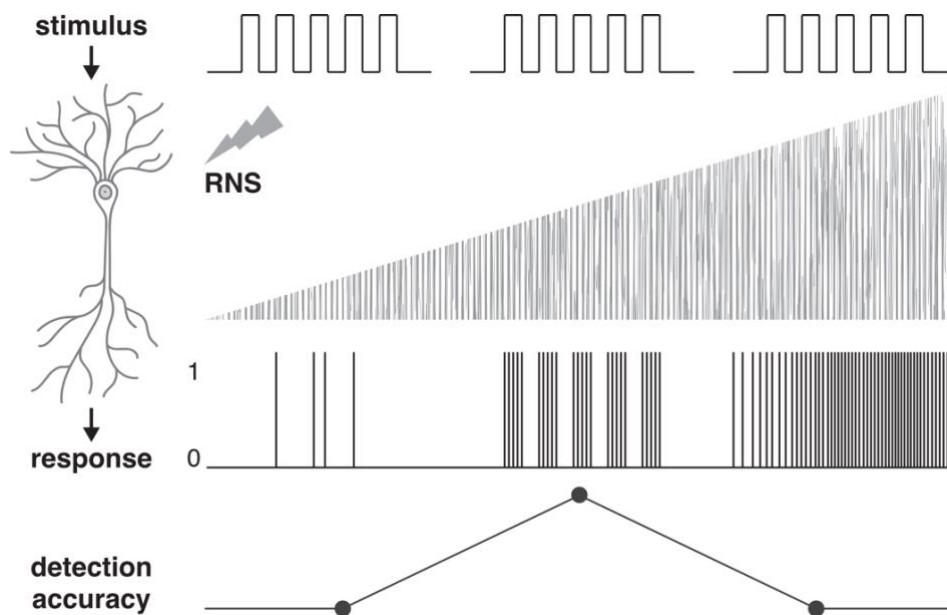


**Figure 2.3** Conceptual representation of how electrical random noise stimulation (RNS) may enhance the neural signal and influence the neural response according to the Stochastic Resonance phenomenon. Weak stimuli of depolarizing steps are delivered to a cell accompanied by white electrical RNS of increasing power (low, optimal or excessive noise level). Stimuli evoke passive changes in membrane potentials resulting in a binary output response when the membrane potential reaches a response threshold. Stimulus input combined with a low level of noise is too weak to evoke an accurate response. For stimuli accompanied by the optimal noise level, the output response corresponds to the exact timing of input stimuli. Excessive noise added to the stimuli results in false alarms in the output response. Detection accuracy of cell firing according to the stimulus is enhanced during the optimal level of noise delivery.

In humans, only one study demonstrated acute online physiological effects of hf-tRNS. It manifested as an immediate decrease in the resting motor threshold measured with TMS,



reflecting the modulation of responsiveness of M1 during very brief hf-tRNS delivery (Potok et al., 2021). This study demonstrated that tRNS can acutely generate noise benefits by enhancing the response of neural populations in human M1 for near-threshold TMS, in line with predictions of SR. Interestingly, pharmacological studies have suggested that activity of the voltage-gated sodium channels is an important determinant of motor threshold (Tergau et al., 2003; Sommer et al., 2012; Ziemann et al., 2015). These findings further support the hypothesis that high-frequency electrical RNS modulates sodium currents.

Taken together, tRNS might acutely modulate voltage-gated sodium channels. This might (i) cause multiple small  $\text{Na}^+$  influxes which are accumulated such that the membrane potential is biased towards depolarization or (ii) change the kinetics of  $\text{Na}^+$  channel activation/inactivation.

In accordance with the SR mechanism, applying an optimal level of electrical noise generates immediate noise benefits such that the cell becomes more responsive to weaker external stimuli than when no noise is added. It has been suggested that these effects might propagate from the single cell to the neuronal population level such that RNS causes large cell ensembles to synchronize their firing (Fröhlich and McCormick, 2010; Reato et al., 2010), thereby increasing the signal-to-noise ratio (Miniussi et al., 2013) and/or enhancing cortical responsiveness (Potok et al., 2021).

**Box 2.1** Definitions of Stochastic Resonance phenomenon and nonlinear system.

**Stochastic resonance** (SR) describes any phenomenon where the presence of noise in a nonlinear system is better for output signal quality than its absence (McDonnell and Abbott, 2009). In a **nonlinear system** the change of the output is not proportional to the change of the input. A good example of a nonlinear system is a neuron, where any stimulus or input signal needs to reach certain threshold in order to evoke an action potential response. One key indicator of the SR phenomenon in a broad sense is that the investigated system “benefits” from noise, which usually refers to better detection, transmission or processing of the input signal than when no noise is present. In its simplest manifestation, SR results from the concurrence of a threshold, a subthreshold stimulus, and noise (Gingl et al., 1995). Another SR feature is that noise benefits are a function of noise intensity exhibiting an inverted U-shape dose–response relationship. It refers to the assumption that there is an *optimal* noise level for enhancing the response of nonlinear systems to weak subthreshold signals, where too low noise does not change the system output and excessive noise degrades performance of the system (e.g., by causing false alarms). It was recently suggested that tRNS can be used as a tool to investigate the SR principle in the human cortex (van der Groen and Wenderoth, 2016).

#### **2.5.4 tRNS induces behavioral after-effects and modulates perceptual learning and motor function in health and disease**

Several studies (N=11) have investigated whether tRNS modulates perceptual learning when applied during the training period. A seminal study showed that 22min of hf-tRNS applied to V1 during a visual perceptual learning task improved orientation discrimination accuracy significantly more than lf-tRNS, a-tDCS, cathodal tDCS, sham, or an active control condition where tRNS was applied to the vertex (Fertonani et al., 2011). Other study replicated and extended these findings by showing that hf-tRNS facilitates perceptual learning only when applied during the learning period and, unlike a-tDCS, not when applied solely beforehand (Pirulli et al., 2013), indicating that mechanisms of action might differ between tRNS and a-tDCS. Similar benefits were demonstrated for other visual learning tasks such that applying hf-tRNS over V1 during training decreased the peripheral crowding threshold (Contemori et al., 2019) and led to fast improvements in a motion discrimination task (Herpich et al., 2019). Likewise, tRNS effects were also reported for visual training paradigms in neurological patients. A series of experiments investigated boosting effects of visual training coupled with hf-tRNS of V1 on visual perceptual learning in individuals with mild myopia (Camilleri et al., 2014, 2016), amblyopia (Campana et al., 2014; Moret et al., 2018a; Donkor et al., 2021) and chronic cortical blindness (Herpich et al., 2019). The recovery of contrast sensitivity, visual acuity, and motion processing observed in these experiments suggested the potential of combining visual training with tRNS to help restoring damaged visual abilities for divergent visual dysfunctions. These positive effects seemed to result from enhanced training efficacy due to tRNS (Camilleri et al., 2014, 2016; Moret et al., 2018a; Herpich et al., 2019; Donkor et al., 2021). For example, in patients with mild myopia the effects of 2 weeks of visual training combined with tRNS were comparable to 8 weeks of solely training (Camilleri et al., 2014) and the improvement in cortical blindness patients after 10 days, was comparable to around 2 months of training only (Herpich et al., 2019).

While the above studies applied tRNS in combination with a perceptual task, others applied tRNS during rest and investigated whether behavioral after-effects were induced (N=2). Offline hf-tRNS applied over parieto-occipital cortex was shown to induce moderate aftereffects in gamma-range brain oscillatory activity measured with EEG during motion direction discrimination task performance. These physiological effects were, however, not accompanied by behavioral task performance modulation (Ghin et al., 2021). Saito et al. (2019) showed that tRNS applied without training, improved tactile spatial discrimination task performance illustrated by a decreased threshold in discriminating grating orientation after 10min of stimulation. The stimulation affected early processing in the primary somatosensory cortex,

modulating neuronal activity by increasing the N20 sensory evoked potential amplitude, that indicates an increase in cortical excitability (Saito et al., 2019).

In the auditory domain, tRNS effects were mainly tested in patients (N=7). Lf-tRNS was demonstrated to induce a large transient suppressive effect on tinnitus loudness and tinnitus-related distress (Vanneste et al., 2013; Joos et al., 2015), outperforming tDCS and alpha tACS (Vanneste et al., 2013). Moreover, studies investigating lf-tRNS delivered over dorsolateral prefrontal cortex and auditory cortex showed the superiority of multisite treatment protocols (To et al., 2017; Mohsen et al., 2018), and multiple sessions (Mohsen et al., 2019b) over sham, one-site or single-session interventions. Lf-tRNS after-effects were illustrated by increased alpha activity that serves an inhibiting role and is usually decreased in auditory cortex of tinnitus patients. Such increase in inhibiting alpha activity most probably leads to a reduction in the hyperexcitability of the auditory cortex and thus, a decrease in tinnitus symptoms (Mohsen et al., 2019a). Despite increasing evidence for the efficacy of lf-tRNS in reducing tinnitus symptoms, the differences in treatment responders suggested the need for individualized treatment procedures, especially when hf-tRNS is utilized (Kreuzer et al., 2019).

Furthermore, 6 studies showed that tRNS also has potential to influence motor performance. tRNS applied at rest improved performance in a visuomotor tracking task (Abe et al., 2019). When delivered during several blocks of a serial reaction time task, tRNS shortened the response times (Terney et al., 2008). Interestingly, lf-tRNS and hf-tRNS were shown to modulate visuomotor learning differentially with hf-tRNS improving and lf-tRNS hindering performance (Saiote et al., 2013). Further, an improvement of complex continuous tracing task performance with the non-dominant hand was observed during both hf-tRNS and a-tDCS (Prichard et al., 2014). The time course of skill gains differed between stimulation types, suggesting likely different mechanisms by which each distinct tES protocol influences motor learning. Yet, application of hf-tRNS failed to enhance skill acquisition and retention in a golf putting task (De Albuquerque et al., 2019). In this regard, a recent study investigating the effects of motor training in combination with tRNS provided at various timepoints (before, during, or after training vs sham) failed to observe differences between these conditions on motor learning (Hoshi et al., 2021). There is also preliminary evidence (N=5) indicating a potentially beneficial influence of tRNS on motor control, pain or perceived motor fatigue in Parkinson's disease (Stephani et al., 2011; Monastero et al., 2020), relapsing-remitting multiple sclerosis (Palm et al., 2016; Salemi et al., 2019) and sub-acute ischemic stroke patients (Arnao et al., 2019). However, further research including studies of greater sample size is required to confirm the observed effects and fully understand their underlying mechanisms.

To this end, the exact mechanism by which tRNS induces long-term behavioral after-effects is not clear. So far, only one study directly linked behavioral after-effects with larger excitability showing increased sensory discrimination performance and greater SEP amplitude after tRNS (Saito et al., 2019). For studies where tRNS was applied together with a learning task, it is difficult to disentangle whether the long-term performance enhancement is caused by tRNS acting on synaptic neuroplasticity per se, or rather on preventing homeostasis of the system or increasing the signal-to-noise ratio for task-related neural activity (Fertonani et al., 2011). Moreover, even though the investigated tRNS-induced modulation seems to be consistent across healthy individuals and patients, one needs to keep in mind that in neurological diseases transmitter availability as well as other functional and structural brain features might differ on a qualitative level and have an impact on the efficacy of non-invasive brain stimulation to alter brain function.

### **2.5.5 tRNS acutely affects perceptual and motor performance**

A series of recent studies focusing on the immediate, i.e., online effects of tRNS on behavior investigated whether perceptual and motor tasks can be acutely improved by hf-tRNS (N=20).

For visual tasks (N=10), hf-tRNS acutely increases sensitivity for low contrast visual stimuli as demonstrated for contrast detection task (van der Groen and Wenderoth, 2016), orientation discrimination task (Melnick et al., 2020), lateral visual masking protocols (Battaglini et al., 2019) and exploring stimulation effects using visual stimuli with various properties (Battaglini et al., 2020). It was further shown that delivering central noise via hf-tRNS influences state-switching dynamics of binocular rivalry (van der Groen et al., 2019) and accelerates perceptual decision-making in a motion discrimination task (Campana et al., 2016; Ghin et al., 2018; van der Groen et al., 2018; Pavan et al., 2019; O'Hare et al., 2021)

Hf-tRNS was also shown to increase auditory detection (N=4), potentially by influencing early sensory processing as indicated by reducing peak latencies of auditory event-related potentials (Rufener et al., 2017, 2018). There is evidence indicating that hf-tRNS can modulate auditory perception more efficiently than tDCS (Prete et al., 2017) and with higher effectiveness when a bilateral rather than an unilateral montage is used (Prete et al., 2018). These results need to be treated with caution, however, as a recent study questioned the beneficial effects of noise in human auditory perception. The authors did not observe improvements in the detection of acoustic stimuli in the presence of noise, irrespective of whether noise was provided in an acoustic or electrical (tRNS) modality (Rufener et al., 2020).

Regarding the motor domain, applying hf-tRNS during an inhibitory “go/no-go” motor task was shown to modulate task performance by a shift in the speed-accuracy trade-off, reflected in slower reaction time and increased accuracy (Jooss et al., 2019).

A first proof-of-concept study has applied tRNS to ipsilesional M1 of stroke survivors, however, clinically relevant improvements varied across individuals and appeared to be independent of stimulation (Hayward et al., 2017). Further research in patients is needed to explore whether tRNS can boost recovery but the rationale for applying tRNS should be matched to the treatment target (Hayward et al., 2017; O'Hare et al., 2021). For example, enhancing corticospinal excitability during strength training targeted at reducing arm weakness, or augmenting learning consolidation during skill practice.

How can these behavioral benefits of acute tRNS be explained? Many of the above studies were motivated by the idea that the brain responds to acute electrical noise stimulation according to the SR phenomenon (see Box 2.1 and *tRNS causes acute physiological effects*). The SR hypothesis makes three important predictions: first, there are “noise benefits”, i.e., adding noise makes the neural system more responsive to external stimuli as indicated by higher detection rates or lower perceptual thresholds. Second, noise benefits depend on the noise intensity according to an inverted U-shaped function (Moss et al., 2004; McDonnell and Abbott, 2009), i.e., the largest noise benefit is observed for an optimal tRNS intensity while too high or too low tRNS results in smaller or no benefits. Third, noise benefits are particularly pronounced when the neural system processes near-threshold stimuli (Gingl et al., 1995) (even though SR effects can also occur for supra-threshold stimuli).

Indeed, the studies cited above could show some “noise benefits” such that performance improved in the presence of tRNS relative to a baseline condition where no tRNS was applied. In line with the second prediction of SR theory, several studies have shown that hf-tRNS at optimal intensity causes performance enhancement while applying higher intensities had a detrimental effect (van der Groen and Wenderoth, 2016; van der Groen et al., 2018; Pavan et al., 2019). Finally, some perceptual detection studies compared tRNS effects for sub-threshold directly with supra-threshold stimuli. These studies revealed that noise stimulation was particularly beneficial for near-threshold signals (van der Groen and Wenderoth, 2016; Rufener et al., 2017; van der Groen et al., 2018; Battaglini et al., 2019) which is in line with the third prediction of SR theory.

Even though tRNS has been shown to affect behavior in accordance with SR for some tasks, it is still not clear which aspect of signal processing has been modulated. A study utilizing drift diffusion framework (DDM) revealed that hf-tRNS-induced performance improvement in perceptual decision-making was accompanied by the increased drift-rate parameter (van der Groen et al., 2018). In DDM, the drift rate reflects the rate at which sensory evidence is accumulated (Ratcliff and McKoon, 2008). Performance improvement during tRNS was, therefore, suggested to occur via an increase in the rate of evidence accumulation, reflecting an enhancement in the quality of sensory information on which the decision is based (Mcintosh

and Mehring, 2017; van der Groen et al., 2018). Interestingly, equivalent noise analysis, a paradigm allowing to parcel motion perception into independent estimates of local and global processing (Dakin et al., 2005) was used to determine whether hf-tRNS modulates internal noise or global sampling (Ghin et al., 2018; Pavan et al., 2019). In this paradigm, internal noise would affect the precision of estimating each moving dot's direction (local processing), whereas sampling reflects the number of such estimates that can be averaged (global processing, (Dakin et al., 2005)). It revealed that hf-tRNS influences sampling, indicating mechanisms modulating effectiveness of perceptual integration of the signal (Ghin et al., 2018; Pavan et al., 2019). In either case, effectiveness of the signal perception but not change of the decision criterion was postulated to be responsible for boosting task performance.

## **2.6 Conclusions and outlook**

There is growing evidence coming from behavioral, physiological, and cell studies demonstrating beneficial influence of electrical RNS on sensory or motor processing manifested either as after-effects following prolonged stimulation or as acute noise benefits. tRNS after-effects manifest as increased cortical excitability and performance improvements for selected tasks, however, there is no evidence that tRNS might act on synaptic plasticity per se. Rather, it seems to act via voltage-gated sodium ion channels in large neuronal populations. This might bring the brain into a slightly facilitated state which is beneficial for neuroplastic changes to occur. The activity of voltage-gated sodium channels has also been proposed to underlie acute noise benefits which manifest as increased effectiveness of responding to weak input signals as tRNS might improve the signal-to-noise ratio of the stimulated neuronal populations.

However, more research is needed to fully understand the neurobiological underpinnings of tRNS which can then inform the design of stimulation protocols to improve sensory and motor function in health and disease. In this regard, there are still several open questions that need to be addressed. So far tRNS effects were shown for stimulation delivered over different cortical areas. However, it remains unknown whether tRNS-induced modulation depends on the neuronal population level of the stimulation delivery within a certain system (e.g., retina vs V1 in the visual system or M1 vs spinal cord in the motor system). Moreover, effectiveness of the current stimulation may vary depending on individual differences in anatomy and could be addressed by individualizing electrode montage or stimulation intensities based on the simulations of the induced electric field. According to the SR theory, the level of noise added to the system needs to be optimized for the individual and task type to improve performance (Moss et al., 2004; McDonnell and Abbott, 2009; van der Groen and Wenderoth, 2016). It is therefore important to consider both these aspects in tRNS study designs.

Although many studies have demonstrated physiological or behavioral after-effects of tRNS consistent with neuroplastic changes, they were shown to be most probably not mediated by NMDA receptor activity (Chaieb et al., 2015). Thus, it is currently not clear how tRNS might affect synaptic plasticity. This question could be addressed by combining tRNS with other brain stimulation protocols that induce neuroplastic effects measured with electrophysiology to provide a better understanding of an underlying mechanism. Finally, as tRNS is a relatively new branch of non-invasive brain stimulation research it is difficult to assess the ratio between effective interventions and null results, the latter being likely underestimated due to the publication bias. Therefore, it is important for the field to share null findings to obtain a full and unbiased picture of the effectiveness of the tRNS method.

### 3 Transcranial Random Noise Stimulation acutely lowers the response threshold of human motor circuits

**Potok, W.**, Bächinger, M., van der Groen, O., Cretu, A. L., & Wenderoth, N. (2021). Transcranial random noise stimulation acutely lowers the response threshold of human motor circuits. *Journal of Neuroscience*, *41(17)*, 3842-3853.

#### **Contributions:**

Experimental Design, Electric Field Modeling, Data Collection, Data Analysis, and Manuscript Writing.

#### **3.1 Abstract**

Transcranial random noise stimulation (tRNS) over cortical areas has been shown to acutely improve performance in sensory detection tasks. One explanation for this behavioral effect is stochastic resonance, a mechanism that explains how signal processing in non-linear systems can benefit from added noise. While acute noise benefits of electrical RNS have been demonstrated at the behavioral level as well as in *in vitro* preparations of neural tissue, it is currently largely unknown whether similar effects can be shown at the neural population level using neurophysiological readouts of human cortex. Here we hypothesized that acute tRNS will increase the responsiveness of primary motor cortex (M1) when probed with transcranial magnetic stimulation. Neural responsiveness was operationalized via the well-known concept of the resting motor threshold (RMT). We showed that tRNS acutely decreases RMT. This effect was small, but it was consistently replicated across four experiments including different cohorts (total  $N=81$ , 46 females, 35 males), two tRNS electrode montages, and different control conditions. Our experiments provide critical neurophysiological evidence that tRNS can acutely generate noise benefits by enhancing the neural population response of human M1.

#### **3.2 Introduction**

Transcranial random noise stimulation (tRNS) is a non-invasive electrical brain stimulation technique whereby currents are randomly drawn from a predefined range of intensities and frequencies (Antal and Herrmann, 2016). Until now most studies applied tRNS for several minutes over primary motor cortex (M1), which typically leads to an increase in corticomotor excitability relative to baseline for up to 60 min after stimulation (Terney et al., 2008; Chaieb et al., 2011, 2015; Abe et al., 2019; Moret et al., 2019) with occasional reports suggesting



inhibitory effects for low intensities (Moliadze et al., 2012). The exact mechanism causing this temporary facilitation of cortical activity is unknown, however, it has been hypothesized to reflect neuroplastic changes (Terney et al., 2008).

By contrast, acute (i.e., online) effects of tRNS have been studied much less. One general hypothesis is that the brain responds to electrical noise according to a stochastic resonance (SR) phenomenon (Terney et al., 2008; Miniussi et al., 2013; van der Groen and Wenderoth, 2016; van der Groen et al., 2018, 2019; Pavan et al., 2019). SR is a general mechanism that enhances the response of nonlinear systems to weak subthreshold signals by adding an optimal level of random noise (Gingl et al., 1995; McDonnell and Abbott, 2009). One key indicator of the SR phenomenon in a broad sense (McDonnell and Abbott, 2009) is that the investigated system “benefits” from noise, which usually refers to better detection, transmission or processing of the input signal than when no noise is present. In humans, SR effects have been mainly demonstrated via behavioral signal detection tasks whereby noise was added to the periphery. For example, the detection of low-contrast visual stimuli was significantly enhanced when the stimuli were superimposed with visual noise (Simonotto et al., 1997). Recently, a similar enhancement of visual perception has been reported when noise was directly added to visual cortex via tRNS, which improved the detection of low contrast visual stimuli (van der Groen and Wenderoth, 2016), visual decision making (Ghin et al., 2018; Pavan et al., 2019; van der Groen et al., 2019), binocular rivalry (van der Groen et al., 2018), and visual training in healthy participants (Fertonani et al., 2011; Pirulli et al., 2013) and patients (Moret et al., 2018b; Herpich et al., 2019). However, until now the beneficial effect of adding external electrical random noise to neural activity has mainly been studied via behavioral outcome measures in humans or via physiological single cell studies in animals (Onorato et al., 2016; Remedios et al., 2019). By contrast, it is largely unknown whether tRNS causes acute benefits when applied in-vivo to neural populations within the cortex. Here we seek to answer this question by delivering electrical noise transcranially to human primary motor cortex (M1). We hypothesized that if M1 benefits from externally added noise in accordance to the SR phenomenon, neural responsiveness to transcranial magnetic stimulation (TMS) (i.e., reflecting the processing and/or transmission of the external stimulation) would be increased (McDonnell and Abbott, 2009). Neural responsiveness was operationalized via the well-known concept of the resting motor threshold (RMT), which is defined as the stimulation intensity required to evoke motor evoked potentials (MEPs) of a given amplitude in at least 50% of trials, i.e., with a probability of 0.5. Accordingly, our hypothesis would be supported if RMTs were lower during tRNS application when compared to no stimulation because random noise increased the probability of evoking MEPs of sufficient size (**Figure 3.1**).

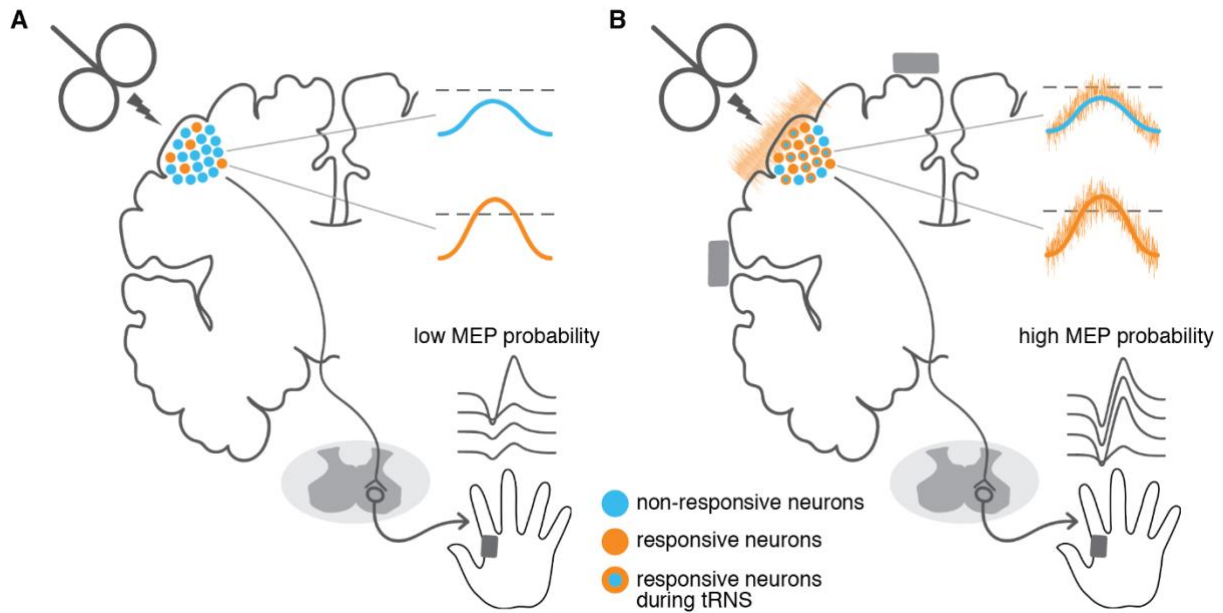


**Figure 3.1** Conceptual representation of how tRNS may enhance the neural signal and influence RMT. **A.** TMS pulse delivered with subthreshold intensity activates small population of neurons (orange circles) eliciting MEPs with a low probability. **B.** When random noise is added to the primary motor cortex with tRNS (orange wave), neurons that did not respond before to TMS (blue circles) can cross the activation threshold (blue circles with orange outline). The enlarged portion of firing neurons results in higher probability of eliciting MEPs, which is reflected in a lower RMT.

### 3.3 Materials and Methods

#### 3.3.1 Participants

Eighty-one healthy volunteers (46 females, 35 males, mean age =  $25.4 \pm 5.1$ ; range, 18-46) took part in this study, which consisted of 4 experiments. A new group of participants was recruited for each experiment. All were right-handed and had no identified contraindications for participation according to established TMS exclusion criteria (Rossi et al., 2009; Wassermann, 1998). All provided written informed consent. Upon study conclusion, they were debriefed and financially compensated for their time and effort. None of the participants reported any major side effects resulting from the stimulation. All research procedures were approved by the Cantonal Ethics Committee Zurich (KEK-ZH-Nr. 2014-0242, KEK-ZH-Nr. 2014-0269 and BASEC Nr. 2018-01078) and were performed in accordance with the Helsinki Declaration of the World Medical Association (2013 WMA Declaration of Helsinki).

#### 3.3.2 General study design

To evaluate the acute influence of tRNS on the excitability of motor cortex we performed a series of four experiments in which we combined high frequency (100-500 Hz) tRNS with single-pulse TMS over left M1. tRNS was applied for only 3 seconds per trial, with jittering of

the TMS pulse between 1.3 and 1.7s after tRNS onset (see **Figure 3.2** for an overview of the different experiments). Short tRNS duration was used based on the previously demonstrated acute behavioral effects of 2-5s tRNS (Groen and Wenderoth, 2016; van der Groen et al., 2019) and reports showing that 4s tDCS results in an excitability change during stimulation without producing after-effects (Nitsche et al., 2003). In all experiments the TMS inter-trial-interval was set to 8 seconds with 20% temporal variability. During the measurement participants sat comfortably at rest and directed their gaze toward a fixation cross. Motor evoked potentials (MEPs) of the right first dorsal interosseous (FDI) muscle were used as a primary physiological read-out. Our main outcome parameter in all experiments was the probability of eliciting MEPs with an amplitude greater than or equal to 0.05 mV (i.e., response probability;  $p(\text{MEP}_{0.05\text{mV}})$ ). All experiments consisted of conditions where tRNS was applied to M1 in random order (see below) and no noise control conditions, with the experimenter holding the TMS coil blinded regarding condition type. Since we used a very brief stimulation time (3 seconds only), fade in/out periods were not possible. Accordingly, some participants were able to distinguish the stimulation conditions (see *Additional Control Analyses: Tactile Sensation*). We accounted for this possible bias via various control analyses and by including one experiment where we introduced an active stimulation control condition (see Experiment 4).

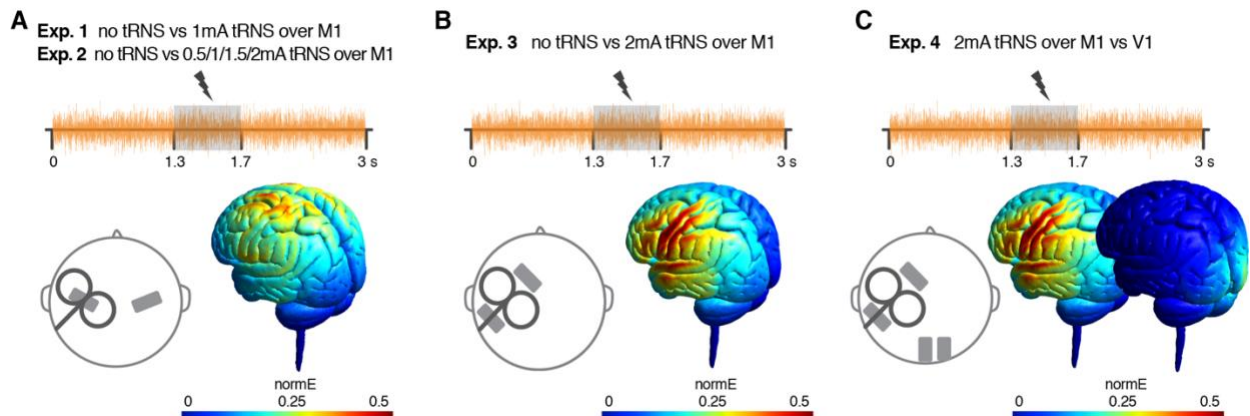


**Figure 3.2** Stimulation protocol, electrode placement (grey rectangles) and electric field modelling for experiments 1-4. tRNS (orange wave) was delivered online for 3 seconds over the M1 with TMS applied in the middle of the noise stimulation window. **A.** In Exp.1 we delivered tRNS at 1mA (vs no tRNS) and probed MEPs with TMS at RMT intensity (jittered 1.3, 1.5 or 1.7 s after tRNS onset), to explore the noise influence on the probability of MEP. In Exp. 2 tRNS was delivered at variable intensity (0.5-2mA tRNS vs no tRNS) with subthreshold TMS (jittered, after 1.5 or 1.7 s) to test the noise dose-response effects. In both experiments, tRNS electrodes were placed over the left and right M1. Electric field modelling shows a 2mA noise intensity condition. **B.** In Exp. 3 RMT<sub>Fit</sub> was measured during the application of tRNS over M1 at 2mA (vs no tRNS) with a TMS threshold estimation approach (i.e., TMS applied in the range  $\text{RMT} \pm 2\%$ , jittered, 1.3 or 1.7 s after tRNS onset). TRNS electrodes were placed 7 cm anterior and posterior to the FDI muscle hotspot (M1). **C.** In Exp. 4 RMT<sub>Fit</sub> was measured during the application of tRNS at 2mA over M1 (vs control stimulation site) with a TMS threshold estimation approach (i.e., TMS applied in the range  $\text{RMT} \pm 2\%$ , jittered, 1.3 or 1.7 s after tRNS onset). tRNS electrodes were placed anterior and posterior to the FDI

muscle hotspot (M1 - main stimulation condition, left) and over the right occipital lobe (the control stimulation site, right).

### 3.3.3 Transcranial Random Noise Stimulation

Random noise (100-500 Hz) was delivered through a battery-driven electrical stimulator (DC-Stimulator PLUS, NeuroConn GmbH, Ilmenau, Germany). Electroconductive gel was applied to the contact side of the rubber electrodes (5 x 7 cm) to reduce skin impedance. Depending on the experiment, the stimulation intensity varied between 0.5 - 2mA amplitude (peak-to-baseline), resulting in maximum current densities ranging from 14.29 - 57.14  $\frac{\mu A}{cm^2}$ , which is below the safety limits for transcranial electrical stimulation (Fertonani et al., 2015). The probability function of the stimulation followed a gaussian distribution with no offset. tRNS power, corresponding to the variance of the electrical noise intensities distribution (Thielscher and Saturnino, 2019), was 0.73 mA<sup>2</sup> in the 2mA condition. The impedance between the electrodes was monitored and kept below 15 k $\Omega$  (on average 8.6  $\pm$  3.9 k $\Omega$  across experiments). tRNS waveforms were created in Matlab (The MathWorks, Inc., Natick, USA), uploaded to Signal (Cambridge Electronic Design, version 2.13) and sent via a CED amplifier (CED Power 1401, Cambridge Electronic Design, Cambridge, UK) to the DC-stimulator which was operated in REMOTE mode. For all experiments we used electric field modelling to ensure optimal electrode placement (**Figure 3.2**). All simulations were run in SimNIBS 2.1 (Thielscher et al., 2015) using the average MNI brain template. The software enables finite-element modelling of electric field distribution of direct current stimulation without taking into account the temporal characteristics. Note, however, that the induced electric field was shown to be independent of the stimulation frequency (Vöröslakos et al., 2018). Since we were mainly interested in the peak of the induced electric field, we run the simulation for the maximum 2mA peak-to-baseline intensity of the stimulation.

tRNS and no noise control conditions were randomized throughout all of the experiments to prevent cumulative effects of tRNS and to minimize the effect of general changes in corticomotor excitability.

### 3.3.4 Transcranial Magnetic Stimulation

Single-pulse monophasic TMS was delivered using a 70mm figure-of-eight coil connected to the Magstim 200 stimulator (Magstim, UK). For all subjects the coil was positioned over the hotspot of the FDI muscle. Depending on the tRNS electrode montage the coil was placed either on top of the electrode (Exp. 1 and 2) or on the scalp in between the electrodes (Exp. 3 and 4; see **Figure 3.2**). The hotspot was defined as the stimulation site where TMS delivery resulted in the most consistent and largest MEPs in the resting muscle. The coil was held

tangential to the surface of the scalp with the handle pointing backward and laterally at 45° away from the nasion-inion mid-sagittal line, resulting in a posterior-anterior direction of current flow in the brain. Such a coil orientation is thought to be optimal for inducing the electric field perpendicular to the central sulcus resulting in the stimulation of M1 neurons (Mills et al., 1992; Rathelot and Strick, 2009). The optimal coil location was marked with a semi-permanent marker on the head and registered using the neuronavigation software (Brainsight® Frameless, Rogue Research Inc., Montreal, QC). The position of the participant's head and TMS coil was constantly monitored in real-time with the Polaris Vicra® Optical Tracking System (Northern Digital Inc., Waterloo, ON, Canada). This ensured that the centre of the coil was kept within 2 mm of the determined hotspot, and that the coil orientation was consistent throughout the experiment. For each participant we determined the resting motor threshold (RMT), defined as the lowest intensity to elicit MEPs with peak-to-peak amplitude greater than or equal to 0.05 mV in the relaxed muscle, in 5 out of 10 consecutive trials (Rossini, Barker, & Berardelli, 1994). Pooling data across all experiments, the mean RMT at baseline corresponded to  $44 \pm 9\%$  of the maximum stimulator output (MSO).

### **3.3.5 Electromyography**

The muscle response was recorded by a surface electromyography (EMG) electrode (Bagnoli™ DE-2.1 EMG Sensors, Delsys, Inc.) placed over the right FDI muscle. Raw signals were amplified (sampling rate, 5 kHz), digitized with a CED micro 1401 AD converter and Signal software V2.13 (both Cambridge Electronic Design, Cambridge, UK), and stored on a personal computer for off-line analysis. Timing of the TMS delivery, remote control of the tRNS stimulator and EMG data recording were synchronized via the CED. Muscular relaxation was constantly monitored through visual feedback of EMG activity and participants were instructed to relax their muscles if necessary.

### **3.3.6 Data processing and analysis**

The EMG data was band-pass filtered (30-800 Hz, notch filter = 50 Hz). Filtering was applied separately for the pre-TMS background EMG (bgEMG) and post-TMS period containing peak-to-peak MEP amplitude in order to avoid "smearing" the MEP into bgEMG data. MEP amplitude was defined as the peak-to-peak amplitude between 15 to 60 ms after the TMS pulse. Next, we excluded trials in which the unwanted background muscle activation could influence the measured MEP amplitude. Trials with root mean square bgEMG above 0.01 mV were removed from further analyses to control for unwanted bgEMG activity (Hess et al., 1986; Devanne et al., 1997). For the remaining trials, the mean and standard deviation of the background EMG was calculated for each participant. Trials with  $\text{bgEMG} > \text{mean} \pm 2.5$  standard deviations were also excluded. Based on these criteria 96.7% of all data were

included for further analysis (96.7% in Exp.1, 97.7% in Exp. 2, 96.2% in Exp. 3 and 97.6% in Exp. 4).

In all experiments our main outcome parameter was the probability of eliciting MEPs with an amplitude greater than or equal to 0.05 mV (for each condition  $\frac{\#MEP \geq 0.05 \text{ mV}}{\# \text{all collected trials}}$ ;  $p(MEP_{0.05mV})$ ). We decided to investigate RMT modulation since it allows us to assess the individual membrane excitability of the corticospinal tract neurons (Kobayashi and Pascual-Leone, 2003; Hallett, 2007; Rossi et al., 2009). RMT serves as one of the most robust TMS measurements (Kobayashi and Pascual-Leone, 2003; Nitsche et al., 2005; Hallett, 2007; Livingston and Ingersoll, 2008; Rossi et al., 2009; Ngomo et al., 2012; Hinder et al., 2014; Schambra et al., 2015; Davila-Pérez et al., 2018; Dissanayaka et al., 2018; Jannati et al., 2019). For all experiments we ran additional control analyses by re-calculating MEP probabilities for other amplitude criteria, i.e., MEP amplitudes larger than or equal to 0.03, 0.04, 0.06 and 0.07 mV to ensure that the observed effects are not purely driven by the definition of the RMT. Additionally, we performed a supplementary analysis to investigate the potential influence of the noise stimulation on MEP amplitude.

### 3.3.7 Statistical analysis

Statistical analyses were performed with repeated measures ANOVAs (rmANOVA) in IBM® SPSS Statistics Version 23.0 (IBM Corp., Armonk, NY, USA) unless otherwise stated. All data were tested for normal distribution using Shapiro-Wilks test of normality. Sphericity was tested using Mauchly's sphericity test. If sphericity was violated, Greenhouse-Geisser correction was applied. The threshold for statistical significance was set at  $\alpha = 0.05$ . All post hoc tests were corrected for multiple comparisons using Bonferroni correction. Effect sizes are reported for each experiment in the form of Partial Eta Squared ( $\eta_p^2$ ; small  $\eta_p^2 = 0.01$ , medium  $\eta_p^2 = 0.06$ , large  $\eta_p^2 = 0.14$  Lakens, 2013) or Cohen's d ( $d_z$ ; small  $d_z = 0.2$ , medium  $d_z = 0.5$ , large  $d_z = 0.8$ ; Lakens, 2013). Variance is reported as standard deviation (SD) in the main text and as standard error (SE) in the figures. Potentially confounding variables (i.e., assessed tactile sensation and bgEMG) were added as covariates whenever applicable (see *Additional Control Analyses* in the results section).

### 3.3.8 Additional information for specific experiments

#### Experiment 1 – Testing effects of 1mA tRNS

In the first experiment, we tested whether tRNS induces an increase in MEP probability when TMS was applied to M1 at RMT intensity. Sixteen right-handed participants (self-report) took part in the experiment (9 females, 7 males, mean age =  $24.7 \pm 5$ , range: 19-35). tRNS

electrodes were placed over (i) the hotspot of the right FDI as determined by single-pulse TMS and (ii) the contralateral, right M1 (**Figure 3.2A**). This bilateral montage was chosen based on modelling results which indicated similar current densities but less current spread for the M1-M1 montage (used here) compared to the M1-supraorbital cortex montage as used in previous studies (Terney et al., 2008; Chaieb et al., 2011). tRNS intensity was set to 1mA peak-to-baseline amplitude and applied in each trial for 3 seconds. TMS pulses were delivered over left M1 at RMT intensity (mean RMT  $49 \pm 13\%$  MSO, range: 36-84%), starting 1.3, 1.5 or 1.7 s after tRNS onset. Testing was split into 4 blocks (60 trials in each block, 240 trials total). We measured MEPs in the FDI muscle either during the 1mA tRNS condition (180 trials total) or the no tRNS condition (control, 60 trials total). We compared MEP probability between the 1mA tRNS vs no tRNS conditions using a paired t-test. Even though we adjusted the TMS intensity to the individuals' RMT prior to the main experiment, closer inspection of the data revealed that RMTs could drift during the experiment (Karabanov et al., 2015) so that some participants were stimulated at sub-threshold TMS intensities (i.e.,  $MEP_{0.05mV}$  probability  $< 0.5$  in the no tRNS condition) while others were stimulated at supra-threshold intensities ( $MEP_{0.05mV}$  probability  $> 0.5$  in the no tRNS condition). Therefore, we evaluated whether tRNS-induced changes in MEP probability were associated with MEP probability in the no tRNS condition using Pearson correlation. The tRNS-induced modulation was calculated as a ratio between  $p(MEP_{0.05mV})$  in the 1mA tRNS condition and  $p(MEP_{0.05mV})$  in the no tRNS condition. Thus, we correlated  $x$  with  $\frac{y}{x}$ , where:

$x = p(MEP_{0.05mV})$  in the no tRNS condition,

$$\frac{y}{x} = \frac{p(MEP_{0.05mV}) \text{ 1mA tRNS}}{p(MEP_{0.05mV}) \text{ no tRNS}}.$$

Given that correlating a fractional increase from  $x$  with  $x$  itself can be problematic as it might lead to spurious correlations (Pearson, 1897; Tu, 2016), we applied a statistical correction method suggested by Tu (2016; Eq. (4-6)). This method compares the above correlation  $r_{x,y/x}$  to the expected "null correlation" ( $r_{null}$ ) which is revealed by

$$r_{null} = -\frac{r_{x,y} - 1}{\sqrt{2(1 - r_{x,y})}}$$

The observed correlation  $r_{x,y/x}$  is then compared to  $r_{null}$  using a z-test of the following form:

$$z = \frac{z_r(r_{x,y/x}) - z_r(r_{null})}{\sqrt{1/(n-3)}}$$

after applying the Fisher's z transform:  $z_r(r) = \frac{1}{2} \ln \left( \frac{1+r}{1-r} \right)$

This allowed us to assess if there is a statistically significant association between  $p(\text{MEP}_{0.05\text{mV}})$  in the no tRNS condition and tRNS-induced modulation.

### Experiment 2 – Testing dose-response effects

The second experiment aimed to determine whether there is an optimal tRNS intensity to modulate MEP probability in M1. Twenty-three right-handed (Edinburgh Handedness Inventory mean laterality quotient [LQ] =  $78.3 \pm 13.8$ ; Oldfield, 1971) participants were recruited. We had to exclude one participant because of technical problems with data acquisition. Twenty-two participants (13 females, 9 males, mean age =  $25.4 \pm 5.4$ , range: 20-46) were included in the subsequent analysis. At the beginning of the session we measured the RMT of each participant (mean RMT =  $43.4 \pm 7.5\%$  MSO, range: 31-54%). Based on the results of experiment 1 and behavioral effects of tRNS (Groen and Wenderoth, 2016; van der Groen et al., 2018) we decided to probe MEP with subthreshold TMS, as the response towards stimuli presented below the threshold are postulated to be particularly susceptible for SR effects (Gingl et al., 1995; Moss et al., 2004). TMS over left M1 was always applied with an intensity slightly below RMT, which was operationally defined as the intensity evoking MEPs with an amplitude of at least 0.05 mV in 3 out of 10 trials ( $p(\text{MEP}_{0.05\text{mV}}) = 0.3$ ; mean subthreshold intensity:  $42 \pm 7.3\%$  MSO, range: 30-53%). The TMS pulse was randomly applied either 1.5 or 1.7 s after tRNS onset to avoid anticipation of the pulse (**Figure 3.2A**). The tRNS electrodes were placed as in experiment 1 (**Figure 3.2A**). We varied tRNS intensity (0.5, 1, 1.5 or 2mA vs no tRNS control condition) to examine whether there is a dose effect on the tRNS induced enhancement of MEP probability. We recorded 10 trials per tRNS condition in randomized order in 3 blocks. Throughout the experiment we monitored MEP probability in the no tRNS control condition and, if required, we adjusted the TMS intensity between blocks to ensure subthreshold level stimulation ( $p(\text{MEP}_{0.05\text{mV}}) = 0.3$ , **Figure 3.9**). This procedure was chosen because it has been shown that state-dependent changes of RMT can occur in absence of overt activity or task involvement and need to be considered in order to keep TMS intensity comparable throughout the experiment (Karabanov et al., 2015). Therefore, we determined MEP probability for the no tRNS condition after each completed block. Since we targeted MEP probability of 0.3, TMS intensity was reduced by 1% MSO when MEP probability was  $\geq 0.5$  or increased when MEP probability was  $\leq 0.1$ . Note that adjusting TMS intensities only between blocks ensured subthreshold TMS throughout the course of the experiment without confounding the comparison between the different tRNS conditions that were sampled equally within each block. 30 MEPs were collected per condition resulting in a total number of 150 TMS pulses. For nineteen participants we collapsed MEPs across the three blocks to estimate the MEP probability for each of the noise conditions. For three participants, post-hoc analysis revealed that they met the criteria for subthreshold TMS during the no tRNS control



condition only in two blocks, i.e., MEP probabilities were estimated from 20 MEPs per condition. MEP probabilities were subjected to a rmANOVA with the within-subject factor *tRNS intensity* (no tRNS, 0.5, 1, 1.5 and 2mA tRNS).

Before starting the main experiment, all experimental tRNS intensities (0.5-2mA) were presented to the participant (for 20 s in a randomized order) and subjectively assessed on a scale from 0 (no sensation) to 10 (strong pain) to make sure that the stimulation did not cause any unpleasant sensations.

### Experiment 3 – Threshold estimation

The third experiment was a conceptual replication of experiment 2, but this time we used a modified electrode montage and tested whether tRNS applied online can influence RMT. The required sample size was estimated based on Experiment 2 ( $\eta_p^2 = 0.18$ ) using a power analysis (G\*Power version 3.1; Faul, Erdfelder, Lang, & Buchner, 2007). It revealed that twenty participants should be included to detect an effect of tRNS on MEP probability with a 2x5 rmANOVA, alpha = 0.05 and 85% power. Twenty-three right-handed (mean LQ =  $88.7 \pm 16.5$ ; Oldfield, 1971) individuals were recruited in experiment 3 to account for potential dropouts, with three removed from further analyses (see below).

RMT was defined at the beginning of the session (mean RMT =  $41.1 \pm 7.4\%$  MSO, range: 28-55%). We then applied TMS intensities centred around the individual RMT level during the main experiment (namely: RMT-2%, RMT-1%, RMT, RMT+1%, RMT+2%). Based on the results of experiment 2, we tested only tRNS intensity of 2mA versus no tRNS. This time we used a modified electrode montage as described by Rawji et al. (2018), whereby electrodes were positioned 7 cm anterior and posterior to the FDI muscle hotspot along the coil axis (45° away from the nasion-inion mid-sagittal line). As described by the authors, in this arrangement current oscillates perpendicular to the central sulcus, which has been hypothesized to be more efficient in modulating corticospinal excitability (Rawji et al., 2018). The electric field modelling showed that this arrangement provides more focal electrical stimulation and induces a slightly higher electric field over M1 (**Figure 3.2B**). Additionally, this montage enables positioning the TMS coil directly on the scalp and avoids delivering TMS pulses through the electrode (see **Figure 3.2**). Different electrode montages can change the directionality of the electric field which has been shown to strongly influence the effect of tDCS (Nitsche et al., 2008). However, noise benefits induced by tRNS should be polarity independent (Pirulli et al., 2016). Here we test whether the increased M1 responsiveness caused by applying tRNS generalize across electrode montages targeting M1. We tested 10 different experimental conditions (no tRNS versus 2mA tRNS x 5 TMS intensities) in total. The experiment consisted of 6 blocks, with 4 trials per condition presented within each block in a randomized order (24 MEPs in each of

the 10 conditions, 240 TMS pulses total). TMS was randomly applied 1.3 or 1.7 s after tRNS onset within each trial (**Figure 3.2B**). We monitored the MEP probability in the control condition (no tRNS with TMS intensity targeted at RMT) and TMS intensity was adjusted between blocks by 1% MSO: it was (i) decreased if the probability of MEPs in the no tRNS condition was  $\geq 0.75$  or (ii) increased if the probability of MEPs was  $\leq 0.25$ , to stay as close as possible to the target RMT level ( $p(\text{MEP}_{0.05\text{mV}}) = 0.5$ ; **Figure 3.9**).

Post-hoc inspection of the data revealed that two participants showed response probabilities consistently above RMT. Thus, they did not fulfil our criteria of probing MEP with TMS intensities centred around the RMT and were excluded from subsequent analyses. Additionally, one outlier was excluded during data analysis due to a tRNS-induced decrease of RMT  $> 2$  SD of the group mean. Data from the final sample of twenty participants (10 females, 10 males, mean age =  $27.5 \pm 6$ , range: 18-42) was entered into a  $2 \times 5$  rANOVA with the within-subject factors *tRNS* (no tRNS versus 2mA tRNS) and *TMS intensity* (RMT-2%, RMT-1%, RMT, RMT+1%, RMT+2%). Additionally, we performed a threshold estimation analysis to determine whether tRNS influenced RMT. To do so, for each participant we calculated the response probability for each of the 5 TMS intensities when either 2mA tRNS or no tRNS was applied. Next, we fitted separate linear models ( $y = ax + b$ , with  $y$  denoting  $p(\text{MEP}_{0.05\text{mV}})$  and  $x$  the stimulation intensity) to each of the datasets and determined  $\text{RMT}_{\text{Fit}} = (0.5 - b)/a$ , i.e., the intensity which would be used to evoke a sufficiently large MEP with a probability of 0.5 (see **Figure 3.3**). Note that this method provides a more accurate estimation of RMT than manually adjusting TMS intensity until  $p(\text{MEP}_{0.05\text{mV}}) = 0.5$  is reached, partly because the model is informed by more data.

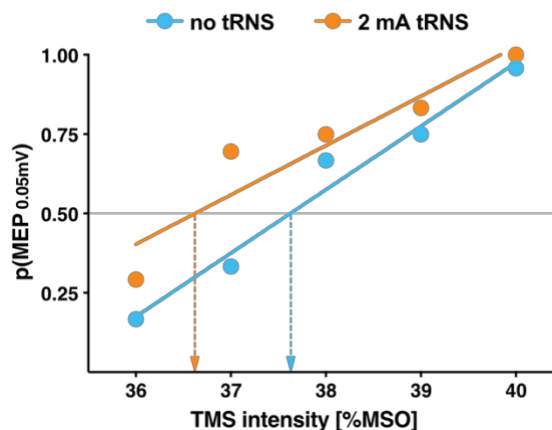


**Figure 3.3.** Representative data of an individual participant to exemplify the threshold estimation procedure. The probability of eliciting a MEP ( $p(\text{MEP}_{0.05\text{mV}})$ ) was determined for five intensities ranging from RMT-2% to RMT+2% (RMT corresponds here to 38% MSO). These values were obtained for the no tRNS control condition (blue symbols) as well as during 2mA tRNS over primary motor cortex (orange symbols). A linear model ( $y = ax + b$ ) was fitted to the data of each condition (represented by the solid lines) and we determined which stimulation intensity would yield  $p(\text{MEP}_{0.05\text{mV}}) = 0.5$  via the following formula  $\text{RMT}_{\text{Fit}} = (0.5 - b)/a$ . The figure symbolizes this procedure

by showing that an intensity of  $RMT_{Fit} = 37.63\%$  was determined for the no tRNS condition (blue arrow), while a slightly smaller  $RMT_{Fit} = 36.62\%$  was determined for the 2mA tRNS condition (orange arrow).

Before the start of the main experiment, participants were familiarized with tRNS and we assessed the detectability of potential sensations. The detection task consisted of 20 trials. Participants received either tRNS (2mA over M1, with and without TMS on half of the trials) or no tRNS (with and without TMS). Their task on each trial was to indicate (after an auditory cue) if they felt something underneath the tRNS electrodes (ignoring TMS pulses) by pressing the appropriate button on a keyboard.

#### Experiment 4 – Threshold estimation with active control condition

The final experiment aimed to replicate the results obtained in experiment 3, but this time we compared tRNS applied over M1 to tRNS applied over right primary visual cortex (V1) to control for unspecific stimulation effects. The sample size estimation was based on the effect size of  $\eta_p^2 = 0.235$  which was obtained by averaging the effect sizes of the tRNS main effect in experiment 2 ( $\eta_p^2 = 0.18$ ) and 3 ( $\eta_p^2 = 0.29$ ) to get a robust estimation across experiments. We further assumed that sphericity might be violated ( $\epsilon = 0.55$  as in Exp. 3) and set alpha = 0.05 and power = 85%. This revealed a sample size of twenty-two participants. Based on this analysis we recruited twenty-nine individuals to account for potential dropouts (see below). Experiment 4 used the same stimulation parameters, electrode montage and general procedures as experiment 3, but this time the no tRNS control condition was replaced with 2mA tRNS over the right occipital lobe. The control site was selected to evoke similar skin sensations as the main experimental condition (i.e., applying 2mA tRNS over M1), but to deliver stimulation that does not interfere with neural processing related to the measured MEPs (see the electrical field modelling, **Figure 3.2C**). The first electrode was placed over theinion and the second electrode was placed to the right (7 cm between the centres of the electrodes, **Figure 3.2C**). tRNS was delivered with a separate battery-driven remote-controlled electrical stimulator (DC-Stimulator PLUS, NeuroConn GmbH, Ilmenau, Germany), with the same high frequency (100-500 Hz) tRNS waveform of 2mA intensity (peak-to-baseline amplitude with a 0mA offset) created in Matlab (The MathWorks, Inc., Natick, USA).

We applied tRNS either over the left M1 or the control stimulation site and probed the muscle response with single-pulse TMS using 5 intensities around threshold level (RMT-2%, RMT-1%, RMT, RMT+1%, RMT+2%). As in experiment 3, the TMS intensity was adjusted between blocks if necessary, based on the data obtained during the control stimulation over right V1 (**Figure 3.9**).

From the original sample of twenty-nine right-handed (mean LQ =  $85 \pm 20.3$ ; Oldfield, 1971) participants, six were excluded for various reasons. One could not complete the session due

to technical problems. Three participants revealed response probabilities consistently above RMT and one substantially below RMT during the experiment. Additionally, one outlier was removed post-hoc because tRNS caused the RMT to decrease by more than 2 SD of the group mean. This resulted in the final sample of twenty-three participants (14 females, 9 males, mean age =  $24.3 \pm 3.9$ , range: 19-34; mean RMT =  $44.1 \pm 7.2\%$  MSO, range: 33-59%).

Similar to the previous experiment, we used the threshold estimation analysis ( $RMT_{Fit}$ ) and a 2x5 rmANOVA with the within-subject factors of *tRNS* (tRNS over M1 vs V1) and *TMS intensity* (RMT-2%, RMT-1%, RMT, RMT+1%, RMT+2%) for the statistical analysis of MEP probability. As in experiment 3, we assessed the detectability of skin sensation due to electrical stimulation via a detection task, which was performed before and after the main experiment. Detection task was similar to experiment 3, but included three stimulation conditions: no tRNS, 2mA tRNS over M1 or 2mA tRNS over right V1.

### 3.4 Results

#### 3.4.1 Exp. 1 – tRNS induced increase in MEP probability for subthreshold TMS

In the first experiment we investigated whether tRNS modulates the probability of eliciting MEPs. We measured MEPs during 1mA tRNS versus no tRNS and calculated the probability of evoking MEPs with an amplitude  $\geq 0.05$  mV ( $p(\text{MEP}_{0.05\text{mV}})$  1mA tRNS and  $p(\text{MEP}_{0.05\text{mV}})$  no tRNS, respectively). We did not observe a significant difference between the overall MEP probability in the noise vs control condition ( $t_{(15)} = 0.31$ ,  $p = 0.77$ , mean difference [MD] =  $0.007 \pm 0.09$ ).

Even though we aimed for stimulating each participant with a TMS intensity corresponding to RMT as determined prior to the main experiment, post-hoc analysis of the no tRNS condition revealed that some participants were stimulated with subthreshold TMS intensities (i.e.,  $p(\text{MEP}_{0.05\text{mV}})$  no tRNS  $< 0.5$ ) while others were stimulated with suprathreshold TMS intensities (i.e.,  $p(\text{MEP}_{0.05\text{mV}})$  no tRNS  $> 0.5$ ). Therefore, we calculated a Pearson correlation to test whether a potential increase in  $p(\text{MEP}_{0.05\text{mV}})$  in the 1mA tRNS condition (i.e., indicating a noise benefit) depended on the MEP probability in the no tRNS condition (**Figure 3.4**). We found a clear negative correlation  $r_{x,y/x} = -0.68$ , which was highly significant when compared to the null model  $r_{\text{null}} = 0.16$  ( $z = -3.56$ ,  $p < 0.001$ , see *Materials and Methods* for details). This finding suggests that tRNS modulates M1's response probability most strongly when TMS stimuli are delivered with an intensity slightly below the individual RMT (i.e.,  $p(\text{MEP}_{0.05\text{mV}})$  no tRNS  $< 0.5$ ), a result that is consistent with van der Groen et al. (2016) who showed that tRNS enhances detection performance for subthreshold stimuli.

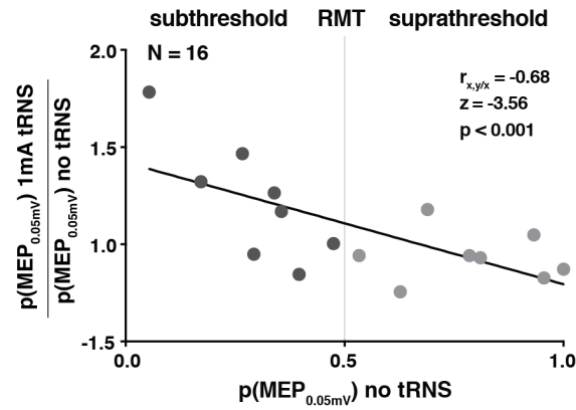


**Figure 3.4** tRNS induced an increase in motor evoked potential (MEP) probability relative to the probability of eliciting MEPs in the no tRNS control condition. The Y axis represents MEP probability in the noise condition normalized to the individual MEP probability in the no tRNS condition, i.e.,  $[p(\text{MEP}_{0.05\text{mV}}) \text{ 1mA tRNS}] / [p(\text{MEP}_{0.05\text{mV}}) \text{ no tRNS}]$ . Participants that were stimulated with subthreshold TMS intensities (i.e.,  $p(\text{MEP}_{0.05\text{mV}}) \text{ no tRNS} < 0.5$ , dark grey symbols on the left) benefited more from 1mA tRNS than participants that were stimulated at suprathreshold TMS intensities (i.e.,  $p(\text{MEP}_{0.05\text{mV}}) \text{ no tRNS} > 0.5$ , light grey symbols on the right). Grey dots indicate single subject data. Statistics for  $r_{x,y/x}$  are reported relative to the null correlation ( $r_{\text{null}}$ ), see methods for details.

### 3.4.2 Exp. 2 - increase in MEP probability for higher tRNS intensity over M1

Next, we aimed to examine if there is an optimal tRNS intensity to enhance the probability of evoking MEPs. Therefore, we applied tRNS over both M1s at intensities ranging from 0.5, 1, 1.5 to 2mA vs no tRNS control condition (**Figure 3.2A**). Based on our previous finding, we ensured that M1 was probed with TMS at sub-RMT intensities. Accordingly,  $p(\text{MEP}_{0.05\text{mV}}) = 0.26 \pm 0.06$  for the no tRNS condition but gradually increased for higher tRNS intensities as indicated by a significant main effect of tRNS intensity ( $F_{(4, 84)} = 4.57$ ,  $p = 0.002$ ,  $\eta_p^2 = 0.18$ , **Figure 3.5**). Post-hoc comparisons revealed that the 2mA stimulation was most effective in boosting MEP probability, which differed significantly from the no tRNS control condition ( $p = 0.04$ ,  $\text{MD} = 0.082 \pm 0.1$ ) and 0.5mA stimulation ( $p = 0.03$ ,  $\text{MD} = 0.079 \pm 0.1$ ). This indicates that the probability of inducing MEPs scales with increasing tRNS intensities.

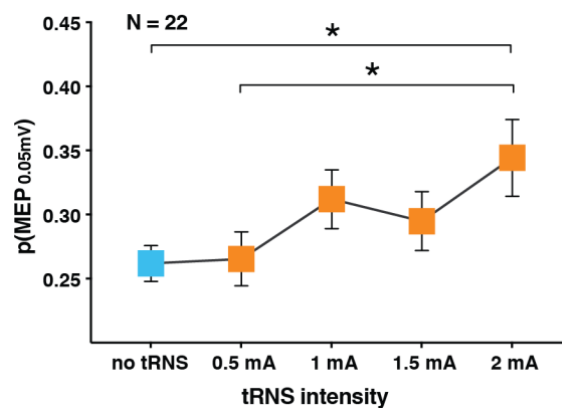


**Figure 3.5** Probability of eliciting MEPs ( $p(\text{MEP}_{0.05\text{mV}})$ ) at different tRNS intensities, revealing a significant increase in the probability of evoking a MEP during 2mA tRNS. Error bars indicate SE. \* indicates  $p < 0.05$ .

### 3.4.3 Exp. 3 - tRNS over M1 induced decrease in RMT

Next, we performed a conceptual replication of the previous experiment and applied 2mA tRNS versus no tRNS (control condition) but changed the electrode placement (**Figure 3.2B**) to probe whether acute noise benefits on responsiveness generalize across different electrode montages targeting M1. Even though specific electrode positions can possibly affect the directionality of the electrical field to target neurons and result in divergent effects regarding polarity and potentially also the effective amount of the induced current, we again observed tRNS-induced enhancement in cortical responsiveness. We found a general increase in MEP probability when 2mA tRNS was applied over M1 (main effect of tRNS,  $F_{(1, 19)} = 7.58$ ,  $p = 0.01$ ,  $\eta_p^2 = 0.29$ , **Figure 3.6A**). The interaction between tRNS and TMS intensity was not significant ( $F_{(4, 76)} = 2$ ,  $p = 0.11$ ). Next, we calculated  $\text{RMT}_{\text{Fit}}$  as an additional outcome parameter. Note that RMT is tightly related to MEP probability since it is defined as the intensity which evokes sufficiently large MEPs with  $p(\text{MEP}_{0.05\text{mV}}) = 0.5$ . We estimated  $\text{RMT}_{\text{Fit}}$  for each condition in each individual and found that  $\text{RMT}_{\text{Fit}}$  was significantly lower when 2mA tRNS versus no tRNS was applied ( $t_{(19)} = 2.3$ ,  $p = 0.03$ ,  $\text{MD} = 0.37 \pm 0.73$ ,  $d_z = 0.51$ ; **Figure 3.6B**). This effect was generally small ( $\leq 2.1\%$  MSO), but relatively consistent across individuals as 14 out of 20 participants exhibited a slight decrease in RMT (**Figure 3.6C**). The results confirm that tRNS influences cortical responsiveness, which was reflected by a lower threshold at rest.

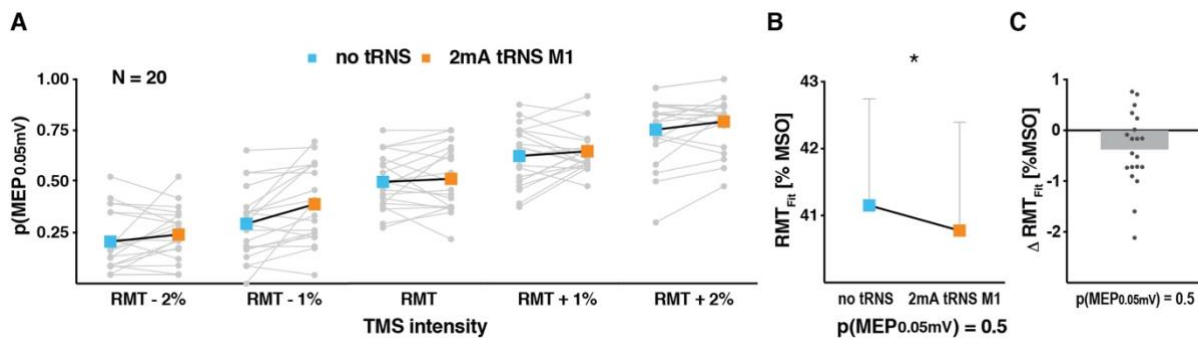


**Figure 3.6** Results of experiment 3: increase in MEP probability [ $p(\text{MEP}_{0.05\text{mV}})$ ] and decrease in the fitted RMT ( $\text{RMT}_{\text{Fit}}$ ) during tRNS over M1 in comparison to the no tRNS control condition. **A** Single-subject data and average change in MEP probability in the no tRNS control and tRNS conditions at different levels of TMS. **B** Decrease in  $\text{RMT}_{\text{Fit}}$  during tRNS over M1 in comparison to the no tRNS control condition.  $\text{RMT}_{\text{Fit}}$  refers to the TMS intensity needed to obtain a 0.5 MEP probability level in both conditions. Individual  $\text{RMT}_{\text{Fit}}$  values were assessed in the threshold estimation analysis based on responses from A. **C** Modulation of  $\text{RMT}_{\text{Fit}}$ : individual differences between  $\text{RMT}_{\text{Fit}}$  in the 2mA tRNS and no tRNS condition (from B). Error bars indicate SE, grey dots indicate single subject data, grey bar indicates group mean, \* indicates  $p < 0.05$ .

### 3.4.4 Exp. 4 - decrease in RMT is specific for M1 stimulation

In experiment 4 we enrolled a new cohort of participants to control for the potentially unspecific effects of tRNS (e.g. arousal or tactile stimulation; Fertoni et al., 2015) by comparing 2mA tRNS over M1 to 2mA tRNS over right V1, with the latter serving as a control area that is unlikely to influence RMT. Our results confirmed the principal finding from the previous experiment, revealing that the probability of evoking MEPs is higher when stimulating M1 compared to the control site (main effect of tRNS,  $F_{(1, 22)} = 13.09$ ,  $p = 0.002$ ,  $\eta_p^2 = 0.37$ , but no significant tRNS x TMS intensity interaction,  $F_{(4, 88)} = 0.42$ ,  $p = 0.8$ ; **Figure 3.7A**). We found that  $RMT_{Fit}$  was lower when 2mA tRNS was delivered over left M1 compared to right V1 ( $t_{(22)} = 4.5$ ,  $p < 0.001$ ,  $MD = 0.67 \pm 0.71$ ,  $d_z = 0.94$ ; **Figure 3.7B**). Even though the absolute decrease was small ( $\leq 2.3\%$  MSO), 20 out of 23 participants exhibited a slight reduction in  $RMT_{Fit}$ . Our results demonstrate that 2mA tRNS modulates the responsiveness of cortical motor circuits, as indicated by the decrease in individual motor threshold, an effect that is specific for the stimulation of M1.

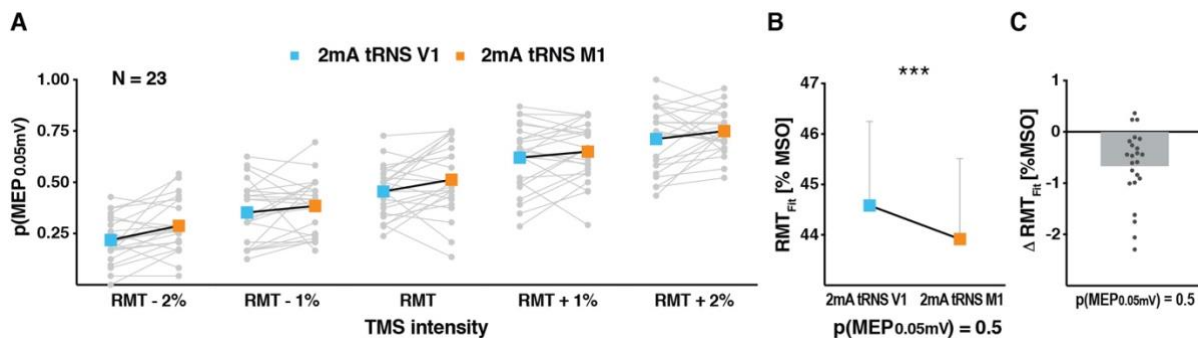


**Figure 3.7** Results of experiment 4: increase in MEP probability [ $p(\text{MEP}_{0.05\text{mV}})$ ] and decrease in the fitted RMT ( $RMT_{Fit}$ ) during noise stimulation over M1 in comparison to the control stimulation condition. **A**. Single-subject data and average changes in MEP probability during noise stimulation over M1 and the control site at different levels of TMS. **B**. Decrease in  $RMT_{Fit}$  during tRNS application over M1 in comparison to the control stimulation site (V1).  $RMT_{Fit}$  refers to the estimated TMS intensity needed to obtain a 0.5 MEP probability level in both conditions. Individual  $RMT_{Fit}$  values were assessed in the threshold estimation analysis based on responses from A. **C**. Modulation of  $RMT_{Fit}$ : individual differences between  $RMT_{Fit}$  during 2mA tRNS over M1 and the control site (from B). Error bars indicate SE, grey dots indicate single subject data, grey bar indicates group mean, \*\*\* indicates  $p < 0.001$ .

### 3.4.5 Additional control analyses

#### MEP Amplitude

We analysed whether tRNS over M1 at 0.5mA up to 2mA versus the control condition (i.e., no tRNS or 2mA tRNS over right V1) influenced average MEP amplitude. Over all experiments this effect did not reach significance (all  $p \geq 0.23$ ), except for experiment 3 where we found a

significant increase in MEP amplitude in the 2mA tRNS vs no tRNS condition (main effect of tRNS,  $F_{(1, 19)} = 10$ ,  $p = 0.005$ ,  $\eta_p^2 = 0.35$ ; **Figure 3.8**).

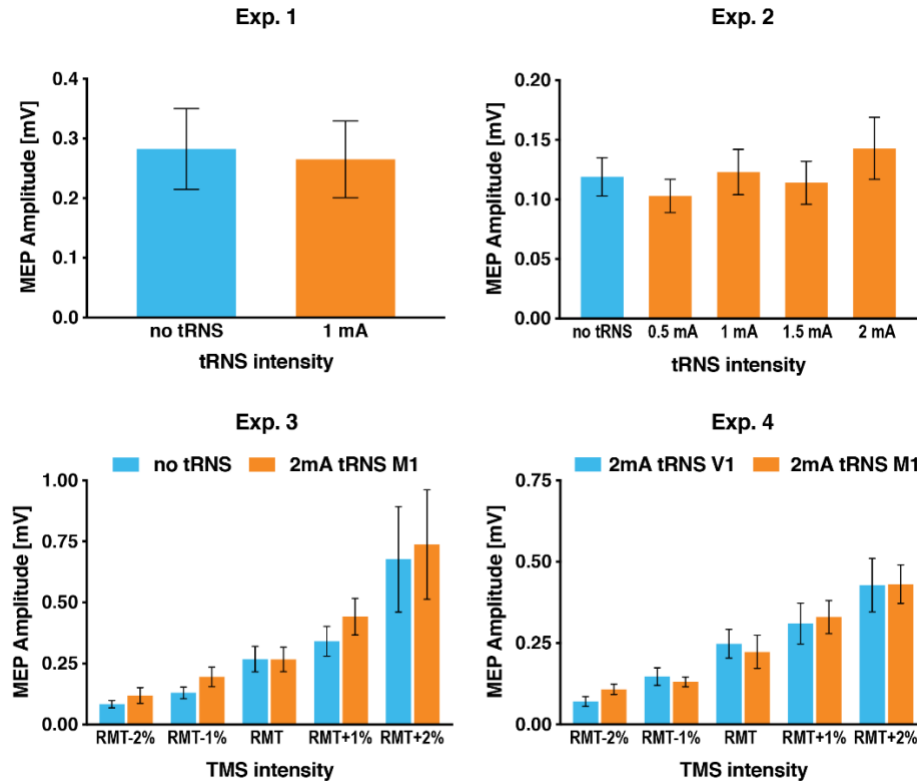


**Figure 3.8** Average MEP amplitude elicited by single-pulse TMS in the experimental and control conditions. tRNS modulated MEP amplitude to a minor extent resulting in significant effects only in Exp. 3, but not in Exp. 1, 2 and 4. Error bars indicate SE.

### Tactile sensation

In experiments 2-4 we performed assessments of the possible tactile effects caused by electrical stimulation. We found that most of our participants could distinguish between no tRNS and tRNS conditions. In experiment 2 we recorded the subjective assessment (on a 0-10 scale) of the tactile sensation evoked by tRNS (mean for 0.5mA =  $0.3 \pm 0.7$ ; 1mA =  $0.6 \pm 1.4$ ; 1.5mA =  $1.2 \pm 1.8$ ; 2mA =  $1.9 \pm 1.9$ ). In experiment 3 we measured the detectability of potential sensations due to 2mA tRNS via a detection task (mean accuracy =  $89\% \pm 18$ ). We extended the detectability estimation in experiment 4, by repeating the task before (Pre) and after (Post) the experiment (mean accuracy Pre =  $85 \pm 17\%$ ; mean accuracy Post =  $77 \pm 18\%$ , resulting in general average accuracy of  $80 \pm 16\%$ ). Additionally, we distinguished hit rates (HRs) for correct detection of M1 (mean =  $0.71 \pm 0.4$ ) versus V1 stimulation (mean =  $0.74 \pm 0.3$ ), showing that sensation detectability did not significantly differ between stimulated areas ( $t_{(22)} = -0.27$ ,  $p = 0.79$ ). In order to test whether our TMS results might have been driven by the tactile sensation, we reanalysed our main outcome parameters (MEP probability and  $RMT_{Fit}$  change) from experiments 2-4 after adding sensation (Exp. 2) or detection accuracy (Exp. 3-



4) as a covariate (all covariates were z-scored due to non-normal distribution). After the covariates were added, all the effects reported in experiments 2-4 remained significant (all  $p \leq 0.04$ ) making it unlikely that tactile sensation was the main driver of our results. Furthermore, strength or accuracy of stimulation-induced sensations did not correlate with the measured effects, i.e., MEP probability and  $RMT_{Fit}$  change in experiments 2 and 3 (Exp.2:  $r = 0.22$ ,  $p = 0.34$ ; Exp.3:  $r = 0.04$ ,  $p = 0.88$ ). Only Exp.4 showed a significant correlation ( $r = 0.5$ ,  $p = 0.02$ ) which, however, could not have driven our results because better detection of tRNS diminished its effect on lowering  $RMT_{Fit}$ . Similarly, there was also no significant correlation between the monitored impedance between the electrodes (which was always  $< 15 \text{ k}\Omega$ ) and the observed effects related to tRNS (all  $r \leq 0.21$ ,  $p \geq 0.4$ ).

### Background EMG

Analysis of bgEMG across the experimental conditions demonstrated that muscle activity was generally low (on average less than  $0.0025 \text{ mV}$  across experiments). Moreover, additional analyses using bgEMG as a covariate in experiments 2-4 revealed that all reported TMS effects remained significant (all  $p \leq 0.03$ ).

### tRNS induced effects do not depend on MEP criteria

The above results used MEP probability as the main outcome measurement. Importantly, the reported effects were not driven by our MEP amplitude criterion (i.e., MEP amplitude  $\geq 0.05 \text{ mV}$ ), as control analyses with slightly different criteria (i.e., MEP cut-off amplitudes of  $0.03\text{-}0.07 \text{ mV}$ ) revealed a similar pattern of results in all our experiments. Namely, irrespective of the adopted MEP criterion, we confirmed tRNS-induced enhancement in MEP probability in Exp. 1 (all  $r \leq -0.56$ ,  $z \leq -2.86$ ,  $p \leq 0.004$ ), we found a gradual increase in MEP probability for higher tRNS intensities in Exp. 2 (all  $F \geq 2.5$ ,  $p \leq 0.05$ ) and observed the decrease in  $RMT_{Fit}$  during  $2\text{mA}$  tRNS over M1 (vs no tRNS in Exp. 3: all  $t \geq 2.3$ ,  $p \leq 0.03$  and vs  $2\text{mA}$  tRNS over V1 in Exp. 4: all  $t \geq 2.3$ ,  $p \leq 0.03$ ).

### TMS intensity adjustments

It is well known that the individual responsiveness to TMS can drift slightly throughout a TMS experiment due to state-dependent changes, which affect measurements close to RMT intensities in particular (Karabanov et al., 2015). As recommended by the Karabanov et al, we adjusted TMS intensities between experimental blocks to ensure subthreshold stimulation (i.e.,  $p(\text{MEP}_{0.05\text{mV}}) \text{ no tRNS} \leq 0.3$  or  $\leq 0.5$ ) throughout Experiments 2, 3 and 4 as shown in **Figure 3.9**. Importantly, once TMS intensity was adjusted, we collected an equal amount of data for each of the tRNS conditions ensuring that the direct comparison of  $2\text{mA}$  tRNS versus the control condition was not confounded by the between-block adjustments.

Next, we analysed whether the intensity adjustments followed a systematic trend by pooling these data across experiments and comparing the first to the last block. We found no systematic changes in TMS intensity ( $t_{(63)} = 1.15$ ,  $p = 0.25$ ,  $MD = 0.22 \pm 1.5\%$ , **Figure 3.9**) making it unlikely that tRNS or other aspects of our experimental procedure caused any longer-lasting effects on M1 responsiveness.

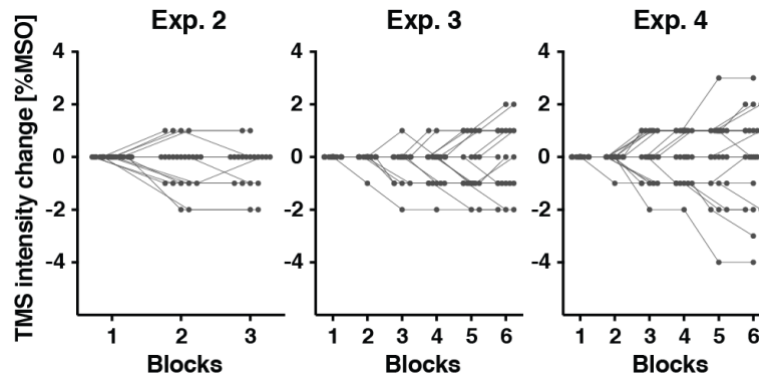


**Figure 3.9** Changes in the adjusted TMS intensity between measurement blocks in experiments 2-4. Grey dots represent TMS intensity change for each individual between the different blocks of experiments 2-4.

### Electric field measurement

Finally, we also tested electric field induced by TMS pulse with and without tRNS. The induced electric field was measured by oscilloscope using a search coil placed under the TMS coil. tRNS was delivered to a conducting phantom medium soaked in saline solution through two electrodes placed on either side of the coils (impedance = 2 k $\Omega$ ). We measured 20 TMS pulses with and without electrical noise stimulation (2mA tRNS) in an alternating manner. We showed that tRNS did not influence the electric field induced by the TMS pulse ( $t_{(19)} = 0.6$ ,  $p = 0.53$ ,  $MD = 0.05 \pm 0.3 \mu\text{V}$ ). This confirmed that all changes in MEP probability originated from the modulation of M1 responsiveness and not stronger magnetic stimulation.

## 3.5 Discussion

This study provides direct evidence that online tRNS over M1 enhances the responsiveness of cortical motor circuits via a shift in response threshold. Across four separate experiments we showed that acute tRNS effects manifested as (i) a higher probability of evoking MEPs when TMS was applied with intensities at or slightly below resting motor threshold (**Figure 3.4**, **Figure 3.5**, **Figure 3.6A**, **Figure 3.7A**), and (ii) lower estimated resting motor thresholds ( $RMT_{\text{Fit}}$  shown in **Figure 3.6B-C**, **Figure 3.7B-C**). Importantly, the observed effects appeared to be specific for tRNS delivery over M1 but not over V1 (**Figure 3.7B**), making it unlikely that our results were driven by any unspecific tRNS effects. Our findings consistently indicate that tRNS enhances the responsiveness of cortical motor circuits by lowering the response

threshold and provide important proof-of-principle evidence of noise benefits at the neural population level in humans.

### **3.5.1 Acute tRNS-induced noise benefits are partly consistent with SR theory**

We consistently observed that adding electrical noise to M1 can acutely increase its responsiveness to TMS. One potential explanation for the observed results is signal enhancement during acute noise delivery to a non-linear system. Such noise benefits are one hallmark feature of SR theory (McDonnell and Abbott, 2009). A second important feature is that noise benefits are a function of noise intensity exhibiting an inverted U-shape dose-response relationship, i.e., too much noise is detrimental. While our neurophysiological study provided proof-of-principle evidence of noise benefits at the neural population level in human cortex, we did not demonstrate the inverted U-shape function for higher tRNS intensities (**Figure 3.5**) and can draw no inference about how much noise would be optimal for increasing the responsiveness of M1.

Previous studies (van der Groen and Wenderoth, 2016; van der Groen et al., 2018; Pavan et al., 2019) demonstrated an inverted U-shape function of tRNS effects using behavioral outcome parameters that are typically acquired in accordance with detection theory. One explanation for the detrimental effect of excessive noise is that it causes the system to respond even if there is no signal to detect and reduces the detection rate by causing too many “*false alarms*”. However, in our experiments a *false alarm* would mean that tRNS alone would occasionally evoke MEPs. Thus, probing the detrimental effect of adding too much noise to the resting motor system via tRNS would require much higher intensities than used here, which would certainly cause strong discomfort in human participants (Fertonani et al., 2015).

Accordingly, we cannot claim that we added the optimal level of noise to M1 based on our data. In fact, the absolute changes in RMT were relatively small (even though statistical effect sizes were medium to large). This can be partly attributed to the fact that we aimed to modulate resting motor threshold, which is one of the most robust and reliable TMS measurements (Ngomo et al., 2012; Dissanayaka et al., 2018). Indeed, RMT has rarely been modulated by other forms of electrical stimulation (Nitsche et al., 2005), including long-lasting effects of tRNS (Terney et al., 2008). However, another explanation for the relatively small absolute effects is that tRNS induced a suboptimal amount of noise.

### **3.5.2 Alternative accounts of the observed acute tRNS-induced noise benefits**

Until now, a change in corticomotor excitability measurements has been demonstrated after prolonged tRNS delivery and has been hypothesized to reflect long-lasting neuroplastic changes (Terney et al., 2008; Chaieb et al., 2011, 2015; Abe et al., 2019; Moret et al., 2019).

However, neuroplastic changes are unlikely to have driven the acute tRNS effects in our study since tRNS conditions were always interleaved with no noise or other control conditions, thereby minimizing the influence of long-term excitability changes. Moreover, there was no systematic change in adjusted TMS intensity for the no tRNS condition over time, making it unlikely that our results were affected by long-term neuroplasticity (**Figure 3.9**).

Another possible mechanism is that repeated subthreshold stimulations with tRNS induced consecutive openings of sodium channels which might lead to temporal summation of small membrane potentials, cause depolarization of the neural membrane due to an increased influx of inward sodium currents and/or prevent the homeostasis of the system (Terney et al., 2008; Fertoni et al., 2011). This may affect excitability of M1 in a similar manner as reported here. Finally, the effects of tRNS may also be attributed to the increased synchronization of neural firing through amplification of subthreshold oscillatory activity, reducing the amount of endogenous noise (Miniussi et al., 2013).

### **3.5.3 Possible neurophysiological substrate mediating tRNS-induced noise benefits**

We showed that a short tRNS bout of less than 3 seconds acutely influences the neurophysiology of human motor cortex. Using threshold estimation analysis as our primary outcome measurement (Vucic et al., 2018), we showed that tRNS specifically affected the response threshold of cortical motor circuits. By contrast, tRNS had no systematic effect on MEP amplitude. It has been argued that motor threshold and MEP amplitude reflect independent neural processes (Paulus et al., 2008; Vucic and Kiernan, 2017; Vucic et al., 2018).

From a neurophysiological point of view, the motor threshold reflects the efficacy of a chain of synapses from cortical interneurons in layer II/III to the muscles (Kobayashi and Pascual-Leone, 2003). Pharmacological studies have implicated voltage-gated sodium channels as a major determinant of motor threshold since blocking sodium channels increases RMT (Tergau et al., 2003; Sommer et al., 2012; Ziemann et al., 2015).

Even though the neurophysiological mechanism of tRNS is not completely understood, previous studies (Onorato et al., 2016) suggested that such enhancing a neurons response via electrical noise occurred by the concurrent activation of voltage-gated sodium channels. A recent study measured sodium currents in somatosensory and auditory pyramidal neurons *in vitro* while stimulating the cells with different levels of electrical random noise (Remedios et al., 2019). The authors showed that some neurons exhibited higher peak amplitudes of sodium currents, elicited by a voltage-clamp-ramp protocol, which correlated with shorter latencies of the neuronal response during brief electrical noise delivery. In other words, in those neurons,

less voltage was needed to evoke the sodium current peak when the optimal level of electrical noise was delivered. Additionally, tRNS might affect neuronal populations by increasing the probability of synchronized firing within neuronal populations (Miniussi et al., 2013). In this regard, it has been estimated that alternating currents at 100 Hz polarize a single neuron by a relatively small amount (Deans et al., 2007). However, networks of many synaptically connected active neurons reveal higher sensitivity to field modulation than single cells, thus, amplifying the stimulation effect (Fröhlich and McCormick, 2010; Reato et al., 2010). Accordingly, even subthreshold stimulation that induces very weak electric fields in cortex can modulate membrane potentials (Gluckman et al., 1996; Francis et al., 2003; Bikson et al., 2006). Based on these findings we propose that tRNS might have reduced  $RMT_{Fit}$  by slightly increasing the responsiveness of voltage-gated sodium channels (Ziemann et al., 2015) in large populations of cortical cells.

Interestingly, unlike short 4s-bouts of tDCS (Nitsche et al., 2003; but see example for large variability of tDCS effects on MEP amplitude Jonker et al., 2021), acute tRNS induced no changes in MEP amplitudes. In line with this finding and the supposed role of sodium channels, previous pharmacological studies have shown that blocking voltage-gated sodium channels had no or only inconsistent effects on MEP amplitudes (Paulus et al., 2008; Vucic et al., 2018).

#### **3.5.4 Increased cortical responsiveness via tRNS is unlikely to result from tactile stimulation**

In our study, many participants felt a slight but noticeable skin sensation (Fertonani et al., 2015). This constitutes a potential confound because participants were not blinded to tRNS conditions and because some effects might be driven by transcutaneous stimulation of peripheral nerves rather than by transcranial stimulation of cortical neurons (Asamoah et al., 2019). We reanalysed all our experiments accounting for tactile sensation and showed that they did not contribute to the observed effects. Most importantly, in the final experiment we utilized an active control condition. Behavioral results revealed that the intensity of the skin sensation was similar but only M1 stimulation lowered the response threshold of cortical motor circuits (**Figure 3.7**). Moreover, a study in non-human primates found significant neuromodulation effects despite blocking or substantially suppressing somatosensory input (Vieira et al., 2020). Thus, we argue that the effects observed in our study are most likely caused by adding electrical noise to M1 rather than by unspecific effects of tRNS.

### 3.6 Conclusions

Our results demonstrate that tRNS changes the responsiveness of M1 circuits. We observed acute modulation of  $RMT_{Fit}$ , which seems to reflect immediate signal enhancement rather than neuroplastic changes. Such increase in responsiveness of a nonlinear system in the presence of noise seems to be consistent with one of the two hallmarks of SR theory showing noise benefits at the neural population level in humans (McDonnell and Abbott, 2009). Our study provides evidence that online tRNS influences the neurophysiology of the human motor cortex and sheds new light on understanding the impact of acute electrical noise stimulation on neural processing at the network level.

#### 4 Transcranial random noise stimulation of the primary visual cortex but not retina modulates visual contrast sensitivity.

**Potok, W.**, Post, A., Bächinger, M., Kiper, D. and Wenderoth, N. (2022). Transcranial random noise stimulation of the primary visual cortex but not retina modulates visual contrast sensitivity. *bioRxiv*.

##### **Contributions:**

Experimental Design, Electric Field Modeling, Data Collection, Data Analysis, and Manuscript Writing.

##### **4.1 Abstract**

Transcranial random noise stimulation (tRNS) has been shown to significantly improve visual perception. Previous studies demonstrated that tRNS delivered over cortical areas acutely enhances visual contrast detection of stimuli when tRNS intensity is optimized for the individual. However, it is currently unknown whether tRNS-induced signal enhancement could be achieved within different neural substrates along the retino-cortical pathway and whether the beneficial effect of optimal tRNS intensities can be reproduced across sessions. In 3 experimental sessions, we tested whether tRNS applied to the primary visual cortex (V1) and/or to the retina improves visual contrast detection. We first measured visual contrast detection threshold (VCT; N=24, 16 females) during tRNS delivery separately over V1 (no tRNS, 0.75, 1, 1.5mA) and over the retina (no tRNS, 0.1, 0.2, 0.3mA), determined the optimal tRNS intensities for each individual (ind-tRNS), and retested the effects of ind-tRNS within the sessions. We further investigated whether we could reproduce the ind-tRNS-induced modulation on a different session (N=19, 14 females). Finally, we tested whether the simultaneous application of ind-tRNS to the retina and V1 causes additive effects. We found that at the group level tRNS of 0.75mA decreases VCT compared to baseline when delivered to the V1. Beneficial effects of ind-tRNS could be replicated when retested within the same experimental session but not when retested in a separate session. Applying tRNS to the retina did not cause a systematic reduction of VCT, irrespective of whether the individually optimized intensity was considered or not. We also did not observe consistent additive effects of V1 and retina stimulation. Our findings demonstrate that V1 seems to be more sensitive than the retina to tRNS-induced modulation of visual contrast processing.

## 4.2 Introduction

Transcranial random noise stimulation (tRNS) has been shown to significantly improve visual perception (see Potok et al., 2022 for review) when applied to visual cortex. Such performance improvements can manifest as both after-effects of visual training combined with tRNS (Fertonani et al., 2011; Pirulli et al., 2013; Contemori et al., 2019; Herpich et al., 2019) or acute effects during tRNS (van der Groen and Wenderoth, 2016; Ghin et al., 2018; van der Groen et al., 2018, 2019; Battaglini et al., 2019, 2020; Pavan et al., 2019). Studies exploring the acute effects of tRNS on visual processing have shown that noise stimulation of the primary visual cortex (V1) improves stimulus contrast detection, particularly, when visual stimuli are presented with near-threshold intensity (van der Groen and Wenderoth, 2016; Battaglini et al., 2019). What remains unknown is whether tRNS-induced signal enhancement, and related contrast sensitivity benefits, could be achieved at the retinal level. Modelling studies suggest noise benefits in retinal ganglion cells (Patel and Kosko, 2005) induced by both visual (Ghosh et al., 2009) and electrical noise (Wu et al., 2017). Moreover, previous research has suggested that the retina is susceptible to 8-20Hz alternating currents (Schutter and Hortensius, 2010; Kar and Krekelberg, 2012) which induce phosphenes even if the stimulation electrodes are placed over distal locations of the scalp (Laakso and Hirata, 2013; see Schutter, 2016 for review). Interestingly, improvement in vision was reported after repetitive transorbital alternating current stimulation at 5-30 Hz over the retina of patients with optic neuropathy or after optic nerve lesions (Gall et al., 2010, 2011; Fedorov et al., 2011; Sabel et al., 2011). They suggested that observed improvements were mediated by increased neuronal synchronization of residual structures and higher cortical areas within the visual system (Sabel et al., 2011). The retina and the optic nerve are interesting targets because they can be reliably reached even with low transcranial electrical stimulation intensities since the eyeball is an excellent conductor (Haberbosch et al., 2019). However, it remains unknown whether noise benefits resulting from tRNS can be induced at different levels of the retino-cortical processing pathway.

In this preregistered study, we investigated the effects of tRNS stimulation of the retina, primary visual cortex (V1) or both on visual detection performance.

## 4.3 Materials and methods

This study was preregistered on the Open Science Framework platform (<https://osf.io/gacjw>). The only difference to preregistered original plan concerns the included sample population. We stated that only participants who completed all three sessions will be included in our study. During data collection not all the individuals who completed the 1<sup>st</sup> and 2<sup>nd</sup> sessions participated in the 3<sup>rd</sup> session, due to the COVID-19 pandemic (Bikson et al., 2020).



Nevertheless, we decided to keep all the data collected in session 1 and 2 (N=24) despite dropouts and lower sample size in session 3 (N=19, see *Participants* below).

#### 4.3.1 Participants

Only individuals with no identified contraindications for participation according to established brain stimulation exclusion criteria (Rossi et al., 2009; Wassermann, 1998) were recruited for the study. All study participants provided written informed consent before the beginning of each experimental session. Upon study conclusion, they were debriefed and financially compensated for their time and effort. All research procedures were approved by the Cantonal Ethics Committee Zurich (BASEC Nr. 2018-01078) and performed in accordance with the Helsinki Declaration of the World Medical Association (2013 WMA Declaration of Helsinki).

The required sample size was estimated using an a priori power analysis (G\*Power version 3.1; Faul, Erdfelder, Lang, & Buchner, 2007). Based on previous finding from van der Groen and Wenderoth (2016) we expected the effect of maximum contrast sensitivity improvement to correspond to Cohen's  $d = 0.77$ . The power analysis revealed that fourteen participants should be included in an experiment to detect an effect of tRNS on contrast detection with repeated measures analysis of variance (rmANOVA, 4 levels of stimulation condition),  $\alpha = 0.05$ , and 90% power, assuming the correlations among repeated measures = 0.5. However, there was no prior data available to investigate whether applying tRNS to two separate neural structures can cause additive effects. Therefore, we include more participants to ensure sufficient power. Moreover, this estimation hinges on the assumption that approx. 80% of the participants exhibit a behavioral response to tRNS (as indicated by Groen and Wenderoth, 2016). Thus, we collected data until N = 20 responders have been included. Responders were defined as individuals who exhibited improved detection in at least one tRNS condition in V1 and retina stimulation. Visual contrast detection is potentially prone to floor effects if the contrast detected at baseline approaches the technical limits of the setup. We decided to exclude participants that were exceptionally good in the visual task and present visual contrast threshold below 0.1 in the no tRNS baseline condition. We also excluded individuals with exceptional contrast threshold modulation (>100%) to avoid accidental results, e.g., due to participants responding without paying attention to the task. From the initially recruited sample of 32 participants, we excluded 8 individuals [5 participants had a contrast threshold below 0.1 in the baseline condition of one of the stimulation sessions (V1 or retina), 1 participant revealed exceptional contrast threshold modulation (>100%), 2 participants did not come back for the second session]. The final sample consisted of 24 healthy volunteers (16 females, 8 males;  $24.4 \pm 4.1$ , age range: 21-38) with normal or corrected-to-normal vision (see **Figure 4.1**). The total number of 24 individuals participated in both 1<sup>st</sup> (tRNS over V1) and 2<sup>nd</sup> (tRNS over the

retina) sessions. Due to the COVID-19 pandemic, we were forced to stop data collection for several months (Bikson et al., 2020). After returning to the lab, 5 participants dropped-out from the initial sample (2 had newly acquired contraindications for brain stimulation and 3 were not able to participate). 19 healthy volunteers (14 females, 5 males;  $25.5 \pm 5.2$ , age range: 21-39) were included into 3<sup>rd</sup> session (tRNS over V1 and retina, see **Figure 4.1**).

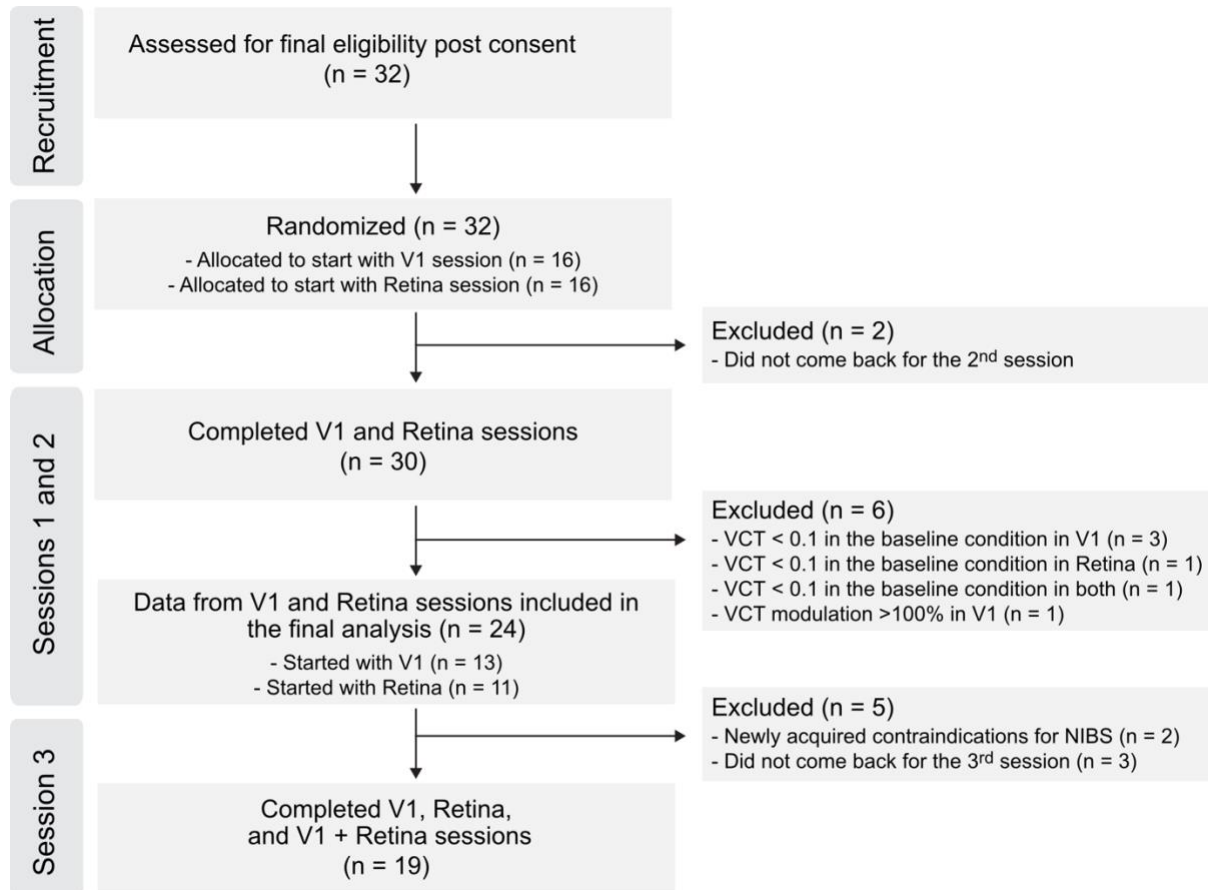


**Figure 4.1** Flow diagram of the data collection progress through the phases of the study.

### 4.3.2 General Study design

To evaluate the influence of tRNS on visual contrast detection, we performed a series of three experimental sessions in which we delivered tRNS over different levels of the visual system, namely: V1, retina, or simultaneously over both V1 and retina (V1+Retina), during visual task performance (see **Figure 4.2A**). In each experiment, tRNS at low, medium and high intensity and a control no tRNS condition were interleaved in a random order (see *tRNS characteristics* below).

The order of experimental sessions for V1 and retina stimulation were counterbalanced across participants (13 participants started with V1 and 11 with retina stimulation). These experimental sessions took place on different days which were on average 2 weeks apart. Due to COVID-19 restrictions, the third session had to be delayed by 5 months on average.

Our main outcome parameter in all experimental sessions was a threshold of visual contrast detection (VCT) that was determined for each of the different tRNS conditions. VCT was independently estimated twice, in two separate blocks within each session (see **Figure 4.2B**). During the first two sessions we determined the individual optimal tRNS intensity (defined as the intensity causing the lowest VCT, i.e., biggest improvement in contrast sensitivity) for each participant in the V1 session (ind-tRNS<sub>V1</sub>) and the retina session (ind-tRNS<sub>retina</sub>). In the third session we then applied ind-tRNS<sub>V1</sub> and ind-tRNS<sub>retina</sub> to investigate the effect on VCT when V1 and retina are stimulated simultaneously.

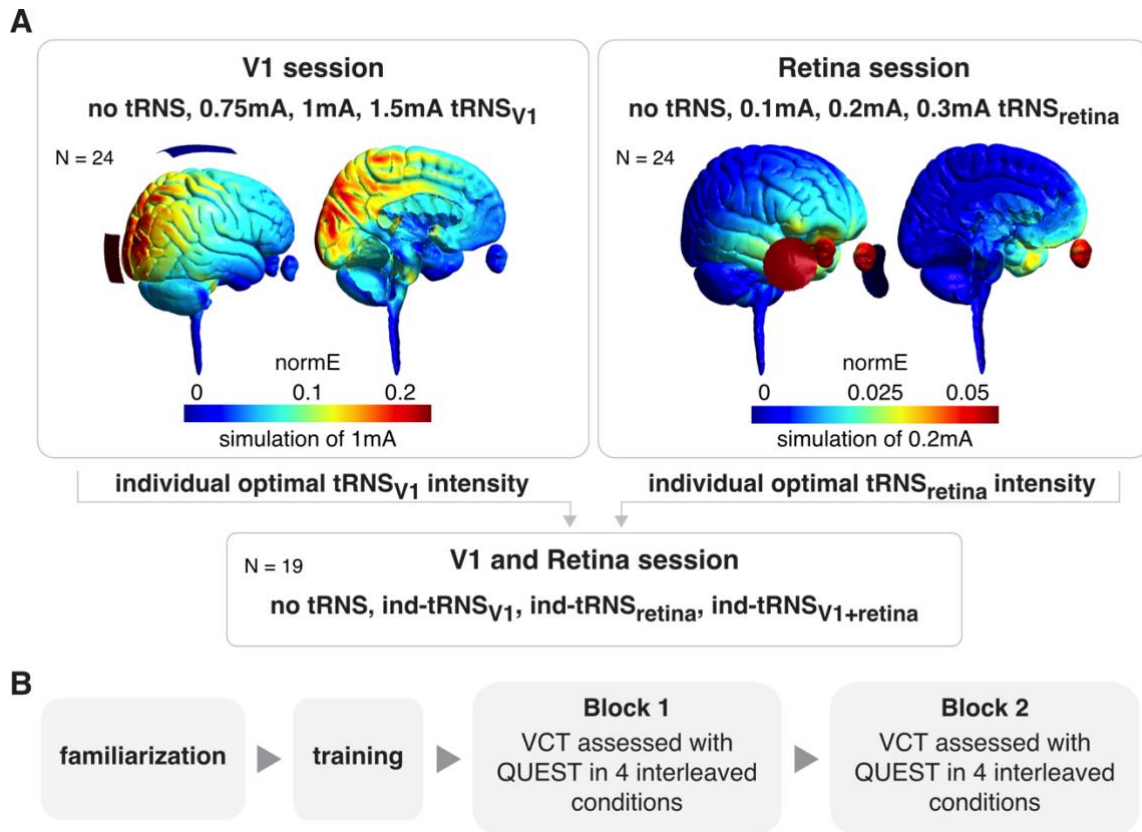


**Figure 4.2** Stimulation protocol in V1, Retina and V1+Retina sessions. **A.** Experimental design and stimulation parameters. First, participants completed experimental sessions in which they received tRNS over V1 or retina (counterbalanced in order) in which the optimal individual tRNS intensity (ind-tRNS) was defined based on the behavioral performance. Next, the ind-tRNS was applied on the third session separately or simultaneously over V1 and retina. **B.** The order of measurements within each session. Each experimental session consisted of a familiarization protocol, followed by task training and two independent visual contrast threshold (VCT) assessments in 4 interleaved tRNS condition (as specified in A).

### 4.3.3 Visual stimuli

All experiments took place in a dark and quiet room, ensuring similar lighting conditions for all participants. Participants sat comfortably, 0.85m away from a screen, with their head supported by a chinrest. Visual stimuli were generated with Matlab (Matlab 2019b, MathWorks, Inc., Natick, USA) using the Psychophysics Toolbox extension (Brainard, 1997;

Pelli, 1997; Kleiner et al., 2007) and displayed on a CRT computer screen (Sony CPD-G420). The screen was characterized by a resolution of 1280 x 1024 pixels, refresh rate of 85Hz, linearized contrast, and a luminance of 35 cd/m<sup>2</sup> (measured with J17 LumaColor Photometer, Tektronix™). The target visual stimuli were presented on a uniform gray background in the form of a Gabor patch – a pattern of sinusoidal luminance grating displayed within a Gaussian envelope (full width at half maximum of 2.8 cm, i.e., 1° 53' visual angle, with 7.3 cm, i.e., 4° 55' presentation radius from the fixation cross). The Gabor patch pattern consisted of 16 cycles with one cycle made up of one white and one black bars (grating spatial frequency of 8 c/deg). Stimuli were oriented at 45° tilted to the left from the vertical axis (see **Figure 4.3B**), since it was shown that tRNS enhances detection of low contrast Gabor patches especially for non-vertical stimuli of high spatial frequency (Battaglini et al., 2020).

#### **4.3.4 Four-alternative forced choice visual detection task**

In all three experiments participants performed a four-alternative forced choice (4-AFC) visual task, designed to assess an individual VCT, separately for each tRNS condition. Such protocol was shown to be more efficient for threshold estimation than commonly used 2-AFC (Jäkel and Wichmann, 2006). In the middle of each 2.04s trial, a Gabor patch was presented for 40ms in one of the 8 locations (see **Figure 4.3A**). To account for potential differences in the extent to which tRNS affects different retinotopic coordinates and to avoid a spatial detection bias, the visual stimuli were presented pseudo-randomly and appeared the same number of times (20) in each of the eight locations on the screen within each experimental block (van der Groen and Wenderoth, 2016). The possible locations were set on noncardinal axes, as the detection performance for stimuli presented in this way is less affected (i.e. less variable) than when stimuli are positioned on the cardinal axes (Cameron et al., 2002; van der Groen and Wenderoth, 2016). The trial was followed by 1s presentation of fixation cross after which the 'response screen' appeared. Participants' task was to decide in which quadrant of the screen the visual stimulus appeared and indicate its location on a keyboard. The timing of the response period was self-paced and not limited. Participants completed a short training (10 trials) at the beginning of each session, with the stimulus presented always at high contrast, in order to ensure that they understand the task (**Figure 4.2B**).

During the main experiment, VCT was estimated using the QUEST staircase maximum likelihood procedure (Watson and Pelli, 1983) implemented in the Psychophysics Toolbox in Matlab (Brainard, 1997; Pelli, 1997; Kleiner et al., 2007). The thresholding procedure starts with a presentation of the visual stimulus displayed with 0.5 contrast intensity (for visual contrast intensity range of minimum 0 and maximum 1). When participants answer correctly QUEST lowers the presented contrast intensity, when participants answer incorrectly QUEST

increases the presented contrast. The estimated stimulus contrast is adjusted to yield 50% detection accuracy (i.e., detection threshold criterion, see **Figure 4.3C**). Note that for 4-AFC task 25% accuracy corresponds to a chance level. The remaining parameters used in the QUEST staircase procedure included: steepness of the psychometric function,  $\beta = 3$ ; fraction of trials on which the observer presses blindly,  $\delta = 0.01$ ; chance level of response,  $\gamma = 0.25$ ; step size of internal table grain = 0.001; intensity difference between the largest and smallest stimulus intensity,  $\text{range} = 1$ . VCT was assessed across 40 trials per tRNS condition (40 trials  $\times$  4 conditions  $\times$  2 blocks; total number of 320 trials per experimental session).

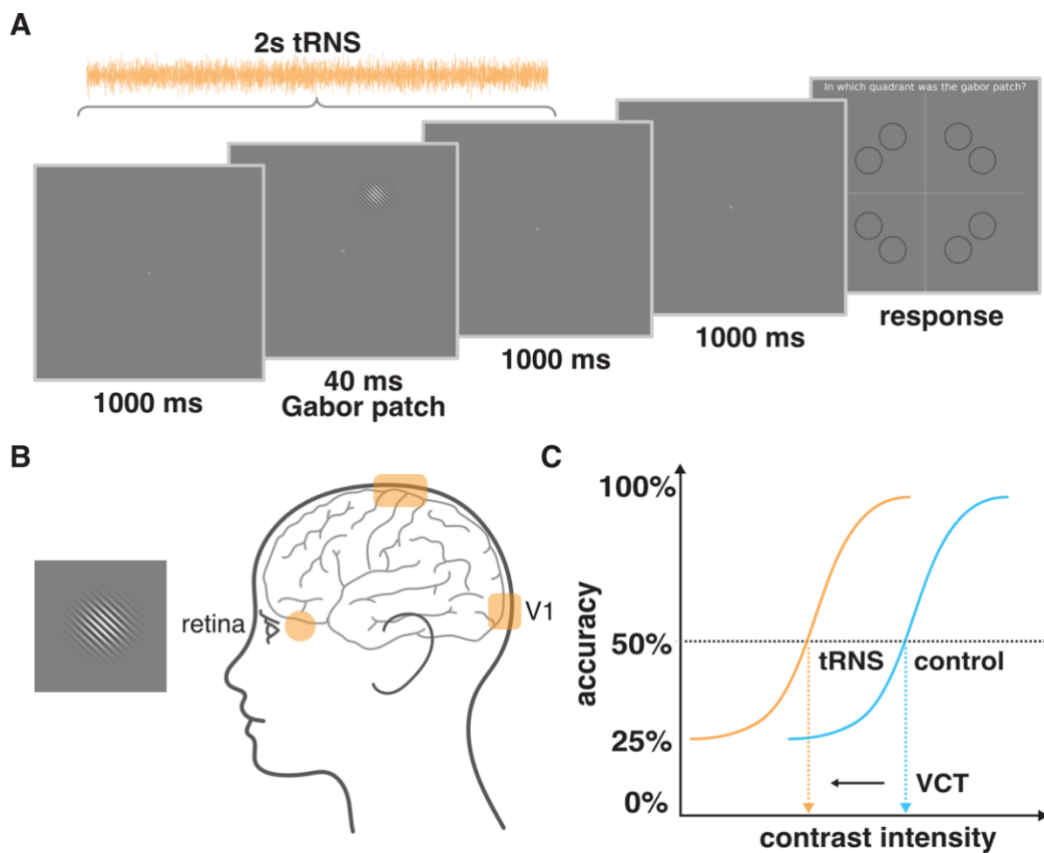


**Figure 4.3** Experimental design. **A**. Example trial of 4-alternative forced choice task measuring visual contrast detection threshold (VCT). tRNS started 20ms after trial onset and was maintained for 2s **B**. Exemplary Gabor patch stimulus to be detected during the visual task and tRNS electrodes montage targeting V1 (rectangle) or retina (round, only the left side is shown but electrodes were mounted bilaterally). **C**. Example of dose-response psychometric curves and the detection of VCT for the 50% detection accuracy level. We hypothesize that the VCT will be lower (indicating better contrast detection performance of the participant) in one of the tRNS conditions (orange) than in the no tRNS control condition (blue).

#### 4.3.5 tRNS characteristics

In tRNS trials, high-frequency tRNS (hf-tRNS, 100-640Hz) with no offset was delivered. The probability function of random current intensities followed a Gaussian distribution with 99% of

the values lying between the peak-to-peak amplitude (Potok et al., 2022b). Stimulation started 20ms after trial onset and was maintained for 2s (**Figure 4.3A**). Subsequently a fixation cross was displayed for 1 s, followed by the self-paced response time. tRNS waveforms were created within Matlab (Matlab 2020a, MathWorks, Inc., Natick, USA) and sent to a battery-driven electrical stimulator (DC-Stimulator PLUS, NeuroConn GmbH, Ilmenau, Germany), operated in REMOTE mode, via a National Instruments I/O device USB-6343 X series, National Instruments, USA). The active tRNS conditions and no tRNS control condition were interleaved and presented in random order. Timing of the stimuli presentation, remote control of the tRNS stimulator, and behavioral data recording were synchronized via Matlab (Matlab 2020a, MathWorks, Inc., Natick, USA) installed on a PC (HP EliteDesk 800 G1) running Windows (Windows 7, Microsoft, USA) as an operating system. The impedance between the electrodes was monitored and kept below 15 k $\Omega$ . For all experiments we used electric field modelling to ensure optimal electrode placement. All simulations were run in SimNIBS 2.1 (Thielscher et al., 2015) using the average MNI brain template (**Figure 4.2A**). The software enables finite-element modelling of electric field distribution of direct current stimulation without taking into account the temporal characteristics. Note, that the software enables simulation of electric field within the brain and eyeball but does not include the optic nerve.

Before the start of the main experiment, participants were familiarized with tRNS and we assessed the detectability of potential sensations (**Figure 4.2B**). The detection task consisted of 20 trials. Participants received either 5s tRNS (0.75, 1, and 1.5mA tRNS in V1 session; 0.1, 0.2, and 0.3mA tRNS in the retina session; or ind-tRNS<sub>V1</sub>, ind-tRNS<sub>retina</sub>, ind-tRNS<sub>V1+retina</sub> in V1+Retina session) or no tRNS. Their task after each trial was to indicate on a keyboard whether they felt something underneath the tRNS electrodes. The determined detection accuracy (hit rates, HR) of the cutaneous sensation induced by tRNS served as a control to estimate whether transcutaneous effects of the stimulation might have confounded the experimental outcomes (Potok et al., 2021).

#### V1 session – testing the effect of no, low, medium or high intensity tRNS targeting V1 on visual detection performance

In the V1 session, we asked whether tRNS over V1 modulates VCT. To target V1 we used an electrode montage that was previously shown to be suitable for V1 stimulation (van der Groen and Wenderoth, 2016; Herpich, 2019). One tRNS 5x5cm rubber electrode was placed over the occipital region (3 cm above inion, Oz in the 10-20 EEG system) and one 5x7cm rubber electrode over the vertex (Cz in the 10-20 EEG system). Electroconductive gel was applied to the contact side of the rubber electrodes (NeuroConn GmbH, Ilmenau, Germany) to reduce skin impedance.

tRNS was delivered with 0.75mA (low), 1mA (medium), and 1.5mA (high) amplitude (peak-to-baseline), resulting in maximum current density of  $60 \frac{\mu A}{cm^2}$ , which is below the safety limits for transcranial electrical stimulation (Fertonani et al., 2015). tRNS power, corresponding to the variance of the electrical noise intensities distribution, was 0.109, 0.194 and  $0.436mA^2$  in the 0.75, 1 and 1.5mA condition, respectively (Potok et al., 2022b).

#### Retina session – testing the effect of no, low, medium or high intensity tRNS targeting the retina on visual detection performance

To further explore the influence of electrical random noise on visual processing we delivered tRNS over the retina during a visual contrast detection task. To stimulate the retina, face skin-friendly self-adhesive round electrodes with a diameter of 32mm (TENS-EMS pads Axion GmbH, Germany) were placed on the sphenoid bones of the right and left temples. Electroconductive gel was applied to the contact side of each electrode to additionally reduce skin impedance.

Dose-response effects were assessed with VCT during tRNS applied with the intensity of 0.1mA (low), 0.2mA (medium), and 0.3mA (high) amplitude (peak-to-baseline), resulting in a maximum current density of  $29.3 \frac{\mu A}{cm^2}$ , which is well below the safety limits for transcranial electrical stimulation (Fertonani et al., 2015). tRNS power, corresponding to the variance of the electrical noise intensities distribution, was 0.002, 0.008 and  $0.017mA^2$  in the 0.1, 0.2 and 0.3mA condition, respectively (Potok et al., 2022b). The selected intensities are commonly used in transorbital alternating current stimulation studies that have reported stimulation induced effects (Gall et al., 2010, 2011; Fedorov et al., 2011; Sabel et al., 2011). Furthermore, we had performed a pilot experiment (N = 30) to assess a flickering threshold when low-frequency tRNS was used (0.1-100Hz). We found that flickering was perceived for a mean intensity of  $0.146 \pm 0.08mA$  (peak-to-baseline) suggesting that the stimulation intensities chosen in this experiment should be suitable for reaching the retina. Our pilot experiment further revealed that flickering was induced by low-frequency tRNS but not by high-frequency tRNS (as used in the main experiments).

#### V1+Retina session – testing the additive effect of simultaneously applying tRNS to V1 and the retina on visual detection performance

The final experimental session aimed to investigate potential additive effects of delivering electrical random noise simultaneously to V1 and the retina on visual contrast sensitivity.

In this session, we combined the electrodes montages over V1 and the retina and applied tRNS with individual optimal intensities as determined in the first two experimental sessions (i.e., ind-tRNS<sub>V1</sub> and ind-tRNS<sub>retina</sub>).

In the V1+Retina session, we compared the VCT in four conditions: (i) tRNS over V1 at its optimal intensity (ind-tRNS<sub>V1</sub>), (ii) tRNS over retina at its optimal intensity (ind-tRNS<sub>retina</sub>), (iii) simultaneous tRNS over V1 and the retina at their respective optimal intensities (ind-tRNS<sub>V1+retina</sub>), and (iv) no tRNS. All conditions were interleaved and presented in a randomized order.

#### 4.3.6 Statistical Analysis

All the statistical analyses were preregistered and did not deviate from the original plan. Statistical analyses were performed in IBM SPSS Statistics version 26.0 (IBM Corp.). All data was tested for normal distribution using the Shapiro-Wilks test. Variance is reported as SD in the main text and as SE in the figures.

First, we tested whether baseline VCT in the no tRNS condition differed across the three experimental sessions using a Bayesian rmANOVA with the factor *time* (blocks 1-2 in sessions 1-3, i.e., six consecutive time points) using the Bayes factor testing for evaluation the absence versus presence of an effect.

For all rmANOVA models, sphericity was assessed with Mauchly's sphericity test. The threshold for statistical significance was set at  $\alpha = 0.05$ . Bonferroni correction for multiple comparisons was applied where appropriate (i.e., post hoc tests). Partial eta-squared (small  $\eta_p^2 = 0.01$ , medium  $\eta_p^2 = 0.06$ , large  $\eta_p^2 = 0.14$ ; Lakens, 2013) values are reported as a measure of effect-sizes.

VCT data collected in the V1 session (tRNS<sub>V1</sub>) was analyzed with a rmANOVA with the factor *tRNS* (no, 0.75, 1, and 1.5mA tRNS) and the factor *block* (1<sup>st</sup>, 2<sup>nd</sup>). For each individual and each block, we determined the maximal behavioral improvement, i.e., lowest VCT measured when tRNS was applied, and the associated "optimal" tRNS intensity (ind-tRNS<sub>V1</sub>). The maximal behavioral improvements in the 1<sup>st</sup> and the 2<sup>nd</sup> block were compared using a t-test (2-tailed) for dependent measurements. We further tested whether ind-tRNS<sub>V1</sub> of the 1<sup>st</sup> and 2<sup>nd</sup> block were correlated using Spearman's rank correlation coefficient (because of categorical characteristics of ind-tRNS<sub>V1</sub> variable). Importantly, we determined ind-tRNS<sub>V1</sub> in the 1<sup>st</sup> block, and then used the VCT data of the separate 2<sup>nd</sup> block to test whether the associated VCT is lower compared to the no tRNS condition using t-tests for dependent measures. Since we had the directional hypothesis that VCT is lower for the optimal tRNS intensity compared to no tRNS this test was 1-tailed. Determining ind-tRNS<sub>V1</sub> and testing its effect on VCT in two separate datasets is important to not overestimate the effect of tRNS on visual detection behavior.



VCT data collected in the Retina session ( $tRNS_{retina}$ ) was analyzed with a rmANOVA with the factor of *tRNS* (no, 0.1, 0.2, and 0.3mA tRNS) and the factor *block* (1<sup>st</sup>, 2<sup>nd</sup>). Again, for each individual and each block, we determined the maximal behavioral improvement and the associated ind-tRNS<sub>retina</sub>. We compared results obtained in the first and second block using the same statistical tests as for the V1 session. The maximal behavioral improvements were compared using a t-test (2-tailed) for dependent measurements. Correlation of ind-tRNS<sub>retina</sub> of the 1<sup>st</sup> and 2<sup>nd</sup> block was tested using Spearman's rank correlation coefficient. We examined whether the ind-tRNS<sub>retina</sub> determined based on the best behavioral performance in 1<sup>st</sup> block, caused VCT to be lower compared to the no tRNS condition when retested on the independent dataset (2<sup>nd</sup> block) using t-tests (1-tailed) for dependent measures.

VCT data collected in the V1+Retina session ( $tRNS_{V1+retina}$ ) was analyzed with a rmANOVA with the factor *tRNS site* (ind-tRNS<sub>V1</sub>, ind-tRNS<sub>retina</sub>, ind-tRNS<sub>V1+retina</sub>, and no tRNS) and the factor *block* (1<sup>st</sup>, 2<sup>nd</sup>). Moreover, we compared behavioral improvement for ind-tRNS<sub>V1</sub> and ind-tRNS<sub>retina</sub> between sessions ( $tRNS_{V1}$  and  $tRNS_{V1+retina}$ ,  $tRNS_{retina}$  and  $tRNS_{V1+retina}$ , respectively) using a Pearson correlation coefficient.

As a control analysis we repeated the main analyses of VCT (rmANOVA were we observed tRNS-induced significant difference) with adding cutaneous sensation as covariate (see *tRNS characteristics*).

#### 4.4 Results

We first tested whether VCT measured during the no tRNS condition differed between the experimental sessions or blocks (i.e., six consecutive time points, see **Figure 4.4**). Bayesian rmANOVA with the factor *time* (1-6) revealed that the baseline VCT measured in the no tRNS condition did not differ over time ( $BF_{10} = 0.06$ , i.e., strong evidence for the  $H_0$ ) indicating that detection performance was rather stable across sessions.

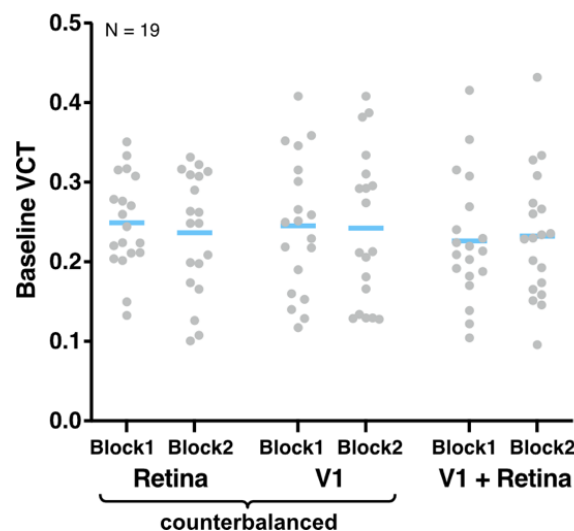


**Figure 4.4** Baseline VCT measured in the no tRNS condition in both blocks in V1, Retina and V1+Retina sessions. Blue lines indicate mean, gray dots indicate single subject data.

#### 4.4.1 tRNS over V1 modulates visual contrast threshold

In the V1 session, we investigated whether tRNS modulates the visual contrast detection when applied to V1. We measured VCT during tRNS<sub>V1</sub> at intensities of 0.75, 1, to 1.5mA versus no tRNS control condition. We found a general decrease in VCT when tRNS was applied (*tRNS* main effect:  $F_{(3, 69)} = 4.54$ ,  $p = 0.006$ ,  $\eta_p^2 = 0.165$ ) indicating that adding noise to V1 improved contrast sensitivity (**Figure 4.5A**). Post hoc comparisons revealed that the 0.75mA stimulation was most effective in boosting contrast processing, which differed significantly from the no tRNS control condition ( $p = 0.045$ , MD =  $-8.69 \pm 15.99\%$ ). As we observed that most of our participants could detect tRNS<sub>V1</sub> conditions (mean HR =  $76.04 \pm 22.16\%$  measured via cutaneous sensations detection task) we reanalyzed our main outcome parameter by adding sensation detection HR as a covariate. The main effect of *tRNS* remained highly significant ( $F_{(3, 66)} = 4.17$ ,  $p = 0.009$ ,  $\eta_p^2 = 0.159$ ), making it unlikely that cutaneous sensation was the main driver of our results. Neither the main effect of *block* ( $F_{(1, 23)} = 0.18$ ,  $p = 0.678$ ) nor *tRNS\*block* interaction ( $F_{(3, 69)} = 0.82$ ,  $p = 0.488$ ) reached significance.

When comparing tRNS-induced effects between the 1<sup>st</sup> and 2<sup>nd</sup> block we found that the maximal behavioral improvement (i.e. the maximal tRNS<sub>V1</sub>-induced lowering of the VCT relative to the no tRNS condition) differed only insignificantly between the 1<sup>st</sup> (MD =  $-17.98 \pm 19.6\%$ ) and the 2<sup>nd</sup> block (MD =  $-16.63 \pm 15.11\%$ ,  $t_{(23)} = -0.304$ ,  $p = 0.764$ ). However, participants' optimal ind-tRNS<sub>V1</sub> of block 1 and 2 (i.e., the tRNS intensity causing the largest VCT reduction in each block) were not correlated ( $\rho = 0.225$ ,  $p = 0.290$ ).

Finally, we determined ind-tRNS<sub>V1</sub> in the 1<sup>st</sup> block (**Figure 4.5B**) and tested whether it caused a decrease in VCT compared to the no tRNS condition using the data of block 2. Indeed, VCT decreased in 15 out of 24 individuals (MD =  $-4.45 \pm 17.9\%$ ) and this effect reached statistical significance ( $t_{(23)} = 1.72$ ,  $p = 0.049$ , **Figure 4.5C**). Note that the optimal ind-tRNS<sub>V1</sub> intensity and the associated VCT effect were determined on independent data sets to avoid circularity.

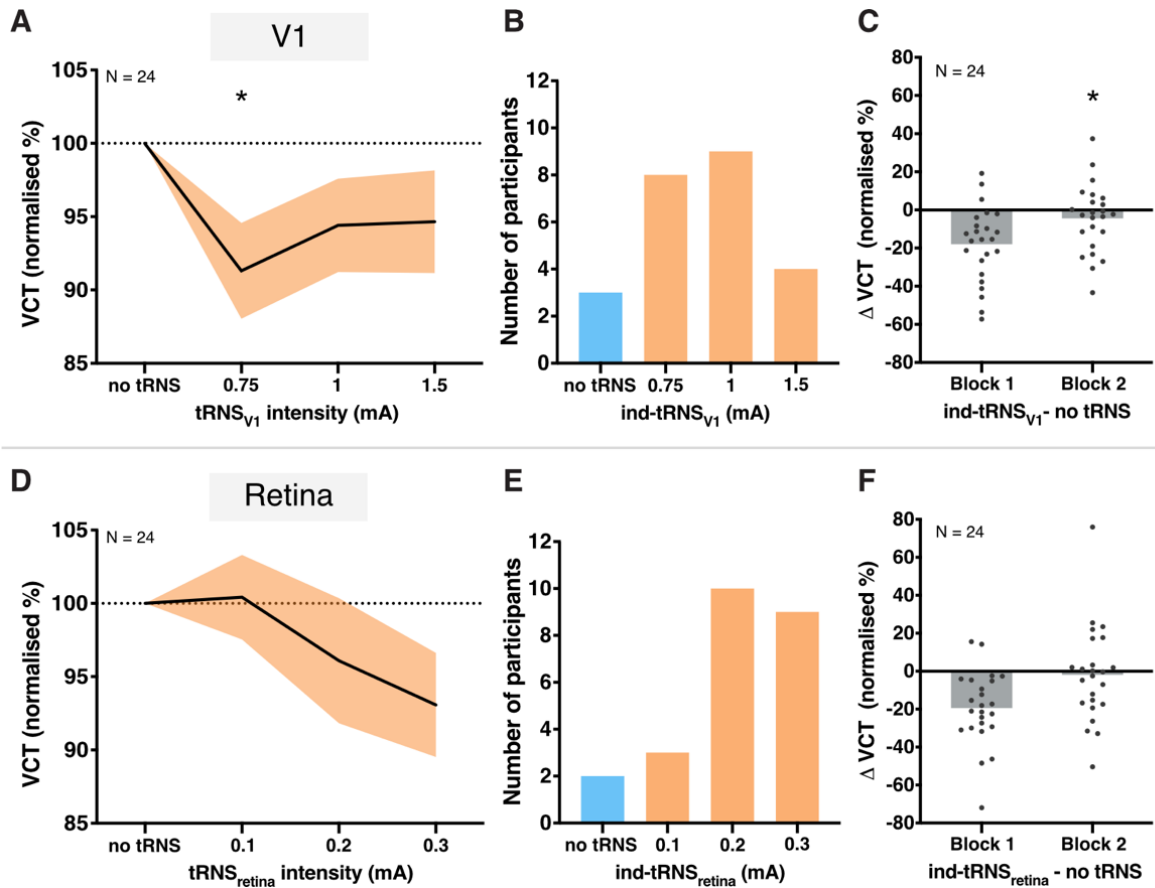


**Figure 4.5** Results of V1 and Retina sessions. **A.** Effect of tRNS<sub>V1</sub> on VCT on a group level measured across 1<sup>st</sup> and 2<sup>nd</sup> block in V1 session. Decrease in VCT reflects improvement of visual contrast sensitivity. All data mean  $\pm$  SE. **B.** Individually defined optimal tRNS<sub>V1</sub> based on behavioral performance during the 1<sup>st</sup> block. **C.** Detection improvement effects of individualized tRNS<sub>V1</sub>. **D.** Effect of tRNS<sub>retina</sub> on VCT on a group level measured across 1<sup>st</sup> and 2<sup>nd</sup> block in Retina session. All data mean  $\pm$  SE. **E.** Individually defined optimal tRNS<sub>retina</sub> based on behavioral performance during the 1<sup>st</sup> block. **F.** Detection modulation during individualized tRNS<sub>retina</sub>. Gray dots indicate single subject data, gray bars indicate group mean; \* $p < 0.05$ .

#### 4.4.2 tRNS over the retina does not modulate visual contrast threshold consistently

In the Retina session, we explored the effects of tRNS applied over the retina on visual contrast detection. VCT was measured during tRNS<sub>retina</sub> at intensities of 0.1, 0.2, to 0.3mA versus no tRNS control condition. Even though, on the group level, we observed decrease in VCT with increasing tRNS<sub>retina</sub> intensity (MD =  $-6.93 \pm 17.39\%$  on average in the 1<sup>st</sup> and 2<sup>nd</sup> block for 0.3mA) the effect was not significant ( $F_{(3, 69)} = 1.69$ ,  $p = 0.177$ , **Figure 4.5D**). There was also no main effect of *block* ( $F_{(1, 23)} = 0.04$ ,  $p = 0.840$ ) or *tRNS\*block* interaction ( $F_{(3, 69)} = 0.55$ ,  $p = 0.652$ ). The maximal behavioral improvements, defined as the maximal tRNS<sub>retina</sub>-induced lowering of the VCT were not significantly different between the 1<sup>st</sup> (MD =  $-19.44 \pm 19.43\%$ ) and the 2<sup>nd</sup> (MD =  $-11.96 \pm 22.79\%$ ) block ( $t_{(23)} = -1.197$ ,  $p = 0.243$ ). Similar to the ind-tRNS<sub>V1</sub>, the optimal ind-tRNS<sub>retina</sub> intensity defined in the 1<sup>st</sup> and 2<sup>nd</sup> block were not significantly correlated among participants ( $\rho = 0.321$ ,  $p = 0.126$ ). The ind-tRNS<sub>retina</sub>

determined in the 1<sup>st</sup> block (**Figure 4.5E**) did not significantly lower the VCT compared to the no tRNS condition when retested on the independent VCT dataset of block 2 ( $t_{(23)} = 1.05$ ,  $p = 0.15$ , VCT decrease in 13 out of 24 individuals,  $MD = -1.89 \pm 25.29\%$ ).

#### 4.4.3 No effects of simultaneous tRNS of V1 and retina on visual contrast threshold

The aim of V1+Retina session was to explore whether the effects of ind-tRNS<sub>V1</sub> and ind-tRNS<sub>retina</sub> determined in sessions 1 and 2 would have additive effects when combined during simultaneous V1 and retina stimulation (**Figure 4.6A**). Against our hypothesis, we did not observe a consistent decrease in VCT on the group level, neither when considering *tRNS site* ( $F_{(3, 54)} = 0.54$ ,  $p = 0.660$ ), *block* ( $F_{(1, 18)} = 2.73$ ,  $p = 0.116$ ) nor *tRNS site\*block* interaction ( $F_{(3, 54)} = 0.31$ ,  $p = 0.822$ ). Although the simultaneous stimulation with ind-tRNS<sub>V1+retina</sub> led to a decrease in VCT in the 1<sup>st</sup> block ( $MD = -4.12 \pm 25.64\%$ ), this difference was not significant ( $t_{(18)} = 0.83$ ,  $p = 0.21$ , **Figure 4.6B**).

In the 3<sup>rd</sup> session we also retested the effects of individually optimized tRNS intensities defined in V1 and Retina sessions. The effect of ind-tRNS<sub>V1</sub> found in V1 session was not reproduced between sessions when VCT was measured during ind-tRNS<sub>V1</sub> in session 3 ( $t_{(18)} = -0.18$ ,  $p = 0.43$ , VCT decrease in 9 out of 19 individuals,  $MD = 2.24 \pm 23.63\%$ , and  $t_{(18)} = -1.37$ ,  $p = 0.09$ , VCT decrease in 6 out of 19 individuals,  $MD = 4.1 \pm 14.28\%$ , in the 1<sup>st</sup> and 2<sup>nd</sup> block respectively, **Figure 4.6B**). There was also no association between behavioral improvements measured during ind-tRNS<sub>V1</sub> in the 1<sup>st</sup> blocks of V1 and V1+Retina sessions ( $r = 0.12$ ,  $p = 0.961$ ,  $N=19$ ), indicating that once-optimized tRNS intensity does not lead to consistent effects between sessions. Similarly to Retina session, participants' ind-tRNS<sub>retina</sub> did not lower the VCT compared to the no tRNS condition when retested on the VCT data in session 3 ( $t_{(18)} = 0.12$ ,  $p = 0.45$ , VCT decrease in 11 out of 19 individuals,  $MD = 1.02\% \pm 24.57\%$ , and  $t_{(18)} = -0.17$ ,  $p = 0.44$ , VCT decrease in 9 out of 19 individuals,  $MD = 2.91 \pm 26.51\%$ , in the 1<sup>st</sup> and 2<sup>nd</sup> block respectively, **Figure 4.6B**). There was also no association between behavioral improvements measured during ind-tRNS<sub>retina</sub> in the 1<sup>st</sup> blocks of Retina and V1+Retina sessions ( $r = -0.252$ ,  $p = 0.297$ ,  $N=19$ ).

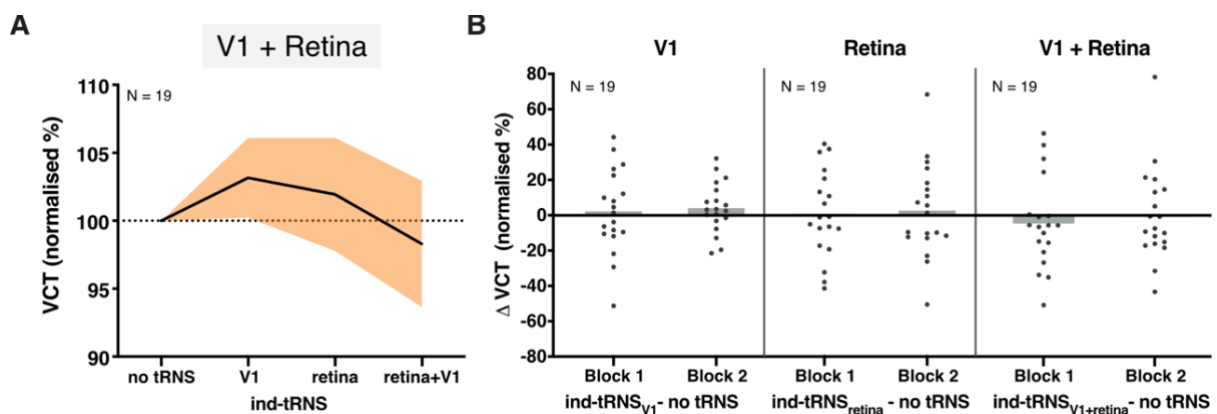


**Figure 4.6** Results of V1+Retina session. **A.** Effect of individualized tRNS<sub>V1</sub>, tRNS<sub>retina</sub>, and tRNS<sub>V1+retina</sub> on VCT on a group level measured across blocks 1 and 2 in V1+Retina session. All data mean  $\pm$  SE. **B.** The detection modulation during participants' optimal ind-tRNS<sub>V1</sub>, ind-tRNS<sub>retina</sub>, and simultaneous ind-tRNS<sub>V1+retina</sub> in blocks 1 and 2 of V1+Retina session. Gray dots indicate single subject data, gray bar indicates group mean.

## 4.5 Discussion

The present study investigated the effects of tRNS on visual contrast sensitivity, when applied to different neuronal substrates along the retino-cortical pathway. We measured VCT during tRNS<sub>V1</sub> and tRNS<sub>retina</sub> and tRNS<sub>V1+retina</sub> across 3 experimental sessions. We found consistent tRNS-induced enhancement of visual contrast detection during V1 stimulation (**Figure 4.5A-C**) but not retina stimulation (**Figure 4.5D-F**). We also did not observe any additive effects on contrast detection when noise stimulation was simultaneously applied to V1 and retina (**Figure 4.6A-B**). The online modulation effects of individually optimized tRNS<sub>V1</sub> intensities were replicated within session (i.e., across two separate blocks) (**Figure 4.5C**), but not between experimental sessions (**Figure 4.6B**). Our findings likely reflect acute effects on contrast processing rather than after-effects, as stimulation was only applied for short intervals (2 s) and always interleaved with control (no tRNS) conditions.

### 4.5.1 tRNS improves visual sensitivity in V1

Our findings confirm previous evidence that the detection of visual stimuli is enhanced when tRNS is added centrally to V1 at optimal intensity (**Figure 4.5A**; van der Groen and Wenderoth, 2016) even though a different outcome measurement was used (i.e., VCT instead of detection accuracy of subthreshold stimuli). As such, it constitutes to a conceptual replication of the earlier study. The modulation observed here was characterized by large effect size ( $\eta_p^2 = 0.165$ , **Figure 4.5A**), stronger than the intermediate effect size (Cohen's  $d = 0.77$ ) found by van der Groen and Wenderoth (2016). Thus, the threshold tracking procedure (Watson and Pelli, 1983; Brainard, 1997; Pelli, 1997; Kleiner et al., 2007) used in our experiments seems to provide a sensitive and reliable estimate of behavioral effects of tRNS<sub>V1</sub>. Moreover, the 4-AFC task protocol used in our study was shown to be more efficient for threshold estimation than commonly used 2-AFC (Jäkel and Wichmann, 2006).

It has been argued previously that tRNS benefits visual detection via the stochastic resonance (SR) mechanism, i.e. the detection probability of weak, subthreshold signals in nonlinear systems can be enhanced if optimally adjusted random noise is added (Moss et al., 2004; McDonnell and Abbott, 2009). One important feature indicative of the SR phenomenon is that noise benefits are a function of noise intensity and exhibit an inverted U-shape relationship, i.e. while the optimal level of noise benefits performance, excessive noise is detrimental (van der Groen and Wenderoth, 2016; van der Groen et al., 2018; Pavan et al., 2019). In the V1

session, we could show that task performance accuracy changed according to an inverted-U-shaped function with increasing tRNS<sub>V1</sub> intensities (ranging from 0 to 1.5mA, **Figure 4.5A**) which is consistent with a SR mechanism. Visual detection enhancement was reflected in lower VCT and this improvement was most likely driven by effective stimulation of V1 rather than unspecific tRNS effects such as cutaneous stimulation and associated effects on arousal, as confirmed in the additional analysis using cutaneous sensation detection during tRNS as a covariate.

Based on the behavioral task performance, we determined which tRNS<sub>V1</sub> intensity was optimal on the individual level (i.e., ind-tRNS<sub>V1</sub> causing the lowest VCT for each participant, **Figure 4.5B**). The optimal noise intensities varied across individuals, similar to effects previously shown for noise added both to the stimulus (Collins et al., 1996b; Martínez et al., 2007) or centrally to V1 (van der Groen and Wenderoth, 2016). Even though the ind-tRNS<sub>V1</sub> intensities defined separately in 1<sup>st</sup> and 2<sup>nd</sup> blocks of V1 session were not correlated, we demonstrated that the ind-tRNS<sub>V1</sub> (from 1<sup>st</sup> block) results in consistent online enhancement effects when retested on the independent data set (VCT in 2<sup>nd</sup> block) within the experimental session (**Figure 4.5C**). This indicates that an individually optimized tRNS<sub>V1</sub> intensity can be considered stable and effective when applied across multiple blocks of a measurement. Notably, the effect of ind-tRNS<sub>V1</sub> was not replicable on different session (see *Intersession variability in the effects of individualized tRNS protocol on contrast sensitivity* below).

Our study contributes to the evidence for SR as a mechanism underlying online visual processing modulation when tRNS is applied to neural networks in human cortex (van der Groen and Wenderoth, 2016; van der Groen et al., 2018, 2019; Battaglini et al., 2019, 2020; Pavan et al., 2019).

#### **4.5.2 Inconsistencies in the effects of noise on retinal processing of contrast**

The present study did not demonstrate systematic noise benefits at the level of the retina. Thus, suggesting that previously reported SR effects on contrast detection might derive mainly from cortical rather than retinal processing. It also shows that SR effects might differ based on the specific characteristic of the stimulated neural tissue.

In our study, we targeted the retina bilaterally with tRNS, to investigate its effects on contrast sensitivity. Although increases in tRNS<sub>retina</sub> intensity resulted in decreases in VCT, reflecting relative task performance improvements (**Figure 4.5D**), the effects did not reach statistical significance. Similar to tRNS<sub>V1</sub>, the effects of tRNS<sub>retina</sub> were variable across study participants. However, even individually determined optimal intensities of tRNS<sub>retina</sub> did not result in consistent visual processing improvements when retested in separate blocks, both within or between sessions (**Figure 4.5F**).

Why did tRNS improve contrast detection when applied to V1 but not when applied to retina? In contrast to V1, the retina is characterized by much larger temporal frequency bandwidth toward which it is responsive. One study measured cat ganglion cell responsivity towards temporal frequencies ranging from 0.1 to 100Hz (Frishman et al., 1987). Further studies have shown a similar range of temporal frequency bandwidth in monkey retina (Benardete and Kaplan, 1999) and even higher cut-off frequencies in response to electrical stimulation in rabbit retina (Cai et al., 2011). Moreover, a fMRI study in humans showed a much higher temporal frequency bandwidth cut-off in human Lateral Geniculate Nucleus (LGN – recipient of retinal ganglion cells' signals) compared to human V1 (Bayram et al., 2016), where the strongest effects are observed for narrow bandwidth of around 4-8Hz (Fawcett et al., 2004). Taken together, stimulus processing at the level of the retina seems to cover a much wider range of temporal frequencies than in V1 and to be more variable. Thus, it is possible that the range of tRNS frequencies used in our experiments, i.e., 100-640 Hz might have been too close to the intrinsic signaling frequencies in the retinal circuitry and in ganglion cells to induce the typical SR effect. V1 neurons, by contrast, respond to frequencies which are one to two magnitudes lower than the tRNS frequencies, and therefore, larger noise benefits could be observed.

Alternatively, the weak effects of tRNS<sub>retina</sub> might simply be due to filtering properties of retinal neurons. A recent study utilized amplitude modulated tACS (AM-tACS) applied to the retina to investigate the efficacy of different carrier frequencies to induce phosphenes. AM-tACS waveforms comprised of different carrier (50Hz, 200Hz, 1000Hz) and modulation frequencies (8Hz, 16Hz, 28Hz). They found that from the conditions using different carrier frequencies only the lowest one was able to induce phosphenes (Thiele et al., 2021). Thus, suggesting the low-pass nature of retinal neurons which greatly reduces the stimulation effectiveness of evoking suprathreshold response (Deans et al., 2007; Thiele et al., 2021). The researchers point out, however, that their findings do not rule out potential sub-threshold modulations of neural activity during AM-tACS with high carrier frequencies.

In the Retina session we observed gradual decrease of VCT with increasing tRNS<sub>retina</sub> intensity on the group level (**Figure 4.5D**). Even though this effect was not significant, we cannot exclude that VCT would decrease further when higher tRNS<sub>retina</sub> intensities were used. We have based our stimulation intensities on studies utilizing repetitive transorbital alternating current stimulation with similar intensities (Gall et al., 2010, 2011; Fedorov et al., 2011) and demonstrated improved vision in patients with damaged optic nerve (see also Sabel et al., 2020). However, it is possible that the induced current is more strongly attenuated in our study (which used much higher stimulation frequencies) due to the filter properties of retinal neurons. Moreover, in these studies the alternating current was delivered using set of four electrodes positioned above and below participants' eyes. Such electrodes placement results in different

direction of the current and related orientation of the induced electric field than bilateral placement used in this study (**Figure 4.2A**). Thus, electrodes montage used here might have been suboptimal for retinal ganglion cell stimulation (Dmochowski et al., 2012; Lee et al., 2021).

In summary, we found no evidence that tRNS affects contrast detection at the retinal level. This is interesting from a methodological perspective since it rules out that applying tRNS over V1 elicits confounding effects in the retina, as previously discussed for tACS experiments (Schutter and Hortensius, 2010; Schutter, 2016).

#### **4.5.3 Intersession variability in the effects of individualized tRNS protocol on contrast sensitivity**

The influence of individually optimized tRNS on VCT, defined separately for both V1 and the retina in experimental sessions 1 and 2, were retested in session 3. The effects of neither ind-tRNS<sub>V1</sub>, nor ind-tRNS<sub>retina</sub> were replicated (**Figure 4.6A-B**). This indicates that optimal tRNS intensity for maximum task performance improvement needs to be individually re-adjusted on each experimental session. These results confirm the well-known variability in the effectiveness of non-invasive brain stimulation (Polanía et al., 2018) and the necessity of carefully designing optimal protocols (Bergmann et al., 2016; Bergmann and Hartwigsen, 2020). The differences in effectiveness of preselected tRNS intensities could result from intrinsic factors such as the participants' arousal levels or attentional states. Additionally, even though we made sure that our procedure was well standardized, there might have been slight differences in the precise electrodes montage or amount of electroconductive gel, potentially resulting in variability of the electric field induced by tRNS of selected intensity across sessions (Polanía et al., 2018). It is also worth noting that the substantial delay between V1/Retina sessions, and V1+Retina session (5 months on average) because of the COVID-19 pandemic (Bikson et al., 2020) could have also influenced this variability. As the modulation of VCT with ind-tRNS<sub>V1</sub> or ind-tRNS<sub>retina</sub> was not replicated in session 3, we also did not observe consistent beneficial additive effects of ind-tRNS delivered simultaneously to V1 and the retina (**Figure 4.6A-B**).

## **4.6 Conclusions**

Our study confirms previous findings that tRNS might enhance visual signal processing of cortical networks via the SR mechanism (van der Groen and Wenderoth, 2016; Potok et al., 2021). When probing the effects of tRNS on contrast sensitivity along the retino-cortical pathway, we demonstrated that V1 seems to be more sensitive than the retina to tRNS-induced modulation of visual processing. Moreover, we found that the individual optimal tRNS



intensity applied to V1 to enhance contract detection appears to vary across sessions. The appropriate adjustment of optimal tRNS intensity is therefore important to consider when designing tRNS protocols for perceptual enhancement.

## 5 Contrast detection is enhanced by non-stochastic, high-frequency transcranial alternating current stimulation

**Potok, W.**, van der Groen, O., Sivachelvam, S., Bächinger, M., Kish, L.B. and Wenderoth, N. (2022). Contrast detection is enhanced by non-stochastic, high-frequency transcranial alternating current stimulation. *In preparation*.

### **Contributions:**

Experimental Design, Electric Field Modeling, Data Collection, Data Analysis, and Manuscript Writing (except from sections 5.2.1 and 5.2.2 written by L.B. Kish, expert in physics and technical applications of stochastic fluctuations in physical, biological and technological systems).

### **5.1 Abstract**

Stochastic Resonance (SR) describes a phenomenon where presence of noise in a nonlinear system has beneficial effects on signal detection. Neural elements of the human nervous system exhibit such nonlinear system properties and the SR phenomenon has been repeatedly demonstrated for visual detection tasks, recently also by adding noise directly to cortical areas via transcranial random noise stimulation (tRNS). However, theoretical considerations predict that also non-stochastic signals can cause resonance effects. Here we tested this prediction empirically and investigated whether non-random, high-frequency transcranial alternating current stimulation (hf-tACS) applied to visual cortex could induce resonance-like effects and enhance visual detection task performance. We showed in 28 participants that applying 80 Hz triangular-waves or sine-waves with hf-tACS reduced visual contrast detection threshold for optimal intensities. These effects differed only insignificantly from using tRNS for reducing detection threshold. Our findings suggest that a resonance-like mechanism can also emerge when non-stochastic electrical waveforms are applied via tACS.

### **5.2 Introduction**

#### **5.2.1 On stochastic resonance**

Stochastic resonance (SR) was discovered in the context of the hysteresis features of climate (ice age) (Benzi et al., 1981) and since then it has been generalized and studied in many systems resulting in a vast body of literature. Here, without the possibility of completeness, we survey a few basic features that are directly relevant for our paper.

SR is a phenomenon where the transfer of a periodic or aperiodic signal in a nonlinear system is optimized by an additive -typically Gaussian- noise at the input and there is an optimal strength of noise for this purpose (Dykman and McClintock, 1999). Note that originally when SR was studied in binary systems, it represented a frequency resonance matching the period times of the periodic signal and the mean residence time in the potential wells of the binary system. Later, in more advanced threshold based, or monostable SR systems the "resonance" means an optimal mean-square amplitude value of the noise, i.e., amplitude resonance.

In the initial phase of SR research, the nonlinear systems were bistable (e.g. Benzi et al., 1981). At a later stage it was discovered that monostable systems (including neurons) also offer SR (Stocks et al., 1993). Moreover, it was realized that the memory/hysteresis effects of the bistable systems actually cause a phase delay that negatively impacts on the quality of the transferred signal (Kiss, 1996). Due to this fact, the best stochastic resonators are the memory-free Threshold Elements (TE), such as the Level Crossing Detector (LCD) (Gingl et al., 1995) and the Comparator (Stocks, 2000). The LCD device (the simplest model of a neuron) produces a short, uniform spike whenever its input voltage amplitude is crossing a given threshold level in a chosen, typically positive direction. On the other hand, the Comparator has a steady binary output where the actual value is dictated by the situation of the input voltage amplitude compared to a given threshold level: for example, in the sub-threshold case the output is "high" while in the supra-threshold case, it is "low".

At the output of a stochastic resonator, the signal strength (SS), the signal-to-noise-ratio (SNR), the information entropy and the Shannon information channel capacity show maxima versus the intensity of the additive input noise. However, these maxima are typically located at different noise intensities. An exception is the SNR vs information entropy which are interrelated by a monotonic function; thus they have the same location of their maxima, see the arguments relevant for neural spike trains (DeWeese and Bialek, 1995). On the other hand, the information channel capacity of SR in an LCD and in neural spike trains has the bandwidth as an extra variable controlled by the input (the higher the input noise the higher the bandwidth); thus the different location of its maximum is at higher input noise than for the maximum of the SNR (Kish et al., 2001).

It is important to note that, in the linear response limit, that is, when the input signal is much smaller than the input (Gaussian) noise, the SNR at the output is always less than at the input, see the mathematical proof in (Dykman et al., 1995). As a consequence, the information content at the output is always less than at the input. On the contrary, in the nonlinear response limit, the SNR at the output can be enhanced by several orders of magnitude compared to its input value provided the signal has a small duty cycle, such as neural spikes do (Kiss, 1996; Loerincz et al., 1996). Yet, due to the unavoidable noise at the output, the information in the

output signal (plus output noise) is obviously always less than in the *original* input signal *without the added noise*.

Therefore, if a proper additive, high-frequency, periodic, time function (carrier wave) could be used in a stochastic resonator instead of the additive noise at the input, the fidelity and the information content of the input signal could be preserved while it is passing through the nonlinear device, as we will show below. However, even in this case there is an optimal (range) for the mean-square amplitude of additive wave thus we call this deterministic phenomenon "non-stochastic resonance".

### 5.2.2 Non-stochastic resonance with triangle (or sawtooth) waves

Earlier, in a public debate about the future of SR, one of us proposed a noise-free method to improve signal transmission through threshold devices (Kish, 2007). Here we summarize those arguments.

**Figure 5.1** shows an example of stochastic resonator hardware with triangle wave, as carrier wave, instead of noise. The same argumentation works for sawtooth wave, too. Note: the original threshold-based stochastic resonators (Gingl et al., 1995; Kiss, 1996) contain the same hardware elements where Gaussian random noise is used instead of the triangle wave. Due to the binary nature of the visual detection experiments described in this paper our focus is on sub-threshold binary signals with some additional comments about the case of analog signals.

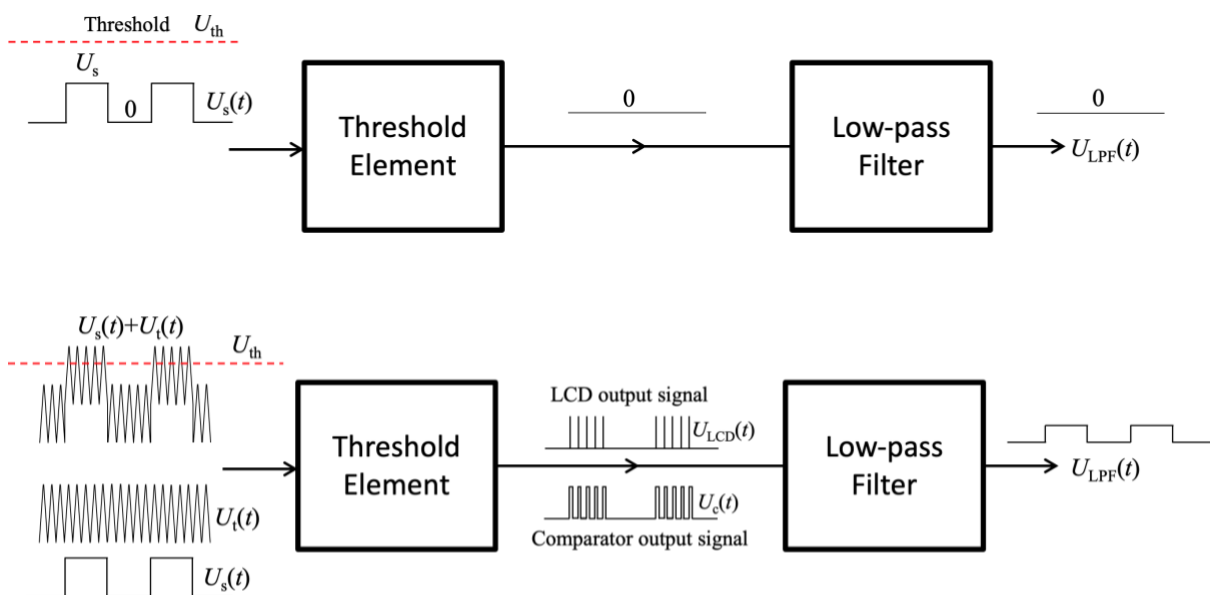


**Figure 5.1** Deterministic transfer of sub-threshold binary signal through simple threshold-based stochastic resonators with a Threshold Element (TE: either a Level Crossing Detector (LCD) or a Comparator) and an additive triangle wave at the input. Note: the classical threshold-based stochastic resonators contain the same hardware

elements except the triangle wave that is substituted by a Gaussian random noise. Upper part: the sub-threshold binary signal is unable to trigger the TE thus the output signal is steadily zero. Lower part: an additive, triangle wave (carrier signal) assists the signal to reach the threshold thus it carries the binary signal over the TE. The Low-pass filter takes a short time average in order to smooth out the high-frequency components. For high-fidelity transfer, to avoid problems caused by delays / phase shifts, the frequency of the carrier wave must be much greater than that of the binary signal. In the old stochastic resonance schemes, the carrier signal was a noise that caused a non-deterministic component (noise) a finite signal-to-noise ratio (SNR) at the output. The new system is purely deterministic, and its SNR is infinite. Moreover, if the signal is "analog" (continuum amplitude values), the triangle wave with comparator as TE guarantees a linear transfer of the signal provided the threshold level is between the minimum and the maximum of the sum of the signal and the carrier signal.

The TE is either an LCD or a Comparator. Suppose that the stable output of the LCD is zero and it produces a short uniform positive spike with height  $U_{LCD}$  and duration  $t$  whenever the input level crosses the Threshold in upward direction. The Comparator's output stays at a fixed positive value whenever the input level is greater than the threshold and stays at a lower (zero or negative) otherwise. Suppose when the input level is greater than the Threshold,  $U_{th}$ , the Comparator output voltage  $U_c = U_H$  and otherwise it is 0. The Low-pass Filter creates a short-time moving-average in order to smooth out the high-frequency components (frequency components due to switching) and it keeps only the low-frequency part with the input signal component. The parameters, such as the frequency  $f_s$  of the signal, the frequency  $f_t$  of the triangle wave and the cut-off frequency  $f_c$  of the Low-pass Filter satisfy

$$f_s \ll f_c \ll f_t < \frac{1}{t} \quad (1)$$

in order to transfer the signal with the highest possible fidelity.

The upper part of **Figure 5.1** shows the situation without carrier wave: the sub-threshold binary signal is unable to trigger the TE thus the output signal is steadily zero. The lower part of **Figure 5.1** shows the situations where an additive, triangle wave assists the signal to reach the threshold thus it carries the binary signal over the TE resulting in a nonzero output signal.

i) The case of Level Crossing Detector

If a constant input signal plus triangle wave can cross the threshold, the LCD produces a periodic spike sequence with the frequency of the triangle wave. In this situation, the time average of this sequence is  $f_t t U_{LCD}$  therefore, for the binary input signal, the output of the LPF will be binary with amplitude values:

$$U_{LPF}(t) = f_t t U_{LCD} \quad \text{or} \quad 0 \quad (2)$$

Thus, the binary input signal is restored at the output of the LPF without any stochasticity (noise) in it. The only deviation from the input signal is a potentially different amplitude (non-zero amplification) and some softening of the edges due to the LPF depending on how well Relation 1 is satisfied.

In conclusion, with an LCD as TE, regarding the amplitude resonance versus the carrier wave amplitude  $U_t$ , there are three different input amplitude ranges:

- (a)  $U_s + U_t < U_{th}$  then there is no output signal
- (b)  $U_{th} < U_s + U_t$ ,  $U_s < U_{th}$ ,  $U_t < U_{th}$  then the binary signal is restored at the output
- (c)  $U_{th} < U_t$  then the output is steadily at the high level  $U_{LPF}(t) = f_t t U_{LCD}$

Therefore, the binary signal can propagate to the output only in the (b) situation when it does that without any noise (the SNR is infinite).

#### ii) The case of Comparator

Note, this system is very different from "Stocks's suprathreshold SR" (Stocks, 2000), where a large number of independent comparators with independent noises are used with a common signal and an adder to reach a finite SNR. For the sake of simplicity, but without limiting the generality of the argumentation, suppose that the binary signal,  $U_s(t)$ , values are 0 and  $U_s$ , where  $U_s \leq U_{th}$ , and the maximum amplitude of the triangle signal,  $U_t(t)$  is  $U_t$  and its minimum value is 0. In conclusion:

$$\text{when } U_s(t) + U_t(t) > U_{th}, U_c = U_H \text{ otherwise } U_c = 0 \quad (3)$$

To evaluate the average output voltage of the comparator the first question is the fraction of time that the input spends over the threshold, see **Figure 5.2**.

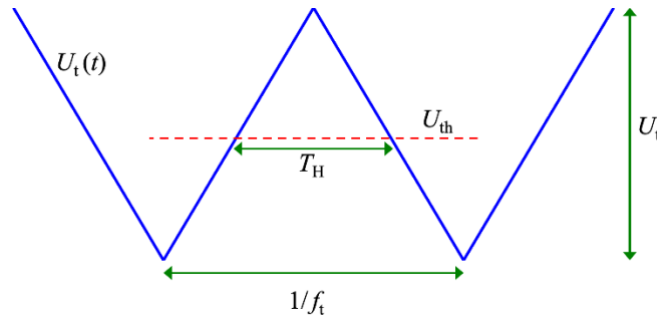


**Figure 5.2** The triangle wave vs. the threshold.

This time  $T_H$  within a period of the triangle wave is the period duration  $1/f_t$  minus the double of the time  $t_r$  spent for rising from the minimum to the threshold:

$$T_H = \frac{1}{f_t} - 2t_r = \frac{1}{f_t} - 2 \frac{U_{th} - U_s}{2U_t f_t} = \frac{U_t - U_{th} - U_s}{U_t f_t}, \quad (4)$$

where we used that the slope  $s$  of the triangle signal with peak-to-peak amplitude is

$$s = 2f_t U_t, \quad (5)$$

assumed that the signal amplitude  $U_s$  is present at the input and assumed condition (3) that the signal alone is subthreshold, but the sum of the signal and the triangle wave is suprathreshold:

$$U_s + U_t \geq U_{th} \quad (6)$$

From (3) and (4), the smoothed value of the output voltage  $U_{LPF}(t)$  of the LPF when the input signal amplitude is  $U_S(t) = U_H$ :

$$U_{LPF} = \langle U_{LPF}(t) \rangle = U_H \frac{T_H}{1/f_t} = U_H \frac{U_t - U_{th} + U_s}{U_t} = U_H \frac{U_t - U_{th}}{U_t} + \frac{U_H}{U_t} U_s, \quad (7)$$

where  $\langle \rangle$  denotes short-range averaged (smoothed) value discussed above.

It is obvious from the last term in the right side of Equation (7) that the signal amplitude transfers linearly through the system. Therefore, this version of our device is working distortion-free also for analog signals, not only for the present digital signal assumption.

This device is not only noise-free but also ideally linear for subthreshold signals satisfying condition (6).

In conclusion, with a Comparators as TE, regarding the amplitude resonance versus the carrier wave amplitude  $U_t$ , there are two different input amplitude ranges:

(a)  $U_s + U_t < U_{th}$  then there is no output signal

(b)  $U_{th} < U_s + U_t$ ,  $U_s < U_{th}$ , then the binary signal is restored at the output and its amplitude scales inversely with the amplitude  $U_t$  of the carrier wave. The maximal amplitude is at  $U_t = U_{th}$ .

Therefore, the binary signal can propagate to the output only in the (b) situation when it does that without any noise (the SNR is infinite) and it has a linear transfer for analog signals.

### 5.2.3 Stochastic resonance effects on neural processing

It has been demonstrated that neural responses to externally applied stimuli were maximally enhanced when an optimal level of electrical random noise stimulation was applied. These effects were linked specifically to the induced sodium ( $\text{Na}^+$ ) current in voltage-gated ion channels (Onorato et al., 2016; Remedios et al., 2019; see Potok et al., 2022b for review).

In humans, early SR effects have been mainly demonstrated via behavioral signal detection tasks whereby noise was added to the periphery. For example, the detection of low-contrast visual stimuli was significantly enhanced when the stimuli were superimposed with visual noise (Simonotto et al., 1997)

Recently, similar enhancements of visual perception have been reported when noise was directly added to the cerebral cortex by the means of transcranial random noise stimulation (tRNS) in studies investigating its acute effects on visual processing (Battaglini et al., 2020, 2019; Ghin et al., 2018; Pavan et al., 2019; van der Groen et al., 2019, 2018; van der Groen and Wenderoth, 2016; see Potok et al., 2022b for review) According to the SR theory, while the optimal level of tRNS benefits performance, excessive noise is detrimental for signal processing (van der Groen and Wenderoth, 2016; van der Groen et al., 2018; Pavan et al., 2019), resulting in an inverted U-shape relationship between noise benefits and noise intensity. In consistence with SR, tRNS was shown to be particularly beneficial for visual detection performance when the visual stimuli were presented with near-threshold intensity (van der Groen and Wenderoth, 2016; van der Groen et al., 2018; Battaglini et al., 2019).

However, based on the theoretical consideration described above, a resonance-like phenomenon can be observed for non-stochastic signals. Here we test this prediction empirically and investigate if the response of visual cortex to around-threshold contrast stimuli could also be enhanced via high-frequency deterministic signal. We first tested if triangle waves can modulate signal processing in a resonance-like manner by delivering hf-tACS with triangle waveform ( $\text{hf-tACS}_{\text{triangle}}$ ) targeting the primary visual cortex (V1) of participants performing a visual contrast sensitivity task and measured their visual detection threshold. Subsequently, we also tested whether high-frequency sinusoidal tACS ( $\text{hf-tACS}_{\text{sine}}$ ) in order to test the effects of a different waveform to induce the resonance effects on signal processing during visual contrast detection task performance.

## 5.3 Materials and methods

### 5.3.1 Participants

Only individuals with normal or corrected-to-normal vision and with no identified contraindications for participation according to established brain stimulation exclusion criteria



(Rossi et al., 2009; Wassermann, 1998) were recruited in the study. All study participants provided written informed consent before the beginning of each experimental session. Upon study conclusion participants were debriefed and financially compensated for their time and effort. All research procedures were approved by the Cantonal Ethics Committee Zurich (BASEC Nr. 2018-01078) and were performed in accordance with the Helsinki Declaration of the World Medical Association (2013 WMA Declaration of Helsinki) and guidelines for non-invasive brain stimulation research through the COVID-19 pandemic (Bikson et al., 2020).

The required sample size was estimated using an a priori power analysis (G\*Power version 3.1; Faul, Erdfelder, Lang, & Buchner, 2007) based on the effect of maximum contrast sensitivity improvement with tRNS shown by Potok et al. (2022a) ( $\eta_p^2 = 0.165$ , Effect size  $f = 0.445$ ). It revealed that twenty-eight participants should be included in an experiment to detect an effect with repeated measures analysis of variance (rmANOVA, 4 levels of stimulation condition),  $\alpha = 0.05$ , and 90% power. We included 31 participants in experiment 1 (hf-tACS<sub>triangle</sub>) and 32 participants in experiment 2 (hf-tACS<sub>sine</sub>) to account for potential dropouts. Visual contrast detection is potentially prone to floor effects if the contrast detected at baseline approaches the technical limits of the setup. We decided to exclude participants that are exceptionally good in the visual task and present visual contrast threshold below 0.1 in the no hf-tACS baseline condition. We also excluded individuals with exceptional contrast threshold modulation, induced by the applied brain stimulation, using interquartile range (IQR) exclusion criteria (values below  $Q1 - 1.5IQR$  or above  $Q3 + 1.5IQR$ , where  $Q1$  and  $Q3$  are equal to the first and third quartiles, respectively) to avoid accidental results, e.g., due to participants responding without paying attention to the task.

From the initially recruited sample, we excluded 7 individuals. In hf-tACS<sub>triangle</sub> experiment 1: 1 participant revealed exceptional contrast threshold modulation ( $>Q3 + 1.5IQR$ ), 1 participant had a contrast threshold below 0.1 in the baseline condition (also  $>Q3 + 1.5IQR$ ), 1 participant stopped the session because of unpleasant skin sensations. In hf-tACS<sub>sine</sub> experiment 2: 1 participant revealed exceptional contrast threshold modulation ( $>Q3 + 1.5IQR$ ), 1 participant stopped the session because of unpleasant skin sensations, 2 participants reported frequent (75% accuracy) phosphenes sensation due to stimulation (see *Hf-tACS characteristics*).

The final sample consisted of 28 healthy volunteers (16 females, 12 males;  $26.9 \pm 4.7$ , age range: 21-39) in hf-tACS<sub>triangle</sub> experiment 1, and 28 healthy volunteers (20 females, 8 males;  $26.4 \pm 4.4$ , age range: 20-39) in hf-tACS<sub>sine</sub> experiment 2. Twenty of these participants completed both experimental sessions. For participants who took part in both experiments, 15 participants started with hf-tACS<sub>triangle</sub> and 5 with hf-tACS<sub>sine</sub>. The experimental sessions took place on different days with  $2.6 \pm 1.2$  months on average apart. Delays were caused by COVID-19 pandemic (Bikson et al., 2020).

### 5.3.2 General Study design

To evaluate the influence of hf-tACS on visual contrast detection, we performed two experiments in which we delivered either hf-tACS<sub>triangle</sub>, or hf-tACS<sub>sine</sub> over V1, during visual task performance (see **Figure 5.3A**). In each experiment, three hf-tACS intensities and a control no hf-tACS condition were interleaved in a random order. Our main outcome parameter in all experiments was a threshold of visual contrast detection (VCT) that was determined for each of the different hf-tACS conditions (Potok et al., 2022a). The experimental procedure to estimate VCT followed a previously used protocol to assess the influence of tRNS on contrast sensitivity (Potok et al., 2022a). In brief, VCT was independently estimated twice, in two separate blocks within each session (see **Figure 5.3D**). We determined the individual's optimal hf-tACS intensity (defined as the intensity causing the lowest VCT, i.e., biggest improvement in contrast sensitivity) for each participant in 1<sup>st</sup> block of experiment 1 (ind-tACS<sub>triangle</sub>) and experiment 2 (ind-tACS<sub>sine</sub>) and retested their effects within the same experimental session on VCT data acquired in 2<sup>nd</sup> block.

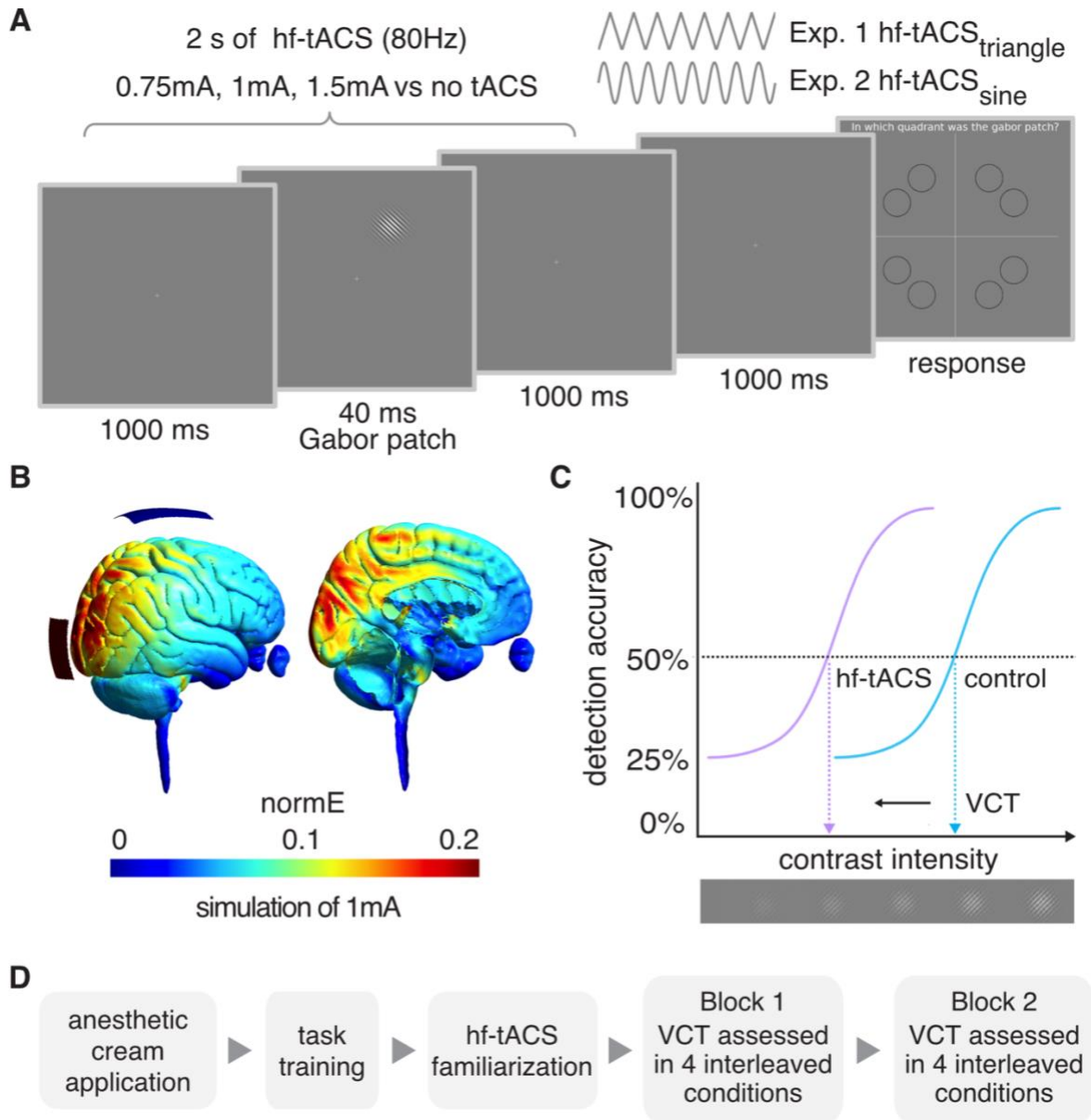


**Figure 5.3** Experimental design. **A.** Example trial of 4-alternative forced choice task measuring visual contrast detection threshold (VCT). Hf-tACS was delivered for 2 s around the Gabor patch presentation. **B.** tACS electrodes montage targeting V1 and simulation of the induced electric field in the brain. **C.** Example of dose-response psychometric curves and the VCT for the 50% detection accuracy level. We hypothesize that the VCT will be lower (indicating better contrast detection performance of the participant) in one of the hf-tACS conditions (violet) than in the no hf-tACS control condition (blue). **D.** The order of measurements within each experiment. Each experimental session consisted of application of an anesthetic cream, followed by task training, familiarization protocol, and two independent VCT assessments in 4 interleaved tACS conditions (as specified in A).

### 5.3.3 Experimental setup and visual stimuli

The experiments took place in a dark and quiet room, ensuring similar lighting conditions for all participants. Participants sat comfortably, 0.85m away from a screen, with their head supported by a chinrest. Visual stimuli were generated with Matlab (Matlab 2020a,

MathWorks, Inc., Natick, USA) using the Psychophysics Toolbox extension (Brainard, 1997; Pelli, 1997; Kleiner et al., 2007) and displayed on a CRT computer screen (Sony CPD-G420). The screen was characterized by a resolution of 1280 x 1024 pixels, refresh rate of 85Hz, linearized contrast, and a luminance of 35 cd/m<sup>2</sup> (measured with J17 LumaColor Photometer, Tektronix™). The target visual stimuli were presented in the form of the Gabor patch – a pattern of sinusoidal luminance grating displayed within a Gaussian envelope (full width at half maximum of 2.8 cm, i.e., 1° 53' visual angle, with 7.3 cm, i.e., 4° 55' presentation radius from the fixation cross). The Gabor patch pattern consisted of 16 cycles with one cycle made up of one white and one black bars (grating spatial frequency of 8 c/deg). Stimuli were oriented at 45° tilted to the left from the vertical axis (see **Figure 5.3A**), since it was shown that tRNS enhances detection of low contrast Gabor patches especially for non-vertical stimuli of high spatial frequency (Battaglini et al., 2020).

#### **5.3.4 Four-alternative forced choice visual detection task**

In both experiments, participants performed a four-alternative forced choice (4-AFC) visual task, designed to assess an individual VCT, separately for each stimulation condition. Such protocol was shown to be more efficient for threshold estimation than commonly used 2-AFC (Jäkel and Wichmann, 2006). In the middle of each 2.04s trial, a Gabor patch was randomly presented for 40ms in one of the 8 locations (see **Figure 5.3A**). A stimulus appeared in each location for the same number of times (20) within each experimental block in pseudo-randomized order to avoid a spatial detection bias. The possible locations were set on noncardinal axes, as the detection performance for stimuli presented in this way is less affected (i.e. less variable) than when stimuli are positioned on the cardinal axes (Cameron et al., 2002; van der Groen and Wenderoth, 2016). The trial was followed by 1s presentation of fixation cross after which the 'response screen' appeared. Participants' task was to decide in which quadrant of the screen the visual stimulus appeared and indicate its location on a keyboard (see **Figure 5.3A**). The timing of the response period was self-paced and not limited. Participants completed a short training session (10 trials), with the stimulus presented always at high contrast, in order to ensure that they understand the task (see **Figure 5.3D**).

VCT was estimated using the QUEST staircase procedure (Watson and Pelli, 1983), implemented in the Psychophysics Toolbox in Matlab (Brainard, 1997; Pelli, 1997; Kleiner et al., 2007). The thresholding procedure starts with a presentation of the visual stimulus displayed with 0.5 contrast intensity (for visual contrast intensity range of minimum 0 and maximum 1). When participants answer correctly, QUEST lowers the presented contrast intensity. Consequently, when participants answer incorrectly QUEST increases the presented contrast. The estimated stimulus contrast is adjusted to yield 50% detection

accuracy (i.e., detection threshold criterion, see **Figure 5.3C**). Note that for 4-AFC task 25% accuracy corresponds to a chance level. The remaining parameters used in the QUEST staircase procedure were set as follows: steepness of the psychometric function,  $\beta = 3$ ; fraction of trials on which the observer presses blindly,  $\delta = 0.01$ ; chance level of response,  $\gamma = 0.25$ ; step size of internal table grain = 0.001; intensity difference between the largest and smallest stimulus intensity,  $\text{range} = 1$ . VCT was assessed across 40 trials per stimulation condition. Four different conditions were randomly interleaved within each of 2 experimental blocks (40 trials  $\times$  4 conditions  $\times$  2 blocks; total number of 320 trials per experimental session, **Figure 5.3D**).

### 5.3.5 Hf-tACS characteristics

In stimulation trials, hf-tACS (80Hz) with symmetrical triangle- (hf-tACS<sub>triangle</sub>) or sinewave (hf-tACS<sub>sine</sub>), with no offset was delivered. Stimulation started 20ms after trial onset and was maintained for 2s (see **Figure 5.3A**). Subsequently a fixation cross was displayed for 1 s, followed by the self-paced response time. Hf-tACS waveforms were created within Matlab (Matlab 2020a, MathWorks, Inc., Natick, USA) and sent to a battery-driven electrical stimulator (DC-Stimulator PLUS, NeuroConn GmbH, Ilmenau, Germany), operated in REMOTE mode, via a National Instruments I/O device USB-6343 X series, National Instruments, USA). The active hf-tACS conditions and no hf-tACS control condition were interleaved and presented in random order. Timing of the stimuli presentation, remote control of the tACS stimulator, and behavioral data recording were synchronized via Matlab (Matlab 2020a, MathWorks, Inc., Natick, USA) installed on a PC (HP EliteDesk 800 G1) running Windows (Windows 7, Microsoft, USA) as an operating system.

In both experiments hf-tACS stimulation (hf-tACS<sub>triangle</sub> in experiment 1 or hf-tACS<sub>sine</sub> in experiment 2) was delivered with 0.75mA, 1mA, and 1.5mA amplitude (peak-to-baseline), resulting in maximum current density of  $60 \frac{\mu\text{A}}{\text{cm}^2}$ , which is below the safety limits for transcranial electrical stimulation (Fertonani et al., 2015). These intensities were selected based on previous studies investigating effects of tRNS on contrast sensitivity (van der Groen and Wenderoth, 2016; Potok et al., 2022a).

Prior to electrode placement, an anesthetic cream (Emla® 5%, Aspen Pharma Schweiz GmbH, Baar, Switzerland) was applied to the intended electrodes position on the scalp to numb potential hf-tACS-induced cutaneous sensations and diminish transcutaneous effects of stimulation. To ensure that the cream got properly absorbed, it was left on the scalp for 20 min (Asamoah et al., 2019; van der Plas et al., 2020) during which participants completed task training (see *Four-alternative forced choice visual detection task* and **Figure 5.3D**).

To target V1 we used an electrode montage that was previously shown to be suitable for visual cortex stimulation (van der Groen and Wenderoth, 2016; Herpich, 2019; Potok et al., 2022a). One tACS 5x5cm rubber electrode was placed over the occipital region (3 cm above inion, Oz in the 10-20 EEG system) and one 5x7cm rubber electrode over the vertex (Cz in the 10-20 EEG system). Electroconductive gel was applied to the contact side of the rubber electrodes (NeuroConn GmbH, Ilmenau, Germany) to reduce skin impedance. The impedance between the electrodes was monitored and kept below 15 k $\Omega$ . We used electric field modelling to ensure optimal electrode placement. Simulations were run in SimNIBS 2.1 (Thielscher et al., 2015) using the average MNI brain template (see **Figure 5.3B**). Note, that the software enables finite-element modelling of electric field distribution of direct current stimulation without taking into account the temporal characteristics of the alternating current.

Before the start of the main experiment, participants were familiarized with hf-tACS and we assessed the detectability of potential sensations (**Figure 5.3D**). The detection task consisted of 20 trials. Participants received either 2s hf-tACS (0.75, 1, and 1.5mA hf-tACS<sub>triangle</sub> in experiment 1 or hf-tACS<sub>sine</sub> in experiment 2) or no hf-tACS. Their task after each trial was to indicate on a keyboard whether they felt something underneath the tACS electrodes. In experiment 2 an additional procedure was repeated to assess potential phosphenes. The protocol was the same with the only difference that this time after each trial participants indicated on a keyboard whether they perceived any visual sensations. The determined detection accuracy (hit rates, HR) of the cutaneous sensation (experiment 1 and 2) and phosphenes (experiment 2) induced by hf-tACS served as a control to estimate whether any unspecific effects of the stimulation might have confounded the experimental outcomes (Potok et al., 2021).

### 5.3.6 Statistical analysis

Statistical analyses were performed in IBM SPSS Statistics version 26.0 (IBM Corp.) unless otherwise stated. All data was tested for normal distribution using Shapiro-Wilks test of normality. Partial eta-squared (small  $\eta_p^2 = 0.01$ , medium  $\eta_p^2 = 0.06$ , large  $\eta_p^2 = 0.14$ ; Lakens, 2013) or Cohen's d (small  $d=0.20-0.49$ , medium  $d=0.50-0.80$ , large  $d > 0.80$ ; Cohen, 1988) values are reported as a measure of effect-sizes. Variance is reported as SD in the main text and as SE in the figures. Statistical analysis of hf-tACS<sub>triangle</sub> and hf-tACS<sub>sine</sub> effects was analogous to the one performed to test hf-tRNS effects (Potok et al., 2022a).

#### Analysis of VCT modulation in hf-tACS<sub>triangle</sub> and hf-tACS<sub>sine</sub> experiments

First, we tested whether baseline VCT in the no hf-tACS condition differed across the two experimental sessions using a Bayesian independent samples t-test (average baseline VCT

in blocks 1-2 in experiments 1-2) using the Bayes factor ( $BF_{10}$ ) testing for evaluation the absence versus presence of an effect.

For all repeated measures analysis of variance (rmANOVA) models, sphericity was assessed with Mauchly's sphericity test. The threshold for statistical significance was set at  $\alpha = 0.05$ . Bonferroni correction for multiple comparisons was applied where appropriate (i.e., post hoc tests).

To test the influence of hf-tACS<sub>triangle</sub> on contrast sensitivity, VCT data collected in experiment 1 (hf-tACS<sub>triangle</sub>) was analyzed with a rmANOVA with the factor of hf-tACS<sub>triangle</sub> (no, 0.75mA, 1mA, and 1.5mA hf-tACS<sub>triangle</sub>) and the factor *block* (1<sup>st</sup>, 2<sup>nd</sup>). For each individual and each block, we determined the maximal behavioral improvement, i.e., lowest VCT measured when hf-tACS<sub>triangle</sub> was applied, and the associated "optimal" hf-tACS<sub>triangle</sub> intensity (ind-tACS<sub>triangle</sub>). The maximal behavioral improvements in the 1<sup>st</sup> and the 2<sup>nd</sup> block were compared using a t-test (2-tailed) for dependent measurements. Importantly, we determined ind-tACS<sub>triangle</sub> in the 1<sup>st</sup> block, and then used the VCT data of the separate 2<sup>nd</sup> block to test whether the associated VCT is lower compared to the no hf-tRNS condition using t-tests for dependent measures. Since we had the directional hypothesis that VCT is lower for the ind-tACS<sub>triangle</sub> intensity compared to no hf-tACS this test was 1-tailed. Determining ind-tACS<sub>triangle</sub> and testing its effect on VCT in two separate datasets is important to not overestimate the effect of tRNS on visual detection behavior.

Similarly, VCT data collected in experiment 2 (hf-tACS<sub>sine</sub>) was analyzed with a rmANOVA with the factor of hf-tACS<sub>sine</sub> (no, 0.75mA, 1mA, and 1.5mA hf-tACS<sub>sine</sub>) and the factor *block* (1<sup>st</sup>, 2<sup>nd</sup>). Again, for each individual and each block, we determined the maximal behavioral improvement and the associated ind-tACS<sub>sine</sub>. We compared results obtained in the first and second block using the same statistical tests as for the experiment 1. The maximal behavioral improvements were compared using a t-test (2-tailed) for dependent measurements. We examined whether the ind-tACS<sub>sine</sub> determined based on the best behavioral performance in 1<sup>st</sup> block, caused VCT to be lower compared to the no hf-tACS condition when retested on the independent dataset (2<sup>nd</sup> block) using t-tests (1-tailed) for dependent measures.

In both experiments to assess a general modulation of VCT induced by hf-tACS we calculated mean of all active hf-tACS conditions from 1<sup>st</sup> and 2<sup>nd</sup> blocks normalized to baseline no hf-tACS condition (hf-tACS-induced modulation).

To control for any potential unspecific effects of hf-tACS we repeated main analyses of VCT (i.e., rmANOVA) with adding mean HR of cutaneous sensation (experiment 1, hf-tACS<sub>triangle</sub> and 2, hf-tACS<sub>sine</sub>) and phosphene detection (experiment 2, hf-tACS<sub>sine</sub>) as covariate. We also tested correlations between the average HR of cutaneous sensation (experiment 1 and 2) and

phosphene (experiment 2) detection and average hf-tACS-induced modulation using a Pearson correlation coefficient.

#### Comparison of stimulation-induced VCT modulation in hf-tACS<sub>triangle</sub>, hf-tACS<sub>sine</sub>, and hf-tRNS experiments

We compared the effects of non-stochastic transcranial electrical stimulation (tES, i.e., hf-tACS<sub>triangle</sub> and hf-tACS<sub>sine</sub>) and stochastic tES (i.e., hf-tRNS) on VCT. The data demonstrating the effect of hf-tRNS on VCT were taken from a previous study (Potok et al., 2022a).

First, we tested whether baseline VCT in the no tES (no hf-tACS, no hf-tRNS) conditions differed across the three experiments using a Bayesian independent samples t-test (average baseline VCT in blocks 1-2 in hf-tACS<sub>triangle</sub>, hf-tACS<sub>sine</sub> and hf-tRNS) using the BF<sub>10</sub> testing for evaluation the absence versus presence of an effect.

Next, we tested whether a general tES-induced modulation of VCT (mean of all active stimulation conditions from two blocks normalized to baseline no stimulation condition) differed across the three experiments using a Bayesian ANOVA (tES-induced modulation in hf-tACS<sub>triangle</sub>, hf-tACS<sub>sine</sub> and hf-tRNS experiments) using the BF<sub>10</sub> testing for evaluation the absence versus presence of an effect.

Finally, we depicted tES-induced modulation of VCT as paired Cohen's d bootstrapped sampling distributions employing an online tool (<https://www.estimationstats.com>; Ho et al., 2019). For each pair of control no tES (i.e., no hf-tACS in hf-tACS<sub>triangle</sub>, hf-tACS<sub>sine</sub> and no hf-tRNS) and tES conditions (hf-tACS<sub>triangle</sub>, hf-tACS<sub>sine</sub>, hf-tRNS) two-sided permutation t-test was conducted. 5000 bootstrap samples were taken. The confidence interval was bias-corrected and accelerated. The reported P values are the likelihoods of observing the effect sizes, if the null hypothesis of zero difference is true. For each permutation P value, 5000 reshuffles of the control and test labels were performed.

## 5.4 Results

We first tested whether VCT measured during the no hf-tACS conditions differed between the experiments (i.e., average baseline VCT in hf-tACS<sub>triangle</sub> and hf-tACS<sub>sine</sub> experiments, see **Figure 5.4**). Bayesian independent samples t-test revealed that the baseline VCT measured in the no hf-tACS condition did not differ between experiments (BF<sub>10</sub> = 0.29, i.e., moderate evidence for the H<sub>0</sub>).



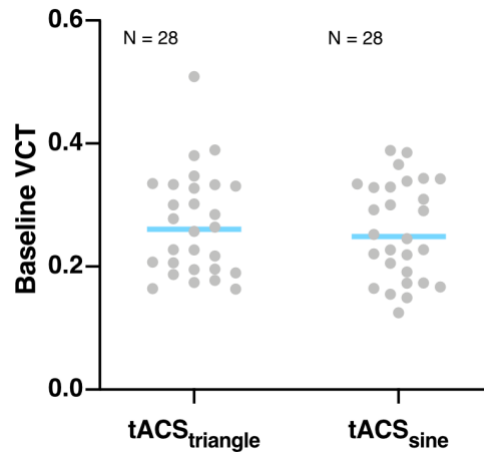


**Figure 5.4** Average baseline VCT measured in the no hf-tACS conditions in hf-tACS<sub>triangle</sub> and hf-tACS<sub>sine</sub> experiments. Blue lines indicate mean, gray dots indicate single subject data.

#### 5.4.1 Hf-tACS<sub>triangle</sub> over V1 modulates visual contrast threshold

In the first experiment, we investigated whether hf-tACS<sub>triangle</sub> modulates the visual contrast detection when applied to V1. We measured VCT during hf-tACS<sub>triangle</sub> at intensities of 0.75, 1, to 1.5mA peak-to-baseline versus no hf-tACS control condition. We found a general decrease in VCT ( $F_{(3, 81)} = 3.41$ ,  $p = 0.021$ ,  $\eta_p^2 = 0.112$ ) reflecting improved contrast sensitivity during hf-tACS<sub>triangle</sub> (**Figure 5.5A**). Post hoc comparisons revealed that the 1mA stimulation was most effective in boosting contrast processing at a group level, which differed significantly from the no hf-tACS control condition ( $p = 0.049$ , MD =  $-6.33 \pm 10.45\%$ ). Neither the main effect of block ( $F_{(1, 27)} = 2.43$ ,  $p = 0.13$ ) nor hf-tACS<sub>triangle</sub>\*block interaction ( $F_{(3, 81)} = 1.6$ ,  $p = 0.195$ ) reached significance.

When comparing hf-tACS<sub>triangle</sub>-induced effects between the 1<sup>st</sup> and 2<sup>nd</sup> block we found that the maximal behavioral improvement (i.e., maximal hf-tACS<sub>triangle</sub>-induced lowering of the VCT relative to the no hf-tACS condition) were not significantly different between the 1<sup>st</sup> (MD =  $-14.64 \pm 12.6\%$ , VCT decrease in 25 out of 28 individuals) and the 2<sup>nd</sup> block (MD =  $-15.75 \pm 15.73\%$ , VCT decrease in 24 out of 28 individuals;  $t_{(27)} = 0.604$ ,  $p = 0.551$ ), additionally showing that no time effects arose from the first to the second block of measurement.

Next, we defined the optimal ind-tACS<sub>triangle</sub> for each participant and examined whether its effects can be reproduced. We observed that the ind-tACS<sub>triangle</sub> determined in 1<sup>st</sup> block (**Figure 5.5B**) caused decrease in VCT compared to the no hf-tACS condition when retested within the same experimental session ( $t_{(27)} = 1.84$ ,  $p = 0.039$ , VCT decrease in 18 out of 28 individuals, MD =  $-5.26 \pm 18.23\%$ , **Figure 5.5C**). Note, that the above analysis does not contain an element of intrinsic circularity because the ind-tACS<sub>triangle</sub> and the VCT measure were based on the independent data sets.

Some of our participants could detect hf-tACS<sub>triangle</sub> conditions (HR at 0.75mA =  $12.5 \pm 25\%$ , 1mA =  $18.75 \pm 27.74\%$ , 1.5mA =  $41.07 \pm 43.68\%$ , mean HR =  $24.11 \pm 27.34\%$  measured via cutaneous sensation detection task). We reanalyzed our main outcome parameter by adding mean sensation detection HR as a covariate. The main effect of hf-tACS<sub>triangle</sub> remained significant ( $F_{(3, 78)} = 3.04$ ,  $p = 0.034$ ,  $\eta_p^2 = 0.105$ ). Moreover, the mean HR of cutaneous sensation detection did not correlate with the average hf-tACS<sub>triangle</sub>-induced VCT modulation ( $r = 0.181$ ,  $p = 0.357$ ), making it unlikely that transcutaneous sensation was the main driver of our results.

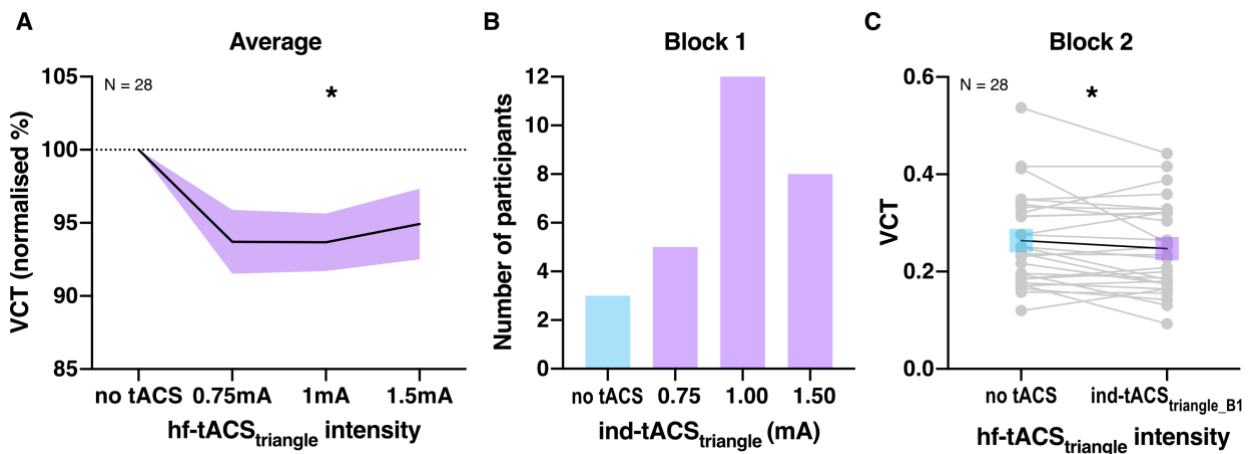


**Figure 5.5** Results of experiment 1 **A.** Effect of tACS<sub>triangle</sub> on VCT on a group level measured across 1<sup>st</sup> and 2<sup>nd</sup> blocks. Decrease in VCT reflects improvement of visual contrast sensitivity. All data mean  $\pm$  SE. **B.** Individually defined optimal hf-tACS<sub>triangle</sub> based on behavioral performance during the 1<sup>st</sup> block. **C.** Detection improvement effects of individualized hf-tACS<sub>triangle</sub> measured on the independent VCT data of block 2. Gray dots indicate single subject data; \* $p < 0.05$ .

#### 5.4.2 Hf-tACS<sub>sine</sub> over V1 modulates visual contrast threshold

In the second experiment, we explored the effects of hf-tACS<sub>sine</sub> applied over V1 on visual contrast detection. VCT was measured during hf-tACS<sub>sine</sub> at intensities of 0.75, 1, to 1.5mA peak-to-baseline versus no hf-tACS control condition. We observed a general decrease in VCT with increasing hf-tACS<sub>sine</sub> intensity ( $F_{(3, 81)} = 4.78$ ,  $p = 0.004$ ,  $\eta_p^2 = 0.15$ ) reflecting improved contrast sensitivity during hf-tACS<sub>sine</sub>. Post hoc comparisons revealed that the 1.5mA stimulation was most effective in enhancing contrast processing, which differed significantly from the no hf-tACS control condition ( $p = 0.015$ , MD =  $-8.04 \pm 13.82\%$  **Figure 5.6A**). There was no main effect of block ( $F_{(1, 27)} = 0.02$ ,  $p = 0.878$ ) or hf-tACS<sub>sine</sub>\*block interaction ( $F_{(3, 81)} = 0.5$ ,  $p = 0.684$ ).

When comparing hf-tACS<sub>sine</sub>-induced effects between the 1<sup>st</sup> and 2<sup>nd</sup> block we found that the maximal behavioral improvement, defined as maximal hf-tACS<sub>sine</sub> induced lowering of the VCT were not different between the 1<sup>st</sup> (MD =  $-17.78 \pm 15.82\%$ , VCT decrease in 25 out of 28

individuals) and the 2<sup>nd</sup> block (MD =  $-18.37 \pm 16.67\%$ , VCT decrease in 22 out of 28 individuals;  $t_{(27)} = 0.95$ ,  $p = 0.353$ ).

We determined the optimal ind-tACS<sub>sine</sub> and tested whether its effects can be reproduced. Similar to the ind-tACS<sub>triangle</sub>, the optimal ind-tACS<sub>sine</sub> determined in 1<sup>st</sup> block (**Figure 5.6B**) significantly lowered the VCT compared to the no hf-tACS condition when retested on the independent VCT data set of the 2<sup>nd</sup> block ( $t_{(27)} = 2.59$ ,  $p = 0.008$ , VCT decrease in 18 out of 28 individuals, MD =  $-7.85 \pm 21.84\%$ , **Figure 5.6C**).

Similarly to experiment 1, we assessed the HR of cutaneous sensation detection (HR at 0.75mA =  $16.07 \pm 27.4\%$ , 1mA =  $21.43 \pm 30.21\%$ , 1.5mA =  $50.89 \pm 43.29\%$ , mean HR =  $29.46 \pm 27.36\%$ ). We reanalyzed our main outcome parameter by adding mean cutaneous sensation detection HR as a covariate. The main effect of hf-tACS<sub>sine</sub> lost its significance ( $F_{(3, 78)} = 1.557$ ,  $p = 0.206$ ,  $\eta_p^2 = 0.057$ ) even though the mean HR of cutaneous sensation did not correlate with the average hf-tACS<sub>sine</sub>-induced VCT modulation ( $r = -0.12$ ,  $p = 0.542$ ). In this experiment we additionally tested phosphene detection (HR<sub>phos</sub> at 0.75mA =  $3.57 \pm 8.91\%$ , 1mA =  $5.36 \pm 12.47\%$ , 1.5mA =  $6.25 \pm 16.14\%$ , mean HR =  $5.06 \pm 10.48\%$ ). The main effect of hf-tACS<sub>sine</sub> remained significant ( $F_{(3, 78)} = 3.058$ ,  $p = 0.033$ ,  $\eta_p^2 = 0.105$ ). Accordingly, the mean HR of phosphene detection did not correlate with the average hf-tACS<sub>sine</sub>-induced VCT modulation ( $r = -0.135$ ,  $p = 0.493$ ).

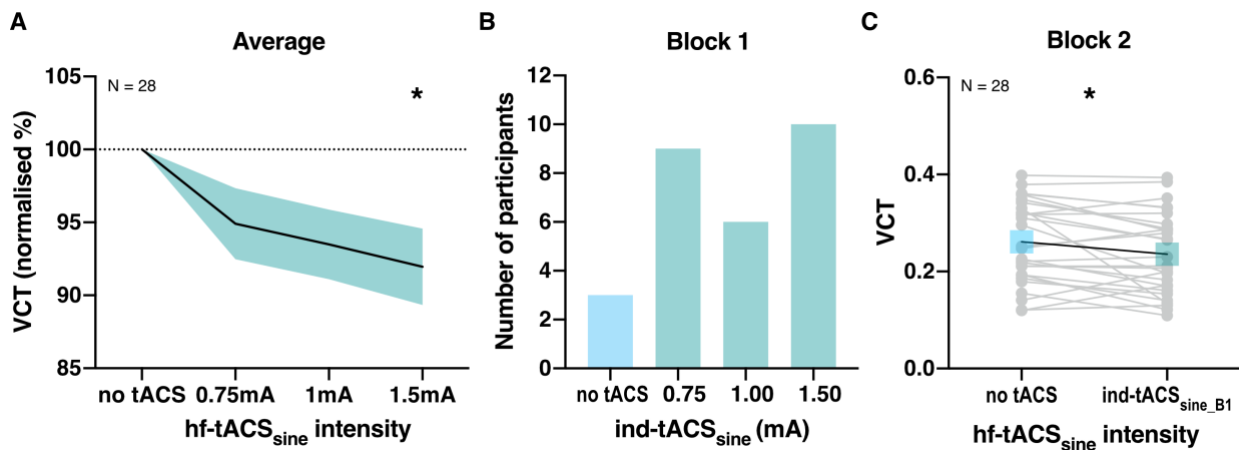


**Figure 5.6** Results of experiment 2 **A**. Effect of tACS<sub>sine</sub> on VCT on a group level measured across 1<sup>st</sup> and 2<sup>nd</sup> blocks. Decrease in VCT reflects improvement of visual contrast sensitivity. All data mean  $\pm$  SE. **B**. Individually defined optimal hf-tACS<sub>sine</sub> based on behavioral performance during the 1<sup>st</sup> block. **C**. Detection improvement effects of individualized hf-tACS<sub>sine</sub> measured on the independent VCT data of block 2. Gray dots indicate single subject data; \* $p < 0.05$ .

#### 5.4.3 Comparison of hf-tACS<sub>triangle</sub>, hf-tACS<sub>sine</sub>, and hf-tRNS-induced modulation

First, we tested whether baseline VCT measured during the no tES conditions differed between the experiments (i.e., average baseline VCT in hf-tACS<sub>triangle</sub>, hf-tACS<sub>sine</sub>, and hf-tRNS

experiments, see **Figure 5.7**). Bayesian independent samples t-test revealed that the baseline VCT measured in the no tES condition did not differ between experiments ( $BF_{10} = 0.21$ , i.e., moderate evidence for the  $H_0$ ).

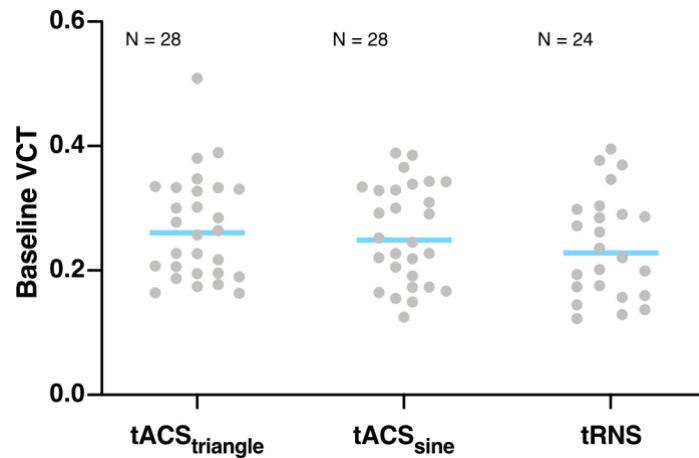


**Figure 5.7** Average baseline VCT measured in the no tES conditions in hf-tACS<sub>triangle</sub>, hf-tACS<sub>sine</sub>, hf-tRNS experiments. Blue lines indicate mean, gray dots indicate single subject data.

Next, we compared tES-induced modulation effects between experiments (hf-tACS<sub>triangle</sub>, hf-tACS<sub>sine</sub> and hf-tRNS experiments, see **Figure 5.8A**). A Bayesian ANOVA revealed that the general tES-induced modulation did not differ between experiments ( $BF_{10} = 0.11$ , i.e., moderate evidence for the  $H_0$ ), suggesting that all three stimulation types were equally effective in lowering VCT.

Finally, we assessed the strength of the tES-induced effects on VCT across hf-tACS<sub>triangle</sub>, hf-tACS<sub>sine</sub> and hf-tRNS experiments defined as paired Cohen's d bootstrapped sampling distributions (see **Figure 5.8B-C**). We found comparable (small) effects of significant differences between no tES baseline VCT and averaged VCT in active tES conditions in all experiments using the two-sided permutation t-test [in hf-tACS<sub>triangle</sub>  $d = -0.17$  (95.0%CI -0.284; -0.0698)  $p = 0.0034$ ; in hf-tACS<sub>sine</sub>  $d = -0.242$  (95.0%CI -0.444; -0.103),  $p = 0.0016$ ; in hf-tRNS  $d = -0.249$  (95.0%CI -0.433; -0.088)  $p = 0.0092$ ]. The effect sizes and CIs are reported above as: effect size (CI width lower bound; upper bound).

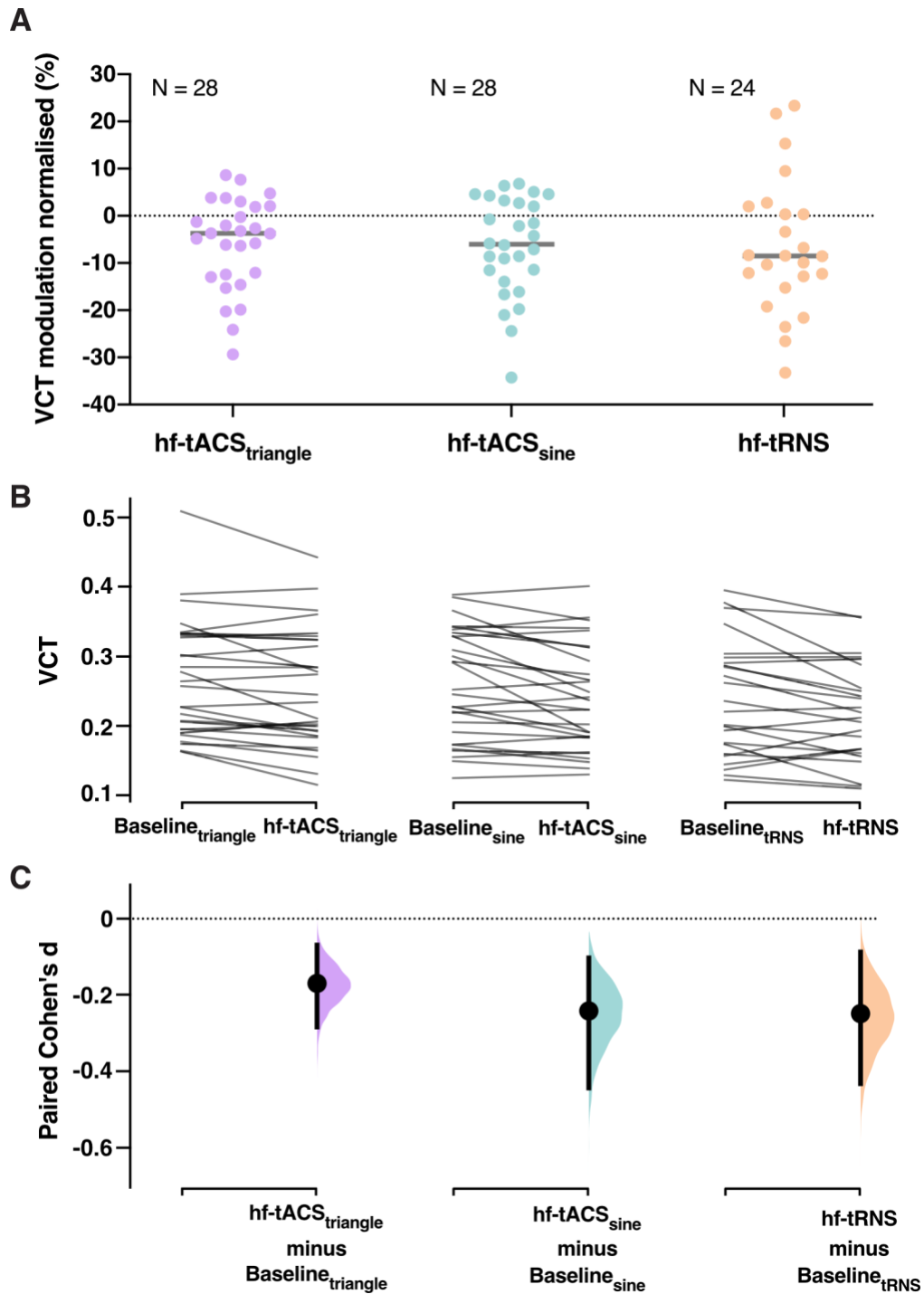


**Figure 5.8** Comparison of effects of hf-tACS<sub>triangle</sub>, hf-tACS<sub>sine</sub>, hf-tRNS. **A.** VCT modulation induced by hf-tACS<sub>triangle</sub>, hf-tACS<sub>sine</sub>, hf-tRNS. The general modulation of VCT induced by tES was calculated as mean of all active tES conditions from 1<sup>st</sup> and 2<sup>nd</sup> blocks normalized to baseline no tES condition in each experiment. **B.** Pairs of raw VCT data from hf-tACS<sub>triangle</sub>, hf-tACS<sub>sine</sub>, hf-tRNS experiments. Lines represent each paired set of observations. **C.** The paired Cohen's d for 3 comparisons shown in the Cumming estimation plot. Each paired mean difference is plotted as a bootstrap sampling distribution. Mean differences are depicted as dots, 95% confidence intervals are indicated by the ends of the vertical error bars.

## 5.5 Discussion

The present study investigated whether stimulation of V1 with deterministic hf-tACS signal instead of stochastic noise leads to the signal enhancement in visual processing. We measured visual contrast sensitivity during hf-tACS<sub>triangle</sub> and hf-tACS<sub>sine</sub>. On the group level, we found consistent hf-tACS<sub>triangle</sub>- and hf-tACS<sub>sine</sub>-induced decrease in VCT, reflecting enhancement in visual contrast processing during V1 stimulation (**Figure 5.5A, Figure 5.6A**). The online modulation effects of individually optimized hf-tACS<sub>triangle</sub> and hf-tACS<sub>sine</sub> intensities (**Figure 5.5B, Figure 5.6B**) were replicated on the independent VCT data (**Figure 5.5C, Figure 5.6C**). Finally, we demonstrated that the effects of non-stochastic stimulation on VCT are comparable to stochastic stimulation of V1 with hf-tRNS (**Figure 5.8A-C**).

### 5.5.1 Hf-tACS with triangle and sine waveform improve visual sensitivity potentially via a resonance-like signal enhancement mechanism

Our findings provide the first proof of concept that non-stochastic hf-tACS<sub>triangle</sub> and hf-tACS<sub>sine</sub> delivered to V1 can modulate the visual contrast sensitivity. Across 2 experiments we showed that the modulatory effects of hf-tACS on visual sensitivity are not waveform specific, as both hf-tACS<sub>triangle</sub> and hf-tACS<sub>sine</sub> induced significant decrease in VCT (**Figure 5.5A, Figure 5.6A**).

One of the main characteristics of SR-like effects is the optimal intensity of noise, which is required in order to yield the improved performance (Dykman and McClintock, 1999; Moss et al., 2004). Here, we did not observe an excessive level of hf-tACS that would be detrimental for visual processing (**Figure 5.5A, Figure 5.6A**). This is consistent with our predictions that adding high frequency deterministic signal should result in a noise-free output where the detection processing is not disturbed by random stimulation effects. The performance curve during hf-tACS resembles linear rather than inverted U-shaped function.

Similar to other studies investigating resonance-like effects, our results have revealed large variability among participants in terms of the intensity resulting in the strongest enhance of visual sensitivity (**Figure 5.5B, Figure 5.6B**). However, consistently with the effects of tRNS-induced online modulation of contrast processing in V1 shown previously (van der Groen and Wenderoth, 2016; Potok et al., 2022a), the effects of individualized hf-tACS intensity were replicated on the independent VCT data set collected within the same experimental session (**Figure 5.5C, Figure 5.6C**), suggesting consistent beneficial resonance-like influence of hf-tACS on signal enhancement.

We conducted several control measures to test whether the improvement in visual processing was driven by effective stimulation of V1 rather than any unspecific effects of hf-tACS. We applied an anesthetic cream to numb potential stimulation-induced cutaneous sensation on the scalp (Asamoah et al., 2019; van der Plas et al., 2020). While the anesthetic cream numbs

the skin and reduces the cutaneous sensation resulting from tACS, it does not eliminate them completely in all individuals. The control cutaneous sensation detection assessment showed that some participants could accurately detect hf-tACS, and that the mean detection rate was rather low (mean HR =  $24.11 \pm 27.34\%$  in hf-tACS<sub>triangle</sub> and mean HR =  $29.46 \pm 27.36\%$  in hf-tACS<sub>sine</sub>). Cutaneous sensation and phosphenes detection (also very low, mean HR<sub>phos</sub> =  $5.06 \pm 10.48\%$ ) did not correlate with the average hf-tACS-induced VCT modulation neither in hf-tACS<sub>triangle</sub>, nor hf-tACS<sub>sine</sub> experiment. Moreover, stimulation effects remained significant in the additional analysis using tactile sensation detection during hf-tACS<sub>triangle</sub> as covariate. However, this was not the case for the hf-tACS<sub>sine</sub>-induced effect. Therefore, we cannot fully exclude potential confounding influence of arousal or transcutaneous effects of the stimulation on task performance during hf-tACS<sub>sine</sub> and its effect needs to be treated with caution.

While tACS<sub>sine</sub> is a well-established and frequently used non-invasive brain stimulation method, hf-tACS<sub>sine</sub> is less common. The effects of 80Hz tACS<sub>sine</sub> were sporadically tested in the past using physiological and behavioral paradigms. Ten minutes of 140Hz tACS<sub>sine</sub> was shown to increase primary motor cortex (M1) excitability as measured by transcranial magnetic stimulation-elicited motor evoked potentials during and for up to 1h after stimulation. Control experiments with sham and 80Hz stimulation did not show any effect, and 250Hz stimulation was less efficient, with a delayed excitability induction and reduced duration (Moliadze et al., 2010b). The researchers postulated that the changes in corticospinal excitability result from externally applied high frequency oscillation in the ripple range (140Hz corresponding to middle, 80Hz lower and 250Hz upper border) that interfere with ongoing oscillations and neuronal activity in the brain (Moliadze et al., 2010b). We cannot directly translate the effects of hf-tACS<sub>sine</sub> of M1 to our stimulation of V1. Additionally, the stimulation effects observed in our study are likely reflecting acute modulation of contrast processing, as stimulation was only applied for short intervals (2 s) always interleaved with control (no hf-tACS) condition. Thus, it is possible that even though 80Hz stimulation did not lead to long term effects in cortical excitability it can still affect acute cortical processes.

In the visual domain, 1.5mA tACS<sub>sine</sub> was applied to V1 for 15-45min in a study investigating the effect of covert spatial attention on contrast sensitivity and contrast discrimination (Laczó et al., 2012). They found that contrast discrimination thresholds decreased significantly during 60Hz tACS<sub>sine</sub>, but not during 40 and 80Hz stimulation. This previous study used, however, different visual stimuli than the utilized here, i.e., a random dot pattern. Moreover, they used more complicated behavioral paradigm, where contrast-discrimination thresholds were tested using in two attention conditions, i.e., with or without peripheral cue, and as the study goal was to explore the influence of attentional processes on visual tasks.

Even though the vast majority of tACS studies to date have used a sinusoidal waveform, an alternating current does not have to be sinusoidal, since it can take any arbitrary waveform such as rectangular wave (Marshall et al., 2006), pulsed (Jaberzadeh et al., 2014), or sawtooth (Dowsett and Herrmann, 2016). Dowsett and Herrmann (2016) investigated the effects of sinusoidal and sawtooth wave tACS on individual endogenous alpha-power enhancement. They observed alpha oscillations both during and after sawtooth stimulation. The effect seemed to depend on the shape of the sawtooth, as they found that positive, but not negative, ramp sawtooth significantly enhanced alpha power during stimulation relative to sham. They postulated that a sudden, instantaneous change in current might be more effective than a sinusoidal current in increasing the probability of neurons firing. In this regard, Fröhlich and McCormick (2010; Supplementary Material) demonstrated that ramps of increasing voltage with a steeper gradient resulted in increased neural firing in vitro, relative to ramps with a low gradient but reaching the same maximum voltage. This suggests that it is not only the total amount of current but also the rate of change of current can modulate neural firing.

Although we postulate that the effect of hf-tACS on VCT in our study results from resonance-like mechanism, this is not the only potential mechanism. Importantly, the commonly accepted mechanism of action of tACS is that it entrains action potential firing, and thus neural oscillations (Fröhlich et al., 2014). Entrainment effect anticipates a linear relationship between the tACS effect and intensity, where increasing stimulation intensity results in greater effects (Thut et al., 2017). It cannot be excluded, though, that sudden current changes in the high-frequency, deterministic, and periodic stimulation waveforms might influence neural processing in accordance with a resonance-like mechanism rather than entrainment. In this regard, it was postulated that a very small amount of applied electric field can bias spike timing or spike probability when a neuron nears the threshold of spike generation. At the same time stronger currents are necessary to entrain network oscillations, as exogenous patterns compete with native brain rhythms (Liu et al., 2018). Accordingly, it was shown that although entrainment effects can arise at field strengths  $<0.5$  mV/mm, physiological effects are more pronounced for higher intensities (around 1mV/mm), according to intracranial recordings in awake nonhuman primates (Johnson et al., 2020). These values are well above the simulated induced electric field in our study (around 0.2 mV/mm, see **Figure 5.3B**). Thus, it is, at least in theory, more probable that the effects observed here result from resonance-like rather than entrainment mechanism. Further studies are required to fully disentangle the underlying neuronal effects of hf-tACS driving the enhancement in visual detection. To exclude the influence of entrainment on VCT modulation a jittered hf-tACS protocol could be employed. A paradigm using stimulation of jittered flickering light, where instead of a rhythmic flicker, inter stimulus intervals of the square wave were jittered with a maximum of  $\pm 60\%$ , was shown to



fail in inducing rhythmic brain response (Notbohm et al., 2016). If a jittered hf-tACS of V1 would still influence contrast sensitivity we could assume the non-entrainment origin of the effect.

### 5.5.2 Comparison of hf-tACS<sub>triangle</sub>, hf-tACS<sub>sine</sub>, and hf-tRNS

In the phenomenon of SR, random noise added to a non-linear system can increase its responsiveness towards weak subthreshold stimuli. One aim of the present study was to explore whether a deterministic and periodic signal can substitute stochastic noise and still lead to response enhancement in a threshold-based stochastic resonator. Non-stochastic characteristics of high-frequency deterministic signal might offer a noise-free output, thus additionally increasing SNR. We found enhancement effects of both hf-tACS<sub>triangle</sub> vs hf-tACS<sub>sine</sub> (**Figure 5.5A**, **Figure 5.6A**), however to test whether these effects are indeed superior to stochastic stimulation, we directly compared the VCT modulation induced by hf-tACS<sub>triangle</sub>, hf-tACS<sub>sine</sub> and hf-tRNS (**Figure 5.8**). The baseline contrast sensitivity between the compared experiments was not different (**Figure 5.7**). Counter to our hypothesis, the noise-free hf-tACS did not result in stronger contrast sensitivity enhancement, as average VCT modulation did not differ between the three stimulation conditions, as confirmed by Bayesian analysis (**Figure 5.8A**). Accordingly, the effects sizes of all three stimulation types were comparable (**Figure 5.8B-C**). Therefore, we showed that both non-stochastic and stochastic hf-stimulations were equally effective in inducing resonance-like effects.

## 5.6 Conclusions

The present study demonstrates the first evidence of the resonance-like neural signal enhancement without stochastic noise component. We showed that ‘non-stochastic’ hf-tACS and ‘stochastic’ hf-tRNS are equally effective in enhancing visual contrast detection. Using hf-tACS provides the possibility to obtain a noise-free output resulting in improved detection. In the range of commonly used intensities of tES to induce SR, hf-tACS did not result in detrimental effects related to excessive interference signal, thus providing increased SNR in all tested intensities. However, these findings await replication and should be interpreted with cautions.

## 6 General Discussion

The aim of this PhD thesis was to investigate the acute effects of stochastic noise added centrally to the nervous system. To test the responsiveness of the nervous system in the presence or absence of added noise, we probed response thresholds of motor and visual cortex when exposed to short bouts of tRNS. Additionally, we tested a high-frequency deterministic stimulation protocol, i.e., a non-stochastic equivalent of noise, on visual signal processing.

In chapter 2, we compiled the existing evidence to date on tRNS-induced modulation of sensory and motor processing from the cellular to the behavioral level. In chapter 3, we investigated for the first time the effect of acute online tRNS on neurophysiology in human participants. In chapter 4, we validated the existing evidence regarding tRNS-modulation of visual processing in V1 and extended this line of research by testing the effects of tRNS applied to the retina. Finally, in chapter 5, we explored the potential of inducing resonance-like effects with non-stochastic deterministic hf-tACS.

In this chapter, we first summarize the significance of the main findings of each study. Next, we discuss the potential neuronal and mechanistic underpinnings of the stimulation-induced effects. We then present the remaining outstanding questions, methodological implications of our findings, and their potential clinical relevance.

### 6.1 Significance of the main findings

#### 6.1.1 tRNS modulates neural processing of sensory and motor systems

In chapter 2, we presented the current state of knowledge about tRNS based on the reviewed literature. tRNS is an emerging non-invasive stimulation method that adds electrical noise to cortical circuits to modulate physiology and behavior. Our analysis reveals that tRNS can enhance neural processing which manifests either as (i) offline after-effects following prolonged stimulation or (ii) acute online noise benefits immediately during stimulation. We synthesized evidence derived from behavioral, physiological and single cell studies, and argue that tRNS is unlikely to act on synaptic plasticity per se but rather modulates neuronal excitability via voltage-gated sodium channels. We further propose that acute online noise benefits result from increasing the signal-to-noise ratio of the stimulated area, particularly in response to weak inputs, with the effect probably driven by a SR mechanism.

### **6.1.2 tRNS delivered centrally acutely lowers the responsiveness of neural populations in human cortex**

In chapter 3, we investigated the effects of tRNS in the context of SR theory predictions in a neurophysiological model. A hallmark feature of SR is that signal processing can benefit from added noise. This has mainly been demonstrated at the single-cell level *in vitro* where the neural response to weak input signals can be enhanced by simultaneously applying random noise. Our finding that tRNS acutely increases the excitability of corticomotor circuits extends the principle of noise benefits to the neural population level in human cortex. Our finding is in line with the notion that tRNS might affect cortical processing via the SR phenomenon. It suggests that enhancing the response of cortical populations to an external stimulus might be one neurophysiological mechanism mediating performance improvements when tRNS is applied to sensory cortex during perception tasks.

### **6.1.3 tRNS affects distinct neural populations within the visual system differently**

In chapter 4, we investigated the effects of acute tRNS delivered to two connected yet anatomically remote neural populations within the visual system, i.e., V1 and the retina. Our findings confirm previous evidence showing online benefits of tRNS applied to V1 on visual contrast detection in accordance with the SR phenomenon. We also demonstrated that the optimal tRNS intensity varies among participants, but when individually tailored, it can improve visual processing when re-tested within the experimental session. The tRNS-induced enhancement in visual sensitivity seems to be specific for cortical contrast processing as stimulation of the retina did not lead to a systematic effect.

### **6.1.4 Signal processing in the visual cortex can be enhanced by non-stochastic high-frequency transcranial alternating current stimulation**

In chapter 5, we explored the potential of using alternative electrical stimulation waveforms to induce resonance-like effects. We tested the effects of hf-tACS<sub>triangle</sub> and hf-tACS<sub>sine</sub> using a visual contrast detection behavioral paradigm. Our findings provide the first evidence showing acute online benefits of hf-tACS<sub>triangle</sub> and hf-tACS<sub>sine</sub> targeting the V1 on contrast sensitivity in accordance with a resonance-like phenomenon. We showed that ‘non-stochastic’ hf-tACS and ‘stochastic’ hf-tRNS are equally effective in enhancing visual contrast detection.

## 6.2 Neural substrate and computational underpinnings of stochastic and non-stochastic electrical stimulation effects

Studies measuring the responsiveness of single cells to externally applied stimuli showed maximal response enhancement when an optimal level of electrical RNS was applied. One likely cellular substrate for mediating this acute random noise stimulation effect are voltage-dependent  $\text{Na}^+$  ion channels (Onorato et al., 2016; Remedios et al., 2019; see Potok et al., 2022 for review). Accordingly, a pharmacological pilot study reported that the facilitatory after-effects of tRNS are suppressed by a voltage-gated sodium channel blocker, while staying unaffected by NMDA receptor antagonists (Chaieb et al., 2015). As such, there is no evidence that tRNS might act on synaptic plasticity per se. Rather, it seems to act via voltage-gated  $\text{Na}^+$  ion channels in large neuronal populations. Our data indirectly supports the hypothesis that tRNS acutely modulates  $\text{Na}^+$  currents. In chapter 3, we demonstrated acute online physiological effects of tRNS. It manifested as an immediate decrease in the RMT, reflecting the modulation of responsiveness of M1 (Potok et al., 2021). In this regard, pharmacological studies have suggested that the voltage-gated  $\text{Na}^+$  channel activity is an important determinant of motor threshold (Tergau et al., 2003; Sommer et al., 2012; Ziemann et al., 2015).

Interestingly repetitive extracellular high-frequency stimulation in cultured rat neurons also activated an inward  $\text{Na}^+$  current, which led to a weak depolarization of the cell membrane (Schoen and Fromherz, 2008). In chapter 5, we showed the acute modulation of contrast detection when hf-tACS was applied to V1. The observed hf-tACS-induced modulation of contrast threshold was equally effective as threshold modulation in the same task during hf-tRNS. It is than possible that hf-tRNS and hf-tACS might in fact share a similar underlying neurophysiological mechanism of action.

Furthermore, in chapter 3, we proposed that the activity of voltage-gated  $\text{Na}^+$  channels underlies acute noise benefits which manifest as increased effectiveness of responding to weak input signals (Potok et al., 2021), showing that tRNS might improve the SNR of the stimulated neuronal populations. Accordingly, at the behavioral level tRNS was shown to improve the quality of sensory information on which the decision is based, thus enhancing visual task performance (Mcintosh and Mehring, 2017; van der Groen et al., 2018). There is growing evidence coming from studies testing the effects of tRNS within the framework of SR theory, demonstrating that tRNS can be used as a source of electrical noise to induce SR effects on signal processing (van der Groen and Wenderoth, 2016; Rufener et al., 2017; Ghin et al., 2018; van der Groen et al., 2018; Battaglini et al., 2019). Our findings described in chapters 3 and 4 (Potok et al., 2021, 2022a) contribute to this line of research and support

previous findings, extending them with neurophysiological evidence of tRNS-induced noise benefits.

In sum, our neurophysiological findings showing the lowered response threshold of neural populations within M1 during tRNS support the evidence that the effects of electrical noise might be driven by Na<sup>+</sup> currents, as Na<sup>+</sup> channel activity was shown to be an important determinant of motor threshold (Tergau et al., 2003; Sommer et al., 2012; Ziemann et al., 2015). The behavioral effects of acute tRNS that we observed confirm the previous findings of tRNS-induced modulation of contrast sensitivity, attributing its computational underpinnings to improved quality of sensory information and increased SNR. Additionally, we showed that this modulation depends on the targeted neural population as tRNS did not lead to equal effects within two distinct areas of the visual system. Moreover, we demonstrated that visual detection can also be modulated by non-stochastic hf-tACS, most likely via a resonance-like mechanism.

### **6.3 Methodological implications**

In this project we utilized several novel procedures to test the predictions of the SR theory in the human brain. First, we employed a threshold tracking approach and probed motor and sensory thresholds to measure responsiveness of the investigated system during noise stimulation. Second, we tested noise effects online in human retina. Finally, we explored the influence of non-stochastic hf-tACS on visual detection.

To investigate the effects of acute electrical noise on the cortical responsiveness, we probed the thresholds of motor and sensory systems. We employed a novel procedure to estimate motor threshold based on the probability of evoking an MEP with different levels of TMS intensity applied in the presence or absence of tRNS (Chapter 3, Potok et al., 2021). We later fitted the data into linear models and determined individual RMT. This method provides a more accurate estimation of RMT than manually adjusting TMS intensity until 50% of responses in consecutive trials is reached (Rossini, Barker, & Berardelli, 1994), partly because the model is informed by more data. Similarly, we measured individual visual contrast sensitivity in the context of electrical stimulation by assessing the detection thresholds (Chapters 4 and 5; Potok et al., 2022a). We utilized an adaptive threshold tracking procedure (QUEST; Watson and Pelli, 1983) that was shown to be more accurate than the constant stimuli method often used in psychophysical experiments (Leek, 2001). In this adaptive approach, the information about the estimated threshold increases systematically as the procedure progresses and is supported by more data (Leek, 2001). In this regard, modulation of contrast processing observed in our study was characterized by larger effect size than found in the previous study (van der Groen and Wenderoth, 2016), where behavioral performance was assessed as

accuracy of detection of stimuli presented at a constant intensity. Therefore, motor threshold estimation as well as the visual threshold tracking procedure (Watson and Pelli, 1983; Brainard, 1997; Pelli, 1997; Kleiner et al., 2007) used in our project provide a sensitive and reliable estimate of neurophysiological and behavioral effects of tRNS delivered to cortical areas.

In chapter 4, we demonstrated that tRNS delivered over the retina did not lead to consistent modulation of visual detection. These findings are interesting from a methodological perspective since it rules out that applying tRNS over V1 elicits confounding effects in the retina, as previously discussed in the tACS literature (Schutter and Hortensius, 2010; Schutter, 2016). As such, it is important to take the retinal effects into account when studying the cortical modulatory effects of tES (Schutter and Hortensius, 2010; Schutter, 2016). To rule out any unspecific effects resulting from possible stimulation of the retina on visual detection performance, van der Groen and Wenderoth (2016) applied tRNS to the forehead in their active control condition. Here, we went one step further and delivered tRNS directly to the retina with an intensity typical for transorbital stimulation (Chapter 4; Potok et al., 2022a). We found no convincing evidence that tRNS affects contrast detection at the retinal level. It is therefore unlikely that, at least for tRNS, stimulation of V1 elicits confounding effects in the retina.

Finally, in chapter 5, we presented the first evidence of hf-tACS-induced modulation of visual contrast threshold. We postulate that hf-tACS influences visual processing of contrast via a resonance-like phenomenon. As such, it contradicts the commonly accepted mechanism of action of tACS that assumes entrainment of action potential firing, and thus neural oscillations during stimulation of a specific frequency (Fröhlich et al., 2014; Thut et al., 2017). Even though we cannot fully exclude entrainment as the mechanism underlying the effects of our experiments, we suggest resonance effect as more probable given the weak induced electrical field during hf-tACS (Liu et al., 2018; Johnson et al., 2020). Thus, these interesting and novel findings require further validation.

#### **6.4 Outstanding questions**

We demonstrated that online stimulation with electrical random noise, delivered via tRNS, leads to immediate modulation of neurophysiology and behavior. Our findings show that tRNS acutely increases the responsiveness of motor or sensory circuits. The enhanced responsiveness was reflected in the improved processing of weak subthreshold stimuli, i.e., TMS pulses or a visual Gabor patch, respectively. Additionally, we provided the first evidence that non-stochastic, high-frequency stimulation can, most probably, also result in resonance-like benefits on signal processing. Nevertheless, the exact underpinnings of tRNS effects are

still unclear. Here we highlight some remaining open questions and future directions to fully understand the mechanism of action of this promising method.

In chapter 3, we presented for the first time the effects of acute online tRNS in a neurophysiological model. The responsiveness of M1 was increased during short bouts of tRNS, as measured with TMS. These neurophysiological effects await replication, ideally, using different outcome measure. EEG is one good candidate to explore online modulation during tRNS with high temporal accuracy, also outside of the motor system. Additionally, using invasive intracranial recordings, e.g., in patients, would enable a deeper and more detailed understanding of the physiological impact of tRNS on neural activity *in vivo*.

The neurophysiological findings presented in this thesis contribute to our mechanistic understanding of the modulation induced by tRNS. However, to this end the origin of long-term and after-effects of tRNS is still not fully clear. Several studies have shown that tRNS modulates perceptual (Fertonani et al., 2011; Pirulli et al., 2013; Contemori et al., 2019; Herpich et al., 2019) and motor learning (Prichard et al., 2014) when applied during the training period. Although behavioral after-effects of training usually reflect the neuroplastic changes underlying the process of skill acquisition (Riout-Pedotti et al., 1998, 2007; Gilbert et al., 2001; Riout-Pedotti and Donoghue, 2003; Li et al., 2004; Carmel and Carrasco, 2008), the exact mechanism through which tRNS contributes to these long-term behavioral after-effects remains unknown. For the reported findings, it is difficult to disentangle whether the long-term performance enhancement reflects tRNS-induced neuroplasticity in the stimulated area, or if the effects are consequences of learning that benefits from noise added during training, e.g. because of immediate improved stimuli processing (Moss et al., 2004; McDonnell and Abbott, 2009). Accordingly, even though physiological or behavioral after-effects of tRNS are consistent with neuroplastic changes, they were shown to be most probably not mediated by NMDA receptor activity (Chaieb et al., 2015). Therefore, it is currently not clear how tRNS might affect synaptic plasticity. One potential mechanism is that increased activity of the voltage-gated Na<sup>+</sup> ion channels (Onorato et al., 2016; Remedios et al., 2019) might bring the cortex into a slightly facilitated state which could be beneficial for neuroplastic changes to occur. We recently ran a pilot study (results not reported in this thesis) to test whether acute tRNS strengthens neuroplastic effects when tested in a neurophysiological model. We combined acute tRNS delivery with a plasticity inducing brain stimulation protocol – Paired Associative Stimulation (PAS; Stefan et al. 2000; Rosenkranz and Rothwell 2006) to investigate whether the combination of acute short bouts of tRNS coinciding with PAS stimuli might facilitate neural transmission at the neural population level, thereby bringing the cortex into a state of heightened plasticity. We did not find significant differences between the effects of the PAS protocol with and without tRNS. Although these findings contradict tRNS

involvement in inducing neuroplastic effects, we cannot fully exclude it based on our pilot data. This question could be further addressed by combining tRNS with other brain stimulation protocols and measuring the induced neuroplasticity effects with electrophysiology to provide a better understanding of the underlying mechanism. To do so, short online bouts of tRNS could be combined with, for example, intermittent bursts of facilitatory theta burst stimulation (iTBS; Huang et al., 2005). The effects of iTBS combined with tRNS could then be compared to an iTBS only intervention by measuring M1 excitability.

Our findings presented in chapter 4 revealed that tRNS affects distinct neuronal populations differently, which is most probably related to the divergent frequency filtering properties of the remote neural areas (i.e., the retina versus V1). It is interesting whether specific cell types can be targeted with specific stimulation frequency ranges. It is additionally of interest in light of the results presented in chapter 5, where stimulation with a specific high-frequency rather than a range of frequencies (as in tRNS) led to improved signal processing. If stimulation frequency could be tailored to target specific cells, then protocols customized for more precise interventions might be a possibility.

In chapter 5, we presented the first results showing an acute decrease of visual detection threshold during brief hf-tACS. We postulated that hf-tACS can modulate brain function by resonance-like effects, i.e., a mechanism different than the commonly presupposed entrainment (Fröhlich et al., 2014; Thut et al., 2017). To exclude the potential involvement of entrainment in visual detection enhancement, the behavioral effects could be validated using a jittered hf-tACS protocol (Notbohm et al., 2016). Since this type of protocol was shown to be ineffective at inducing brain oscillations of a specific frequency, the potential involvement of entrainment could be excluded (Notbohm et al., 2016).

Finally, in our experiments, we always simulated the induced electric field (Thielscher et al., 2015) to ensure the optimal electrode montage for stimulation of the target region (i.e., M1, V1 or retina). It is commonly agreed and recommended that modeling of the induced electric field helps to obtain the optimal electrode placement for targeted brain stimulation (Bikson et al., 2018; Bergmann and Hartwigsen, 2020). Unfortunately, most of the available software enables finite-element modeling of electric field distribution of direct current stimulation without taking into account the temporal characteristics. Thus, simulating the effects of tACS might not be accurate. In particular, until now there is no tool providing a reliable simulation of the electric field induced when current waveforms of variable intensities and frequencies are used, as with tRNS. Therefore, there is an increasing need to design simulation algorithms that could better reflect the effects of an alternating current in the neural tissue. Including accurate modeling of tACS and tRNS induced electrical fields would allow for more targeted stimulation and a comparison of induced electric fields between and within studies.



## 6.5 Potential applications

While other brain stimulation protocols, such as TMS or tDCS, are relatively well established as neurorehabilitation therapies (Lefaucheur et al., 2017; Zhao et al., 2017; Rossi et al., 2021), tRNS is so far not widely utilized, even though it was shown to outperform other stimulation methods in increasing brain excitability (Inukai et al., 2016; Moliadze et al., 2014).

Stimulation with electrical random noise has been used to target different clinical populations within the sensory and motor domains. The data collected so far brings encouraging evidence for employing tRNS as a treatment method for several conditions (for details see Chapter 2, Potok et al., 2022b). In short, tRNS combined with visual training improved visual processing in individuals with mild myopia (Camilleri et al., 2014, 2016), amblyopia (Campana et al., 2014; Moret et al., 2018a; Donkor et al., 2021) and chronic cortical blindness (Herpich et al., 2019). Promising after-effects of tRNS were shown for tinnitus patients, with evidence suggesting that the symptoms of tinnitus loudness and distress were decreased after stimulation (Vanneste et al., 2013; Joos et al., 2015; To et al., 2017; Mohsen et al., 2018, 2019a, 2019b). There is also preliminary evidence suggesting potentially beneficial effects of tRNS on motor control, pain or perceived motor fatigue in Parkinson's disease (Stephani et al., 2011; Monastero et al., 2020), relapsing-remitting multiple sclerosis (Palm et al., 2016; Salemi et al., 2019) and sub-acute ischemic stroke patients (Arnao et al., 2019). Interestingly, the immediate effects of online tRNS have been studied less. The first feasibility studies investigating the acute effects of tRNS have examined visual processing in migraine patients (O'Hare et al., 2021) and the generation of voluntary motor commands in stroke survivors (Hayward et al., 2017).

The broad relevance of the method in enhancing brain function is hypothesized to be attributed to the beneficial influence of the optimal level of electrical noise added to the cortical areas. We showed that in contrast to other stimulation methods, which are typically applied for a longer period of time to induce after-effects, tRNS results in an acute increase in cortical responsiveness (Potok et al., 2021, 2022a). Our findings indicate an immediate increase in cortical responsiveness in motor and visual areas even during very short (2-3 seconds) stimulation epochs. This evidence is especially exciting since the acute neurophysiological effects of transcranial electrical stimulation on the human brain remain until now under debate (Liu et al. 2018). The immediate influence on brain activity provided by our protocol could be used to support neurorehabilitation of motor and perceptual brain function by providing short bouts of stimulation coinciding with movement attempts or visual training in patients whose motor or sensory pathways/circuits are compromised at the cortical level. These optimally adjusted protocols of online boosting stimulation could provide new opportunities to improve

current neurorehabilitation protocols by opening a 'window' of stronger activity in targeted cortical areas during the rehabilitation of patients suffering from neurological impairments.

## **6.6 Conclusions**

The last 14 years of research involving tRNS have been marked by an increasing interest in the method and its appealing potential applications. The work presented in this thesis has contributed substantially to our current understanding of neuromodulation induced by tRNS, and to our understanding of the mechanism underlying the stimulation effects. For the first time we showed that the responsiveness of motor cortex increases immediately with the application of electrical noise. This effect was further tested by comparing the behavioral outcomes of stimulation targeting two distinct neural populations within the visual system. We showed that the immediate effects of tRNS depend on the targeted area as the modulation of visual processing observed in V1 and in the retina were inconsistent, with V1 being more susceptible to noise benefits. Finally, we were among the first to explore the potential of alternative high-frequency stimulation waveforms by demonstrating that non-stochastic deterministic hf-tACS can modulate visual detection in accordance with a resonance-like mechanism.

## References

- Abe T, Miyaguchi S, Otsuru N, Onishi H (2019) The effect of transcranial random noise stimulation on corticospinal excitability and motor performance. *Neurosci Lett* 705:138–142 Available at: <https://doi.org/10.1016/j.neulet.2019.04.049>.
- Ambrus GG, Antal A, Paulus W (2011) Clinical Neurophysiology Comparing cutaneous perception induced by electrical stimulation using rectangular and round shaped electrodes. *Clin Neurophysiol* 122:803–807 Available at: <http://dx.doi.org/10.1016/j.clinph.2010.08.023>.
- Ambrus GG, Paulus W, Antal A (2010) Clinical Neurophysiology Cutaneous perception thresholds of electrical stimulation methods: Comparison of tDCS and tRNS. *Clin Neurophysiol* 121:1908–1914 Available at: <http://dx.doi.org/10.1016/j.clinph.2010.04.020>.
- Antal A, Chaieb L, Moliadze V, Monte-Silva K, Poreisz C, Thirugnanasambandam N, Nitsche MA, Shoukier M, Ludwig H, Paulus W (2010) Brain-derived neurotrophic factor (BDNF) gene polymorphisms shape cortical plasticity in humans. *Brain Stimul* 3:230–237 Available at: <http://dx.doi.org/10.1016/j.brs.2009.12.003>.
- Antal A, Herrmann CS (2016) Transcranial Alternating Current and Random Noise Stimulation: Possible Mechanisms. *Neural Plast* 2016:1–12.
- Antal A, Ivan A, Paulus W (2016) The New Modalities of Transcranial Electric Stimulation: tACS, tRNS, and Other Approaches. In: *Transcranial Direct Current Stimulation in Neuropsychiatric Disorders: Clinical principles and management* (Brunoni A, Nitsche M, Loo C, eds), pp 21–28. Springer International Publishing.
- Arnao V, Riolo M, Carduccio F, Tuttolomondo A, Amelio MD, Brighina F, Gangitano M, Salemi G, Ragonese P, Aridon P (2019) Effects of transcranial random noise stimulation combined with Graded Repetitive Arm Supplementary Program (GRASP) on motor rehabilitation of the upper limb in sub - acute ischemic stroke patients: a randomized pilot study. *J Neural Transm* 126:1701–1706 Available at: <https://doi.org/10.1007/s00702-019-02087-9>.
- Asamoah B, Khatoun A, Mc Laughlin M (2019) tACS motor system effects can be caused by transcutaneous stimulation of peripheral nerves. *Nat Commun* 10:1–16 Available at: <http://dx.doi.org/10.1038/s41467-018-08183-w>.
- Awiszus F (2003) Chapter 2 TMS and threshold hunting. Elsevier B.V. Available at: [http://dx.doi.org/10.1016/S1567-424X\(09\)70205-3](http://dx.doi.org/10.1016/S1567-424X(09)70205-3).
- Awiszus F (2011) Fast estimation of transcranial magnetic stimulation motor threshold: Is it safe? *Brain Stimul* 4:50–57 Available at: <http://dx.doi.org/10.1016/j.brs.2010.09.004>.
- Battaglini L, Contemori G, Fertoni A, Miniussi C, Coccaro A, Casco C (2019) Excitatory and inhibitory lateral interactions effects on contrast detection are modulated by tRNS. *Sci Rep* 9:1–10.
- Battaglini L, Contemori G, Penzo S, Maniglia M (2020) tRNS effects on visual contrast detection. *Neurosci Lett* 717.
- Bayram A, Karahan E, Bilgiç B, Ademoglu A, Demiralp T (2016) Achromatic temporal-frequency responses of human lateral geniculate nucleus and primary visual cortex. *Vision Res* 127:177–185.
- Benardete E, Kaplan E (1999) The dynamics of primate retinal ganglion cells. *Prog Brain Res* 134:355–368.
- Benzi R, Sutera A, Vulpiani A (1981) The mechanism of stochastic resonance. *J Phys A Math Gen*.
- Bergmann TO, Hartwigsen G (2020) Inferring causality from noninvasive brain stimulation in cognitive neuroscience. *J Cogn Neurosci* 33:195–225.
- Bergmann TO, Karabanov A, Hartwigsen G, Thielscher A, Siebner HR (2016) Combining non-invasive transcranial brain stimulation with neuroimaging and electrophysiology: Current approaches and future perspectives. *Neuroimage* 140:4–19 Available at: <http://dx.doi.org/10.1016/j.neuroimage.2016.02.012>.
- Bezrukov SM, Vodyanoy I (1995) Noise-induced enhancement of signal transduction across voltage-dependent ion channels. *Lett to Nat* 378:9213–9214.
- Bezrukov SM, Vodyanoy I (1997) Signal Transduction Across Alamethicin Presence of Noise. *Biophys J* 73:2456–2464.
- Bikson M et al. (2016) Safety of Transcranial Direct Current Stimulation: Evidence Based Update 2016. *Brain Stimul* 9:641–661 Available at: <http://dx.doi.org/10.1016/j.brs.2016.06.004>.
- Bikson M et al. (2018) Rigor and reproducibility in research with transcranial electrical stimulation: An NIMH-sponsored workshop. *Brain Stimul* 11:465–480 Available at: <https://doi.org/10.1016/j.brs.2017.12.008>.

- Bikson M et al. (2020) Guidelines for TMS/tES clinical services and research through the COVID-19 pandemic. *Brain Stimul* 13:1124–1149 Available at: <https://doi.org/10.1016/j.brs.2020.05.010>.
- Bikson M, Radman T, Datta A (2006) Rational modulation of neuronal processing with applied electric fields. 2006 Int Conf IEEE Eng Med Biol Soc:1616–1619.
- Bostock H, Cikurel K, Burke D (1998) Threshold tracking techniques in the study of human peripheral nerve. *Muscle and Nerve* 21:137–158.
- Brainard DH (1997) The Psychophysics Toolbox. *Spat Vis* 10:433–436.
- Cai C, Ren Q, Desai NJ, Rizzo JF, Fried SI (2011) Response variability to high rates of electric stimulation in retinal ganglion cells. *J Neurophysiol* 106:153–162.
- Cameron EL, Tai JC, Carrasco M (2002) Covert attention affects the psychometric function of contrast sensitivity. *Vision Res* 42:949–967.
- Camilleri R, Pavan A, Campana G (2016) The application of online transcranial random noise stimulation and perceptual learning in the improvement of visual functions in mild myopia. *Neuropsychologia* 89:225–231 Available at: <http://dx.doi.org/10.1016/j.neuropsychologia.2016.06.024>.
- Camilleri R, Pavan A, Ghin F, Battaglini L, Campana G (2014) Improvement of uncorrected visual acuity and contrast sensitivity with perceptual learning and transcranial random noise stimulation in individuals with mild myopia. 5:1–6.
- Campana G, Camilleri R, Moret B, Ghin F, Pavan A (2016) Opposite effects of high- and low- frequency transcranial random noise stimulation probed with visual motion adaptation. *Nat Publ Gr*:1–7.
- Campana G, Camilleri R, Pavan A, Veronese A, Giudice G Lo (2014) Improving visual functions in adult amblyopia with combined perceptual training and transcranial random noise stimulation (tRNS): a pilot study. 5:1–6.
- Carmel D, Carrasco M (2008) Perceptual Learning and Dynamic Changes in Primary Visual Cortex. *Neuron* 57:799–801.
- Chaieb L, Antal A, Paulus W (2015) Transcranial random noise stimulation-induced plasticity is NMDA-receptor independent but sodium-channel blocker and benzodiazepines sensitive. *Front Neurosci* 9:1–9.
- Chaieb L, Kovacs G, Cziraki C, Greenlee M, Paulus W, Antal A (2009) Short-duration transcranial random noise stimulation induces blood oxygenation level dependent response attenuation in the human motor cortex. *Exp Brain Res* 198:439–444.
- Chaieb L, Paulus W, Antal A (2011) Evaluating aftereffects of short-duration transcranial random noise stimulation on cortical excitability. *Neural Plast* 2011.
- Cohen J (1988) *Statistical Power Analysis for the Behavioral Sciences*. New York: NY: Routledge Academic.
- Collins JJ, Imhof TT, Grigg P (1996a) Noise-enhanced tactile sensation. *Nature* 383:770.
- Collins JJ, Imhoff TT, Grigg P (1996b) Noise-enhanced information transmission in rat SA1 cutaneous mechanoreceptors via aperiodic stochastic resonance. *J Neurophysiol* 76:642–645.
- Contemori G, Trotter Y, Cottureau BR, Maniglia M (2019) tRNS boosts perceptual learning in peripheral vision. *Neuropsychologia* 125:129–136 Available at: <https://doi.org/10.1016/j.neuropsychologia.2019.02.001>.
- Dakin SC, Mareschal I, Bex PJ (2005) Local and global limitations on direction integration assessed using equivalent noise analysis. *Vision Res* 45:3027–3049.
- Davila-Pérez P, Jannati A, Fried PJ, Cudeiro Mazaira J, Pascual-Leone A (2018) The Effects of Waveform and Current Direction on the Efficacy and Test–Retest Reliability of Transcranial Magnetic Stimulation. *Neuroscience* 393:97–109.
- De Albuquerque LL, Fischer KM, Pauls AL, Pantovic M, Guadagnoli MA, Riley ZA, Poston B (2019) Human Movement Science An acute application of transcranial random noise stimulation does not enhance motor skill acquisition or retention in a golf putting task. *Hum Mov Sci* 66:241–248 Available at: <https://doi.org/10.1016/j.humov.2019.04.017>.
- Deans JK, Powell AD, Jefferys JGR (2007) Sensitivity of coherent oscillations in rat hippocampus to AC electric fields. *J Physiol* 583:555–565.
- DeWeese M, Bialek W (1995) Information flow in sensory neurons. *Nuovo Cim D* 17:733–774.
- Di Lazzaro V, Rothwell JC (2014) Corticospinal activity evoked and modulated by non-invasive stimulation of the intact human motor cortex. *J Physiol* 592:4115–4128.
- Dissanayaka T, Zoghi M, Farrell M, Egan G, Jaberzadeh S (2018) Comparison of Rossini–Rothwell and adaptive threshold-hunting methods on the stability of TMS induced motor evoked potentials amplitudes. *J Neurosci Res* 96:1758–1765.

- Dmochowski JP, Bikson M, Datta A, Richardson J, Fridriksson J, Parra LC (2012) On the role of electric field orientation in optimal design of transcranial current stimulation. *Proc Annu Int Conf IEEE Eng Med Biol Soc EMBS*:6426–6429.
- Donkor R, Silva AE, Teske C, Wallis-Duffy M, Johnson AP, Thompson B (2021) Repetitive visual cortex transcranial random noise stimulation in adults with amblyopia. *Sci Rep*:3029 Available at: <https://doi.org/10.1038/s41598-020-80843-8>.
- Douglass JK, Wilkens L, Pantazelou E, Moss F (1993) Noise enhancement of information transfer in crayfish mechanoreceptors by. *Nature* 395:337–339.
- Dowsett J, Herrmann CS (2016) Transcranial alternating current stimulation with sawtooth waves: Simultaneous stimulation and EEG recording. *Front Hum Neurosci* 10:1–10.
- Dykman MI, Luchinsky DG, Mannella R, McClintock PVE, Stein ND, Stocks NG (1995) Stochastic resonance in perspective. *Nuovo Cim D* 17:661–683.
- Dykman MI, McClintock PVE (1999) Stochastic Resonance. *Sci Prog* 82:113–134.
- Faul F, Erdfelder E, Lang A, Buchner A (2007) G \* Power 3 : A flexible statistical power analysis program for the social, behavioral, and biomedical sciences. *Behav Res Methods* 39:175–191.
- Fawcett IP, Barnes GR, Hillebrand A, Singh KD (2004) The temporal frequency tuning of human visual cortex investigated using synthetic aperture magnetometry. *Neuroimage* 21:1542–1553.
- Fedorov A, Jobke S, Bersnev V, Chibisova A, Chibisova Y, Gall C, Sabel BA (2011) Restoration of vision after optic nerve lesions with noninvasive transorbital alternating current stimulation : a clinical observational study. *Brain Stimul* 4:189–201 Available at: <http://dx.doi.org/10.1016/j.brs.2011.07.007>.
- Fertonani A, Ferrari C, Miniussi C (2015) What do you feel if I apply transcranial electric stimulation? Safety, sensations and secondary induced effects. *Clin Neurophysiol* 126:2181–2188 Available at: <http://dx.doi.org/10.1016/j.clinph.2015.03.015>.
- Fertonani A, Miniussi C (2017) Transcranial electrical stimulation: What we know and do not know about mechanisms. *Neuroscientist* 23:109–123.
- Fertonani A, Pirulli C, Bollini A, Miniussi C, Bortoletto M (2019) Age-related changes in cortical connectivity influence the neuromodulatory effects of transcranial electrical stimulation. *Neurobiol Aging* 82:77–87 Available at: <https://doi.org/10.1016/j.neurobiolaging.2019.07.009>.
- Fertonani A, Pirulli C, Miniussi C (2011) Random Noise Stimulation Improves Neuroplasticity in Perceptual Learning. *J Neurosci* 31:15416–15423 Available at: <http://www.jneurosci.org/cgi/doi/10.1523/JNEUROSCI.2002-11.2011>.
- Fisher RJ, Nakamura Y, Bestmann S, Rothwell JC, Bostock H (2002) Two phases of intracortical inhibition revealed by transcranial magnetic threshold tracking. *Exp Brain Res* 143:240–248.
- Francis JT, Gluckman BJ, Schiff SJ (2003) Sensitivity of Neurons to Weak Electric Fields. *J Neurosci* 23:7255–7261.
- Frishman LJ, Freeman AW, Troy JB, Schweitzer-Tong DE, Enroth-Cugell C (1987) Spatiotemporal frequency responses of cat retinal ganglion cells. *J Gen Physiol* 89:599–628.
- Fröhlich F, McCormick DA (2010) Endogenous electric fields may guide neocortical network activity. *Neuron* 67:129–143.
- Fröhlich F, Sellers KK, Cordle AL (2014) Targeting the neurophysiology of cognitive systems with transcranial alternating current stimulation. *Expert Rev Neurother* 15:145–167.
- Gall C, Fedorov AB, Ernst L, Borrmann A, Sabel BA (2010) Repetitive transorbital alternating current stimulation in optic neuropathy. *Neuro Rehabil* 27:335–341.
- Gall C, Sgorzaly S, Schmidt S, Brandt S, Fedorov A, Sabel BA (2011) Noninvasive transorbital alternating current stimulation improves subjective visual functioning and vision-related quality of life in optic neuropathy. *Brain Stimul* 4:175–188 Available at: <http://dx.doi.org/10.1016/j.brs.2011.07.003>.
- Ghin F, O'Hare L, Pavan A (2021) Electrophysiological aftereffects of high-frequency transcranial random noise stimulation (hf-tRNS): an EEG investigation. *Exp Brain Res* 239:2399–2418 Available at: <https://doi.org/10.1007/s00221-021-06142-4>.
- Ghin F, Pavan A, Contillo A, Mather G (2018) The effects of high-frequency transcranial random noise stimulation ( hf-tRNS ) on global motion processing : An equivalent noise approach. *Brain Stimul* 11:1263–1275 Available at: <https://doi.org/10.1016/j.brs.2018.07.048>.
- Ghosh K, Sarkar S, Bhaumik K (2009) A possible mechanism of stochastic resonance in the light of an extra-classical receptive field model of retinal ganglion cells. *Biol Cybern* 100:351–359.

- Gilbert CD, Sigman M, Crist RE (2001) The neural basis of perceptual learning. *Neuron* 31:681–697.
- Gingl Z, Kiss LB, Moss F (1995) Non-dynamical stochastic resonance: Theory and experiments with white and arbitrarily coloured noise. *Europhys Lett* 29:191–196.
- Gluckman BJ, Spano ML, Netoff TI, Neel EJ, Schiff SJ, Spano WL (1996) Stochastic Resonance in a Neuronal Network from Mammalian Brain. *Phys Rev Lett* 77:4098–4101.
- Groen O Van Der, Wenderoth N (2016) Externally applied noise influences state-switching dynamics of binocular rivalry. *36:1002991*.
- Grondin S (2016) Psychology of perception.
- Haberbosch L, Datta A, Thomas C, Jooß A, Köhn A, Rönnefarth M, Scholz M, Brandt SA, Schmidt S (2019) Safety aspects, tolerability and modeling of retinofugal alternating current stimulation. *Front Genet* 10:1–12.
- Hallett M (2000) Transcranial magnetic stimulation and the human brain. *Nature* 406:147–150.
- Hallett M (2007) Transcranial magnetic stimulation: A primer. *Neuron* 55:187–199 Available at: <http://www.ncbi.nlm.nih.gov/pubmed/17640522>.
- Harmsen IE, Lee DJ, Dallapiazza RF, De Vloo P, Chen R, Fasano A, Kalia SK, Hodaie M, Lozano AM (2019) Ultra-high-frequency deep brain stimulation at 10,000 Hz improves motor function. *Mov Disord* 34:146–148.
- Hayward KS, Brauer SG, Ruddy KL, Lloyd D, Carson RG (2017) Repetitive reaching training combined with transcranial Random Noise Stimulation in stroke survivors with chronic and severe arm paresis is feasible : a pilot , triple-blind , randomised case series. :1–9.
- Herpich F (2019) Boosting learning efficacy with non-invasive brain stimulation in intact and brain-damaged humans Boosting learning efficacy with non-invasive brain stimulation in intact and brain-damaged humans Center for Neuroscience and Cognitive Systems @ UniTn , Ist.
- Herpich F, Contò F, van Koningsbruggen M, Battelli L (2018) Modulating the excitability of the visual cortex using a stimulation priming paradigm. *Neuropsychologia* 119:165–171 Available at: <https://doi.org/10.1016/j.neuropsychologia.2018.08.009>.
- Herpich F, Melnick M, Agosta S, Huxlin K, Tadin D, Battelli L (2019) Boosting learning efficacy with non-invasive brain stimulation in intact and brain-damaged humans. *J Neurosci* 39:5551–5561.
- Hinder MR, Goss EL, Fujiyama H, Canty AJ, Garry MI, Rodger J, Summers JJ (2014) Inter- and intra-individual variability following intermittent theta burst stimulation: Implications for rehabilitation and recovery. *Brain Stimul* 7:365–371 Available at: <http://dx.doi.org/10.1016/j.brs.2014.01.004>.
- Ho J, Tumkaya T, Aryal S, Choi H, Claridge-Chang A (2019) Moving beyond P values: data analysis with estimation graphics. *Nat Methods* 16:565–566 Available at: <http://dx.doi.org/10.1038/s41592-019-0470-3>.
- Ho KA, Taylor JL, Loo CK (2015) Comparison of the effects of transcranial random noise stimulation and transcranial direct current stimulation on motor cortical excitability. *J ECT* 31:67–72.
- Hoshi H, Kojima S, Otsuru N, Onishi H (2021) Effects of transcranial random noise stimulation timing on corticospinal excitability and motor function. *Behav Brain Res* 414:113479 Available at: <https://doi.org/10.1016/j.bbr.2021.113479>.
- Hottinger AF, Pacheco P, Stupp R (2016) Tumor treating fields: A novel treatment modality and its use in brain tumors. *Neuro Oncol* 18:1338–1349.
- Howells J, Trinh T, Burke D, Kiernan MC (2018) Threshold-tracking TMS without an MEP. *Clin Neurophysiol* 129:e6 Available at: <https://doi.org/10.1016/j.clinph.2017.12.026>.
- Huang Y, Liu AA, Lafon B, Friedman D, Dayan M, Wang X, Bikson M, Doyle WK, Devinsky O, Parra LC (2017) Measurements and models of electric fields in the in vivo human brain during transcranial electric stimulation. *Elife* 6:1–26.
- Huang YZ, Edwards MJ, Rounis E, Bhatia KP, Rothwell JC (2005) Theta burst stimulation of the human motor cortex. *Neuron* 45:201–206.
- Huidobro N, Mendez-Fernandez A, Mendez-Balbuena I, Gutierrez R, Kristeva R, Manjarrez E (2017) Brownian optogenetic-noise-photostimulation on the brain amplifies somatosensory-evoked field potentials. *Front Neurosci* 11:1–10.
- Iliopoulos F, Nierhaus T, Villringer A (2013) Electrical noise modulates perception of electrical pulses in humans: sensation enhancement via stochastic resonance. *J Neurophysiol* 111:1238–1248.
- Inukai Y, Saito K, Sasaki R, Tsuike S, Miyaguchi S (2016) Comparison of Three Non-Invasive Transcranial Electrical Stimulation Methods for Increasing Cortical Excitability. *10:1–7*.
- Jaberzadeh S, Bastani A, Zoghi M (2014) Anodal transcranial pulsed current stimulation: A novel technique to

- enhance corticospinal excitability. *Clin Neurophysiol* 125:344–351 Available at: <http://dx.doi.org/10.1016/j.clinph.2013.08.025>.
- Jäkel F, Wichmann FA (2006) Spatial four-alternative forced-choice method is the preferred psychophysical method for naïve observers. *J Vis* 6:1307–1322.
- Jannati A, Fried PJ, Block G, Oberman LM, Rotenberg A, Pascual-Leone A (2019) Test–Retest Reliability of the Effects of Continuous Theta-Burst Stimulation. *Front Neurosci* 13:447 Available at: <https://www.frontiersin.org/article/10.3389/fnins.2019.00447/full>.
- Johnson L, Alekseichuk I, Krieg J, Doyle A, Yu Y, Vitek J, Johnson M, Opitz A (2020) Dose-dependent effects of transcranial alternating current stimulation on spike timing in awake nonhuman primates. *Sci Adv* 6:1–9.
- Jonker ZD, Gaiser C, Tulen JHM, Ribbers GM, Frens MA, Selles RW (2021) No effect of anodal tDCS on motor cortical excitability and no evidence for responders in a large double-blind placebo-controlled trial. *Brain Stimul* 14:100–109 Available at: <https://doi.org/10.1016/j.brs.2020.11.005>.
- Joos K, Ridder D De, Vanneste S (2015) The differential effect of low - versus high - frequency random noise stimulation in the treatment of tinnitus. :1433–1440.
- Jooss A, Haberbosch L, Köhn A, Rönnefarth M, Bathe-Peters R, Kozarzewski L, Fleischmann R, Scholz M, Schmidt S, Brandt SA (2019) Motor Task-Dependent Dissociated Effects of Transcranial Random Noise Stimulation in a Finger-Tapping Task Versus a Go / No-Go Task on Corticospinal Excitability and Task Performance. *Front Neurosci* 13:1–12.
- Kapur L, Yu C, Doust MW, Gliner BE, Vallejo R, Sitzman BT, Amirdelfan K, Morgan DM, Yearwood TL, Bundschu R, Yang T, Benyamin R, Burgher AH (2016) Comparison of 10-kHz High-Frequency and Traditional Low-Frequency Spinal Cord Stimulation for the Treatment of Chronic Back and Leg Pain: 24-Month Results from a Multicenter, Randomized, Controlled Pivotal Trial. *Neurosurgery* 79:667–676.
- Kar K, Krekelberg B (2012) Transcranial electrical stimulation over visual cortex evokes phosphenes with a retinal origin. *J Neurophysiol* 108:2173–2178.
- Karabanov AN, Raffin E, Siebner HR (2015) The resting motor threshold - Restless or resting? A repeated threshold hunting technique to track dynamic changes in resting motor threshold. *Brain Stimul* 8:1191–1194.
- Kilgore KL, Bhadra N (2014) Reversible nerve conduction block using kilohertz frequency alternating current. *Neuromodulation* 17:242–255.
- Kish L (2007) Stochastic Resonance — Trivial or Not? Public debate on May 24, 2007. In: SPIE's Third Symposium on Fluctuations and Noise (FaN'07) (Weissman CM, ed). Florence, Italy.
- Kish LB, Harmer G, Abbott D (2001) Information transfer rate of neurons: stochastic resonance of Shannon's information channel capacity. *Fluct Noise Lett* 1:L13–L19.
- Kiss LB (1996) Possible breakthrough: Significant improvement of signal to noise ratio by stochastic resonance. In: American Institute of Physics Press (Katz ed. R, ed), pp 382–396 Available at: <https://doi.org/10.1063/1.51039>.
- Kleiner M, Brainard D, Pelli D, Ingling A, Murray R, Broussard C (2007) What's new in Psychtoolbox-3? *Perception* 36:1–16.
- Kobayashi M, Pascual-Leone A (2003) Transcranial magnetic stimulation in neurology. *Lancet Neurol* 2:145–156.
- Kortuem V, Ester N, Michael K, Moliadze V (2019) Efficacy of tRNS and 140 Hz tACS on motor cortex excitability seemingly dependent on sensitivity to sham stimulation. *Exp Brain Res* Available at: <https://doi.org/10.1007/s00221-019-05640-w>.
- Kreuzer PM, Poepl TB, Rupprecht R, Vielsm V, Lehner A, Langguth B, Scheckmann M (2019) Daily high-frequency transcranial random noise stimulation of bilateral temporal cortex in chronic tinnitus – a pilot study. :1–6.
- Laakso I, Hirata A (2013) Computational analysis shows why transcranial alternating current stimulation induces retinal phosphenes. *J Neural Eng* 10.
- Laczó B, Antal A, Niebergall R, Treue S, Paulus W (2012) Transcranial alternating stimulation in a high gamma frequency range applied over V1 improves contrast perception but does not modulate spatial attention. *Brain Stimul* 5:484–491.
- Laczó B, Antal A, Rothkegel H, Paulus W (2014) Increasing human leg motor cortex excitability by transcranial high frequency random noise stimulation. *Restor Neurol Neurosci* 32:403–410.
- Lakens D (2013) Calculating and reporting effect sizes to facilitate cumulative science: a practical primer for t-tests and ANOVAs. *Front Psychol* 4:1–12 Available at: <http://journal.frontiersin.org/article/10.3389/fpsyg.2013.00863/abstract>.

- Lee S, Park J, Kwon J, Kim DH, Im CH (2021) Multi-channel transorbital electrical stimulation for effective stimulation of posterior retina. *Sci Rep* 11:1–11 Available at: <https://doi.org/10.1038/s41598-021-89243-y>.
- Leek MR (2001) Adaptive procedures in psychophysical research. *Percept Psychophys* 63:1279–1292.
- Lefaucheur JP et al. (2017) Evidence-based guidelines on the therapeutic use of transcranial direct current stimulation (tDCS). *Clin Neurophysiol* 128:56–92 Available at: <http://dx.doi.org/10.1016/j.clinph.2016.10.087>.
- Levin JE, Miller JP (1996) Broadband neural encoding in the cricket cerebellar sensory system enhanced by stochastic resonance. *Nature* 380:165–168.
- Li W, Pièch V, Gilbert CD (2004) Perceptual learning and top-down influences in primary visual cortex. *Nat Neurosci* 7:651–657.
- Liu A, Vöröslakos M, Kronberg G, Henin S, Krause MR, Huang Y, Opitz A, Mehta A, Pack CC, Kregelberg B, Berényi A, Parra LC, Melloni L, Devinsky O, Buzsáki G (2018) Immediate neurophysiological effects of transcranial electrical stimulation. *Nat Commun* 9:1–12 Available at: <http://dx.doi.org/10.1038/s41467-018-07233-7>.
- Livingston SC, Ingersoll CD (2008) Intra-rater reliability of a transcranial magnetic stimulation technique to obtain motor evoked potentials. *Int J Neurosci* 118:239–256.
- Loerincz K, Gingl Z, Kiss LB (1996) A stochastic resonator is able to greatly improve signal-to-noise ratio. *Phys Lett A* 224:63–67.
- Longstaff A (2000) *Instant Notes: Neuroscience*. London and New York: BIOS Scientific Publishers.
- Lugo E, Doti R, Faubert J (2008) Ubiquitous Crossmodal Stochastic Resonance in Humans: Auditory Noise Facilitates Tactile, Visual and Proprioceptive Sensations. 3.
- Mabil P, Huidobro N, Torres-Ramirez O, Flores-Hernandez J, Flores A, Gutierrez R, Manjarrez E (2020) Noisy Light Augments the Na<sup>+</sup> Current in Somatosensory Pyramidal Neurons of Optogenetic Transgenic Mice. *Front Neurosci* 14.
- Manjarrez E, Rojas-Piloni JG, Méndez I, Martínez L, Vélez D, Vázquez D, Flores A (2002) Internal stochastic resonance in the coherence between spinal and cortical neuronal ensembles in the cat. *Neurosci Lett* 326:93–96.
- Marshall L, Helgadóttir H, Mölle M, Born J (2006) Boosting slow oscillations during sleep potentiates memory. *Nature* 444:610–613.
- Martínez L, Pérez T, Mirasso CR, Manjarrez E (2007) Stochastic Resonance in the Motor System: Effects of Noise on the Monosynaptic Reflex Pathway of the Cat Spinal Cord. *J Neurophysiol* 97:4007–4016.
- McDonnell MD, Abbott D (2009) What is stochastic resonance? Definitions, misconceptions, debates, and its relevance to biology. *PLoS Comput Biol* 5 Available at: <https://doi.org/10.1371/journal.pcbi.1000348>.
- McDonnell MD, Stocks NG, Pearce CEM, Abbott D (2008) *Stochastic resonance: its definition, history, and debates*. Cambridge: Cambridge University Press.
- McDonnell MD, Ward LM (2011) The benefits of noise in neural systems: Bridging theory and experiment. *Nat Rev Neurosci* 12:415–425 Available at: <http://dx.doi.org/10.1038/nrn3061>.
- McIntosh JR, Mehring C (2017) Modifying response times in the Simon task with transcranial random noise stimulation. *Sci Rep*:1–16 Available at: <http://dx.doi.org/10.1038/s41598-017-15604-1>.
- Melnick MD, Park WJ, Croom S, Chen S, Batelli L, Busza A, Huxlin KR, Tadin D (2020) Online Transcranial Random Noise stimulation improves perception at high levels of visual white noise. *bioRxiv*.
- Menon P, Geevasinga N, Yiannikas C, Howells J, Kiernan MC, Vucic S (2015) Sensitivity and specificity of threshold tracking transcranial magnetic stimulation for diagnosis of amyotrophic lateral sclerosis: A prospective study. *Lancet Neurol* 14:478–484.
- Mills KR, Boniface SJ, Schubert M (1992) Magnetic brain stimulation with a double coil: the importance of coil orientation. *Electroencephalogr Clin Neurophysiol Evoked Potentials* 85:17–21.
- Miniussi C, Harris JA, Ruzzoli M (2013) Modelling non-invasive brain stimulation in cognitive neuroscience. *Neurosci Biobehav Rev* 37:1702–1712 Available at: <http://dx.doi.org/10.1016/j.neubiorev.2013.06.014>.
- Mohsen S, Mahmoudian S, Talebian S, Pourbakht A (2018) Prefrontal and auditory tRNS in sequence for treating chronic tinnitus: a modified multisite protocol. *Brain Stimul* 11:1177–1179 Available at: <https://doi.org/10.1016/j.brs.2018.04.018>.
- Mohsen S, Mahmoudian S, Talebian S, Pourbakht A (2019a) Multisite transcranial Random Noise Stimulation ( tRNS ) modulates the distress network activity and oscillatory powers in subjects with chronic tinnitus. *J Clin Neurosci* 67:178–184 Available at: <https://doi.org/10.1016/j.jocn.2019.06.033>.



- Mohsen S, Pourbakht A, Farhadi M, Mahmoudian S (2019b) The efficacy and safety of multiple sessions of multisite transcranial random noise stimulation in treating chronic tinnitus. *Braz J Otorhinolaryngol* 85:628–635 Available at: <https://doi.org/10.1016/j.bjorl.2018.05.010>.
- Moliadze V, Antal A, Paulus W (2010a) Clinical Neurophysiology Electrode-distance dependent after-effects of transcranial direct and random noise stimulation with extracephalic reference electrodes. *Clin Neurophysiol* 121:2165–2171 Available at: <http://dx.doi.org/10.1016/j.clinph.2010.04.033>.
- Moliadze V, Antal A, Paulus W (2010b) Boosting brain excitability by transcranial high frequency stimulation in the ripple range. *J Physiol* 588:4891–4904.
- Moliadze V, Atalay D, Antal A, Paulus W (2012) Close to threshold transcranial electrical stimulation preferentially activates inhibitory networks before switching to excitation with higher intensities. *Brain Stimul* 5:505–511 Available at: <http://dx.doi.org/10.1016/j.brs.2011.11.004>.
- Moliadze V, Fritzsche G, Antal A (2014) Comparing the Efficacy of Excitatory Transcranial Stimulation Methods Measuring Motor Evoked Potentials. *Neural Plast* 2014.
- Monastero R, Baschi R, Nicoletti A, Pilati L, Pagano L, Cicero CE, Zappia M, Brighina F (2020) Transcranial random noise stimulation over the primary motor cortex in PD-MCI patients: a crossover, randomized, sham-controlled study. *J Neural Transm* 127:1589–1597 Available at: <https://doi.org/10.1007/s00702-020-02255-2>.
- Moret B, Camilleri R, Pavan A, Lo G (2018a) Differential effects of high-frequency transcranial random noise stimulation (hf-tRNS) on contrast sensitivity and visual acuity when combined with a short perceptual training in adults with amblyopia. *Neuropsychologia* 114:125–133 Available at: <https://doi.org/10.1016/j.neuropsychologia.2018.04.017>.
- Moret B, Camilleri R, Pavan A, Lo Giudice G, Veronese A, Rizzo R, Campana G (2018b) Differential effects of high-frequency transcranial random noise stimulation (hf-tRNS) on contrast sensitivity and visual acuity when combined with a short perceptual training in adults with amblyopia. *Neuropsychologia* 114:125–133 Available at: <https://doi.org/10.1016/j.neuropsychologia.2018.04.017>.
- Moret B, Donato R, Nucci M, Cona G, Campana G (2019) Transcranial random noise stimulation (tRNS): a wide range of frequencies is needed for increasing cortical excitability. *Sci Rep* 9:1–8 Available at: <http://dx.doi.org/10.1038/s41598-019-51553-7>.
- Moss F, Ward LM, Sannita WG (2004) Stochastic resonance and sensory information processing: A tutorial and review of application. *Clin Neurophysiol* 115:267–281.
- Ngomo S, Leonard G, Moffet H, Mercier C (2012) Comparison of transcranial magnetic stimulation measures obtained at rest and under active conditions and their reliability. *J Neurosci Methods* 205:65–71 Available at: <http://dx.doi.org/10.1016/j.jneumeth.2011.12.012>.
- Nitsche MA, Cohen LG, Wassermann EM, Priori A, Lang N, Antal A, Paulus W, Hummel F, Boggio PS, Fregni F, Pascual-Leone A (2008) Transcranial direct current stimulation: State of the art 2008. *Brain Stimul* 1:206–223.
- Nitsche MA, Fricke K, Henschke U, Schlitterlau A, Liebetanz D, Lang N, Henning S, Tergau F, Paulus W (2003) Pharmacological modulation of cortical excitability shifts induced by transcranial direct current stimulation in humans. *J Physiol*:293–301.
- Nitsche MA, Seeber A, Frommann K, Klein CC, Rochford C, Nitsche MS, Fricke K, Liebetanz D, Lang N, Antal A, Paulus W, Tergau F (2005) Modulating parameters of excitability during and after transcranial direct current stimulation of the human motor cortex. *J Physiol* 568:291–303.
- Notbohm A, Kurths J, Herrmann CS (2016) Modification of brain oscillations via rhythmic light stimulation provides evidence for entrainment but not for superposition of event-related responses. *Front Hum Neurosci* 10.
- O'Hare L, Goodwin P, Sharp A, Contillo A, Pavan A (2021) Improvement in visual perception after high-frequency transcranial random noise stimulation (hf-tRNS) in those with migraine: An equivalent noise approach. *Neuropsychologia* 161:107990 Available at: <https://doi.org/10.1016/j.neuropsychologia.2021.107990>.
- Oldfield RC (1971) The Assessment and Analysis of Handedness: The Edinburgh Inventory. 9:97–113 Available at: [http://ac.els-cdn.com/0028393271900674/1-s2.0-0028393271900674-main.pdf?\\_tid=aaa8e908-59af-11e2-b6b1-00000aacb35e&acdnat=1357662359\\_9cb8b13303b8bd329938d28c6814493b](http://ac.els-cdn.com/0028393271900674/1-s2.0-0028393271900674-main.pdf?_tid=aaa8e908-59af-11e2-b6b1-00000aacb35e&acdnat=1357662359_9cb8b13303b8bd329938d28c6814493b).
- Onorato I, D'Alessandro G, Di Castro MA, Renzi M, Dobrowolny G, Musarò A, Salvetti M, Limatola C, Crisanti A, Grassi F (2016) Noise enhances action potential generation in mouse sensory neurons via stochastic resonance. *PLoS One* 11:1–12.
- Opitz A, Falchier A, Yan CG, Yeagle EM, Linn GS, Megevand P, Thielscher A, Deborah RA, Milham MP, Mehta AD, Schroeder CE (2016) Spatiotemporal structure of intracranial electric fields induced by transcranial electric stimulation in humans and nonhuman primates. *Sci Rep* 6:1–11 Available at: <http://dx.doi.org/10.1038/srep31236>.

- Opitz A, Paulus W, Will S, Antunes A, Thielscher A (2015) Determinants of the electric field during transcranial direct current stimulation. *Neuroimage* 109:140–150 Available at: <http://dx.doi.org/10.1016/j.neuroimage.2015.01.033>.
- Palm U, Chalah MA, Padberg F, Al-Ani T, Abdellaoui M, Sorel M, Dimitri D, Créange A, Lefaucheur JP, Ayache SS (2016) Effects of transcranial random noise stimulation (tRNS) on affect, pain and attention in multiple sclerosis. *Restor Neurol Neurosci* 34:189–199.
- Parkin BL, Bhandari M, Glen JC, Walsh V (2019) The physiological effects of transcranial electrical stimulation do not apply to parameters commonly used in studies of cognitive neuromodulation. *Neuropsychologia* 128:332–339 Available at: <https://doi.org/10.1016/j.neuropsychologia.2018.03.030>.
- Patel A, Kosko B (2005) Stochastic resonance in noisy spiking retinal and sensory neuron models. *Neural Networks* 18:467–478.
- Paulus W (2011) Transcranial electrical stimulation (tES - tDCS; tRNS, tACS) methods. *Neuropsychol Rehabil* 21:602–617.
- Paulus W, Classen J, Cohen LG, Large CH, Di Lazzaro V, Nitsche M, Pascual-Leone A, Rosenow F, Rothwell JC, Ziemann U (2008) State of the art: Pharmacologic effects on cortical excitability measures tested by transcranial magnetic stimulation. *Brain Stimul* 1:151–163.
- Pavan A, Ghin F, Contillo A, Milesi C, Campana G, Mather G (2019) Modulatory mechanisms underlying high-frequency transcranial random noise stimulation ( hf-tRNS ): A combined stochastic resonance and equivalent noise approach. *Brain Stimul* 12:967–977 Available at: <https://doi.org/10.1016/j.brs.2019.02.018>.
- Pearson K (1897) Mathematical contributions to the theory of evolution.—on a form of spurious correlation which may arise when indices are used in the measurement of organs. *Proc R Soc London* 60:489–498.
- Pelli DG (1997) The VideoToolbox software for visual psychophysics: transforming numbers into movies. *Spat Vis* 10:437–442.
- Pirulli C, Fertonani A, Miniussi C (2013) The role of timing in the induction of neuromodulation in perceptual learning by transcranial electric stimulation. *Brain Stimul* 6:683–689 Available at: <http://dx.doi.org/10.1016/j.brs.2012.12.005>.
- Pirulli C, Fertonani A, Miniussi C (2016) On the Functional Equivalence of Electrodes in Transcranial Random Noise Stimulation. *Brain Stimul* 9:621–622 Available at: <http://dx.doi.org/10.1016/j.brs.2016.04.005>.
- Polanía R, Nitsche MA, Ruff CC (2018) Studying and modifying brain function with non-invasive brain stimulation. *Nat Neurosci* 21:174–187.
- Potok W, Bächinger M, Cretu AL, van der Groen O, Wenderoth N (2021) Transcranial Random Noise Stimulation acutely lowers the response threshold of human motor circuits. *J Neurosci* 41:3842–3853.
- Potok W, Post A, Bächinger M, Kiper D, Wenderoth N (2022a) Transcranial random noise stimulation of the primary visual cortex but not retina modulates visual contrast sensitivity. *bioRxiv*.
- Potok W, van der Groen O, Bächinger M, Edwards D, Wenderoth N (2022b) Transcranial random noise stimulation modulates neural processing of sensory and motor circuits – from potential cellular mechanisms to behaviour: A scoping review. *eNeuro* 9:1–13.
- Prete G, Anselmo AD, Tommasi L, Brancucci A (2017) Modulation of Illusory Auditory Perception by Transcranial Electrical Stimulation. 11:1–10.
- Prete G, Anselmo AD, Tommasi L, Brancucci A (2018) Modulation of the dichotic right ear advantage during bilateral but not unilateral transcranial random noise stimulation. *Brain Cogn* 123:81–88 Available at: <https://doi.org/10.1016/j.bandc.2018.03.003>.
- Prichard G, Weiller C, Fritsch B, Reis J (2014) Effects of different electrical brain stimulation protocols on subcomponents of motor skill learning. *Brain Stimul* 7:532–540 Available at: <http://dx.doi.org/10.1016/j.brs.2014.04.005>.
- Qi F, Nitsche MA, Zschorlich VR (2019) Interaction Between Transcranial Random Noise Stimulation and Observation-Execution Matching Activity Promotes Motor Cortex Excitability. *Front Neurosci* 13:1–10.
- Ratcliff R, McKoon G (2008) The Diffusion Decision Model: Theory and Data for Two-Choice Decision Tasks. *Neural Comput* 20:873–922.
- Rathelot J-A, Strick PL (2009) Subdivisions of primary motor cortex based on cortico-motoneuronal cells. *Proc Natl Acad Sci* 106:918–923.
- Rawji V, Ciocca M, Zacharia A, Soares D, Truong D, Bikson M, Rothwell J, Bestmann S (2018) tDCS changes in motor excitability are specific to orientation of current flow. *Brain Stimul* 11:289–298.
- Reato D, Rahman A, Bikson M, Parra LC (2010) Low-Intensity Electrical Stimulation Affects Network Dynamics by

- Modulating Population Rate and Spike Timing. *J Neurosci* 30:15067–15079.
- Remedios L, Mabil P, Flores-Hernández J, Torres-Ramírez O, Huidobro N, Castro G, Cervantes L, Tapia JA, De la Torre Valdovinos B, Manjarrez E (2019) Effects of Short-Term Random Noise Electrical Stimulation on Dissociated Pyramidal Neurons from the Cerebral Cortex. *Neuroscience* 404:371–386.
- Rioul-Pedotti M-S, Donoghue JP (2003) The nature and mechanisms of plasticity. In: *Plasticity in the Human Nervous System* ((Boniface S, Ziemann U eds), ed), pp 1–25. Cambridge, UK: Cambridge UP.
- Rioul-Pedotti MS, Donoghue JP, Dunaevsky A (2007) Plasticity of the synaptic modification range. *J Neurophysiol* 98:3688–3695.
- Rioul-Pedotti MS, Friedman D, Hess G, Donoghue JP (1998) Strengthening of horizontal cortical connections following skill learning. *Nat Neurosci* 1:230–234.
- Rosenkranz K, Rothwell JC (2006) Differences between the effects of three plasticity inducing protocols on the organization of the human motor cortex. *Eur J Neurosci* 23:822–829.
- Rossi S et al. (2009) Safety, ethical considerations, and application guidelines for the use of transcranial magnetic stimulation in clinical practice and research. *Clin Neurophysiol* 120:2008–2039 Available at: <http://dx.doi.org/10.1016/j.clinph.2009.08.016>.
- Rossi S et al. (2021) Safety and recommendations for TMS use in healthy subjects and patient populations, with updates on training, ethical and regulatory issues: Expert Guidelines. *Clin Neurophysiol* 132:269–306 Available at: <https://doi.org/10.1016/j.clinph.2020.10.003>.
- Rossini P, Barker A, Berardelli A (1994) Non-invasive electrical and magnetic stimulation of the brain, spinal cord and roots: basic principles and procedures for routine clinical application. Report of an IFCN. *Electroencephalogr Clin Neurophysiol* 91:79–92.
- Rufener KS, Geyer U, Janitzky K, Heinze HJ, Zaehle T (2018) Modulating auditory selective attention by non-invasive brain stimulation: Differential effects of transcutaneous vagal nerve stimulation and transcranial random noise stimulation. *Neurosci Lett* 678:2301–2309.
- Rufener KS, Kauk J, Ruhnau P, Repplinger S, Heil P, Zaehle T (2020) Inconsistent effects of stochastic resonance on human auditory processing. *Sci Rep* 10:1–10.
- Rufener KS, Ruhnau P, Heinze H-J, Zaehle T (2017) Transcranial Random Noise Stimulation (tRNS) Shapes the Processing of Rapidly Changing Auditory Information. *Front Cell Neurosci* 11:1–11.
- Sabel B, Gao Y, Antal A (2020) Reversibility of visual field defects through induction of brain plasticity: Vision restoration, recovery and rehabilitation using alternating current stimulation. *Neural Regen Res* 15:1799–1806.
- Sabel BA, Fedorov AB, Naue N, Borrmann A, Herrmann C, Gall C (2011) Non-invasive alternating current stimulation improves vision in optic neuropathy. *Restor Neurol Neurosci* 29:493–505.
- Saiote C, Polanía R, Rosenberger K, Paulus W, Antal A (2013) High-Frequency TRNS Reduces BOLD Activity during Visuomotor Learning. *PLoS One* 8:1–8.
- Saito K, Otsuru N, Inukai Y, Miyaguchi S, Yokota H, Kojima S, Sasaki R, Onishi H (2019) Comparison of transcranial electrical stimulation regimens for effects on inhibitory circuit activity in primary somatosensory cortex and tactile spatial discrimination performance. *Behav Brain Res* 375:112168 Available at: <https://doi.org/10.1016/j.bbr.2019.112168>.
- Salemi G, Vazzoler G, Ragonese P, Bianchi A, Cosentino G, Croce G, Gangitano M, Portera E, Realmuto S, Fierro B, Brighina F (2019) Application of tRNS to improve multiple sclerosis fatigue: a pilot, single-blind, sham-controlled study. *J Neural Transm* 126:795–799 Available at: <https://doi.org/10.1007/s00702-019-02006-y>.
- Sánchez-León CA, Sánchez-López Á, Gómez-Cliement MA, Cordones I, Cohen Kadosh R, Márquez-Ruiz J (2021) Impact of chronic transcranial random noise stimulation (tRNS) on GABAergic and glutamatergic activity markers in the prefrontal cortex of juvenile mice. *Prog Brain Res* 264:323–341.
- Schambra HM, Ogden RT, Martínez-Hernández IE, Lin X, Chang YB, Rahman A, Edwards DJ, Krakauer JW (2015) The reliability of repeated TMS measures in older adults and in patients with subacute and chronic stroke. *Front Cell Neurosci* 9:1–18 Available at: <http://journal.frontiersin.org/article/10.3389/fncel.2015.00335>.
- Schoen I, Fromherz P (2008) Extracellular Stimulation of Mammalian Neurons Through Repetitive Activation of Na<sup>+</sup> Channels by Weak Capacitive Currents on a Silicon Chip. *J Neurophysiol* 100:346–357.
- Schoiswohl S, Langguth B, Gebel N, Poepl TB, Kreuzer PM, Schecklmann M (2021) Electrophysiological evaluation of high and low-frequency transcranial random noise stimulation over the auditory cortex, 1st ed. Elsevier B.V. Available at: <http://dx.doi.org/10.1016/bs.pbr.2020.08.009>.
- Schutter DJLG (2016) Cutaneous retinal activation and neural entrainment in transcranial alternating current stimulation: A systematic review. *Neuroimage* 140:83–88 Available at: <https://doi.org/10.1016/j.neuroimage.2016.08.048>.

- <http://dx.doi.org/10.1016/j.neuroimage.2015.09.067>.
- Schutter DJLG, Hortensius R (2010) Clinical Neurophysiology Retinal origin of phosphenes to transcranial alternating current stimulation. *Clin Neurophysiol* 121:1080–1084 Available at: <http://dx.doi.org/10.1016/j.clinph.2009.10.038>.
- Scott AC (2007) *The Nonlinear Universe. Chaos, Emergence, Life*. Springer Berlin Heidelberg.
- Shibuya K, Park SB, Geevasinga N, Huynh W, Simon NG, Menon P, Howells J, Vucic S, Kiernan MC (2016) Threshold tracking transcranial magnetic stimulation: Effects of age and gender on motor cortical function. *Clin Neurophysiol* 127:2355–2361 Available at: <http://dx.doi.org/10.1016/j.clinph.2016.03.009>.
- Simonotto E, Riani M, Seife C, Roberts M, Twitty J, Moss F (1997) Visual Perception of Stochastic Resonance. 256:6–9.
- Sommer M, Gileles E, Knappmeyer K, Rothkegel H, Polania R, Paulus W (2012) Carbamazepine reduces short-interval interhemispheric inhibition in healthy humans. *Clin Neurophysiol* 123:351–357 Available at: <http://dx.doi.org/10.1016/j.clinph.2011.07.027>.
- Stacey WC, Durand DM (2000) Stochastic resonance improves signal detection in hippocampal CA1 neurons. *J Neurophysiol* 83:1394–1402.
- Stefan K, Kunesch E, Cohen LG, Benecke R, Classen J (2000) Induction of plasticity in the human motor cortex by paired associative stimulation. *Brain* 123:572–584.
- Stefani SP, Breen PP, Serrador JM, Camp AJ (2019) Stochastic Noise Application for the Assessment of Medial Vestibular Nucleus Neuron Sensitivity In Vitro. *JoVE*:e60044 Available at: <https://www.jove.com/t/60044>.
- Stephani C, Nitsche MA, Sommer M, Paulus W (2011) Parkinsonism and Related Disorders Impairment of motor cortex plasticity in Parkinson ' s disease , as revealed by theta-burst-transcranial magnetic stimulation and transcranial random noise stimulation q , qq. *Park Relat Disord* 17:297–298 Available at: <http://dx.doi.org/10.1016/j.parkreldis.2011.01.006>.
- Stocks N, Stein N, McClintock P (1993) Stochastic resonance and antiresonance in monostable systems. *J Phys A Math Gen* 26:L385–L390.
- Stocks NG (2000) Suprathreshold stochastic resonance in multilevel threshold systems. *Phys Rev Lett* 84:2310–2313.
- Tergau F, Wischer S, Somal HS, Nitsche MA, Mercer AJ, Paulus W, Steinhoff BJ (2003) Relationship between lamotrigine oral dose, serum level and its inhibitory effect on CNS: Insights from transcranial magnetic stimulation. *Epilepsy Res* 56:67–77.
- Terney D, Chaieb L, Moliadze V, Antal A, Paulus W (2008) Increasing Human Brain Excitability by Transcranial High-Frequency Random Noise Stimulation. *J Neurosci* 28:14147–14155.
- Thiele C, Zaehle T, Haghikia A, Ruhnau P (2021) Amplitude modulated transcranial alternating current stimulation (AM-TACS) efficacy evaluation via phosphene induction. *Sci Rep* 11:1–10 Available at: <https://doi.org/10.1038/s41598-021-01482-1>.
- Thielscher A, Antunes A, Saturnino GB (2015) Field modeling for transcranial magnetic stimulation: A useful tool to understand the physiological effects of TMS? *Proc Annu Int Conf IEEE Eng Med Biol Soc EMBS*:222–225.
- Thielscher A, Saturnino GB (2019) Field calculations with SimNIBS. In: *Brainbox Initiative Conference*.
- Thut G, Bergmann TO, Fröhlich F, Soekadar SR, Brittain JS, Valero-Cabr e A, Sack AT, Miniussi C, Antal A, Siebner HR, Ziemann U, Herrmann CS (2017) Guiding transcranial brain stimulation by EEG/MEG to interact with ongoing brain activity and associated functions: A position paper. *Clin Neurophysiol* 128:843–857 Available at: <http://dx.doi.org/10.1016/j.clinph.2017.01.003>.
- To WT, Ost J, Hart J, Ridder D De, Vanneste S (2017) The added value of auditory cortex transcranial random noise stimulation ( tRNS ) after bifrontal transcranial direct current stimulation ( tDCS ) for tinnitus. *J Neural Transm* 124:79–88.
- Tricco AC et al. (2018) PRISMA extension for scoping reviews (PRISMA-ScR): Checklist and explanation. *Ann Intern Med* 169:467–473.
- Tu YK (2016) Testing the relation between percentage change and baseline value. *Sci Rep* 6:23247.
- van der Groen O, Mattingley JB, Wenderoth N (2019) Altering brain dynamics with transcranial random noise stimulation. *Sci Rep* 9:1–8.
- van der Groen O, Tang MF, Wenderoth N, Mattingley JB (2018) Stochastic resonance enhances the rate of evidence accumulation during combined brain stimulation and perceptual decision-making. *PLoS Comput Biol* 14:1–17.

- van der Groen O, Wenderoth N (2016) Transcranial Random Noise Stimulation of Visual Cortex: Stochastic Resonance Enhances Central Mechanisms of Perception. *J Neurosci* 36:5289–5298.
- van der Plas M, Wang D, Brittain JS, Hanslmayr S (2020) Investigating the role of phase-synchrony during encoding of episodic memories using electrical stimulation. *Cortex* 133:37–47 Available at: <https://doi.org/10.1016/j.cortex.2020.09.006>.
- Van Doren J, Langguth B, Schecklmann M (2014) Electroencephalographic Effects of Transcranial Random Noise Stimulation in the Auditory Cortex. *Brain Stimul* 7:807–812 Available at: <http://dx.doi.org/10.1016/j.brs.2014.08.007>.
- Vanneste S, Fregni F, Ridder D De (2013) Head-to-head comparison of transcranial random noise stimulation , transcranial AC stimulation , and transcranial DC stimulation for tinnitus. 4:31–33.
- Vázquez-Rodríguez B, Avena-Koenigsberger A, Sporns O, Griffa A, Hagmann P, Larralde H (2017) Stochastic resonance at criticality in a network model of the human cortex. *Sci Rep* 7:1–12.
- Vieira PG, Krause MR, Pack CC (2020) tACS entrains neural activity while somatosensory input is blocked. *PLoS Biol* 18:1–14 Available at: <http://dx.doi.org/10.1371/journal.pbio.3000834>.
- Vöröslakos M, Takeuchi Y, Brinyiczki K, Zombori T, Oliva A, Fernández-Ruiz A, Kozák G, Kincses ZT, Iványi B, Buzsáki G, Berényi A (2018) Direct effects of transcranial electric stimulation on brain circuits in rats and humans. *Nat Commun* 9 Available at: <http://dx.doi.org/10.1038/s41467-018-02928-3>.
- Vucic S, Howells J, Trevillion L, Kiernan MC (2006) Assessment of cortical excitability using threshold tracking techniques. *Muscle and Nerve* 33:477–486.
- Vucic S, Kiernan MC (2017) Transcranial Magnetic Stimulation for the Assessment of Neurodegenerative Disease. *Neurotherapeutics* 14:91–106 Available at: <http://dx.doi.org/10.1007/s13311-016-0487-6>.
- Vucic S, van den Bos M, Parvathi M, Howells J, Dharmadasa T, Kiernan MC (2018) Utility of threshold tracking transcranial magnetic stimulation in ALS. *Clin Neurophysiol Pract* 3:164–172 Available at: <https://doi.org/10.1016/j.cnp.2018.10.002>.
- Wassermann EM (1998) Risk and safety of repetitive transcranial magnetic stimulation. *Electroencephalogr Clin Neurophysiol* 108:1–16 Available at: <http://www.ncbi.nlm.nih.gov/pubmed/9474057>.
- Watson AB, Pelli DG (1983) QUEST: A general multidimensional bayesian adaptive psychometric method. *Percept Psychophys* 33:113–120.
- Wiesenfeld K, Pierson D, Pantazelou E, Dames C, Moss F (1994) Stochastic resonance on a circle. *Phys Rev Lett*.
- Woods AJ et al. (2015) A technical guide to tDCS, and related non-invasive brain stimulation tools. *Clin Neurophysiol* 127:1031–1048 Available at: <http://dx.doi.org/10.1016/j.clinph.2015.11.012>.
- Wu J, Jin M, Qiao Q (2017) Modeling electrical stimulation of retinal ganglion cell with optimizing additive noises for reducing threshold and energy consumption. *Biomed Eng Online* 16:1–14.
- Zeng F-G, Fu Q-J, Morse R (2000) Human hearing by noise. *Brain Res* 869:251–255.
- Zhang M, Cheng I, Sasegbon A, Dou Z, Hamdy S (2021) Exploring parameters of gamma transcranial alternating current stimulation (tACS) and full-spectrum transcranial random noise stimulation (tRNS) on human pharyngeal cortical excitability. *Neurogastroenterol Motil* 33:1–10.
- Zhao H, Qiao L, Fan D, Zhang S, Turel O, Li Y, Li J, Xue G, Chen A, He Q (2017) Modulation of Brain Activity with Noninvasive Transcranial Direct Current Stimulation (tDCS): Clinical Applications and Safety Concerns. *Front Psychol* 8.
- Ziemann U, Reis J, Schwenkreis P, Rosanova M, Strafella A, Badawy R, Müller-Dahlhaus F (2015) TMS and drugs revisited 2014. *Clin Neurophysiol* 126:1847–1868 Available at: <http://dx.doi.org/10.1016/j.clinph.2014.08.028>.

## Appendix

### Supplementary material Chapter 2

**Table 2.1** Summary of the purpose, stimulation parameters and findings of tRNS and RNS studies.

Authors, year	Research question and study protocol	Participants population N, gender, age (M±SD)	Stimulation location	Verum stimulation parameters	Control stimulation parameters	Main finding(s)
<b>1. Physiological effects of tRNS</b>						
<b>1.1 Offline after-effects following tRNS</b>						
Terney et al., 2008	Investigated tRNS effects on cortical excitability and motor task performance. Measured RMT, AMT, SI <sub>1mV</sub> , single-pulse TMS-elicited MEPs, SICl, ICF, LICl, recruitment curves, cortical silent period, serial reaction time task performance, and EEG before and after intervention.	80 healthy volunteers; 48F and 32M; 25.74±5.13, age range: 20–44; all right-handed	4x4cm electrode over left M1, 6x14cm electrode over the contralateral orbit	1mA (peak-to-peak) tRNS (0.1-640Hz), lf-tRNS (0.1–100 Hz), and hf-tRNS (101– 640 Hz) with 0mA offset, for 10 min in several experiments	30s tRNS	Increased cortical excitability (probed with MEP amplitude) up to 60 min after tRNS, hf-tRNS was most effective with regard to changing the level of cortical excitability. Decreased reaction time after tRNS (in blocks 5-6 out of 14).
Antal et al., 2010	Investigated whether brain-derived neurotrophic factor (BDNF) gene polymorphism is important for neuromodulation induced by iTBS, tDCS, tRNS. Measured single-pulse TMS-elicited MEPs and SI <sub>1mV</sub> before and after intervention.	64 healthy volunteers with different BDNF gene polymorphisms (retrospective analysis from different studies); 28F, 36M; age range: 19-42 years; all right-handed	tRNS: 4x4cm electrode over left M1, 6x14cm electrode over the contralateral orbit tDCS: 5x7cm electrodes	1mA intensity for tRNS (0.1-640Hz) with 0mA offset, and tDCS 10 min tRNS, 7-9 min a-tDCS and 13 min c-tDCS; 2-second train of iTBS (three pulses at 50 Hz repeated at 5 Hz) was repeated every 10s;	2 groups of different genotypes	tRNS did not affect the 2 genotype groups differently. The impact of BDNF polymorphism on neuromodulation in humans might differ according to the mechanism of plasticity induction.
Moliadze et al., 2010	Investigated the importance of the distance between stimulation electrodes, in various montages, on the ability to induce sustained cortical excitability changes using tDCS and tRNS. Measured single-pulse TMS-elicited MEPs with SI <sub>1mV</sub> before, during and after intervention.	11 healthy volunteers in tRNS experiment; 26 ± 3; all right-handed	4x4cm electrode over left M1, 6x14cm electrode over contralateral forehead vs contralateral upper arm – for tRNS experiment	1mA tRNS (0.1-640Hz) with 0mA offset, for 10 min per electrode montage	2 electrode montages	The effects of tRNS on the targeted area are dependent on the distance between the electrodes. Using extracephalic reference electrodes with tES techniques, the stimulation intensity has to be adapted to account for interelectrode distance.
Chaieb et al., 2011	Investigated whether a shorter duration of tRNS can induce a change in cortical excitability. Measured RMT, AMT, SI <sub>1mV</sub> , and single-pulse TMS-elicited MEPs before and after intervention.	22 healthy volunteers; 4F and 18M; age range: 20–30; 15 right-handed	4x4cm electrode over left M1, 6x14cm electrode over contralateral orbit	1mA hf-tRNS (101-640Hz) with 0mA offset, for 4, 5 or 6 min	30s tRNS	A minimal stimulation duration of 5 minutes is required to induce facilitatory after-effects of tRNS on cortical excitability (increased MEP amplitude). The after-effects persist for up to 10 min.

Moliadze et al., 2012	Investigated the dose-response relationship between tES intensity and the induced after-effects. Measured single-pulse TMS-elicited MEP with $SI_{1mV}$ before and after intervention.	25 healthy volunteers; 6F and 19M; 25.9±2.35; age range: 23–30; all right-handed	4x4cm electrode over left M1, 6x14cm electrode over contralateral orbit	0.2, 0.4, 0.6, 0.8, 1mA of tRNS (0.1-640Hz) with 0mA offset and 140 Hz tACS; 6 sessions of each tES applied for 10 min on separate days, with 5s fade-in/out	sham*	Different intensities of high frequency tES result in enhancement or reduction of M1 excitability. 1mA tES results in excitation, intermediate intensity ranges of 0.6 and 0.8 mA had no effect at all, 0.4 mA induced inhibition (stronger for 140 Hz tACS than that induced by tRNS).
Moliadze et al., 2014	Investigated the efficacy of three stimulation methods inducing excitability enhancement in the motor cortex: a-tDCS, iTBS, and tRNS. Measured single-pulse TMS-elicited MEPs with $SI_{1mV}$ before and after intervention.	12 healthy volunteers; age: 25.7±4.1; range: 23–38; all right-handed	4x4cm electrode over left M1, 6x14cm electrode over contralateral orbit	1mA tRNS (0.1-640Hz) and a-tDCS each for 10 min 2s train of iTBS (bursts of 3 pulses at 50 Hz repeated at 5 Hz and an intensity of 80% AMT) was repeated every 10s for a total of 190s (600 pulses) for 3 min; separate sessions counterbalanced order; double blinded	30s tDCS	Among the stimulation methods, tRNS resulted in the strongest cortical excitability increase, and a-tDCS led to significantly longest excitability enhancement compared to sham. Different time courses of the applied stimulation methods suggest different underlying mechanisms of action.
Laczó et al., 2014	Investigated the efficacy of tRNS and tDCS on the leg area of motor cortex. Measured RMT, IO curve, single-pulse TMS-elicited MEPs with $SI_{1mV}$ before and after intervention.	10 healthy volunteers; 5F, 5M; 27.4±3.95, age range: 22–34; 8 right-handed	5x7cm electrodes over leg M1, and over contralateral orbit	2mA a-tDCS, c-tDCS, (peak-to-peak) hf-tRNS (100-640Hz) with 8s fade-in/out, applied for 10 min on separate days in randomized order (5 days in between)	30 s of 2mA a-tDCS or c-tDCS, with an 8s fade-in/out	Leg area can be reached by weak transcranial currents. Anodal tDCS induced a constant gradual increase of cortical excitability until 60 min post-stimulation, whereas the effect of tRNS was immediate with a duration of 40 min following stimulation. Cathodal tDCS induced a decrease in MEP amplitude which did not reach statistical significance.
Van Doren et al., 2014	Investigated the effects of tRNS over AC on resting state and evoked activity in healthy subjects. Measured ASSRs with EEG during rest and auditory stimulation, before and after intervention.	14 healthy volunteers; 7F, 7M; 24.6±1.9; all right-handed	5x7cm electrodes over T8 and over T7; both oriented in anterior-posterior direction with the inferior center on the T position	2 mA hf-tRNS (101-640 Hz), with 0mA offset, for 20 min with a 10s fade-in/out 1 week between verum and sham	10s fade-in/out 2mA tRNS	tRNS increased excitability of the auditory cortex, reflected by an increased ASSR to auditory stimulation and a non-significant trend toward an increase in mean theta band power.
Chaieb et al., 2015	Investigated the efficacy data with regard to the possible neuronal effect of tRNS using pharmacological intervention. Measured RMT, AMT, $SI_{1mV}$ and TMS-elicited MEPs before and after tRNS and a pharmacological agent vs placebo. Pilot study.	8 healthy volunteers; 0F, 8M; 30.1±5.2; 7 right-handed	4x4cm electrode over left M1, 6x14cm electrode over contralateral orbit;	1mA tRNS (0.1-640Hz) for 10 min; 6 experimental sessions were separated by a 2 weeks interval; double blinded	5 pharmacological interventions vs placebo	Mechanism of tRNS-induced neuroplastic effects is related to sodium channel activity and $\gamma$ -Aminobutyric acid type A (GABA <sub>A</sub> ) receptors, but, unlike tDCS, independent of N-methyl-D-aspartate (NMDA) receptors.
Ho et al., 2015	Investigated the effect of tRNS with and without a DC offset on motor cortical excitability and compared results to tDCS. Measured single-pulse TMS-elicited MEPs, SIC1 and ICF before and after interventions.	15 healthy volunteers; 7F, 8M; 24±6.07; all right-handed	5x7cm electrodes over left M1, and over right contralateral supraorbital area	1mA tDCS, 2mA tDCS, 2mA (peak-to-peak) hf-tRNS (100-640Hz) with 0mA offset, and 2mA (peak-to-peak) hf-tRNS + 1mA DC offset, 10 min with a 30s fade-in/out, on 5 experimental sessions (randomized order) separated by 4 days	30s tRNS with 10s fade in	Although differences between the stimulation conditions did not reach statistical significance, the findings suggest that stimulation involving DC (tDCS and hf-tRNS including DC offset) but not solely tRNS is more likely to lead to an increase in cortical excitability.

Inukai et al., 2016	Investigated the efficacy of a-tDCS, tRNS and tACS methods for increasing cortical excitability using the same subject population and same current intensity. Measured single-pulse TMS-elicited MEPs with $SI_{1mV}$ before and after interventions.	15 healthy volunteers; 7F, 8M; 24±6.07; all right-handed	5x7cm electrodes over left M1, and over right contralateral orbit	1 mA a-tDCS, tRNS (0.1-640Hz) with 0mA offset, and 140 Hz tACS for 10 min with 10s fade-in/out  4 sessions, 3 days apart	30s tDCS	tRNS was shown to be more effective than a-tDCS and 140Hz tACS in increasing cortical excitability compared to both pre-stimulation and sham conditions. tRNS- and tACS-induced effects were correlated across participants.
Herpich et al., 2018	Investigated whether priming the visual cortex with tRNS leads to increased and sustained excitability. Measured visual phosphenes threshold before and after intervention.	Exp.1a: 18 healthy volunteers; 11F, 7M; mean age: 22.9; all right-handed; 6 excluded Exp.1b: 11 healthy volunteers; 7F, 4M; mean age = 20.1; all right-handed; 3 excluded Exp.2: 22 healthy volunteers; 6F, 16M; mean age = 20.9; all right-handed; 10 excluded	35cm <sup>2</sup> electrodes over O1/PO7 and O2/PO8 (tRNS) or over Oz and Cz (a-tDCS)	1mA hf-tRNS (101-640Hz) with 0mA offset and 1mA a-tDCS for 20 min with a 15s fade-in/out	5s tRNS fade-in/fade-out	Phosphene thresholds were significantly reduced after tRNS up to 60 min post stimulation relative to baseline, a behavioral marker of increased excitability of the visual cortex, while a-tDCS had no effect.
Qi et al., 2019	Investigated whether execution-dependent motor cortex excitability is affected by prior interaction between tRNS and action observation. Measured single-pulse TMS-elicited MEPs with $SI_{1mV}$ before action observation, immediately after, and after performing action execution.	129 healthy volunteers; 81F, 48M; 24.42 ± 3.84; age range: 18–37; all right-handed	5x5cm electrodes over left M1, and over contralateral supraorbital region	1mA (peak-to-peak) hf-tRNS (101-640Hz) for 10 min with 5 s fade-in/out	30s tRNS	Prior interaction between hf-tRNS and action observation of mirror-matched movements enhanced M1 excitability. The subsequent congruent goal-directed actions further enhanced the respective excitability alterations.
Parkin et al., 2019	Investigated excitatory and inhibitory tES effects after stimulation delivered via unilateral versus bilateral electrode montage. Measured single-pulse TMS-elicited MEPs with $SI_{1mV}$ before and after tES intervention execution.	51 healthy volunteers; 32F, 19M; mean age: 20.6; age range: 18–27; all right-handed Exp.1a: 8, Exp.1b: 9, Exp.1c: 9, Exp.2a: 17, Exp.2b: 8	5x7cm electrodes over left M1, and over contralateral orbit (unilateral) or right M1(bilateral)	1mA unilateral or bilateral tDCS for 10 min with a 15s fade-in/out 1mA (peak-to-peak) unilateral or bilateral hf-tRNS (101-640Hz) with 0mA offset for 10 or 20 min with 20s fade-in/out	2 electrodes montages	Effects of unilateral tES do not extend to the bilateral montage (for tRNS and tDCS) and to longer (double) stimulation duration (tRNS).
Moret et al., 2019	Investigated whether both the lower and the higher half of the high-frequency band are needed for increasing neural excitability with tRNS. Measured single-pulse TMS-elicited MEPs with $SI_{1mV}$ before and after intervention.	14 healthy volunteers; 14F, 0M; mean age 21 age range: 19–25; all right-handed	16cm <sup>2</sup> electrode over left M1, 60cm <sup>2</sup> electrode over contralateral orbitofrontal area	1.5 mA low-hf-tRNS (100–400 Hz), high-hf-tRNS (400–700 Hz), whole-hf-tRNS (100–700 Hz) with 0mA offset, for 10 min with 30s fade-in; intervals between sessions 1-3 days (and 2 months between experiments low/high and whole hf-tRNS)	30s 1.5mA tRNS (15s fade-in/out)	Efficacy of hf-tRNS is related to the width of the selected frequency range. Only the full-high frequency band condition (100–700 Hz) modulated cortical excitability. Neither the higher nor the lower sub-range of the high-frequency band significantly modulated cortical excitability.



Kortuem et al., 2019	Investigated the effect of corticospinal excitability during sham stimulation on the individual response to tRNS and tACS. Measured single-pulse TMS-elicited MEPs with $SI_{1mV}$ before and after intervention.	30 healthy volunteers; 10F, 20M; 24.2±2.8, age range: 18–30; all right-handed	5x7cm electrodes over left M1, and over contralateral supraorbital area	1mA tRNS (0.1-640Hz) and 140 Hz tACS for 10 min, with 5s fade-in/out; sessions separated by at least 7 days	sham*	Individual responsiveness to sham stimulation can serve as a potential predictor of the variable effects of tRNS. Participants who did not exhibit any modulation of MEP amplitude after sham stimulation showed effects of active tRNS. In contrast, those who respond to sham (in both directions) did not present any response in the verum stimulation condition
Schoiswohl et al., 2021	Investigated the effects of high- and low-frequency tRNS on excitability of AC. Measured ASSR of 20 and 40Hz stimuli as well as power of oscillatory brain activity using EEG before and after tRNS.	22 healthy volunteers; 11F, 11M; 24.18±2.89; age range: 19–31	5x7cm electrodes over the left (FT7, FC5, C5, T7, CP5, TP7) and the right hemisphere (FT8, FC6, C6, T8, CP6, TP8); both oriented in anterior-posterior direction	2mA lf-tRNS (0.1-100Hz) and hf-tRNS (101-640Hz) for 20 min with 10s fade-in/out	10s fade-in/out	Stimulation of both verum tRNS protocols revealed no significant changes either in ASSR or in resting state EEG activity. Sham tRNS resulted in a significant decrease in 20Hz ASSR and an increase in the alpha frequency band (8–12.5Hz).
Zhang et al., 2021	Investigated the effects and optimal stimulation parameters of tACS and tRNS for modulating excitability of human pharyngeal motor cortex. Measured single-pulse TMS-elicited pharyngeal MEPs and thenar MEPs before and after intervention.	15 healthy volunteers; 9F, 6M; 24±8; age range: 18–50	5x7cm electrodes over the “pharyngeal” area of M1 assessed with TMS and over contralateral supraorbital ridge	1.5mA (peak-to-peak) tACS (10Hz alpha, 20Hz beta, and 70Hz gamma) and tRNS (0.1–640Hz) for 10 min with 10s fade-in/out	10s of 20Hz tACS	Both gamma tACS and tRNS enhanced human pharyngeal cortical excitability. A significant MEP interaction was found both in the stimulated pharyngeal cortex and in the ipsilateral thenar cortex. Compared to sham, subsequent post hoc tests showed site-specific and sustained (60–120 min) increases in pharyngeal MEPs with tRNS and gamma tACS, and for thenar MEPs with beta tACS.
<b>1.2 Acute online effects during tRNS</b>						
Potok et al., 2021	Investigated the influence of tRNS on cortical responsiveness. Measured RMT and probability of single-pulse TMS-elicited MEPs during brief tRNS delivery.	81 healthy participants, 46F, 35M; 25.5±5; age range: 18-46, all right-handed Exp.1: 16 (9F, 7M, 24.7±5, age range: 19–35); Exp.2: 22 (13F, 9M; 25.4±5.4; age range: 20–46); Exp.3: 20 (10F, 10M; 27.5±6; age range: 28–42); Exp.4: 23 (14F, 9M; 24.3±3.9; age range: 19–34)	Exp.1 and 2: 5x7cm electrodes over left and right M1 Exp.3 and 4: 5x7cm electrodes placed ±7cm anterior and posterior to the left M1 along the coil axis (45° away from the nasion-inion mid-sagittal line)	0.5-2mA (peak-to-baseline) hf-tRNS (100-500Hz) with 0mA offset for 3 s per trial with 0s fade-in/out vs no tRNS or active control (randomly interleaved)	no tRNS or active control condition (2mA peak-to-baseline hf-tRNS for 3s per trial)	tRNS acutely modulates the responsiveness of neural circuits of human M1 reflected in the immediate decrease in RMT and increase in probability of eliciting MEP for subthreshold TMS.
<b>2. Behavioral effects</b>						
<b>2.1 Offline after- and learning effects following tRNS</b>						
<b>2.1.1 Visual perception</b>						
Fertonani et al., 2011	Investigated the possibility of inducing differential plasticity effects using tDCS and tRNS during visual perceptual	99 healthy volunteers; all right-handed;	16cm <sup>2</sup> electrode over occipital cortex (3.5 ± 0.2 cm above	1.5mA hf-tRNS (100 – 640 Hz), lf-tRNS (0.1–100 Hz) with 0mA offset, a-tDCS, c-tDCS	20s stimulation and active control condition	tRNS modulates learning effects during orientation discrimination task execution.

	learning training as measured with orientation discrimination task performance.	normal or corrected to normal vision Pilot: 6 participants, 4F, 2M; 35.0±7.2; age range 29–48; Main Exp.: 84 participants 42 males, mean age 21.7±2.5; age range 19-30; 6 groups x14sbj; Control hf-tRNS Exp.: 9 participants, 6F 3M, 31.7±3.9; age range 24–38	the inion) or over Cz (active control), and 60cm <sup>2</sup> electrode on the right arm	for 4 min x 5 first blocks (~22 min total)		hf-tRNS significantly improved performance accuracy compared with a-tDCS, c-tDCS, sham, and active control site stimulations.
Pirulli et al., 2013	Investigated how different types of tES (tDCS and tRNS) can modulate behavioral performance in the healthy adult brain in relation to their timing of application. Two protocols tested: before (offline) or during (online) visual perceptual learning training. Measured orientation discrimination task performance.	90 healthy volunteers 45F, 45M, 21.8±2.9, age range: 19-32; all right-handed; normal or corrected to normal vision; 6 groups (online stimulation data from Fertonani 2011)	16cm <sup>2</sup> electrode over occipital cortex V1 (3.5 ± 0.2 cm above the inion), 60cm <sup>2</sup> electrode on the right arm	1.5mA offline-hf-tRNS (101 – 640 Hz) online-hf-tRNS (101 – 640 Hz) with 0mA offset, offline-a-tDCS online-a-tDCS for 4 min x 5 blocks (~total 20 min)	20s tDCS online-sham offline-sham	Timing of tES protocols yields opposite effects on performance. tRNS facilitated task performance only when it was applied during task execution, whereas anodal tDCS induced a larger facilitation if it was applied before task execution.
Pirulli et al., 2016	Investigated differences in visual perceptual learning caused by the position of the so-called reference electrode relative to the active electrode. Measured orientation discrimination task performance before and after tRNS, tRNS-reversed, or sham.	33 healthy volunteers; 20 F, 13 M; 25.1±5.5; 11 per group;	16cm <sup>2</sup> electrode over occipital lobe, 60cm <sup>2</sup> electrode over the right upper arm (in the tRNS-reversed condition the cable connections with the stimulator were reversed)	1.5 mA (peak-to-peak) hf-tRNS (100-640 Hz) for 4 min x 5 blocks	sham*	tRNS over the occipital cortex improved subject performance in the orientation discrimination task irrespective of the electrode configuration used. Effects of both tRNS and tRNS-reversed were different from sham, but not different from each other.
Contemori et al., 2019	Investigated the effect of tRNS on perceptual learning (peripheral crowding task) and transfer in peripheral high-level visual tasks measured before and after intervention.	32 healthy volunteers; 17F, 15M; mean age 25, age range: 20-32; normal or corrected to normal vision	16cm <sup>2</sup> electrode over occipital cortex (3cm above the inion), 27cm <sup>2</sup> electrode over the vertex	1.5mA (amplitude) hf-tRNS (100-640Hz) with 0mA offset for 30 min	15s fade-in/out	Coupling tRNS to the early visual cortex with perceptual learning of a peripheral crowding reduction task is effective in boosting between-session learning but does not increase transfer of learning to untrained visual functions with respect to perceptual learning alone. After training, the tRNS group showed greater learning rate (decrease in crowding threshold) with respect to the sham group. For both groups, learning generalized to the same extent to the untrained retinal location and task.
Fertonani et al., 2019	Investigated tRNS and a-tDCS of the V1 during visual perceptual learning in healthy young and older individuals.	45 young participants; 22F, 23M; 22.3±3.1 with normal or corrected-to-normal vision.	16cm <sup>2</sup> electrode over Oz; 60cm <sup>2</sup> electrode over right shoulder	1.5mA a-tDCS and 1.5mA hf-tRNS (101-600Hz) with 0mA offset for 22 min	20s tES at the beginning and at the end	Only the tRNS in the young, but not in the older, subjects modulated visual perceptual learning, by decreasing performance. TEP-revealed age-related changes in connectivity, that is, a stronger activation of the prefrontal cortex after visual cortex stimulation, and a stronger

	Measured orientation discrimination task performance and TEP over V1 before and after intervention.	36 older participants; 21F, 15M; 66.1±3.6; with normal or corrected-to-normal vision 3 stimulation groups				modulation of the prefrontal cortex after visual perceptual learning in the older subjects.
Herpich et al., 2019	Investigated the effect of tRNS on visual perceptual learning in intact and brain-damaged humans. Tested whether tRNS of V1 during training can enhance and speed up the resultant perceptual learning. Measured motion discrimination task performance.	45 healthy volunteers; 32 F, 13M; mean age: 19, age range: 19–36; normal or corrected to normal vision; all right-handed; 15 per group 11 patients with cortical blindness; normal or corrected to normal visual acuity; all right-handed; 3 tRNS, 2 sham, 6 only training	tRNS: 35cm <sup>2</sup> electrodes positioned bilaterally over O1 and O2 a-tDCS: 35cm <sup>2</sup> electrodes over Oz and Cz active control tRNS: 35cm <sup>2</sup> electrodes positioned bilaterally over P3 and P4	1mA hf-tRNS (101-640Hz) or a-tDCS For 20 min with 20s of fade-in/out, 10 days of training and follow-up after 6 months	sham group: 20s tRNS; no stimulation condition; active control condition	Enhancement of the capacity for long-lasting plastic and restorative changes when a neuromodulatory intervention is coupled with visual training (motion perception). Relative to control conditions and anodal stimulation, tRNS-enhanced learning was at least twice as fast, and, crucially, it persisted for 6 months after the end of training and stimulation. Notably, tRNS also boosted learning in patients with chronic cortical blindness, leading to recovery of motion processing in the blind field after just 10 days of training, a period too short to elicit enhancements with training alone.
Ghin et al., 2021	Investigated the spatial and temporal dynamics of cortical activity modulated by offline hf-tRNS on performance of a motion direction discrimination 2IFC task. Measured amplitude of motion-related VEPs over the parieto-occipital cortex, oscillatory PSD at rest, as well as shift in ERSP in response to the motion stimuli between the pre- and post-stimulation period, using EEG.	16 healthy volunteers; 9F, 7M; age range 19–33 all right-handed	16cm <sup>2</sup> electrodes over PO3 and PO4, bilaterally over the parieto-occipital cortex	1.5mA hf-tRNS (100-600Hz) with 0mA offset for 20 min	30s 1.5mA tRNS	Offline hf-tRNS may induce moderate after-effects in brain oscillatory activity but not behavioral task performance. The accuracy of the motion direction discrimination task was not modulated by offline hf-tRNS. Although the motion task was able to elicit motion dependent VEP components (P1, N2, and P2), none of them showed any significant change between pre- and post-stimulation. There was a time-dependent increase in the PSD in alpha and beta bands regardless of the stimulation protocol. The time–frequency analysis showed a modulation of ERSP power in the hf-tRNS condition for gamma activity when compared to pre-stimulation periods and Sham stimulation.
<b>2.1.2 Somatosensory perception</b>						
Saito et al., 2019	Investigated the effects of tES applied to primary somatosensory cortex on SEP-PPD and tactile discrimination performance. Measured N20/P25_SEP-PPD, N20_SEP-PPD, and P25_SEP-PPD responses and grating orientation task performance assessed before and immediately after tES applied to primary somatosensory cortex.	17 healthy volunteers; 0F, 17M; 22.0±1.1; 16 right-handed	5x5cm electrodes located 3 cm posterior to C3 (left primary somatosensory cortex), and over the contralateral orbit	0.7mA a-tDCS, a-tPCS (50ms pulse, 5ms IPI), tACS (140Hz, Exp.1), tRNS (0.1-640Hz), 0mA offset, for 10 min with 10s fade-in/out 4 (or 3 in Exp.2) sessions with 3 days break	30s tDCS	tRNS and anodal tPCS can improve sensory perception by modulating neuronal activity in primary somatosensory cortex. a-tDCS and a-tPCS decreased N20_SEP-PPD, and tRNS increased the first N20 SEP amplitude. tRNS and a-tPCS improved grating orientation task performance, reflected in decreased discrimination threshold.
<b>2.1.3 Motor function</b>						
Chaieb et al., 2009	Measured BOLD fMRI to monitor modulations in human sensorimotor activity (activation maps for a right-hand index–thumb finger-tapping task) after the application of 4-min tRNS.	9 healthy volunteers; 3F, 6M; age range: 21-32; all right-handed	4x4cm electrode over sensorimotor cortex, 6x14cm electrode over contralateral orbit	1mA tRNS (0.1-640Hz) with 0mA offset for 4 min	sham*	Short-duration application of tRNS can induce a transient decrease in BOLD activity in the human primary sensorimotor cortex, using a classical finger-tapping task.

Saiote et al., 2013	Investigated the effects of tDCS and tRNS in the early and later stages of visuomotor learning, as well as associated brain activity changes using fMRI (throughout the experiment). Measured motor task performance changes after the stimulation.	52 healthy volunteers; 30F, 22M; 27±6; age range: 20-50; all right-handed 5 groups of 10 people a-tDCS, c-tDCS, lf-tRNS, hf-tRNS, sham	5x7cm MRI compatible electrodes over left M1 and over contralateral right orbit	1mA a-tDCS, c-tDCS, lf-tRNS (0.1-100Hz) or hf-tRNS (101-640Hz) for 10 min of a task with 20s fade-in and 10s fade-out	20s fade-in and 10s fade-out	lf-tRNS and hf-tRNS differentially modulate visuomotor learning. Cathodal tDCS and hf-tRNS showed a tendency to improve and lf-tRNS to hinder early learning during stimulation, an effect that remained for 20 minutes after cessation of stimulation in the late learning phase. Motor learning-related activity decreased in several regions, however, there was no significant modulation of brain activity by tDCS. hf-tRNS was associated with reduced motor task-related-activity bilaterally in the frontal cortex and precuneus, probably due to interaction with ongoing neuronal oscillations.
Prichard et al., 2014	Investigated whether tDCS and tRNS alter aspects of learning a tracing task: skill acquisition (online/within session effects) or consolidation (offline/between session effects).	91 healthy volunteers; 52F, 39M; 25.7±4.6; all right-handed 5 groups with 18 participants	16cm <sup>2</sup> electrodes over: tDCS and tRNS: M1 and contralateral supraorbital area; tDCS: left and right M1; tRNS: right T6 and contralateral supraorbital area (control)	1mA tDCS or hf-tRNS (100-640Hz) For 20 min with 15s fade-in/out; during the task 3 consecutive days	30s tRNS or tDCS	Unilateral M1 stimulation using tRNS as well as unilateral and bilateral M1 tDCS all enhanced motor skill learning compared to sham stimulation. In all groups, this appeared to be driven by online effects without an additional offline effect. Unilateral tDCS resulted in large skill gains immediately following the onset of stimulation, while tRNS exerted more gradual effects. Control stimulation of the right temporal lobe did not enhance skill learning relative to sham.
Abe et al., 2019	Investigated the effects of tRNS on both corticospinal excitability and motor performance. Measured single-pulse TMS-elicited MEPs with SI <sub>1mv</sub> and performance of visuomotor tracking task by isometric abduction motion of the right index finger before and after intervention.	16 healthy volunteers; 4F, 12M; 21±0.35; all right-handed	5x7cm electrodes over left M1, and over right front forehead area	1mA of tRNS (0.1-640Hz) for 10 min with 10s fade-in/out tRNS vs sham separated by 1 week	30s tRNS	tRNS over M1 is effective for enhancing cortical excitability as well as for motor performance. Significant increase in MEP amplitudes immediately and 10 min after tRNS, motor performance improved 10 min after tRNS.
De Albuquerque et al., 2019	Investigated the influence of tRNS on motor skill acquisition and retention in a complex golf putting task. Measured task performance before, during and after intervention.	34 healthy volunteers, 0F, 34M; 23.1 ± 2.8; age range: 18-30, all right-handed tRNS vs sham group	7x5cm electrodes over M1 and over the contralateral supraorbital region	2mA hf-tRNS for 20min during task performance	30s tRNS with 10s fade-in/out	Acute application of tRNS failed to enhance skill acquisition or retention in a golf putting task – no difference between tRNS and sham groups
Hoshi et al., 2021	Investigated the effects of tRNS timing on corticospinal excitability and motor function when combined with motor training. Measured single-pulse TMS-elicited MEPs with SI <sub>1mv</sub> and visuomotor tracking task performance before and after tRNS and motor training.	15 healthy volunteers; 0F, 15M; 21.32 ± 0.58; all right-handed	5x7cm electrodes over left M1, and over contralateral orbital area	1mA tRNS (0.1–640 Hz) for 10 min, with 10s fade-in/out, before, during or after motor training. Crossover design with 4 conditions randomly performed with a break of at least one week between each condition.	30s tRNS	The timing of tRNS affects corticospinal excitability but not motor learning. The corticospinal excitability increased after tRNS in the before and during conditions but not in the after condition. Motor function after motor training improved in all conditions, but there were no significant differences between these conditions.
<b>2.1.4 Clinical: visual perception</b>						
Camilleri et al., 2014	Investigated whether a short behavioral training using a contrast detection task combined with online tRNS was as	16 volunteers with mild myopia, mean	16cm <sup>2</sup> electrode over occipital cortex, 3cm above theinion,	1.5mA hf-tRNS (100-640Hz) with 0mA offset for 5min	training without tRNS	The combination of behavioral training and tRNS can be fast and efficacious in improving sight in individuals with mild myopia. After 2 weeks of perceptual training in combination

	effective in improving visual functions in participants with mild myopia compared to a 2-month behavioral training without tRNS. Measured UCVA and UCCS before and after intervention using Landolt-C and Grating tests of the FrACT.	age 24.12, age range: 19 and 27 2 groups of 8 people tRNS+training vs training only	60cm <sup>2</sup> electrode over upper right arm	during 5 first training blocks (total 25min stimulation) 8 sessions		with tRNS, participants showed an improvement of 0.15 LogMAR in UCVA that was comparable with that obtained after 8 weeks of training with no tRNS, and an improvement in UCCS at various spatial frequencies (whereas no UCCS improvement was seen after 8 weeks of training with no tRNS). A control group that trained for 2 weeks without stimulation did not show any significant UCVA or UCCS improvement.
Campana et al., 2014	Investigated whether shorter perceptual training combined with hf-tRNS can improve visual functions in a group of adult participants with amblyopia. Measured VA and CS function using Landolt-C and Grating tests of Freiburg Visual Acuity Test and CRS Psycho 2.36 test. Pilot study.	7 volunteers with anisometric amblyopia, mean age: 39.2, age range: 26-52	16cm <sup>2</sup> electrode over occipital cortex, 3cm above theinion, 60cm <sup>2</sup> electrode over forehead	1.5mA hf-tRNS (100-640Hz) with 0mA offset for 5min during 5 first training blocks (total 25min stimulation) 8 sessions	none	Eight sessions of training in contrast detection under lateral masking conditions combined with hf-tRNS, were able to substantially improve VA and CS function in adults with amblyopia.
Camilleri et al., 2016	Investigated the efficacy of a short training (8 sessions) using a single Gabor contrast-detection task with concurrent hf-tRNS in comparison with the same training with sham stimulation or hf-tRNS with no concurrent training, in improving VA and CS of individuals with uncorrected mild myopia. Measured UCVA and UCCS using Landolt-C and Grating tests of FrACT before and after intervention	30 volunteers with mild myopia, mean age 25.32, age range: 19 and 29 3 groups of 10 people tRNS+training vs sham+training vs tRNS only	16cm <sup>2</sup> electrode over occipital cortex, 3cm above theinion, 60cm <sup>2</sup> electrode over forehead	1.5mA hf-tRNS (100-640Hz) with 0mA offset for 5min during 5 first training blocks (total 25min stimulation) 8 sessions	20s tRNS at the beginning of each block	Hf-tRNS coupled with a short training of contrast detection task is able to improve VA and CS, whereas no effect on VA and marginal effects on CS are seen with the sole administration of hf-tRNS.
Moret et al., 2018	Investigated the efficacy hf-tRNS combined with a short perceptual training (2IFC task contrast detection of a central Gabor patch flanked by two high-contrast collinear Gabors - lateral masking) in adults with amblyopia. Measured VA and CS before and after intervention.	20 volunteers with amblyopia, 12F, 8M, mean age 44, age range: 27 and 58 2 groups of 10 people tRNS+ training vs sham+ training	16cm <sup>2</sup> electrode over occipital cortex, 3cm above theinion, 60cm <sup>2</sup> electrode over forehead	1.5mA hf-tRNS (100-640Hz) with 0mA offset for 5min with 30s fade-in during 5 first training blocks (total 25min stimulation) 8 sessions	30s fade-in/out 1.5mA tRNS	Significant and similar improvement of CS for both groups, suggesting that hf-tRNS is not crucial for the improvement of CS. However, for VA, a significant improvement was only observed in the hf-tRNS group with a mean VA improvement of 0.19 LogMAR in the amblyopic eye after 8 sessions.
Donkor et al., 2021	Investigated whether five daily sessions of tRNS over V1 would improve perceptual learning measured with CS, crowded and uncrowded VA in adults with amblyopia measured during and after stimulation.	19 volunteers with amblyopia, 9F, 10M, 44.2±14.9 tRNS: 9 sham: 10	5x5cm electrodes over Oz, and over Cz	2mA tRNS (0.1-640Hz) for 25min with 30s fade in/out over 5 consecutive days	30s fade-in/out 2mA tRNS	tRNS induced short-term contrast sensitivity improvements in adult amblyopic eyes, and the effects may extend to uncrowded visual acuity. However, multiple sessions of tRNS did not lead to enhanced or long-lasting effects.

### 2.1.5 Clinical: auditory perception

Vanneste et al., 2013	Investigated the efficacy of three different tES techniques: tDCS, tACS, and tRNS applied to AC in tinnitus patients. Measured tinnitus loudness and distress before and after intervention.	111 tinnitus patients 77F, 34M, 49.46±14.37 tinnitus duration 4.18±4.05 tDCS (reversed placement): 16 and 20 tRNS: 38 tACS: 37	35cm <sup>2</sup> electrodes over T3, and over T4 (AC bilaterally)	1.5mA tDCS for 20min with 10s fade in 1.5mA tACS (at IAF peak within the range of 6–13 Hz) for 20min with 10s fade in 1.5mA lf-tRNS (0.1-100Hz) with 0mA offset for 20min with 10s fade in	none	Lf-tRNS induced the larger transient suppressive effect on tinnitus loudness and tinnitus related distress as compared to tDCS and tACS
Joos et al., 2015	Investigated the efficacy of lf-tRNS, hf-tRNS and tRNS on non-pulsatile tinnitus. Measured tinnitus loudness and distress before and after intervention.	154 patients with non-pulsatile tinnitus, 30F, 124M; 53.28±12.11; tinnitus duration 6.92±6.64 lf-tRNS: 119 hf-tRNS: 19 tRNS: 16	35cm <sup>2</sup> electrodes over T3, and over T4	2mA lf-tRNS (0.1-100Hz), hf-tRNS (100-640Hz) and tRNS (0.1-640Hz) with 0mA offset for 20min with 10s fade in	none	Reduction in tinnitus loudness when lf-tRNS and hf-tRNS were applied as well as a reduction in tinnitus-related distress with lf-tRNS. Significantly more pronounced reduction in loudness and distress in pure tone tinnitus compared to narrow band noise tinnitus when hf-tRNS was applied, a difference that could not be obtained with lf-tRNS.
To et al., 2017	Investigated the effects of treatment protocol using multisite tES over tinnitus network (combined bifrontal tDCS and bilateral tRNS) on tinnitus intensity and distress. Measured tinnitus loudness and distress before and after intervention.	40 patients with tinnitus 18F, 22M, 48.33±10.74; tinnitus duration 10.82±14.35 3 groups: tDCS: 12 tDCS+tRNS: 14 waiting list: 14	35cm <sup>2</sup> electrode over left DLPFC (c-tDCS), and over right DLPFC (a-tDCS) 35cm <sup>2</sup> electrode over T3 and T4 (tRNS)	1.5mA tDCS for 20 min with 10s fade in 2mA lf-tRNS (0.1-100Hz) with 0mA offset for 20min with 10s fade in 8 sessions (2x per week for 4 weeks) Waiting list – no treatment	no stimulation group	Multisite treatment tES protocol resulted in more pronounced effects when compared with the bifrontal tDCS protocol or the waiting list group, suggesting an added value of auditory cortex tRNS to the bifrontal tDCS protocol for tinnitus patients.
Mohsen et al., 2018	Investigated the multisite protocol of tRNS by applying lf-tRNS over the AC preceded by hf-tRNS over the right DLPFC in a sham-controlled clinical trial and compare the results to the auditory lf-tRNS. Measured tinnitus loudness and annoyance before and after intervention.	32 patients with tinnitus 9F, 23M, 42±10.96 AC: 16 DLPFC+AC: 16 Each group sham 30min break and real session	35cm <sup>2</sup> electrodes over F4 and FP1 (DLPFC) 35cm <sup>2</sup> electrodes over T3 and T4 (AC)	2mA lf-tRNS (0.1-100Hz) for 20min For multisite protocol 10 min over PFC followed by 10 min over AC	sham*	The multisite tES protocol was more effective in reducing the loudness and annoyance of tinnitus in comparison with auditory cortex tRNS, while the sham stimulation session had no effect.
Mohsen et al., 2019b	Investigated the role of applying eight sessions of multisite tRNS in decreasing tinnitus loudness and annoyance without exerting additional adverse effects. Measured tinnitus loudness and annoyance before and after intervention.	29 patients with tinnitus 8F, 21M, 45.34±9.57 1 session: 17 8 sessions: 12	35cm <sup>2</sup> electrodes over F4 and FP1 (DLPFC) 35cm <sup>2</sup> electrodes over T3 and T4 (AC)	2mA lf-tRNS (0.1-100Hz) over AC and hf-tRNS (100-640Hz) over DLPFC with 0mA offset for 10 min over PFC followed by 10 min over AC with 30s fade-in/out	none	Statistically and clinically significant reduction in tinnitus loudness and annoyance in both groups, while the amount of annoyance suppression in the multiple-sessions group was significantly greater than the single-session group. The patients of the multiple session tRNS group reported an improvement in their sleep and lower tinnitus handicap inventory scores without experiencing any additional adverse effects of the intervention.
Mohsen et al., 2019a	Investigated the modulatory effects of multisite tRNS on the tinnitus network. EEG recorded before and after the session.	32 patients with tinnitus 9F, 23M, 42±10.96 AC: 16 DLPFC+AC: 16	35cm <sup>2</sup> electrodes over F4 and FP1 (DLPFC)  35cm <sup>2</sup> electrodes over T3 and T4 (AC)	2mA lf-tRNS (0.1-100Hz) for 20min  For multisite protocol 10 min over PFC followed by 10 min over AC	10s tRNS	Increased power in the alpha-1 band at the AC and PFC accompanied by decreased power in the delta and beta-2 bands in the PFC after the multisite-tRNS real session. Standardized low-resolution brain electromagnetic tomography (sLORETA) showed a significant decrease in beta-2 activity in the PFC, ACC, and the paraHC and

		Each group sham 30min break and real session				decreased alpha connectivity between the right PFC and the left AC. No significant effects were observed for the sham session.
Kreuzer et al., 2019	Investigated the use of hf-tRNS in a one-arm pilot study in patients with chronic tinnitus. Measured primary (treatment response - tinnitus questionnaire) and secondary outcomes (tinnitus numeric rating scales, depressivity, and quality of life) before and after intervention. Pilot study.	30 patients with tinnitus 4F, 26M, 49.2±10.9 tinnitus duration: 96.0±73.7 months who underwent rTMS treatment before	5x7cm electrodes over T7, and over T8	2mA hf-tRNS (100-640Hz) with 0mA offset for 20 min with 10s fade-in/out 10 sessions (2 weeks Mon-Fri)	none	hf-tRNS is feasible for daily treatment in chronic tinnitus. However, summarizing low treatment response, increase of tinnitus loudness in 20% of patients and missing of any significant secondary outcome, the use of hf-tRNS as a general treatment for chronic tinnitus cannot be recommended at this stage. Differences in treatment responders between tRNS and rTMS highlight the need for individualized treatment procedures.
<b>2.1.6 Clinical: pain and motor function</b>						
Stephani et al., 2011	Investigated stimulation-induced cortical plasticity of iTBS and tRNS in patients with Parkinson's disease. Single-pulse TMS-elicited MEP with SI <sub>1mV</sub> measured before and after intervention.	8 non-tremor-dominant idiopathic Parkinson's disease patients; 1F, 7M; 62.23±8.3	16cm <sup>2</sup> electrode over abductor digiti minimi muscle hotspot and 35cm <sup>2</sup> electrode over contralateral orbital region	iTBS with 80% of RMT or 1mA (peak-to-peak) tRNS (0.1-640Hz) for 10 min	sham iTBS with shielded figure-of-eight coil	Decrease in MEP amplitude after tRNS. No statistical significance for the factor of time or interaction. Anti-parkinsonian drugs were not discontinued in the study and dopaminergic drugs may have contributed to the paradoxical effects of tRNS. No "off" medication control group.
Palm et al., 2016	Investigated the effects of tRNS over DLPFC on attention and neuropathic pain in Multiple Sclerosis patients. Measured pain, attention, mood and electrophysiological parameters (EEG).	16 Multiple Sclerosis patients; age range: 18-70 years; right-handed	25cm <sup>2</sup> electrodes over F3, and over AF8	2mA (peak-to-peak) tRNS (0-500Hz) with 1mA DC offset Two blocks (3 consecutive daily sessions) tRNS/sham separated by 3-week wash-out interval	15s fade-in tRNS	Compared to sham, tRNS showed a trend to decrease the N2-P2 amplitudes of pain related evoked potentials and improve pain ratings. Attention performance and mood scales did not change after stimulations.
Salemi et al., 2019	Investigated the effects of tRNS on fatigue in subjects with relapsing-remitting Multiple Sclerosis with low physical disability. Pilot study	17 Multiple Sclerosis patients; 9 received real tRNS, 6F, 2M, 8 received sham, 6F, 3M,	5x5cm electrode over dominant M1 or contralateral to the most compromised limb; 5x5cm over C3 + FP2 or C4 + FP1	1.5mA hf-tRNS (100-640Hz) with 0mA offset for 15 min over two consecutive weeks (for 10 days)	30s tRNS	In the tRNS group, beneficial effects were observed using the Modified Fatigue Impact Scale (physical subscale), the subscales 'change in health' and 'role limitations due to physical problems' of the Multiple Sclerosis Quality of Life-54, and by assessing the patient impression of perceived fatigue.
Arnao et al., 2019	Investigated the combined use of tRNS with the Graded Repetitive Arm Supplementary Program in sub-acute ischemic stroke patients suffering from arm impairment. Measured upper limb impairment with Fugl-Meyer Assessment-Upper extremity before and after treatment. Pilot study.	18 ischemic stroke patients with upper limb disability, evaluated by FMA-UE, 1-6 weeks after stroke 9 in experimental group, 5F, 4M, 75.5±11.7; 9 in control group, 4F, 5M, 76.6±6.6	One electrode was placed over M1 opposite the upper limb impairment, and the reference electrode was placed over the contralateral orbit	1mA hf-tRNS (101-640Hz) for 20 min on 5 sessions	30s tRNS	Proposed protocol might have a positive impact on clinical rehabilitation programs, given it is effective, easy to carry out, well tolerated by the patient and can be initiated in the sub-acute phase bedside at a Stroke Unit. Beneficial effects in the tRNS group correlated with better Fugl-Meyer Assessment-Upper extremity score than sham stimulation group and these results did not correlate to stroke severity.
Monastero et al., 2020	Investigated the effects of tRNS applied over M1 in Parkinson's disease patients with mild cognitive impairment in cognitive and motor tasks.	10 Parkinson's disease patients with mild cognitive impairment; 0F, 10M;	4.5x4.5cm electrodes over the left M1 and the contralateral shoulder	1.5mA hf-tRNS (100-600Hz) for 15 min with 10s fade-in/out Double-blind	30s 1.5mA tRNS with 10s fade-in/out	tRNS improved the motor ability (measured with Unified Parkinson's Disease Rating Scale) in comparison to sham control condition. No other significant differences were found in other motor

	Measured cognitive and motor function before and after each session.	70.2±8.7; age range: 59-80				tasks and cognitive assessment both after real and sham stimulations.
<b>2.2 Acute online effects during tRNS</b>						
<b>2.2.1 Visual perception</b>						
Campana et al., 2016	Investigated the effects of hf- vs lf-tRNS on motion adaptation and recovery employing motion after-effect phenomenon. Measured the estimated motion after-effect duration during tRNS stimulation.	36 healthy volunteers; normal or corrected-to-normal vision Exp.1 hf-tRNS: 12 lf-tRNS: 12 control: 12	25cm <sup>2</sup> electrodes placed bilaterally over a site located ~3 cm above theinion and ~5 cm anteriorly on the left and on the right (hMT <sup>+</sup> ) or over frontal areas	1.5mA lf-tRNS (0.1-100Hz), hf-tRNS (100-640Hz) with 0mA offset for 17-18 min with 30s fade-in sham on the same session	30s fade in/out 1.5mA tRNS, Active control condition	Hf- and lf-tRNS have opposite effects on the adaptation-dependent imbalance between neurons tuned to opposite motion directions. When applied to the bilateral hMT <sup>+</sup> , hf-tRNS caused a significant decrease in motion after-effect duration whereas lf-tRNS caused a significant corresponding increase in motion after-effect duration. No effects on motion after-effect duration were induced by stimulating frontal areas.
van der Groen and Wenderoth, 2016	Investigated whether noise added directly to cortical networks acutely enhances sensory detection. Tested the hypothesis that SR phenomenon underlies the tRNS mechanism of action. Measured visual contrast detection 2AFC task performance during tRNS.	52 healthy volunteers; 26F, 26M; mean age 24; age range: 18-30 all right-handed; normal or corrected to normal vision Exp.1: 31 (14F, 17M; 24; age range: 19–30) Exp.2: 38 (21F, 17M; 25; age range: 19–30) Exp.3: 20 (9F, 11M; 25; age range: 21–30) 2 groups in each	5x7cm electrodes over Oz, and over Cz in Exp.2 5x7cm electrodes over forehead (Fpz), and over Cz in Exp.3	0.5, 0.75, 1 or 1.5mA (peak-to-baseline) hf-tRNS (100-640Hz) with 0mA offset for 2.04 s twice per trial, randomized order	no tRNS or active control condition	When the optimal level of noise was added to V1, detection performance improved significantly relative to a zero-noise condition and to a similar extent as optimal noise added to the visual stimuli. Results demonstrate that adding noise to cortical networks can improve human behavior and that tRNS is an appropriate tool to exploit the mechanism of SR.
Mcintosh and Mehring, 2017	Investigated modulation of perceptual decisions with conflicting biases by applying tRNS. Measured performance of a Simon task, a paradigm where irrelevant spatial cues influence the response times of subjects to relevant color cues, measured during tRNS. Utilized DDM framework to analyse the data.	24 healthy volunteers; 7F, 16M; age range: 20-40; all right-handed	7x5cm electrodes over FT7 and FT8	1mA (peak-to-peak) tRNS (0.1-640Hz) for 18 first trial within each block (alternating with sham) first and last trial to ramp up and down (18 trials tRNS + 18 trials sham) x 6 blocks x 4 sessions	sham*	Non-specific to the Simon task tRNS-induced reduction in the response time of subjects independent of the congruence between spatial and color cues, but dependent on the baseline response time (tRNS reduces response time particularly when baseline response times are long). Different baseline responses resulted from interaction of noise with models of evidence accumulation.
Ghin et al., 2018	Investigated the effects of hf-tRNS to those of a-tDCS and c-tDCS in a global motion direction discrimination task. An equivalent noise paradigm was used to assess how hf-tRNS modulates the mechanisms underlying local and global motion processing. Measured motion coherence threshold and slope of the psychometric function using an 8AFC task in which observers had to discriminate the motion direction of a random dot kinematogram	53 healthy volunteers; all right-handed; normal or corrected to normal vision Exp.1: 16, Exp.2: 24 Exp.3: 13	Exp.1 and 3 16cm <sup>2</sup> electrode over left hMT <sup>+</sup> (3 cm dorsal to inion and 5 cm leftward) 60cm <sup>2</sup> electrode over Cz Exp.2a: 16cm <sup>2</sup> electrode over Cz 60cm <sup>2</sup> electrode over the left forehead	1.5mA (peak-to-peak) hf-tRNS (100-600Hz) with 0mA offset 1.5mA a-tDCS and c-tDCS for 18 min	30s stimulation	hf-tRNS interacts with the output neurons tuned to directions near to the directional signal, incrementing the signal-to-noise ratio and the pooling of local motion cues and thus increasing the sensitivity for global moving stimuli. hf-tRNS reduced the motion coherence threshold but did not affect the slope of the psychometric function, suggesting no modulation of stimulus discriminability. Anodal and cathodal tDCS did not produce any modulatory effects. Equivalent noise analysis in the last experiment found that hf-tRNS modulates sampling but not internal noise, suggesting that hf-tRNS modulates the integration of local motion cues.



	presented either in the left or right visual hemi-field.		Exp.2b: 16cm <sup>2</sup> electrode over Cz 60cm <sup>2</sup> electrode over the left V1 (i.e., 3 cm dorsal to the inion and 1 cm leftward)			
van der Groen et al., 2018	Investigated whether perceptual decisions made by human observers obey the SR principles, by adding noise directly to the visual cortex using tRNS while participants judged the direction of coherent motion in random dot kinematograms presented at the fovea. Measured random dot motion task performance during tRNS. Utilized DDM to analyse the data.	45 healthy volunteers; 17F, 28M; mean age 22.5; age range: 18-27 all with normal or corrected to normal vision 15 per group (bilateral, unilateral left and right)	Exp.1 bilateral: 4x4cm electrodes placed 3.5 cm above the inion and 6.5 cm left and right of the midline in the sagittal plane Exp.2 unilateral left: 4x4cm electrodes placed over left V1 (as in Exp.1) and Cz Exp.3 unilateral right: 4x4cm electrodes placed over right V1 (as in Exp.1) and Cz	0.25, 0.375, 0.5 and 0.75mA hf-tRNS (100-640 Hz) with 0mA offset during 20 trials followed by 20 no stimulation trials within each block of 6min randomized order	no tRNS; 3 electrodes montages	Found that adding tRNS bilaterally to visual cortex enhanced decision-making when stimuli were just below perceptual threshold, but not when they were well below or above threshold. Bilateral tRNS selectively increased the drift rate parameter, which indexes the rate of evidence accumulation.
Battaglini et al., 2019	Investigated whether inhibitory/facilitatory contrast sensitivity effects related to lateral masking are modulated by tRNS. Measured contrast detection task performance. Signal detection theory was used to measure sensitivity ( $d'$ ) and the criterion in a detection task.	68 healthy volunteers, 46F, 24M; 24 ± 3; with normal or corrected to normal vision Exp.1: 19 Exp.2: 19 Exp.3: 30 Exp.4: 15	5x7cm electrodes over Oz and Cz (Exp.1 and 2) or over the forehead (between Fpz and nasion) and Cz (Exp.3 and 4)	1.5mA hf-tRNS (100-600Hz) with 0mA offset for 12 min with 15s fade-in/out	30s tRNS with 15s fade-in/out	Occipital stimulation results in a tRNS-dependent increased sensitivity for the single Gabor signal of low but not high contrast. Dissociation of the tRNS effects when the Gabor signal is presented with the flankers, consisting in a general increased sensitivity at 2λ where the flankers had an inhibitory effect (reduction of inhibition) and a decreased sensitivity at 6λ where the flankers had a facilitatory effect on the Gabor signal (reduction of facilitation). After a frontal stimulation, no specific effect of tRNS was found.
Pavan et al., 2019	Investigated whether modulatory effects of hf-tRNS rely on the SR phenomenon, and what is the specific neural mechanism producing SR. Measured performance of 2AFC motion direction discrimination task with a coherence near threshold measured during intervention.	Exp.1: 24 healthy volunteers; 13F, 11M; age range: 18-40; all right-handed; with normal or corrected to normal vision 12 in Exp.1A and 12 in Exp.1B; Exp.2: 24 healthy volunteers; 15F, 9M; age range: 18-40; all right-handed; with normal or corrected to normal vision 12 in tRNS and 12 in sham	16cm <sup>2</sup> electrodes over left and right hMT <sup>+</sup> (3 cm dorsal to inion and 5 cm leftward and rightward from there for the localization of the hMT <sup>+</sup> )	0.5, 0.75, 1.0, 1.5, and 2.25mA hf-tRNS (100-600Hz) with 0mA offset, for 20 min sessions on different, non-consecutive days	30s 1.5mA tRNS; 30s 2.25mA tRNS;	The results showed a significant improvement in performance when hf-tRNS was applied at 1.5mA, representing the optimal level of external noise. However, stimulation intensity at 2.25mA significantly impaired direction discrimination performance. An equivalent noise analysis, used to assess how hf-tRNS modulates the mechanisms underlying global motion processing, showed an increment in motion signal integration (increase in sampling level) with the optimal current intensity, but reduced motion signal integration at 2.25 mA.

		Exp.3: 20 healthy volunteers; 10F, 10M; age range: 18-40 4 groups of 5 participants				
van der Groen et al., 2019	Investigated the effect of noise on perceptual dominance durations. Used a computational model and compared the model prediction to measured binocular rivalry dynamics when noise was added either to the visual stimulus or directly to V1 by tRNS.	50 healthy volunteers; mean age 23.5 with normal or corrected to normal vision Exp.1 peripheral noise: low contrast: 10, high contrast: 10 Exp.2 tRNS: low contrast: 15, high contrast: 15	5x7cm electrodes over Oz, and over Cz	1mA hf-tRNS (100-640Hz) with 0mA offset for 5 s per trial tRNS/no tRNS randomized (total 6 min stimulation)	no tRNS	Adding noise significantly reduced dominance duration of the mixed percept for low contrast visual stimuli for noise delivered both to the stimuli and to the cortex. Both central and peripheral noise can influence state-switching dynamics of binocular rivalry under specific conditions (e.g., low visual contrast stimuli), in line with a SR-mechanism.
Battaglini et al., 2020	Investigated tRNS effects on multiple spatial frequencies and orientation to unravel whether the long-term perceptual improvements are due to early-stage perceptual enhancements of contrast sensitivity or later stage mechanisms such as learning consolidation. Measured visual contrast detection task performance.	20 healthy volunteers, 13F, 7M; 25 ± 3.4; age range: 21-31; with normal or corrected to normal vision	7.2x6cm electrode over Oz, 11.5x9.5cm electrode over Cz	1.5mA hf-tRNS (100-600Hz) with 0mA offset for 15 min with 15s fade-in/out 4 session each participant (tRNS vs. Sham) × Gabor patch orientations (vertical vs. diagonal) in 2 days; 30min break between sessions	30s tRNS with 15s fade-in/out	Online tRNS effects on visual perception are the result of a complex interaction between stimulus intensity and cortical anatomy. tRNS enhances detection of a low contrast Gabor, but only for oblique orientation and high spatial frequency. No improvement was observed for low contrast and vertical stimuli.
Melnick et al., 2020	Investigated underlying mechanisms of visual improvements caused by tRNS using equivalent noise approach. Measured visual orientation discrimination task performance during and after intervention.	10 healthy volunteers, 7F, 3M; age range: 18-32; with normal or corrected to normal vision; 1 excluded	5x7cm electrodes bilaterally over occipital cortex at O1 and O2	2mA hf-tRNS (100-600Hz) during 400 trials of the task for ~ 20 min 3 sessions: baseline, tRNS and sham (the last 2 counterbalanced)	no tRNS	tRNS improves visual processing when stimulation is applied during task performance, but only at high levels of external visual white noise - a signature of improved external noise filtering. There were no significant effects of tRNS on task performance after the stimulation period.
<b>2.2.2 Auditory perception</b>						
Prete et al., 2017	Investigated whether tES can modulate illusory perception in the auditory domain. Hypothesized that the hyperactivity of the temporal cortex induced by tES could interfere with auditory processing, making the emergence of illusory percepts more difficult.	Exp.1 tDCS 60 healthy volunteers; c-tDCS: 30, 15F, 15M; 21.67±0.65; a-tDCS: 30, 15F, 15M; 20.33±0.19; 6 left-handed Exp.2 tRNS 45 healthy volunteers; 28F, 17M; 22.67±0.42; all right-handed; no auditory impairments and no different hearing thresholds (±5 dBA)	tDCS: 5x7cm electrode over AC, between C3/4 and T3/4 sites (specifically C5 and C6 sites) 5x7cm electrode over contralateral shoulder tRNS: 5x9.5cm electrode and 5x5cm electrode between C3/T3 and C4/T4 (specifically	2mA a-tDCS, c-tDCS for 20 min with 60s fade in/out 3 sessions: left AC, right AC, sham 1.5mA hf-tRNS (100-640Hz) with 0mA offset, for 20 min with 15s fade-in/out	15s tDCS 15s tRNS	Hf-tRNS can modulate auditory perception more efficiently than tDCS. Hf-tRNS applied bilaterally on the temporal cortex reduced the number of times the sequence of sounds was perceived as the Deutsch's illusion with respect to the sham control condition. Neither anodal nor cathodal tDCS applied over the left/right temporal cortex modulated the perception of the illusion.

		between left and right ears	centered on C5 and C6 sites), AC			
Rufener et al., 2017	Investigated AC tRNS-induced modulations in the participants' temporal and spectral auditory resolution ability. Measured gap detection task performance, pitch discrimination task performance and continuous EEG.	20 healthy volunteers; 10F, 10M; age range: 20-35; all right-handed	5x7cm electrodes horizontally over T7, and over T8	1.5mA hf-tRNS (100-640Hz) with 0mA offset, for 20 min (threshold evaluation), 15 min break, and 20 min (EEG + task) with 10s fade-in/out	30s tRNS	Auditory tRNS increased the detection rate for near-threshold stimuli in the temporal domain only, while no such effect was present for the discrimination of spectral features. Reduced peak latencies of the P50 and N1 component of the auditory event-related potentials indicating an impact on early sensory processing The facilitating effect of tRNS was limited to the processing of near-threshold stimuli while stimuli clearly below and above the individual perception threshold were not affected by tRNS.
Prete et al., 2018	Investigated the impact of hf-tRNS on auditory speech perception using the dichotic listening task. Measured the right ear advantage effect, which in dichotic listening positively correlates with speech sound processing.	Exp.1 Bilateral 46 healthy volunteers; 31F, 15M; 22.79±0.41; all right-handed Exp.2 Unilateral 24 healthy volunteers; 12F, 12M; 24.42±0.46; all right-handed; no auditory impairments and no different hearing thresholds (±5 dBA) between left and right ears	Exp.1 Bilateral montage: 5x9.5cm electrode and 5x5cm electrode over T3 and T4, AC Exp.2 Unilateral montage: 5x5cm electrode over T3 or T4, AC 5x9.5cm electrode over contralateral shoulder	1.5mA hf-tRNS (100-640Hz) with 0mA offset, for 20min with 15s fade-in/out Exp.1 2 sessions separated at least 2h Exp.2 3 sessions on 3 different days	15s tRNS	Higher effectiveness of bilateral than unilateral hf-tRNS in modulating basic speech processing mechanisms. Significant enhancement of the right ear advantage was found during bilateral (but not unilateral) hf-tRNS with respect to sham.
Rufener et al., 2018	Investigated the involvement of the locus coeruleus-norepinegic system and a large-scale fronto-parietal cortical network in the regulation of auditory selective attention by applying tVNS and tRNS over the frontal cortex using auditory oddball paradigm and simultaneous EEG	20 healthy volunteers; 10F, 10M; 24.85±2.62; age range: 21-30; normal hearing acuity	tRNS: 5x5cm electrodes over left DLPFC (F3), and over right shoulder	1.5mA hf-tRNS (100-640Hz) with 0mA offset, for 30min (twice: first not part of this study, second oddball task), 10 min break, with 10s fade-in/out, started 5 min before the task tVNS 0.5mA stimulation via the concha cymbae of the left ear; 25 Hz, pulse width 250 µs; with alternating on/off phases of 30 s; 90 min prior to the oddball task and lasted until the end, 100.5 min total. 3 sessions with 3 days break	10s tRNS 10s tVNS	tRNS over the frontal cortex specifically modulates processes involved in stimulus evaluation and in the subjects' behavioral response. Compared to sham, tVNS increased the P3 amplitude, while tRNS reduced the response time to target stimuli. Moreover, both techniques reduced the P3 latency.
Rufener et al., 2020	Investigated detection rate for near-threshold acoustic stimuli, with 3AFC task performance, during application of different levels of noise, either acoustically or electrically via tRNS.	Study 1 (acoustic noise): 29 healthy volunteers; 18F, 11M; 23.7±3.6 Study 2 (tRNS): 26 healthy volunteers; 16F, 10M; 24.5±3.9	5x7cm electrodes horizontally over T7, and over T8 over the left and right auditory cortex	0.3, 0.6, 0.9, 1.2 and 1.5mA (amplitude) hf-tRNS (100-640Hz) delivered during task performance (6 blocks of different intensities; started 250 ms prior to the onset of the first observation interval	no tRNS or acoustic noise	Participants do not benefit from noise, irrespective of its modality (acoustic or tRNS). The results question the existence of SR in the human auditory system.

				and ended 250 ms after the offset of the last observation interval)		
<b>2.2.3 Somatosensory perception</b>						
Ambrus et al., 2010	Investigated the cutaneous perception thresholds of tDCS and tRNS for current intensities ranging from 0.2 to 2mA	30 healthy volunteers; 15F, 15M; 25.9±3.6 3 groups: 10 naïve to tES methods, 4F, 6M, 24.3±3.1; 10 subjects with previous experience with tES, 6F, 4M, 26.2±3.9 and 10 investigators, who use tES in their research, 5F, 5M, 27.4±3.4	3x3.5cm electrode over left supraorbital area, and over contralaterally C3, M1	0.2 – 2mA (with 0.1mA increments) tRNS (0.1-640Hz), a-tDCS, c-tDCS for 15 s with 8s fade-in/out per trial 3 sessions with 24h break 19 trials verum stimulation, + 7 non-stimulation trials	only fade-in/out of certain tES	tRNS as a possible alternative with a better blinding control. Higher cutaneous perception threshold for tRNS (1.2mA) than tDCS (0.4mA). Investigators better than naïve subjects in non-stimulation discrimination.
Ambrus et al., 2011	Investigated the cutaneous perception differences for tDCS and tRNS between rectangle-shaped, and circle-shaped electrodes with the same surface area, and thus, same nominal current distribution.	12 healthy volunteers; 6F, 6M; age range: 20-27	6.7cm diameter circle-shaped, round sponge wrappers, and the standard 5x7cm electrode wrappers for comparison. Both with an area of 35cm <sup>2</sup> ; over left supraorbital area and contralaterally C3, M1	0.2 – 2mA (with 0.1mA increments) tRNS (0.1-640Hz), a-tDCS, c-tDCS for 15 s with 8s fade-in/out per trial 6 sessions with 24h break 19 trials verum stimulation, + 7 non-stimulation trials	only fade-in/out of certain tES	No difference between the round and the rectangular electrode configurations regarding their blinding potentials. No substantial differences between detection thresholds, detection rates, false positive rates or consistent alterations in the sites of perceived stimulation.
<b>2.2.4 Motor function</b>						
Jooss et al., 2019	Investigated the task dependency of tRNS-induced neuromodulation in the motor system using a finger-tapping task versus a go/no-go task. Measured single-pulse TMS-elicited MEPs before and after tRNS, finger-tapping and go/no-go performance assessed during and after tRNS	30 healthy volunteers; 4 F, 12 M; 21±0.35; all right-handed	12.5cm <sup>2</sup> circular electrode over left M1, 30cm <sup>2</sup> rectangular electrode over the contralateral frontopolar cortex	1.51mA peak-to-peak (0.8 mA effective current intensity) of hf-tRNS (100-640Hz), with 0mA offset for 10 min tRNS vs sham separated by at least 7 days	15s fade-in/out tRNS	tRNS-induced neuromodulatory effects are task-dependent and the resulting enhancements are specific to the underlying task-dependent brain state. tRNS enhances the endogenous task-dependent brain state of healthy subjects. In an 'activating' motor task, tRNS during finger-tapping significantly facilitated corticospinal excitability. There was no difference in finger-tapping task performance between tRNS and sham stimulation. In an 'inhibitory' motor task, tRNS during go/no-go left corticospinal excitability was unchanged while inhibitory control was enhanced as shown by slowed reaction times and enhanced task accuracy during and after stimulation.
<b>2.2.5 Clinical: visual perception</b>						
O'Hare et al., 2021	Investigated whether tRNS modulates levels of internal noise in the brain of migraine patients and healthy controls. Measured global motion direction discrimination task performance and	15 migraine patients, 11F, 4M; 30.93±10.85 16 healthy volunteers, 12F, 4M; 31.7±11.35;	4x4cm electrodes over left and right hMT <sup>+</sup> (3cm from theinion and 5cm to the right and left from this point)	1.5mA hf-tRNS (100-600Hz) with 0mA offset for 20 min during task performance	30s tRNS	Hf-tRNS can decrease internal noise levels in migraine. The migraine group demonstrated increased baseline internal noise levels compared to the control group. Internal noise levels, and sampling, were reduced using hf-tRNS but not sham stimulation. There were no differences in terms of

	visually based equivalent noise task performance.					coherence thresholds, slopes, and lapse rate for global motion discrimination between the two groups.
<b>2.2.6 Clinical: motor function</b>						
Hayward et al., 2017	Investigated the feasibility of tRNS, timed to coincide with the generation of voluntary motor commands, during reaching training. Measured the effects with adverse events, training outcomes, clinical outcomes, corticospinal tract structural integrity, and reflections on training through in-depth interviews from each individual case.	4 stroke survivors with chronic (6-months to 5-years) and severe arm paresis; age range 49-73 tRNS: 2 sham: 2	Electrodes over the ipsilesional M1 C3/C4 and over contralateral supraorbital region	2mA tRNS with 0mA offset triggered to coincide with a voluntary movement attempt, for 5 s with 0s fade-in/out. At this point, peripheral nerve stimulation enabled full range reaching. 12 sessions of reaching training (45min each) over 4-weeks	no tRNS	There were no adverse events. All training sessions were completed, repetitive practice performed and clinically relevant improvements across motor outcomes demonstrated. The amount of improvement varied across individuals and appeared to be independent of group allocation and corticospinal tract integrity.
<b>3. Potential cellular mechanisms of RNS</b>						
Onorato et al., 2016	Investigated how externally applied RNS influences action potential firing in mouse primary sensory neurons of dorsal root ganglia, modelling a basic process in sensory perception. Measured the effects of sub-threshold depolarizing current steps with superimposed random fluctuations.	20 to 30 cultured neurons of dorsal root ganglia isolated from the full length of the spine, derived from four months old FVB and C57J mice of both sexes	Patch pipettes made of borosilicate glass for patch-clamp whole-cell recordings	RNS (variance scaled together with step) either before and during, or only during the 5 current depolarizing steps (0.5nA - 3.5nA) applied in alternation, for 30 or 40ms, delivered at 1 Hz	no RNS	External RNS enhances, via SR, the recruitment of transient voltage-gated Na <sup>+</sup> channels, responsible for action potential firing in response to rapid stepwise depolarizing currents. Stimuli of depolarizing step combined with RNS triggered significantly more action potentials than steps alone. The normalized power norm had a clear peak at intermediate noise levels, demonstrating that the phenomenon is driven by SR.
Remedios et al., 2019	Investigated the physiological mechanism underlying electrical RNS. Measured the effects of short-term electrical noise applied to the voltage-clamp ramps on the kinetics of the Na <sup>+</sup> current. Assessed correlation between the peak amplitude of the Na <sup>+</sup> current and its latency for different levels of RNS.	34 in-vitro, acutely-isolated brain pyramidal neurons from the somatosensory (N=16) and auditory (N=18) cerebral cortex of 7 Wistar rats (mean weight 100–150 g)	Glass microelectrode for whole-cell voltage clamp recordings	0.045mV, 0.080mV, 0.142mV, 0.250mV, 0.445mV electrical RNS (0-5000Hz) for 250ms (short-term) delivered during Na <sup>+</sup> currents eliciting six groups of 10 voltage-clamp-ramp protocol of 100ms, from -100 to +40 mV, with a holding potential of -80 mV	no RNS	There is an intermediate level of RNS that enhances the activation or inactivation processes occurring in the Na <sup>+</sup> channels of the pyramidal neurons. A Hodgkin–Huxley neuron model, involving the kinetics of activation and inactivation of the Na <sup>+</sup> channels, explains differences in the impact of noise on three groups of pyramidal cells exhibiting a positive, negative or no correlation between peak amplitude of the Na <sup>+</sup> current and its latency for different levels of RNS.
*no further methodological details were specified; Abbreviations: AC – auditory cortex; AFC – alternative forced choice; AMT – active motor threshold; ASSRs - auditory steady state responses; a-tDCS – anodal transcranial direct current stimulation; a-tPCS – anodal transcranial pulsed current stimulation; c-tDCS – cathodal transcranial direct current stimulation; CS - contrast sensitivity; DDM – drift-diffusion model; DLPFC - dorsolateral prefrontal cortex; EEG – Electroencephalography; ERSP - event-related spectral perturbation; fMRI – functional magnetic resonance imaging; hf-tRNS – high-frequency transcranial random noise stimulation; ICF – intracortical facilitation; IFC - interval forced choice; iTBS - intermittent theta- burst stimulation; lf-tRNS – low- frequency transcranial random noise stimulation; LICl - long-interval intracortical inhibition; M1 – primary motor cortex; MEP – motor evoked potential; MS – multiple sclerosis; PFC - prefrontal cortex; PSD - power spectral density; RMT – rest motor threshold; RNS – random noise stimulation; SEP-PPD - somatosensory evoked potential paired-pulse depression; SI <sub>1mV</sub> – TMS intensity to evoke MEP of 1 mV peak-to-peak amplitude; SICl - short-interval intracortical inhibition; SR – Stochastic Resonance; tACS – transcranial alternating current stimulation; tDCS – transcranial direct current stimulation; TEP - transcranial magnetic stimulation evoked potentials; tRNS – transcranial random noise stimulation; TMS – transcranial magnetic stimulation; tVNS - transcutaneous vagal nerve stimulation; UCVA - uncorrected visual acuity; UCCS - uncorrected contrast sensitivity; V1 – primary visual cortex; VA – visual acuity; VEP - visual evoked potentials						

## Curriculum Vitae